BioMed Research International

Aquatic Environmental Health and Toxicology

Guest Editors: Zhi-Hua Li, Kaiyu He, Chunsheng Liu, Ping Li, and Vladimir Zlabek

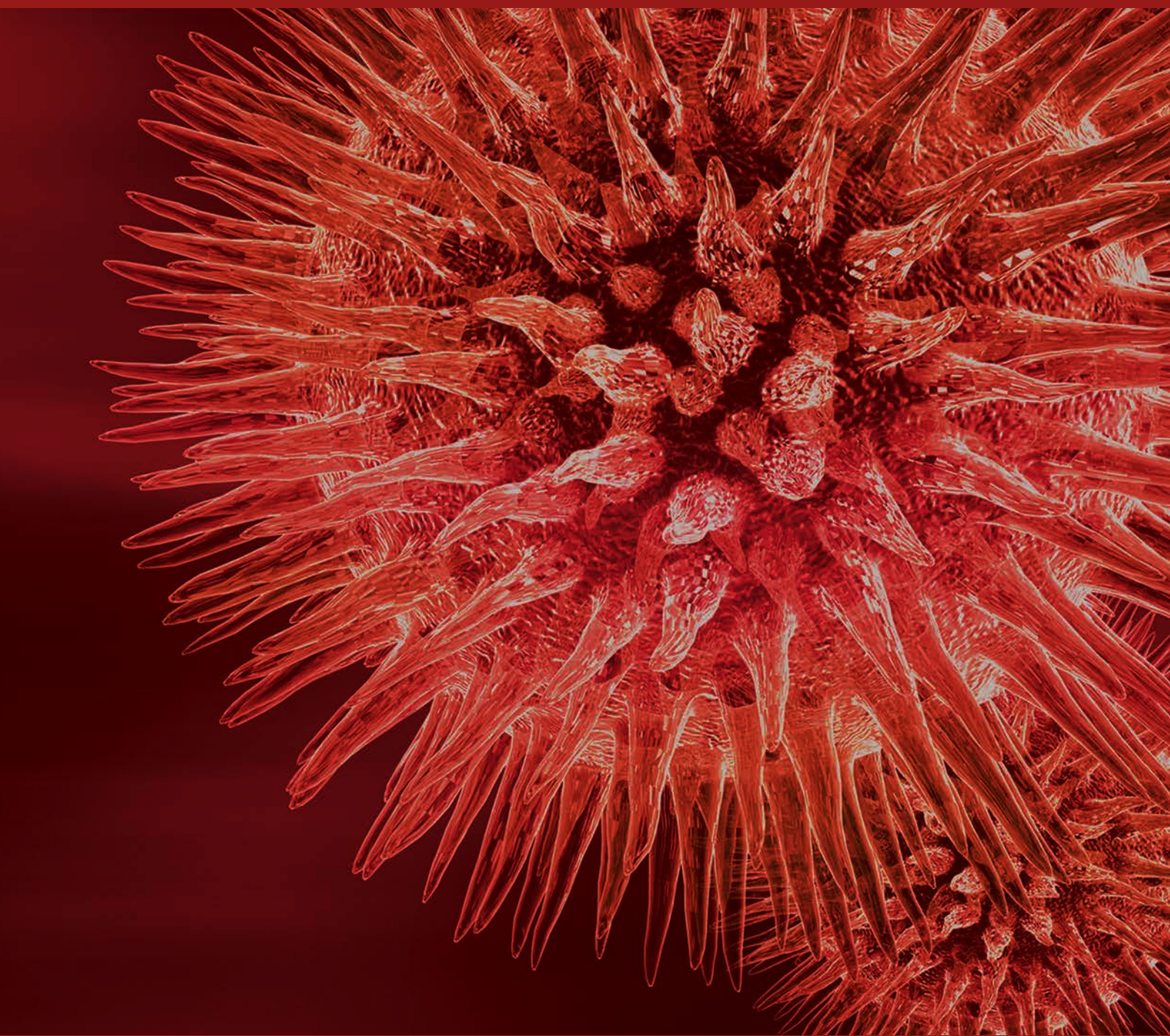

Aquatic Environmental Health and Toxicology

BioMed Research International

Aquatic Environmental Health and Toxicology

Guest Editors: Zhi-Hua Li, Kaiyu He, Chunsheng Liu, Ping Li, and Vladimir Zlabek

Contents

Hindawi Publishing Corporation
BioMed Research International
Volume 2016, Article ID 3514898, 2 pages
http://dx.doi.org/10.1155/2016/3514898

Editorial
Aquatic Environmental Health and Toxicology

Zhi-Hua Li,[1,2] Kaiyu He,[3] Chunsheng Liu,[4] Ping Li,[1,2] and Vladimir Zlabek[2]

[1] *Yangtze River Fisheries Research Institute, Chinese Academy of Fishery Sciences, No. 8, 1st Wudayuan Road, East Lake Hi-Tech Development Zone, Wuhan, Hubei 430223, China*
[2] *Faculty of Fisheries and Protection of Waters, University of South Bohemia in České Budějovice, Zátiší 728/II, 389 25 Vodňany, Czech Republic*
[3] *Biomedical Sciences Research Building (BSRB), University of Michigan, 109 Zina Pitcher Place, Ann Arbor, MI 48109-2200, USA*
[4] *College of Fisheries, Huazhong Agricultural University, No. 1 Shizishan Street, Hongshan District, Wuhan, Hubei 430070, China*

Correspondence should be addressed to Zhi-Hua Li; zhihuali06@yahoo.com

Received 5 December 2016; Accepted 7 December 2016

Nowadays, thousands of pollutants enter into the water environment and exert various kinds of stress on aquatic organisms, which can in many cases result in negative changes in water quality. Water-inhabiting organisms constitute one of the essential components of the ecosystem. Recently, awareness of the adverse effects of chemical contamination is growing as investigations into these pollutants increase and analytical detection techniques improve. The aquatic environment, as an important component of the biosphere, has been termed "the ultimate sink" for natural and man-made chemicals. Given the finite supply of water available, the continued chemical contamination of the aquatic environment may pose a significant environmental health hazard. Laboratories from Turkey, Brazil, India, and China submitted 19 papers. Altogether, 9 original papers were accepted after the reviewing process.

For the part *bookmarks and mechanisms of aquatic toxicology*, six papers have been accepted. Toxicity tests were conducted with sea cucumber (*Apostichopus japonicus*) exposed to heavy metals by L. Li et al., who found that, under acute or chronic heavy metal stress, the sea cucumber has many physiological adaption mechanisms including decrease or increase of oxygen consumption rate and adjusted activity of metabolic enzymes. L. Geng et al. evaluated the individual and combined effects of salinity and alkalinity on gill Na^+/K^+-ATPase enzyme activity, plasma ion concentration, and osmotic pressure in *Luciobarbus capito*. The toxic effects of carbon quantum dots (CDs) on rare minnow (*Gobiocypris rarus*) embryos at different developmental stages were investigated by Y.-Y. Xiao et al., who found that the mechanism of CDs exposure might result from the pressure of induced oxidative stress coordinate with the dysregulated development related gene expression mediated. L. Luo et al. demonstrated that adding strain SP1 to aquaculture wastewater could effectively reduce the COD, TAN, and SS and accelerate biofloc formation.

For the part *environmental factors and aquatic environmental health*, three papers have been accepted. J. Li et al. studied the impacts of dam construction on fish, which provided basic knowledge of spatiotemporal distribution and assemblages of fishes in the extended reaches downstream of Gezhouba Dam. X. Bi et al. found that heavy metals with different stimulatory effects on different stages of the formation of *Microcystis* colonies might be one factor that contributes to the occurrence of *M. aeruginosa* blooms in natural conditions, through investigating the sequestration and distribution characteristics of Cd(II) by *Microcystis aeruginosa* and its role in *Microcystis* colony formation. To provide more reasonable references for remedying underground water, Y. Cheng et al. carried out a study that was conducted to achieve a better understanding of the migration and distribution of benzene, toluene, ethyl benzene, and xylene (BTEX). And they concluded that alleviating BTEX pollution in underground water by increasing the concentrations of electric acceptors, such as nitrate, and by enhancing microbial activities is an effective and noteworthy method.

The papers of this special issue comprise critical and new areas of research and recent advances on challenging issues in different fields of aquatic environmental health and toxicology, which tried to stimulate the continuing efforts to

understand the adverse effects and toxicological mechanisms of chemical contaminants in aquatic systems. We hope that the special issue will attract more interest from many people, including scientists, researchers, and related governments concerned about aquatic environmental health.

Zhi-Hua Li
Kaiyu He
Chunsheng Liu
Ping Li
Vladimir Zlabek

Hindawi Publishing Corporation
BioMed Research International
Volume 2016, Article ID 4605839, 7 pages
http://dx.doi.org/10.1155/2016/4605839

Research Article

Effect of Salinity and Alkalinity on *Luciobarbus capito* Gill Na^+/K^+-ATPase Enzyme Activity, Plasma Ion Concentration, and Osmotic Pressure

Longwu Geng, Guangxiang Tong, Haifeng Jiang, and Wei Xu

Heilongjiang River Fisheries Research Institute, Chinese Academy of Fishery Sciences, Harbin 150070, China

Correspondence should be addressed to Wei Xu; xwsc23@163.com

Received 30 March 2016; Accepted 17 October 2016

Academic Editor: Vladimir Zlabek

We evaluated the individual and combined effects of salinity and alkalinity on gill Na^+/K^+-ATPase enzyme activity, plasma ion concentration, and osmotic pressure in *Luciobarbus capito*. Increasing salinity concentrations (5, 8, 11, and 14 g/L) were associated with an initial increase and then decrease in *L. capito* gill Na^+/K^+-ATPase activity. Activity was affected by the difference between internal and external Na^+ ion concentrations and osmotic pressure ($P < 0.05$). Both plasma ion (Na^+, K^+, and Cl^-) concentration and osmotic pressure increased significantly ($P < 0.05$). An increase in alkalinity (15, 30, 45, and 60 mM) caused a significant increase in plasma K^+ and urea nitrogen concentrations ($P < 0.05$) but had no effect on either plasma osmotic pressure or gill filament ATPase activity. In the two-factor experiment, the saline-alkaline interaction caused a significant increase in plasma ion (Na^+, Cl^-, and urea nitrogen) and osmotic pressure ($P < 0.05$). Variance analysis revealed that salinity, alkalinity, and their interaction significantly affected osmotic pressure, with salinity being most affected, followed by alkalinity, and their interaction. Gill filament ATPase activity increased at first and then decreased; peak values were observed in the orthogonal experiment group at a salinity of 8 g/L and alkalinity of 30 mM.

1. Introduction

In China, saline-alkaline water is an important territorial resource. This resource is primarily located in northwestern plateau lakes, in northeastern plain wetlands, and underground in the northern littoral region in China and has an estimated capacity of 539.8 billion m^3 [1]. The distinguishing features of this water resource include high salinity-alkalinity, poor buffering capacity, and ion imbalance. Coincidentally, these features are also limiting to aquatic animal survival [2]. The availability of water resources is decreasing but demand for aquatic products is increasing [3, 4]. Thus, the use of saline waters will become important to the development of sustainable fisheries. In recent years, China has attempted to breed some fish species in partially saline waters. The species used to date have been restricted to waters with salinity of $<5\ g\ L^{-1}$ and alkalinity <10 mM. However, there is considerable effort being devoted to successfully rearing fish in higher-salinity waters [5–7]. In 2003, China introduced the salt-tolerant fish *Luciobarbus capito* from the Aral Sea in Uzbekistan. This Cyprinidae (Barbinae, *Barbus* genus) is found primarily in the Aral Sea but migrates into the rivers to spawn. In addition to its high salt tolerance, it has a varied diet, has fast growth rate, produces meat that has desirable traits, and is economically important for the region [8].

Gill is the main organ of osmotic regulation in teleosts and chloride cells are the sites of ion transport across gill epithelium [9–11]. ATPases are membrane-bound enzymes responsible for the transport of ions through cell membranes and thus help in regulation of cellular volume, osmotic pressure, and membrane permeability [12]. Salinity tolerance is typically evaluated by measuring gill filament Na^+/K^+-ATPase enzyme activity, plasma ion concentration, and osmotic pressure [13–18]. However, because most studies have looked at either salinity [12, 19] or alkalinity [20, 21] alone, it is difficult to evaluate the interactive effect of both factors on aquatic animals. Our objectives were to evaluate the effect of salinity and alkalinity, alone and

Table 1: The orthogonal test of salinity and alkalinity.

Experience group number	Treatment level	
	NaCl (g/L)	$NaHCO_3$ (mM)
0	0	0
1	5	15
2	5	30
3	5	45
4	8	15
5	8	30
6	8	45
7	11	15
8	11	30
9	11	45

in combination, on *L. capito* gill Na^+/K^+-ATPase activity, plasma ion concentration, and osmotic pressure. Our results can be used to inform the range of saline-alkaline conditions suitable for survival during aquaculture.

2. Materials and Methods

2.1. Study Species. The experimental fish were 1-year-old, pool-bred fish (40–60 g, 16.57–24.61 cm fork length). The fish were held in a glass-steel circular cylinder (1 m diameter) containing 300 L aerated water (pH 7.51, salinity 0.28‰, total alkalinity 1.39 mM, total hardness 1.10 mM, total phosphorus 0.11 mg/L, total nitrogen 2.95 mg/L, total iron 0.002 mg/L, SO_4^{2-} 31.19 mg/L, Ca^{2+} 19.81 mg/L, and Mg^{2+} 2.03 mg/L) at room temperature. The fish were acclimated to experimental conditions for 3 d. The analytical reagents (AR) were NaCl and $NaHCO_3$.

2.2. Experimental Design. First, we evaluated the individual effect of salinity or alkalinity. The fish were divided into four treatment groups for each factor: 5, 8, 11, and 14 g/L NaCl and 15, 30, 45, and 60 mM $NaHCO_3$. Second, we evaluated the combined effects of salinity and alkalinity. The fish were divided into 9 treatment groups to test all combinations of salinity (5, 8, and 11 g/L) and alkalinity (15, 30, and 45 mM), based on orthogonal table L_9 (3^4) (Table 1). Each treatment group consisted of three replicates with eight specimens per replicate, and the number of the experimental fish was 480. The experiment was performed for 60 days without aeration at 22 ± 0.5°C. A third of the water was changed daily and the corresponding concentration was adjusted with a pre-prepared master mix.

2.3. Sample Collection and Testing. After the experiment, the fish were anaesthetized by immersion in Tricaine Methanesulphonate (MS-222) at 200 mg/L. Approximately 1.5–2.0 mL blood was drawn from the caudal vessels, just behind the anal fin, with a 2.5 mL syringe. The samples were centrifuged at 4000 ×g for 10 min and the plasma was collected and frozen at −70°C until required. After collecting the blood, the fish were put into an ice box. The gills were then removed and washed with cold saline water (0.7 g/L), the surface moisture was dried with filter paper, and the gill filament was then accurately weighed to the nearest 0.2 g. The gill tissue was then homogenized in 1.8 mL saline water according to weight and volume and centrifuged at 1200 ×g for 10 min, and the clear supernatant was eluted for testing. Plasma and gill filament test samples were taken from three fish.

Plasma Na^+, Cl^-, and K^+ concentrations were measured by using the detection kits (Nanjing Jiancheng Bioengineering Institute, Nanjing, China). The urea nitrogen was spectrophotometrically measured with Nessler's reagent as the chromogenic reagent according to Lu export method [22]. The activity of Na^+/K^+-ATPase was determined by Spectrophotometry using ATP as substrate; thus, 1 μmol inorganic phosphorus generated by ATPase enzyme decomposition is equal to one ATPase enzyme activity unit (μmol Pi/mg prot/h). Coomassie blue staining and calf plasma protein as a standard were used for protein determination [23]. Plasma osmotic pressure was determined using an autofreezing point osmometer (Labsun Technology Development Co. Ltd., Beijing, China).

2.4. Statistical Analysis. Count experimental data and significance tests were performed in SPSS 11.5 software (SPSS Inc., Chicago, IL, USA). Each parameter was analyzed separately by one-way ANOVA. Comparisons between different groups and between the treatment groups and control were performed by ANOVA followed by Duncan's *post hoc* test.

3. Results

3.1. Influence of Salinity-Alkalinity on Plasma Ion Concentration. The plasma ion concentrations for *L. capito* reared at different salinities are shown in Table 2. The concentration of plasma ions K^+, Na^+, and Cl^- increased significantly with increasing salinity ($P < 0.05$), and the concentration of these three ions peaked when salinity was 14 g/L (234.21 ± 3.69 mM for K^+, 292.82 ± 7.23 mM for Na^+, and 0.57 ± 0.04 mM for Cl^-). Urea nitrogen concentration was significantly higher than that of the control group ($P < 0.05$) at 14 g/L salinity but was not different in the other groups ($P > 0.05$).

The plasma ion concentrations for *L. capito* reared at different alkalinities are shown in Table 3. K^+ ion concentration in the experimental groups was significantly higher than in the control group. Na^+ and Cl^- ion concentrations were not significantly affected by changes in alkalinity ($P > 0.05$). Urea nitrogen concentration in the experimental groups was significantly higher than in the control group ($P < 0.05$), and urea nitrogen concentration increased gradually with increasing alkalinity.

The single-factor experiment results revealed that salinity significantly influenced Na^+, K^+, and Cl^- plasma concentrations but had only a small influence on urea nitrogen concentration. Alkalinity had little effect on plasma Na^+ and Cl^- concentrations but significantly affected K^+ and urea nitrogen concentrations ($P < 0.05$).

The *L. capito* plasma ion concentrations in the saline-alkaline orthogonal test are shown in Table 4. With increasing

Table 2: Plasma Na^+, Cl^-, and K^+ concentration, ammonia content, and osmolarity in *L. capito* at different salinity conditions.

NaCl (g/L)	Na^+ (mM)	Cl^- (mM)	K^+ (mM)	BUN (mM)	Osmolarity (mosmol/kg)
0	153.77 ± 8.72^a	105.81 ± 3.85^a	0.35 ± 0.05^a	1.36 ± 0.08^a	280.10 ± 4.76^a
5	161.84 ± 4.44^b	119.17 ± 3.18^b	0.49 ± 0.06^b	1.43 ± 0.11^a	291.02 ± 2.57^b
8	216.41 ± 8.82^c	174.85 ± 5.75^c	0.52 ± 0.03^b	1.47 ± 0.10^a	354.95 ± 4.83^c
11	276.11 ± 5.99^d	232.18 ± 4.23^d	0.53 ± 0.04^b	1.53 ± 0.06^a	457.81 ± 2.79^d
14	292.82 ± 7.23^e	234.21 ± 3.69^d	0.57 ± 0.04^{bc}	1.63 ± 0.12^b	449.32 ± 4.81^e

Different letters in the columns indicate significant differences between variables evaluated ($P < 0.05$).

Table 3: Plasma Na^+, Cl^-, and K^+ concentration, ammonia content, and osmolarity in *L. capito* at different alkalinity conditions.

$NaHCO_3$ (mM)	Na^+ (mM)	Cl^- (mM)	K^+ (mM)	BUN (mM)	Osmolarity (mosmol/kg)
0	153.77 ± 8.72^a	105.81 ± 3.85^a	0.35 ± 0.05^a	1.36 ± 0.08^a	280.10 ± 4.76^a
15	161.22 ± 5.87^a	109.61 ± 7.33^a	0.58 ± 0.06^b	5.06 ± 0.15^c	286.27 ± 5.63^a
30	153.30 ± 6.89^a	105.21 ± 5.71^a	0.61 ± 0.03^b	5.04 ± 0.24^c	284.16 ± 3.11^a
45	152.21 ± 6.57^a	104.37 ± 5.55^a	0.64 ± 0.04^b	4.87 ± 0.19^c	287.88 ± 4.85^a
60	151.78 ± 6.03^a	103.00 ± 4.21^a	0.65 ± 0.05^b	4.57 ± 0.38^{bc}	288.98 ± 5.62^a

Different letters in the columns indicate significant differences between variables evaluated ($P < 0.05$).

Table 4: Plasma Na^+, Cl^-, and K^+ concentration, ammonia content, and osmolarity in *L.capito* at different saline-alkaline conditions.

Group number (salinity × alkalinity)	Na^+ (mM)	Cl^- (mM)	K^+ (mM)	BUN (mM)	Osmolarity (mosmol/kg)
0 × 0	153.77 ± 8.72^a	105.81 ± 3.85^a	0.35 ± 0.05^a	1.36 ± 0.08^a	280.10 ± 4.76^a
5 × 15	155.68 ± 3.84^a	113.33 ± 1.85^b	0.32 ± 0.05^a	1.30 ± 0.08^a	296.66 ± 3.69^b
5 × 30	164.77 ± 1.88^b	116.70 ± 2.88^b	0.39 ± 0.04^a	1.76 ± 0.05^b	308.84 ± 2.16^c
5 × 45	169.91 ± 2.49^b	118.40 ± 2.62^b	0.39 ± 0.05^a	1.71 ± 0.03^b	320.21 ± 4.31^d
8 × 15	180.40 ± 3.70^c	118.00 ± 2.81^b	0.43 ± 0.05^a	1.79 ± 0.03^b	350.91 ± 1.41^e
8 × 30	189.20 ± 2.31^c	144.50 ± 2.26^c	0.49 ± 0.07^b	1.71 ± 0.04^b	359.94 ± 5.46^f
8 × 45	191.25 ± 3.61^d	156.33 ± 2.23^d	0.55 ± 0.06^b	1.87 ± 0.03^c	363.15 ± 3.12^f
11 × 15	195.68 ± 2.66^d	173.71 ± 3.19^f	0.64 ± 0.03^c	3.31 ± 0.06^e	376.81 ± 4.67^g
11 × 30	205.06 ± 3.69^e	177.87 ± 2.75^f	0.56 ± 0.04^b	3.19 ± 0.06^d	389.65 ± 3.96^h
11 × 45	209.64 ± 2.25^e	169.23 ± 1.50^e	0.54 ± 0.06^b	3.38 ± 0.09^e	405.52 ± 4.80^i
ANOVA	$S > A$, $S \times A$ not significant	$S > A > S \times A$	$S > S \times A$, A not significant	$S > A > S \times A$	

S, salinity effect. A, alkalinity effect. $S \times A$, interaction of salinity and alkalinity. Different letters in the columns indicate significant differences between variables evaluated ($P < 0.05$).

salinity and alkalinity, the concentration of plasma ions Na^+, K^+, Cl^-, and urea nitrogen increased to different degrees, suggesting that salinity and alkalinity have an interactive effect on the concentrations of these four plasma ions. The variance analysis revealed that salinity and the saline-alkaline interaction significantly affected K^+ ion concentrations ($P < 0.05$) but that alkalinity had no significant effect ($P > 0.05$). The effect of salinity on Na^+ ion concentration was most significant ($P < 0.05$), followed by alkalinity, and their interaction had no significant effect ($P > 0.05$). Both Cl^- ion and urea nitrogen concentrations were significantly affected by salinity, alkalinity, and their interaction ($P < 0.05$).

3.2. Influence of Salinity-Alkalinity on Plasma Osmotic Pressure. The influence of salinity, alkalinity, and saline-alkaline orthogonal function on plasma osmotic pressure is shown in Table 2 and Figures 1–3. In the single-factor experiment, plasma osmotic pressure significantly increased with increasing salinity ($P < 0.05$) (Figure 1). Increasing alkalinity had no significant effect on plasma osmotic pressure ($P > 0.05$) (Figure 2). In the orthogonal experiment, plasma osmotic pressure gradually increased with increasing salinity and alkalinity concentrations ($P < 0.05$) (Figure 3). The variance analysis revealed that salinity, alkalinity, and their interaction significantly affected osmotic pressure; salinity had the most significant effect, followed by alkalinity, with their interaction being the smallest. The regression equation for plasma osmotic pressure (Y), salinity (S), and alkalinity (A) is $Y = 260.148 + 10.726S + 0.306A$ ($R^2 = 0.904$).

3.3. Influence of Salinity-Alkalinity on Gill Na^+/K^+-ATPase Enzyme Activity. The influence of salinity, alkalinity, and

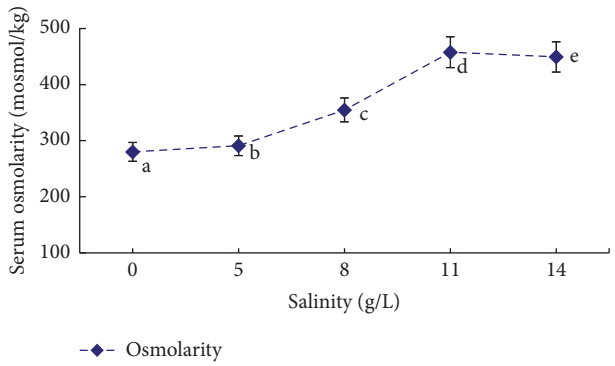

Figure 1: The influence of different salinity conditions on plasma osmolarity in *L. capito*.

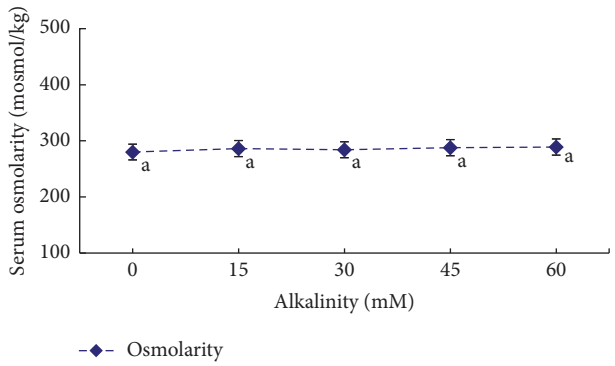

Figure 2: The influence of different alkalinity conditions on plasma osmolarity in *L. capito*.

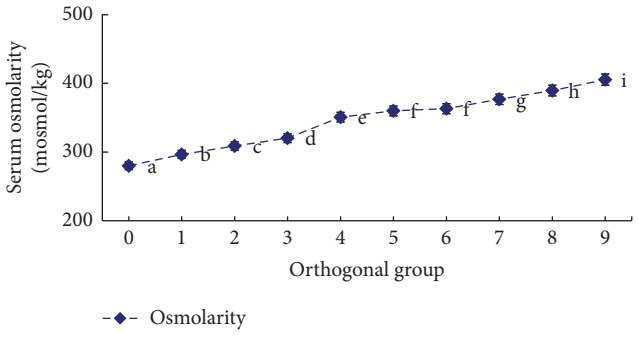

Figure 3: The influence of different saline-alkaline conditions on plasma osmolarity in *L. capito*.

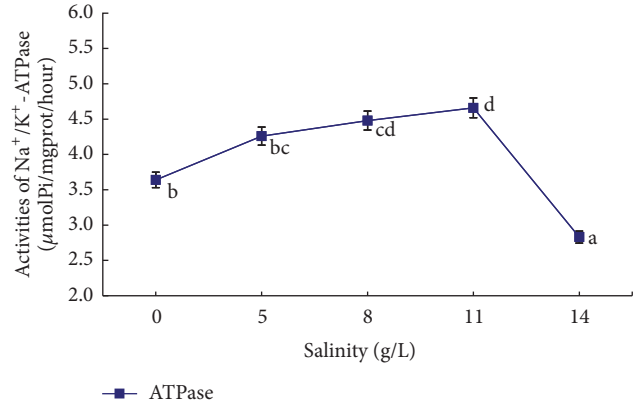

Figure 4: The influence of different salinity conditions on Na^+/K^+-ATPase activities in *L. capito*.

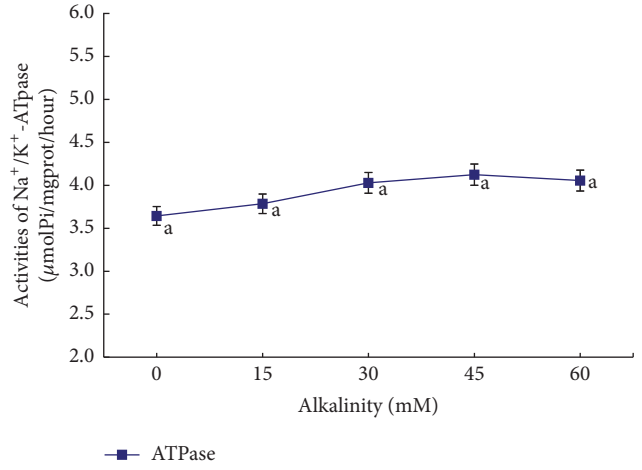

Figure 5: The influence of different alkalinity conditions on Na^+/K^+-ATPase activities in *L. capito*.

their interaction on gill filament Na^+/K^+-ATPase enzyme activity is shown in Figures 4–6. In the single-factor experiment, gill filament Na^+/K^+-ATPase enzyme activity significantly increased when salinity was between 5 and 11 g/L ($P < 0.05$), whereas it was significantly lower at salinity >11 g/L ($P < 0.05$) (Figure 4). The influence of increasing alkalinity on gill filament ATPase enzyme activity was not significant ($P > 0.05$) (Figure 5). In the orthogonal experiment, gill filament ATP enzyme activity increased at first and then decreased with the interactive effects of increasing salinity and alkalinity. ATPase enzyme activity peaked in group 5 (salinity 8 g/L and alkalinity 30 mM) and was lowest in group 9 (salinity 11 g/L and alkalinity 45 mM) (Figure 6).

For the single-factor salinity experiment, the difference between gill filament Na^+/K^+-ATPase enzyme activity and Na^+ ion concentration in the water, plasma, and water osmotic pressure and the difference between plasma Na^+ concentration and Na^+ concentration in the water are shown in Table 5. In the water, Na^+ concentration and ATPase enzyme activity were positively correlated but the degree of correlation was not high. Differences in osmotic pressure and Na^+ concentration were strongly positively correlated with ATPase enzyme activity. ATPase enzyme activity gradually increased with increasing osmotic pressure differences and was highest (4.66 ± 0.07) when the osmotic pressure difference was at its peak (97.17 ± 4.34). The results of the single-factor salinity experiment suggest that differences in plasma osmotic pressure and plasma Na^+ concentration

Table 5: The correlation of water Na^+ concentration, serum osmosis, and Na^+ concentration difference to the Na^+/K^+-ATPase of *L. capito* at different salinity conditions.

NaCl (g/L)	Na^+ concentration (mM)	Serum osmosis difference (mosmol/kg)	Na^+ concentration difference (mM)	Na^+/K^+-ATPase (μmolPi/mgprot/hour)
5	90.47 ± 5.78	92.46 ± 5.53	71.38 ± 5.20	4.26 ± 0.13
8	139.56 ± 7.31	94.41 ± 10.41	76.85 ± 15.82	4.48 ± 0.13
11	194.29 ± 3.90	97.17 ± 4.34	81.81 ± 4.91	4.66 ± 0.07
14	243.92 ± 3.25	12.87 ± 3.18	48.90 ± 4.98	2.83 ± 0.20
Regression equation	$Y = 3.889 + 0.004X$ ($R^2 = 0.684$)	$Y = 2.599 + 0.020X$ ($R^2 = 0.922$)	$Y = 1.319 + 0.038X$ ($R^2 = 0.872$)	—

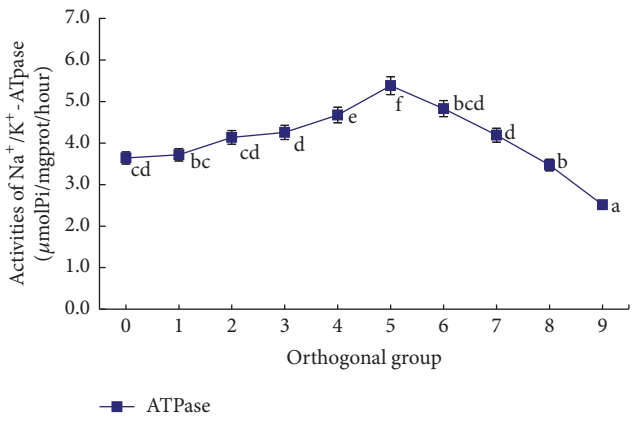

Figure 6: The influence of different saline-alkaline conditions on Na^+/K^+-ATPase activities in *L. capito*.

are important factors affecting gill filament Na^+/K^+-ATPase enzyme activity in *L. capito* both *in vitro* and *in vivo*.

4. Discussion

4.1. Changes in Luciobarbus capito Gill Na^+/K^+-ATPase Enzyme Activity. All freshwater and saltwater fish exhibit Na^+/K^+-ATPase enzyme activity in the gill epithelia. The main function of this is to maintain ion permeability in the cytoplasmic membrane, relative stability of various ion concentrations in the intracellular environment, and osmotic pressure balance between the intracellular and external environments [24–26]. Gill filament ATPase enzyme activity adjusts accordingly when ion concentrations in the external environment change. Generally, ATPase enzyme activity is positively correlated with the external salinity concentration [13, 18, 27, 28]. Based on our single-factor experimental results, changes in gill filament ATPase enzyme activity follow the above-mentioned rule when salinity is <11 g/L. ATPase enzyme activity increased with increasing salinity in the water. This increased the permeability of the gill epithelium membrane, accelerated the discharge of Na^+ and Cl^- ions, and discharged excess salt ions out of the body. This maintained plasma ion concentration at a level required for physical activity, thus ensuring normal activity and energy metabolism [18].

When salinity was >11 g/L and under high salinity stimulus, gill filament Na^+/K^+-ATPase enzyme activity in *L. capito* decreased. Some researchers have reported a similar phenomenon in *Chanos chanos* [29]; ATPase enzyme activity in juvenile cobia was lower at 20 g/L salinity than at 10 g/L. Xu et al. have suggested that salinity is not the only factor affecting juvenile cobia gill ATPase activity but that it may be associated with a different regulatory mechanism [15]. Our salinity experimental results revealed that the influence of differences in osmotic pressure or Na^+ ion concentration *in vivo* and *in vitro* on gill filament ATPase enzyme activity in *L. capito* was significant and did not increase with increasing salinity in the water. The fish improve ATPase enzyme activity and discharged excess salt ions from the body when there was a large difference between plasma osmotic pressure *in vivo* and water osmotic pressure *in vitro*. In contrast, the ATPase enzyme activity was decreased, when the difference was smaller.

In the saline-alkaline orthogonal experiment, the overall trend of changes in gill filament Na^+/K^+-ATPase enzyme activity was similar to that for salinity, but peak ATPase enzyme activity was higher than that in the single-factor salinity experiment. The salinity concentration corresponding to peak ATPase activity was lower than in the single-factor, suggesting that the saline-alkaline interaction has a greater influence on ATPase enzyme activity than salinity alone. At certain concentrations, alkalinity impedes ion exchange in gill tissue exposed to a salt solution. The gill tissue needs to maintain a smooth ion channel; therefore, gill filament ATPase enzyme activity must increase. A similar phenomenon was observed in our experiment; alkalinity stimulus increased mucus secretion from the fish body. Much of the mucus condensed on the surface of the gill filament, directly affecting normal breathing and other gill tissue functions.

4.2. Osmotic Pressure Regulation in Luciobarbus capito. The plasma osmotic pressure of stenohaline marine bony fishes is 370–480 mOsm/kg, but that of stenohaline freshwater bony fishes is 260–330 mOsmol/kg [15]. The plasma osmotic pressure range in *L. capito* is 280–457 mOsm/kg. Thus,

L. capito is considered a euryhaline fish because its plasma osmotic pressure range is between those of marine and freshwater bony fishes. Typically, when a euryhaline bony fish enters high salinity water, osmotic pressure regulation occurs in two stages. First, as a result of passive water loss, the osmotic pressure increases because of a relative increase in plasma ion concentrations. Second, gill filament Na^+/K^+-ATPase enzyme activity increases and the ion discharge mechanism is activated, which causes osmotic pressure to gradually decrease and finally level off [13, 15, 30–32]. Plasma osmotic pressure in *L. capito* initially increased with increasing salinity in the water, as normal, yet it did not gradually decrease and level off. Thus, the change in plasma osmotic pressure in *L. capito* is a response to the external hypertonic environment. Whether this is a unique reaction of this species to saline-alkaline waters requires further study.

Urea nitrogen content in *L. capito* changed under different saline-alkaline concentrations, suggesting that plasma urea also participates in osmotic pressure regulation. However, the regulation of urea to osmotic pressure was only significantly affected by alkalinity and saline-alkaline mixed water. In the single-factor salinity experiment, the regulation of urea to osmotic pressure was lower. Urea is a key factor in maintaining the balance between water and salt in elasmobranchs. When urea content is higher in the blood, the blood osmotic pressure is higher than the surrounding environment and close to isotonic, thus reducing moisture loss [26]. Alkalinity is the limiting factor for aquatic animal survival and growth in saline-alkaline waters; most euryhaline fishes find it difficult to overcome alkalinity putting them at a disadvantage in saline-alkaline waters [33]. Our results show that, in alkaline water environments, urea supplements other ions regulating osmotic pressure, enhances the osmotic regulation ability of *L. capito* in saline-alkaline waters, and thus improves its tolerance for saline-alkaline waters.

5. Conclusions

Luciobarbus capito gill Na^+/K^+-ATPase activity, plasma ion (Na^+, K^+, and Cl^-) concentration, and osmotic pressure were increased at first and then decreased with increasing salinity. *L. capito* plasma K^+ and urea nitrogen concentrations increased with increasing alkalinity. All these concentrations gradually increased with increasing salinity and alkalinity concentrations in the orthogonal experiment.

Competing Interests

The authors declare that they have no competing interests.

Acknowledgments

Financial support for this work was provided by The Central-Level Non-profit Scientific Research Institutes Special Funds (HSY201403), Special Scientific Research Funds for Central Non-profit Institutes, Chinese Academy of Fishery Sciences (2016HY-ZD0602) Harbin Science and Technology Project (2012AA6CN037), and Technology Support Program (2012BAD25B09).

References

[1] L. Q. Liang, B. Ren, Y. M. Chang, R. Tang, and L. M. Zhang, "Inland brackish (alkaline-saline) water resources and fisheries utilization in China," *Chinese Fisheries Economics*, vol. 31, no. 3, pp. 138–145, 2013.

[2] H. Wang, Q. F. Lai, and Z. L. Yao, *100 Questions about Aquatic Cultural Techniques in Saline-Alkaline Land*, China Agriculture Press, Beijing, China, 2010.

[3] C. Mao, N. Zhai, J. Yang et al., "Environmental kuznets curve analysis of the economic development and nonpoint source pollution in the Ningxia Yellow River irrigation districts in China," *BioMed Research International*, vol. 2013, Article ID 267968, 7 pages, 2013.

[4] M. Hasanuzzaman, K. Nahar, M. M. Alam et al., "Potential use of halophytes to remediate saline soils," *BioMed Research International*, vol. 2014, Article ID 589341, 12 pages, 2014.

[5] J. Liu, "Application of the grey prediction model to forecast *Gymnocypris przewalskii* production," *Journal of Dalian Fisheries University*, vol. 21, no. 4, pp. 390–393, 2006.

[6] Y. P. Han, "Analysis of the status of fishery resources survey in Dali Lake," *Inner Mongolia Conservancy*, no. 1, pp. 45–46, 2007.

[7] D. F. Lin and Q. H. Cai, "Comparison of fish fauna structure and main economic fish growth among different saline and alkaline waters," *Acta Hydrobiologica Sinica*, vol. 24, pp. 493–501, 2000.

[8] X. Z. Liao, F. S. Lin, and M. C. Tian, *The Taxonomy of Fishes*, Higher Education Press, Beijing, China, 1958.

[9] N. B. Caberoy and G. F. Quinitio, "Changes in Na^+,K^+-ATPase activity and gill chloride cell morphology in the grouper *Epinephelus coioides* larvae and juveniles in response to salinity and temperature," *Fish Physiology & Biochemistry*, vol. 23, no. 1, pp. 83–94, 2000.

[10] P. Sreejith, R. S. Beyo, G. Prasad, F. Sunny, and O. V. Oommen, "Thyroid status alters gill ionic metabolism and chloride cell morphology as evidenced by scanning electron microscopy in a teleost *Anabas testudineus* (Bloch): short and long term *in vivo* study," *Indian Journal of Experimental Biology*, vol. 45, no. 12, pp. 1015–1021, 2007.

[11] D. H. Evans, P. M. Piermarini, and K. P. Choe, "The multifunctional fish gill: dominant site of gas exchange, osmoregulation, acid-base regulation, and excretion of nitrogenous waste," *Physiological Reviews*, vol. 85, no. 1, pp. 97–177, 2005.

[12] B. Kulac, G. Atli, and M. Canli, "Response of ATPases in the osmoregulatory tissues of freshwater fish *Oreochromis niloticus* exposed to copper in increased salinity," *Fish Physiology & Biochemistry*, vol. 39, no. 2, pp. 391–401, 2013.

[13] F. Zhao, P. Zhuang, and L. Z. Zhang, "The influence of salinity acclimation on activity of Na^+/K^+-ATPase in branchial epithelium, concentration of ions and osmolarity in serum of *Acipenser schrenckii*," *Journal of Fisheries of China*, vol. 30, no. 4, pp. 444–449, 2006.

[14] X. H. Wang, Y. H. Lin, and Q. L. Jiang, "Effects of NaCl on concntration of serum ions, cortisol and activities of Na^+/K^+-ATPase on tissue in *Chalcalburnus chalcoides aralensis*," *Journal of Jilin Agricultural University*, vol. 29, no. 5, pp. 576–580, 2007.

[15] L. W. Xu, G. F. Liu, R. X. Wang, Y. L. Su, and Z. X. Guo, "Effects of abrupt salinity stress on osmoregulation of juvenile *Rachycentron canadum*," *Chinese Journal of Applied Ecology*, vol. 18, no. 7, pp. 1596–1600, 2007.

[16] F. Y. Yang, X. J. Li, C. S. Zhao, and Y. Chen, "Prawn adaptability to saline-alkali soda lakes of northeast China," *Chinese Journal of Eco-Agriculture*, vol. 15, no. 5, pp. 115–119, 2007.

[17] Q. L. Jiang, Y. H. Lin, X. H. Wang, and B. Liu, "Effect of $NaHCO_3$ on growth and osmoregulation of *Chalcalbumus chalcoides aralensis*," *Journal of Jilin Agricultural University*, vol. 30, no. 1, pp. 106–110, 2008.

[18] C.-Q. Liu, J.-X. Wang, Y.-J. Zhang, and L.-J. Liu, "Effects of salinity and Na^+/K^+ in percolating water from saline-alkali soil on the growth of Litopenaeus vannamei," *Chinese Journal of Applied Ecology*, vol. 19, no. 6, pp. 1337–1342, 2008.

[19] Y. K. Ip, C. G. L. Lee, W. P. Low, and T. J. Lam, "Osmoregulation in the mudskipper, *Boleophthalmus boddaerti* I. Responses of branchial cation activated and anion stimulated adenosine triphosphatases to changes in salinity," *Fish Physiology & Biochemistry*, vol. 9, no. 1, pp. 63–68, 1991.

[20] S. Thomas and J. Poupin, "A study of the effects of water carbonate alkalinity on some parameters of blood acid-base status in rainbow trout (*Salmo gairdneri* R.)," *Journal of Comparative Physiology B*, vol. 156, no. 1, pp. 29–34, 1985.

[21] C. M. Wood, H. L. Bergman, A. Bianchini et al., "Transepithelial potential in the Magadi tilapia, a fish living in extreme alkalinity," *Journal of Comparative Physiology B: Biochemical, Systemic, and Environmental Physiology*, vol. 182, no. 2, pp. 247–258, 2012.

[22] F. Lü, L. Pan, A. Wang, and Y. Hu, "Effects of salinity on oxygen consumption rate and ammonia excretion rate of allogynogemetic crucian carp," *Acta Hydrobiologica Sinica*, vol. 34, no. 1, pp. 184–189, 2010.

[23] M. M. Bradford, "A rapid and sensitive method for the quantitation of microgram quantities of protein utilizing the principle of protein-dye binding," *Analytical Biochemistry*, vol. 72, no. 1-2, pp. 248–254, 1976.

[24] J. K. Foskett and C. Scheffey, "The chloride cell: definitive identification as the salt-secretory cell in teleosts," *Science*, vol. 215, no. 4529, pp. 164–166, 1982.

[25] K. J. Karnaky Jr., "Structure and function of the chloride cell of *Fundulus heteroclitus* and other teleosts," *Integrative & Comparative Biology*, vol. 26, no. 1, pp. 209–224, 2015.

[26] H. R. Lin, *Fish Physiology*, Guangdong Higher Education Press, Guangzhou, China, 2002.

[27] J. M. Mancera and S. D. McCormick, "Rapid activation of gill Na^+,K^+-ATPase in the euryhaline teleost *Fundulus heteroclitus*," *Journal of Experimental Zoology*, vol. 287, no. 4, pp. 263–274, 2000.

[28] C. K. Tipsmark, S. S. Madsen, M. Seidelin, A. S. Christensen, C. P. Cutler, and G. Cramb, "Dynamics of Na^+,K^+,$2Cl^-$ cotransporter and Na^+,K^+-ATPase expression in the branchial epithelium of brown trout (*Salmo trutta*) and Atlantic salmon (*Salmo salar*)," *Journal of Experimental Zoology*, vol. 293, no. 2, pp. 106–118, 2002.

[29] Y. M. Lin, C. N. Chen, and T. H. Lee, "The expression of gill Na^+, K^+-ATPase in milkfish, *Chanos chanos*, acclimated to seawater, brackish water and fresh water," *Comparative Biochemistry and Physiology—A Molecular and Integrative Physiology*, vol. 135, no. 3, pp. 489–497, 2003.

[30] C. M. Wood and W. S. Marshall, "Ion balance, acid-base regulation, and chloride cell function in the common killifish, *Fundulus heteroclitus*-a euryhaline estuarine teleost," *Estuaries & Coasts*, vol. 17, no. 1, pp. 34–52, 1994.

[31] G. T. O. LeBreton and F. W. H. Beamish, "The influence of salinity on ionic concentrations and osmolarity of blood serum in lake sturgeon, *Acipenser fulvescens*," *Environmental Biology of Fishes*, vol. 52, no. 4, pp. 477–482, 1998.

[32] X. He, P. Zhuang, L. Zhang, and C. Xie, "Osmoregulation in juvenile Chinese sturgeon (*Acipenser sinensis* Gray) during brackish water adaptation," *Fish Physiology & Biochemistry*, vol. 35, no. 2, pp. 223–230, 2009.

[33] H. G. Fu, "The opinion on our province saline alkali waters in inland fishery utilization," *Hebei Fishery*, vol. 4, p. 12, 2002.

Hindawi Publishing Corporation
BioMed Research International
Volume 2016, Article ID 7040872, 8 pages
http://dx.doi.org/10.1155/2016/7040872

Research Article

Migration of BTEX and Biodegradation in Shallow Underground Water through Fuel Leak Simulation

Yaping Cheng,[1,2] Yudao Chen,[1,2] Yaping Jiang,[1,2] Lingzhi Jiang,[1] Liqun Sun,[1] Liuyue Li,[1] and Junyu Huang[1]

[1] *College of Environmental Science and Engineering, Guilin University of Technology, Guilin 541004, China*
[2] *Guangxi Scientific Experiment Center of Mining, Metallurgy and Environment, Guilin University of Technology, Guilin 541004, China*

Correspondence should be addressed to Yudao Chen; cyd0056@vip.sina.com

Received 22 July 2016; Accepted 19 September 2016

Academic Editor: Ping Li

To provide more reasonable references for remedying underground water, fuel leak was simulated by establishing an experimental model of a porous-aquifer sand tank with the same size as that of the actual tank and by monitoring the underground water. In the tank, traditional gasoline and ethyl alcohol gasoline were poured. This study was conducted to achieve better understanding of the migration and distribution of benzene, toluene, ethyl benzene, and xylene (BTEX), which are major pollutants in the underground water. Experimental results showed that, compared with conventional gasoline, the content peak of BTEX in the mixture of ethyl alcohol gasoline appeared later; BTEX migrated along the water flow direction horizontally and presented different pollution halos; BTEX also exhibited the highest content level at 45 cm depth; however, its content declined at the 30 and 15 cm depths vertically because of the vertical dispersion effect; the rise of underground water level increased the BTEX content, and the attenuation of BTEX content in underground water was related to the biodegradation in the sand tank, which mainly included biodegradation with oxygen, nitrate, and sulfate.

1. Introduction

With the development of the oil industry, petroleum leakage during petroleum use, transport, and storage has resulted in serious water pollution from fuel hydrocarbon, which became a substantial threat to underground water safety [1]. At the beginning of 1990s, 90,000 out of 2 million underground gasoline tanks were found with leaks in the United States [2, 3]. According to statistics, 70% of underground gasoline tanks with service lives of over 15 years are more likely to leak [4] and filling stations are potential pollution source of organic pollution. This concern has then become a global problem [5, 6]. Benzene, toluene, ethyl benzene, and xylene (BTEX) are prime contaminants that have attracted wide attention because of their high water solubility and toxicity. BTEX can cause cancers, mucosal pain, blood diseases, damage to the central nervous and respiratory systems, and liver and kidney functional impairment [7, 8]. Six benzene series including BTEX were placed on the top blacklist of pollutants for priority control in China [9]. In China, underground water pollution derived from petroleum use and other activities is also fairly common. For example, BTEX was detected in the shallow groundwater of Yangtze River Delta [10] and benzene series was discovered in Taihu Lake Basin [11], Nanyang Oilfield, Liulin Spring in Shanxi [12], and the Shuanghe River and Weigang water sources near Henan Oilfield [13].

A porous-aquifer sand tank with similar size as that of the actual tank was constructed in our laboratory for simulation experiments on fuel leakage after traditional petroleum and ethanol gasoline pouring. The underground water was monitored for a long period to determine the migration features of BTEX in underground water and to provide the literature for pollution control and water recovery.

2. Materials and Methods

2.1. Sand Tank Model. The constructed sand tank (Figure 1) was 5.8 m long in a brick-concrete structure with antiseepage.

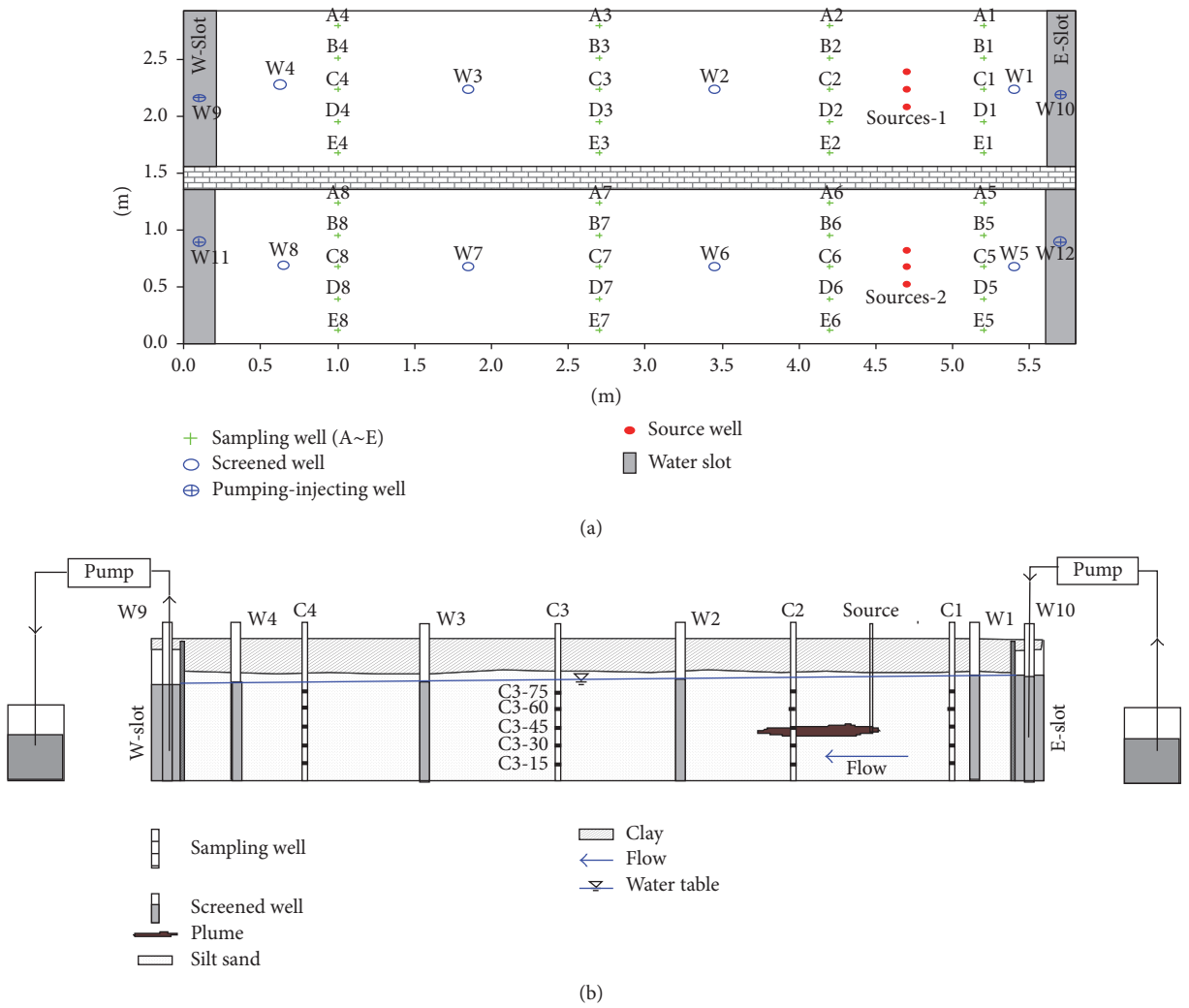

Figure 1: Experimental plan view and cross-sectional view of the sand tank.

The tank included two narrow-slit water sinks of 0.25 m length on two ends and a 5.3 m long porous aquifer. The tank was 2.9 m wide. For comparative analysis, the tank was divided into two parts by a 0.2 m thick wall, and the porous aquifers on the north and south ends were 1.36 m in width. The diameter of the pure fine sands in this tank ranged from 0.25 mm to 0.05 mm. Oil orifices, specifically multilayered (five layers of 15, 30, 45, 60, and 75 cm heights, resp.) sampling observation holes and a water-level observation hole, were designed.

2.2. Experimental Setup. This experiment was performed on July 13, 2015. The water level was 50 cm when the fuel was poured through orifices sw-1 and sw-2. A hose was placed in the tank and the hose's bottom altitude was 45 cm, which corresponded to the level of the 45 cm layered sample tap. Before the experiment was commenced, the average background concentrations of the constituents in the tank were 4.2 mg/L nitrate, 14.3 mg/L sulfate, 4.0 mg/L chloridion, 1.5 mg/L acetate, and 4.1 mg/L dissolved oxygen, at pH 7.6 and 25.9°C. To stimulate the underground water flow, water was directed to flow in from the east side and flow out from the west side at an initial constant flow of 30 mL/min and an average hydraulic slope of around 0.0013. Furthermore, the pumping-filling cyclic experiment was performed, when the porosity was 0.3 at a speed of 30 mL/min and Darcy's underground water velocity of 0.07 m/d (actual flow is 0.24 m/d). After MODFLOW simulation, the seepage was observed as a one-dimensional horizontal flow. To determine the migration and distribution features of gasoline and ethanol gasoline in underground water, we poured 3 L traditional gasoline through sw-1 (northern part) and 3 L 10% ethanol gasoline in sw-2 (southern part) at the speed of transfusion (about 500 mL/h). Meanwhile, 1 L of the 500 mg/L KBr solution was filled in two parts as tracer agent. To maintain their synchronization, the speed of the poured KBr solution was 1/3 that of the poured gasoline.

2.3. Sampling and Analysis. Fifteen milliliters of water was sampled from each sample hole with injectors, and 0.5 mL

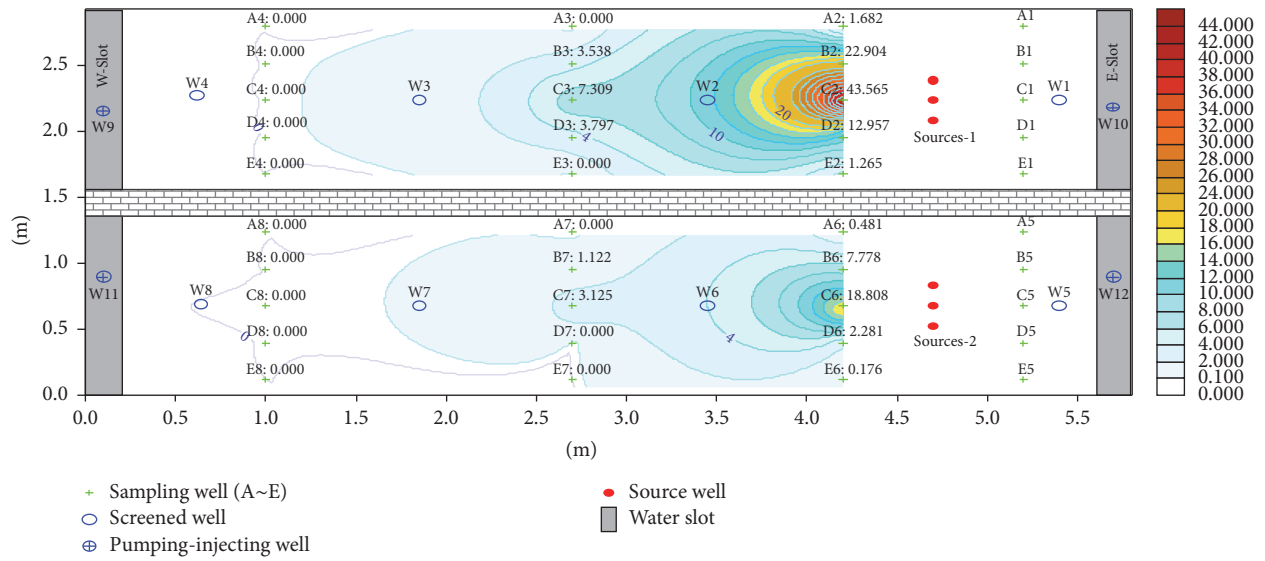

Figure 2: Distribution of BTEX pollution halo on the 30th day.

mercuric chloride (800 mg/L) was used for sterilization. Five milliliters of water was placed in a headspace bottle sealed by an aluminium cap for ethyl alcohol and BTEX determination. Meanwhile, 10 mL water was placed in a Dionex alumina injector for the analysis of acetic acid, nitrate, nitrite, sulfate, and bromide ion. The interval of the large-volume sampling was 15–30 days.

Ethyl alcohol and BTEX compounds were tested through a gas chromatograph (agilent 6890N) with a flame ionization detector. The chromatographic conditions were as follows: column temperature, 50°C (5 min), at rates of 20 and 150°C/min; injection port-temperature 200°C; detector temperature, 250°C; flow rate of carrier nitrogen, 1.0 mL/min; headspace bottle temperature, 60°C; equilibrium time, 10 min; frisking time, 5 min; clamping time, 0.13 min; injecting time, 1 min; lower limit of ethyl alcohol detection, 0.1 mg/L; and limit of BTEX detection, 0.002 mg/L.

Acetic acid, nitrate, nitrite, sulfate, and bromide ion were measured through an ion chromatograph (Dionex ICS-1000); the detection limit was 0.1 mg/L. The chromatographic conditions were column temperature, 30°C; tank temperature, 35°C; suppressor type-ASRS-4MM, SRS current, 50 mA; leachate flow rate (3.5 mmol Na_2CO_3 and 1 mmol $NaHCO_3$), 1.20 mL/min; and sample size, 25 μL.

Dissolved oxygen, pH, and water temperature were measured in site through water-level observation holes (w1–w10) using electrodes matching the multifunctional water quality analyzer made in Italy (HANAA, HI9804D).

3. Results and Discussion

3.1. Distribution Law of BTEX Pollution Halo. Fuel was filled at 45 cm depth; the BTEX content in the tank at this height corresponded to the highest value and dropped at 30 and 15 cm from the monitoring results. The distribution of the BTEX pollution halo in the tank during the first 71 days is shown in Figures 2, 3, and 4.

Figures 2–4 reveal that the BTEX contents at C2-45 in the north tank on the 30th, 56th, and 71th days are 43.565, 31.277, and 20.250 mg/L, respectively, and the content reaches the peak during 30–60 days and declined afterwards. In the south tank where ethanol gasoline was filled, the contents at C6-45 on the 30th, 56th, and 71th days were 18.808, 33.921, and 28.894 mg/L, respectively. Because of ethyl alcohol [14], the pollution halo is small in this tank and the content peak lags behind. However, with time progression, the pollution halo shrank inward because of volatilization [15–17], adsorption [18, 19], and biodegradation [20–22]. As a result, BTEX content diminished.

In the first 78 days, the underground water level remained at 45–50 cm in the sand tank. To simulate the influences of rain on BTEX, we added water in the tank until the 69 cm level was reached. Figure 5 shows the distribution of the BTEX pollution halo on the 118th day, from which the BTEX content clearly rose, especially in the south tank, reaching as high as 79.41 mg/L. This result indicates that the rise of water level after rainfall achieved fuller contact between gasoline near the pollution source and underground water. Consequently, a great amount of BTEX dissolved in the water. The increased pollutants content deteriorated the underground water quality.

3.2. Longitudinal Distribution Law of BTEX. Water sample monitoring results show that, at the same depth, the BTEX content on the C row of central axis was the highest and decreased along two sides, at the order of C > B > A and C > D > E. The longitudinal monitoring results of the BTEX pollutant concentration on the C row at 45 cm depth are shown in Figure 6.

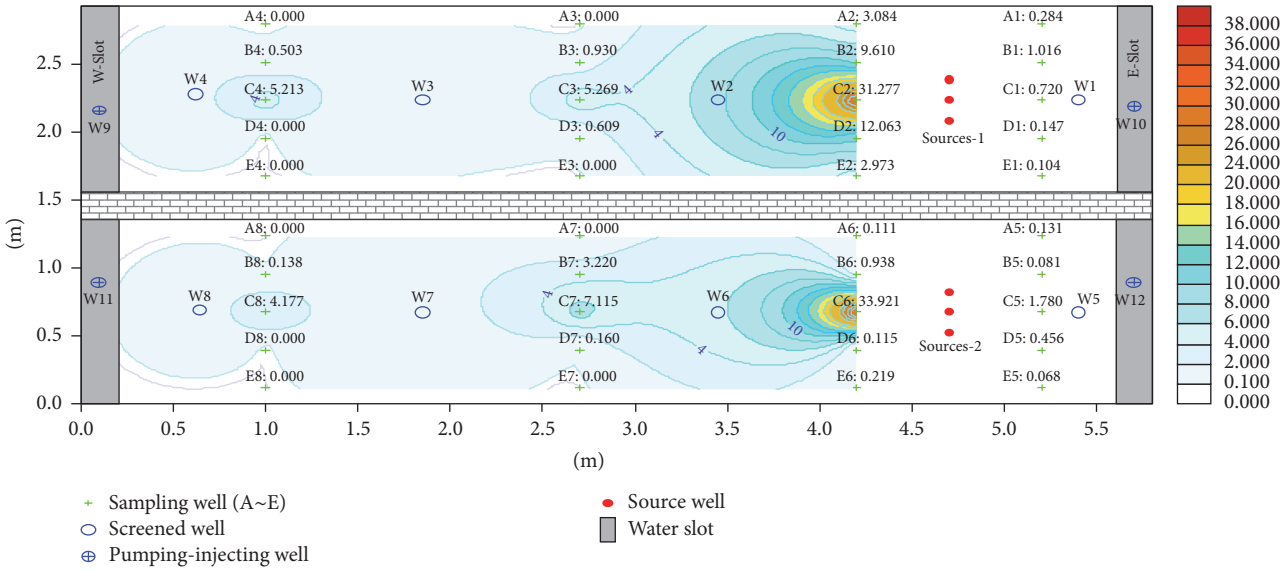

Figure 3: Distribution of BTEX pollution halo on the 56th day.

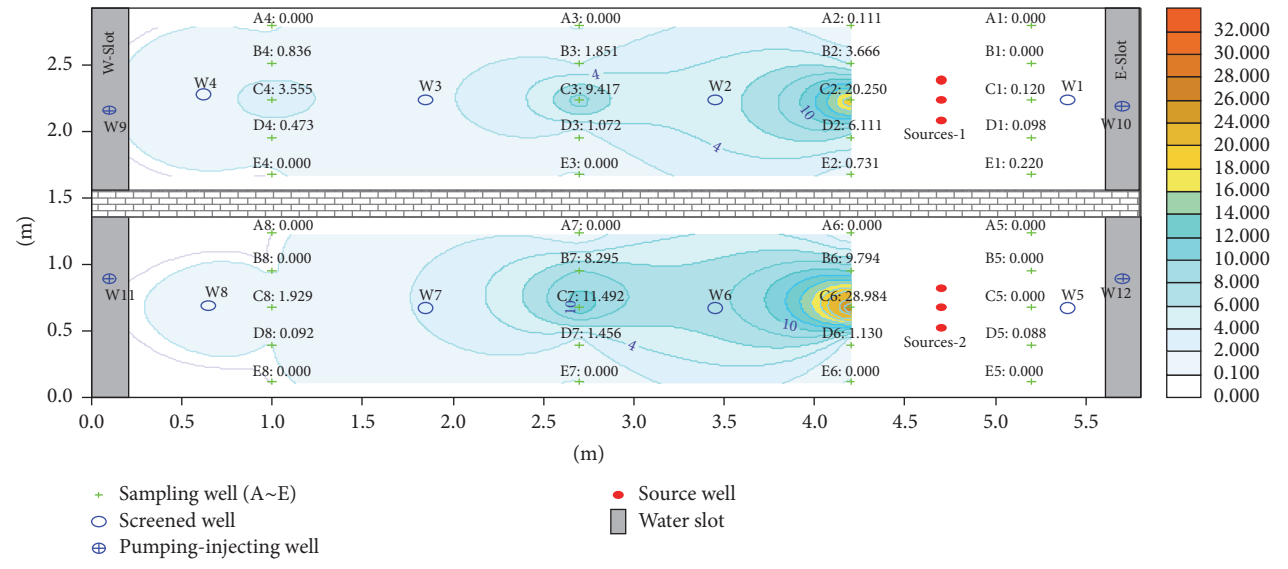

Figure 4: Distribution of BTEX pollution halo on the 71th day.

Figure 6 reveals that BTEX was detected but with the lowest content upstream of pollution sources C1 and C5, where the pollutants mainly originated from the dispersion. By contrast, particularly downstream, the contents at the same height dropped (C2 > C3 > C4 and C6 > C7 > C8) because of the underground water flow.

3.3. Vertical Distribution Law of BTEX. The vertical migration and distribution of BTEX on each row were almost identical between the north (traditional gasoline) and the south (ethanol gasoline) tanks. At the C row, the content was highest but declined along two sides. For instance, in C2 of the north tank and C6 of the south tank, the vertical monitoring results of the BTEX pollutant concentration at the depths 15, 30, and 45 cm are shown in Figure 7.

Figure 7 shows that, in either tank, the BTEX content was the highest at the 45 cm depth, followed by the 30 and 15 cm depths. 78 days after adding water, the content at 45 cm depth rose more rapidly than those at the 30 and 15 cm levels, which only changed slightly. The density of BTEX is lower than that of water; hence, downward vertical migration was rarely observed, and BTEX contents were found at lower water levels.

3.4. Declining Features of BTEX by Biodegradation. Biodegradation is a major mechanism of destructive declination which

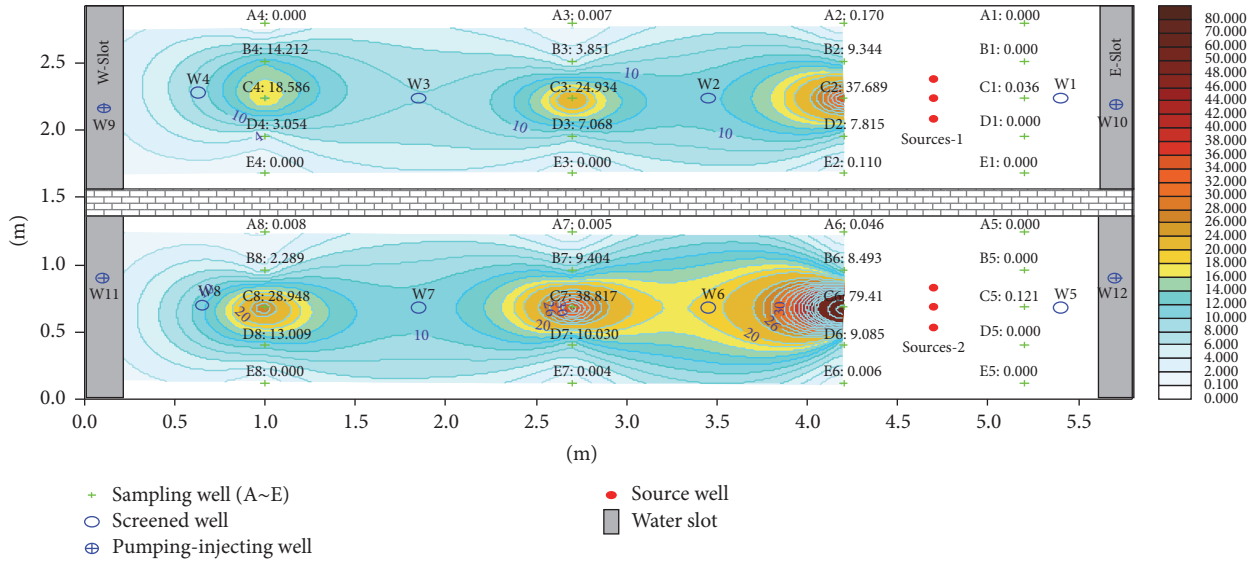

Figure 5: Distribution of BTEX pollution halo on the 118th day.

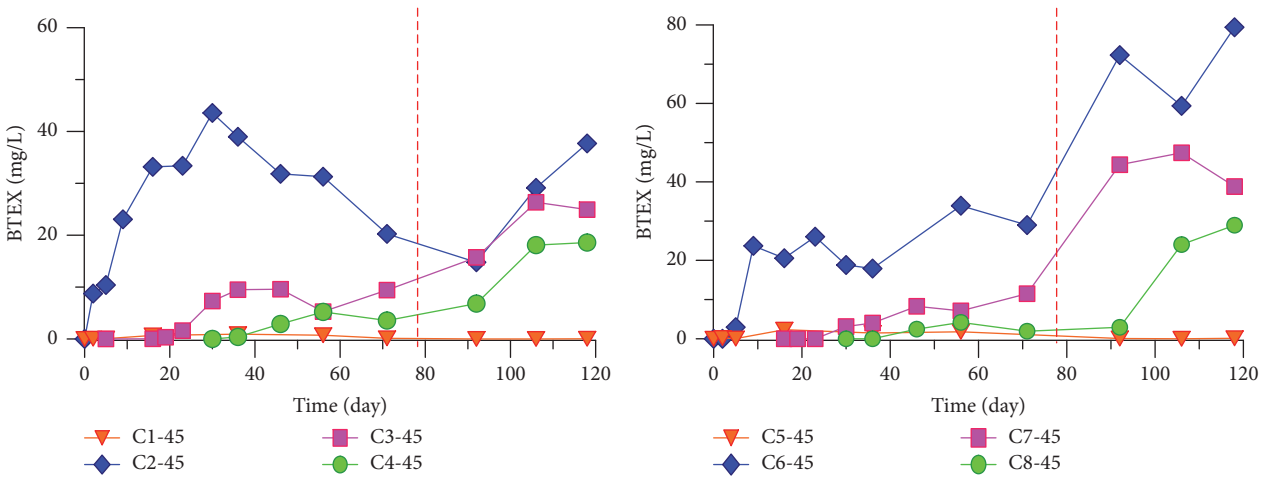

Figure 6: Longitudinal monitoring results of BTEX pollutant concentration on C row at the same depth.

can essentially remove pollutants by transforming pollutants in aquifers from macromolecules into small molecules or converting toxic compounds into nontoxic substances. Degradation is classified based on electron acceptor type; the respiratory action of a microorganism is called "aerobic degradation" when oxygen is used as the electron acceptor; "anaerobic degradation" for nitrate, ferric ion, sulfate, or carbon dioxide; and "facultative degradation" for dissolved oxygen and nitrate.

Microbial activity is active and common in an underground environment, including those of simple microorganisms, such as prokaryotic bacteria and cyanobacteria, as well as complicated eukaryotic algae, fungi, and prokaryotes. Since the 1970s, 28 kinds of bacteria and fungi capable of degrading hydrocarbon were extracted from the underground environment [23]. In aerobic conditions, almost all of the oil-hydrocarbon can be degraded by organisms [24]. In the underground water which is seriously short of dissolved oxygen, microorganisms can degrade petroleum hydrocarbon through electron acceptors, such as nitrate, ferric irons, and sulfate, resulting in reduction reactions.

3.4.1. Changes of Dissolved Oxygen. The dissolved oxygen in each sample was detected. In the first 92 days, the injector (early stage) and peristaltic pump (middle stage) were used in sampling. Hence, aeration occurred in the water sample. As a result, the detected values were higher than the actual levels and did not reflect the real situation. After 92 days, dissolved oxygen was detected through a probe from the water-level monitoring hole. The results are shown in Table 1.

The background value of dissolved oxygen at each hole was 3–5 mg/L. After gasoline was poured, the content

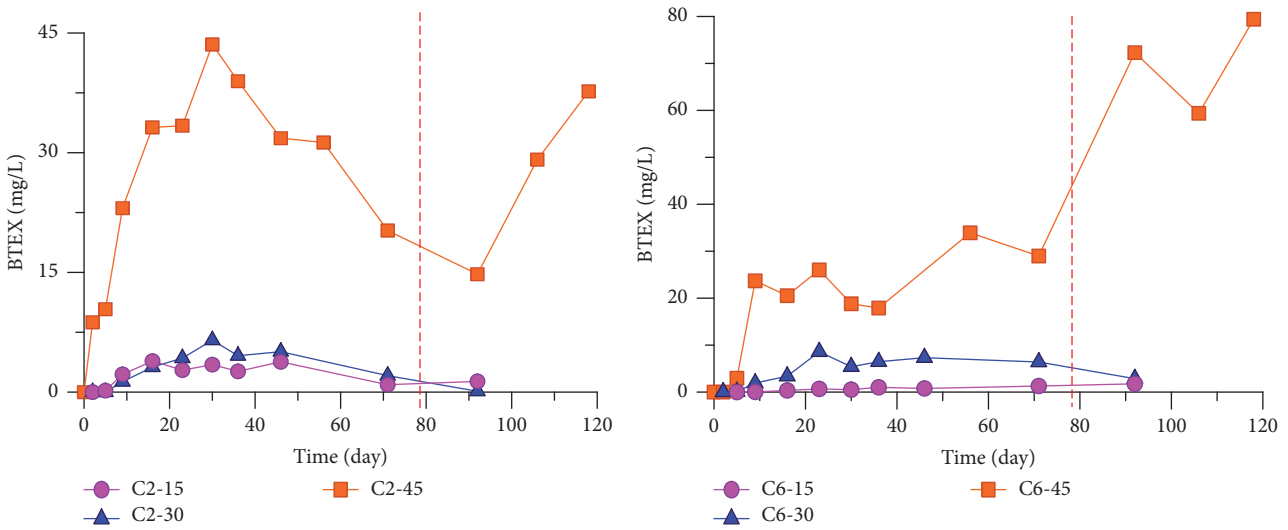

Figure 7: Vertical monitoring results of BTEX pollutant concentration on C2 and C6 in the sand tank.

Table 1: The monitoring results of dissolved oxygen concentration in the water level monitoring hole of sand tank (mg/L).

Time (day)	W1	W2	W3	W4	W5	W6	W7	W8
92	6.43	0.23	0.2	0.17	7.19	0.33	0.06	0.13
106	6.98	0.23	0.24	0.72	6.73	1.07	0.91	1.06
117	7.61	1.11	0.47	0.5	7.92	1.43	0.78	0.32
142	8.0	1.0	0.5	0.3	8.1	0.8	0.4	0.3

increased upstream the pollution source (water continued flowing in), but the dissolved oxygen was almost consumed downstream. This observation indicates that biodegradation with oxygen took place in the tank and some BTEX was degraded [25–27].

3.4.2. Changes of NO_3^-, SO_4^{2-}, and NO_2^- Contents. The fuel was filled to the 45 cm level; hence, the BTEX content at this point was the highest, whereas the contents of NO_3^- and SO_4^{2-} were basically the same. The concentration monitoring results from C2-45 and C6-45 are displayed in Figure 8.

Figure 8 shows that the contents of NO_3^- and NO_2^- at C2-45 and C6-45 are much lower, approximately 0, implying that biodegradation with nitrate occurred in the tank when NO_3^- was degraded as the electron acceptor. When the dissolved oxygen was nearly consumed, some anaerobes can replace O_2 with NO_3^- to serve as the final electron acceptor for later hydrocarbon degradation [25–27]. The content of SO_4^{2-} was elevated initially but fluctuated slightly after filling with water close to the background value. The content then began to drop on the 91st day to 0 on the 118th day. This observation implies that oxidation-reduction environment changed from oxidation to a reduction environment, when biodegradation with sulfate ensured. When some electron acceptor with strong oxidizability is consumed, SO_4^2 serves as the electron acceptor in the hydrocarbon degradation of contaminants by anaerobes. For these reasons, BTEX is degraded [25–27].

4. Conclusions

The BTEX content near the injection point was the highest. The lateral dispersion of the BTEX pollution halo laterally extended continuously. Longitudinally, the BTEX pollution migrated downstream mainly because of the water flow and longitudinal dispersion. Given the slight vertical dispersion, BTEX content reached the highest level at the 45 cm depth but dropped successively at the 30 and 15 cm depths. Meanwhile, effect of ethyl alcohol caused the concentration peak of BTEX in ethanol gasoline in the underground water to lag behind that of tradition gasoline.

When the underground water level rose, the BTEX content at 45 cm increased more rapidly than those at 30 and 15 cm, which changed only slightly. The density of BTEX is lower than that of water; hence, vertical migration downward was rarely observed, and lower contents were found at lower water levels.

The geochemical characteristics of the underground water environment revealed that downstream the pollution source, the concentration of dissolved oxygen and NO_3^- decreased more rapidly, whereas the concentration of SO_4^{2-} changed slightly initially and then decreased slowly. This observation indicated that oxidation, denitrification, and desulfurization took place. The fall of the BTEX content in the underground water was related to many kinds of biodegradations, such as biodegradation with oxygen, nitrate,

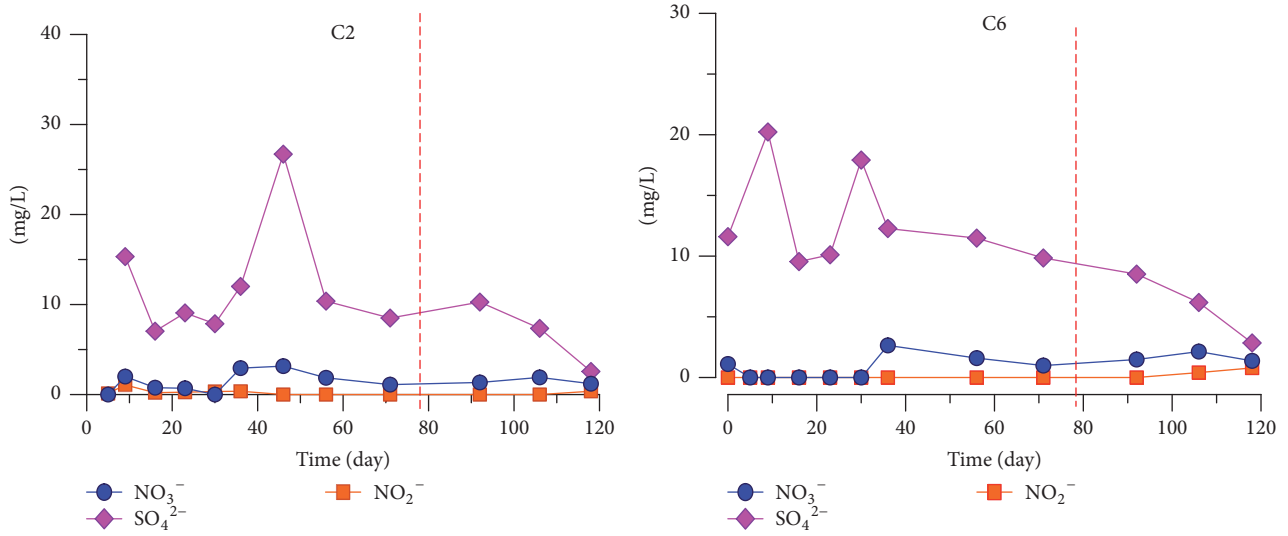

Figure 8: Monitoring results of electron acceptors on C2 and C6 at the 45 cm depth in the sand tank.

and sulfate. Thus, alleviating BTEX pollution in underground water by increasing the concentrations of electric acceptors, such as nitrate, and by enhancing microbial activities is an effective and noteworthy method.

Competing Interests

The authors declare that they have no competing interests.

Acknowledgments

The authors gratefully acknowledge the financial support of the National Natural Science Foundation of China [NSFC41362012 and 41172229] and the research funds of the Guangxi Key Laboratory of Theory and Technology for Environmental Pollution Control [GuiKeNeng1401Z003].

References

[1] R.-F. Liu, H.-H. Chen, Y.-L. Wang, and F. Liu, "Ways of groundwater pollution by oil in an oilfield," *Geology in China*, vol. 34, no. 1, pp. 153–159, 2007.

[2] Environmental Protection Agency. Public Housing, Proposed notification requirements for owners of underground storage tanks: U.S.,UST1-1-SB-001.07/02/85, Spatial Distribution of Characteristic Pollutants at a Gas Station in Shallow Groundwater Area_Yang Qing.caj356774.

[3] J. W. Weaver, J. Lewis, and B. H. Daniel, "Predicted ground water, soil and soil gas impacts from US gasoline (2004): first analysis of the autumnal data," Tech. Rep. EPA/600/R-05/032, United States Environmental Protection Agency, Washington, DC, USA, 2005.

[4] H. J. Zuo, W. F. Jin, and J. C. Gao, "An investigation of tank bottom corrosion in Karamay Petroc Hemical Company and its countermeasures," *Journal of Xinjiang Petroleum Institute*, vol. 14, no. 3, pp. 70–73, 2002.

[5] C. M. Kao and J. Prosser, "Evaluation of natural attenuation rate at a gasoline spill site," *Journal of Hazardous Materials*, vol. 82, no. 3, pp. 275–289, 2001.

[6] Q. L. Zhang, "The oil tank in gas station should be standardized quickly," *Oil Depot and Gas Station*, vol. 12, no. 2, pp. 22–24, 2003.

[7] X.-F. Li and Q.-X. Zhou, "Environmental quality standard of BTEX: a review," *Chinese Journal of Ecology*, vol. 30, no. 2, pp. 369–375, 2011.

[8] H. Nourmoradi, M. Nikaeen, and H. Khiadani, "Removal of benzene, toluene, ethylbenzene and xylene (BTEX) from aqueous solutions by montmorillonite modified with nonionic surfactant: equilibrium, kinetic and thermodynamic study," *Chemical Engineering Journal*, vol. 191, pp. 341–348, 2012.

[9] W. M. Zhou, D. Q. Fu, and Z. G. Sun, "Determination of black list of China's priority pollutants in water," *Research of Environmental Sciences*, vol. 4, no. 6, pp. 9–12, 1991.

[10] B. H. Li, H. H. Chen, J. T. He et al., "Characteristics and cause of monocyclic aromatic hydrocarbon contamination in shallow groundwater in an area of the Yangtze River delta," *Geology in China*, vol. 23, no. 5, pp. 1124–1130, 2006.

[11] H. H. Chen, J. T. He, and F. Liu, "Organic contamination characteristics of shallow groundwater in a study area of the Taihu Lake basin," *Geological Bulletin of China*, vol. 24, no. 8, pp. 735–739, 2005.

[12] H. M. Guo and Y. X. Wang, "Remediation of organic contaminants in groundwater state of the art and perspectives," *Geological Science and Technology Information*, no. 19, pp. 69–72, 1999.

[13] Y. M. Wang and J. F. Dang, "Analysis on underground water pollution in oil and gas fields," *Journal of Geological Hazards and Environment Preservation*, vol. 11, no. 3, pp. 271–273, 2000.

[14] Y. Chen, Y. Jiang, Y. Zhu et al., "Fate and transport of ethanol-blended dissolved BTEX hydrocarbons: a quantitative tracing study of a sand tank experiment," *Environmental Earth Sciences*, vol. 70, no. 1, pp. 49–56, 2013.

[15] C. Y. Chiang, J. P. Salanitro, E. Y. Chai, J. D. Colthart, and C. L. Klein, "Aerobic biodegradation of benzene, toluene, and xylene in a sandy aquifer. Data analysis and computer modeling," *Ground Water*, vol. 27, no. 6, pp. 823–834, 1989.

[16] L. Tong, X.-L. Zheng, M. Li, and Z.-F. Hu, "Volatilization behavior of BTEX on different underlying materials," *Environmental Science*, vol. 29, no. 7, pp. 2058–2062, 2008.

[17] Y. Zhao, *Volatilization of BTEX in Underground Environment and the Influence to Air Sparging*, JiLin University, Changchun, China, 2009.

[18] S. W. Chang Chien, C. Y. Chen, J. H. Chang, S. H. Chen, M. C. Wang, and M. R. Mannepalli, "Sorption of toluene by humic acids derived from lake sediment and mountain soil at different pH," *Journal of Hazardous Materials*, vol. 177, no. 1–3, pp. 1068–1076, 2010.

[19] L. Seifi, A. Torabian, H. Kazemian et al., "Kinetic study of BTEX removal using granulated surfactant-modified natural zeolites nanoparticles," *Water, Air, & Soil Pollution*, vol. 219, no. 1–4, pp. 443–457, 2011.

[20] Y. D. Chen, J. L. Liu, J. F. Wu et al., "Hydrochemical identification of biodegradation in the groundwater," *Geological Journal of China Universities*, vol. 5, no. 3, pp. 306–310, 1999.

[21] Y. D. Chen, Y. N. Zhu, Y. P. Jiang et al., "Natural removal and biodegradation of monoaromatic hydrocabons (BTEX) in groundwater contaminated by gasoline: a pilot scale physical model," *Geochimica*, vol. 33, no. 5, pp. 515–520, 2004.

[22] R. Zhou, Y.-S. Zhao, H.-J. Ren et al., "Natural attenuation of BTEX in the underground environment," *Environmental Science*, vol. 30, no. 9, pp. 2804–2808, 2009.

[23] J. S. Davies and D. W. S. Westlake, "Crude oil utilization by fungi," *Canadian Journal of Microbiology*, vol. 25, no. 2, pp. 146–156, 1979.

[24] R. C. Borden, C. A. Gomez, and M. T. Becker, "Natural Bioremediation of a gasoline spill," *Hydrocarbon Bioremediation*, vol. 20, no. 5, pp. 290–295, 1994.

[25] Y. D. Chen and X. Y. Zhu, "Mechanisms of biodegradation of hydrocarbon contaminants in the groundwater in DaWu well field in ZiBo," *Guangxi Geology*, vol. 12, no. 2, pp. 31–34, 1999.

[26] Y. Su, C. Sun, Y. S. Zhao et al., "Spatial changes of redox environment in aquifer contaminated by BTEX," *Journal of Civil, Architectural & Environmental Engineering*, vol. 36, no. 2, pp. 126–130, 2014.

[27] X. Wang, D. Qu, S. Zhao, Y. Su, Y. Tao, and R. Zhou, "Anaerobic biogeochemical process in BTEX contaminated aquifer," *Journal of Central South University*, vol. 44, no. 6, pp. 2617–2622, 2013.

Hindawi Publishing Corporation
BioMed Research International
Volume 2016, Article ID 4016402, 11 pages
http://dx.doi.org/10.1155/2016/4016402

Research Article

Developmental Toxicity of Carbon Quantum Dots to the Embryos/Larvae of Rare Minnow (*Gobiocypris rarus*)

Yuan-Yuan Xiao, Li Liu, Yao Chen, Yu-Lian Zeng, Ming-Zhi Liu, and Li Jin

Key Laboratory of Freshwater Fish Reproduction and Development, Key Laboratory of Aquatic Science of Chongqing, School of Life Sciences, Southwest University, Ministry of Education, Chongqing 400715, China

Correspondence should be addressed to Li Jin; jinll@swu.edu.cn

Received 15 July 2016; Accepted 20 September 2016

Academic Editor: Kaiyu He

The toxic effects of CDs on rare minnow (*Gobiocypris rarus*) embryos at different developmental stages were investigated. The results showed that rare minnow embryos had decreased spontaneous movements, body length, increased heart rate, pericardial edema, yolk sac edema, tail/spinal curvature, various morphological malformations, and decreased hatching rate. Biochemical analysis showed the CDs exposure significantly inhibited the activity of Na^+/K^+-ATPase and Ca^{2+}-ATPase and increased the MDA contents and the activity of SOD, CAT, and GPX. Further examination suggested that the CDs exposure induced serious embryonic cellular DNA damage. Moreover, the CDs exposure induced upregulation of development related genes (*Wnt8a* and *Mstn*) along with the downregulation of *Vezf1*. Overall, the present study revealed that the CDs exposure has significant development toxicity on rare minnow embryos/larvae. Mechanistically, this toxicity might result from the pressure of induced oxidative stress coordinate with the dysregulated development related gene expression mediated by the CDs exposure.

1. Introduction

Carbon quantum dots (CDs) denote a class of less than 10 nm sized nanoparticles composed of carbon, hydrogen, oxygen, nitrogen, and other elements [1]. Bearing the advantage as higher thermostability, photostability, quantum yield, and lower release rate of heavy metal ions than the traditional semiconductor quantum dots [2], CDs have been proposed broadly to the potential application in analytical chemistry, biological probing and imaging, drug delivery, and so forth [3–5]. Further, with the advent of nanotechnology, CDs are becoming more prevalent in the environment. This raises increasing public concerns about biosafety and the potential health risks of long term exposure to CDs. Previous study has shown that concentration of the TiO_2 in surface waters is 21 ng/L and the C_{60} in sewage is 4 ng/L, which could increase to 35 mg/L through the suspension process in the natural water system [6]. Further, a series of studies has shown the nanomaterials including CdSe/ZnS and TiO_2 could induce the fishes embryos' developmental defect such as embryonic pericardial edema, yolk sac edema, and tail malformation [7], suggesting the potential risky impact of CDs on the natural water ecosystem. Thus, the biological and environmental toxicity of CDs gradually attracted great research interest which is required for the safety evaluation for further application.

However, only limited studies regarding this issue have been reported while the comprehensive toxic effects and the exact underlying mechanism are still not clear. In 16 HBE cells, high concentration of CDs treatment results in oxidative damage and decreased proliferation rate. Besides, CDs could form a complex with BSA leading to the structural alteration of some functional proteins [8]. In animal models, when CDs were administrated through the tail vein injection in rats, the oxidative damage and the disrupted immunologic balance were observed in the target organs which eventually induced the compensable pathological lesions [9].

Here we report a biosafety research of CDs on rare minnow (*Gobiocypris rarus*), an endemic cyprinid fish in China [10]. With serious features such as short life cycle, high fertilization rates, and hatching rates, rare minnow has

Table 1: Primers sequences used for real-time PCR.

Gene	Forward primers	Reverse primers
β-Actin	CCCCATTGAGCACGGTATTG	GGGAGCCTCTGTGAGCAGGA
Wnt8a	CCAAAGGCTTACCTCACA	AACCCAACCACGACCC
Vezf1	GTGGCGGGCATCCTCACCAC	GCCGCACATCTCACAGCCGT
Mstn	CACCGCCTTTGCAACAACTT	CCGATCTACTTGAACGATGG

been regarded as one of the suitable aquatic organisms for the biological toxicity assessment [11].

In our study, we have investigated the developmental toxicity of the CDs on the embryos/larvae of rare minnow. Our data would not only enrich the scientific understanding for the biocompatibility and risk assessment of CDs, but also promote the early diagnosis of potential pollution in fishery water area introduced by nanomaterials.

2. Materials and Methods

2.1. CDs. CDs (W-900-440) were purchased from Beida Jubang Science & Technology Co. Ltd. (Beijing, China). Monodispersed CDs were 2–6 nm sized and prepared as 10 mg/mL (water solution). The fluorescence emission wavelength of the CDs is 440 nm.

2.2. Fish Husbandry and Embryo Collection. Sexually matured and healthy rare minnow were selected as parent fish. Following long term acclimation (more than 4 weeks) in the circulating water system with the sex ratio as 1 : 1, the spawning time points were set to 20:00 daily through the circadian rhythm manipulation. Once the sexual chasing behavior of the parent fishes was observed, the fertilized eggs were collected followed by artificial insemination (fertilization rate > 95%). The parent fishes were fed three times daily to visual satiation (twice with commercial granular food and once with fairy shrimp). Culture condition was set as 25 ± 1°C with the daily photoperiod cycle as 12 : 12 (light : dark).

2.3. Embryo Toxicity Assay. The toxicity assay was designed according to the established protocol [12]. Briefly, the rare minnow embryos were collected immediately after fertilization; at blastocyst stage, normal embryos were selected and introduced individually into 24-well plates filled with 1 mL/well daily renewed solutions or controls per well. The plates were incubated at 25 ± 1°C in water bath for 96 h with the photoperiod of 12 : 12 h (light : dark). The toxicity effects of CDs on the subsequent embryonic development of rare minnow were evaluated by exposing fertilized eggs to a range of concentrations (0, 1, 5, 10, 20, 40, and 80 mg/L). The standard dilution solution served as the control. Three wells for concentration groups and three replicates were set for the tests, with 20 embryos per replicate. In our study, embryos/larvae from the five early embryonic development stages (12 hpf, 24 hpf, 48 hpf, 72 hpf, and 96 hpf) were sampled and analyzed.

2.4. Microexamination. The developmental parameters were monitored and documented every six hours between 12 hpf (hours after fertilization) and 96 hpf. Toxicological endpoints were determined by the observation through microscopy (Nikon SMZ 25, Japan). Between 12 hpf and 96 hpf stage, the hatching rate, the mortality rate, and the malformation rate were calculated. The spontaneous movement frequency at 36 hpf stage and the heart rate at 60 hpf stage were calculated, respectively, as well. The body length (mm), the area of pericardial edema (μm^2), area of sac-yolk edema (μm^2), and SV-BA distance (μm) at 96 hpf stage were photographed with a digital camera and measured from these digital images using Image pro plus 6.0 software (Media Cybernetics, America).

2.5. Measurement of Antioxidant Enzymes, Na^+/K^+-ATPase, Ca^{2+}-ATPase Activity, and Malondialdehyde (MDA) Content. 20 embryos/larvae were collected from each group. Each sample was defrosted and homogenized on ice with 0.65% ice-cold saline. Following centrifuging at 2500 ×g at 4°C for 10 min, the supernatants were collected and subject to the measurement of the MDA content and the activity of the antioxidant enzymes, Na^+/K^+-ATPase, Ca^{2+}-ATPase based on the kits manual (Nanjing Jiancheng Bioengineering Institute, Nanjing, China).

2.6. Comet Assay. 20 embryos/larvae were collected from each group. Samples were completely digested in 37°C water bath with 0.25% trypsin. Following centrifuging at 2500 ×g for 10 min and the supplementation with moderate amount of PBS (pH 7.4), the single-cell suspension (10^4–10^6/mL) was prepared and subject to the single-cell gel electrophoresis (SGCE). For each treatment group, about 100 cells per slide were randomly scored with an image analysis through fluorescent microscopy. The comet images were analyzed by the auto comet image analysis system [13]. The DNA damage of the samples was evaluated by comet tail length, percentage of total DNA in the tail, tail moment, and olive tail moment.

2.7. Gene Expression Analysis. According to the gene sequences in GenBank, primers were designed by the primer 5.0 software (Table 1) and synthesized by biotechnology company (Invitrogen). The total RNA of tested rare minnow embryos/larvae was extracted using the RNAiso Plus (Takara, Kyoto, Japan). The total RNA contents were determined by measuring the absorbance at 260 nm and the RNA quality was verified by the ratio of the absorbance at 260/280 nm (range within 1.8~2.0). The first-strand cDNA synthesis was

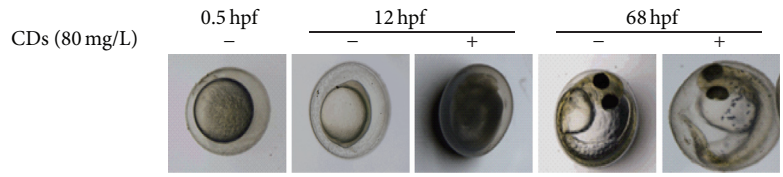

(a) Effects of exposure to CDs on developing rare minnow embryos

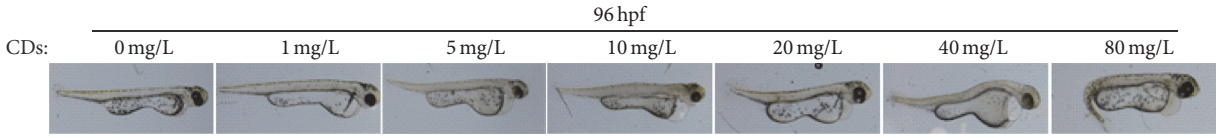

(b) Effects of exposure to CDs on developing rare minnow larvae

Figure 1: Effects of exposure to CDs on developing rare minnow embryos/larvae.

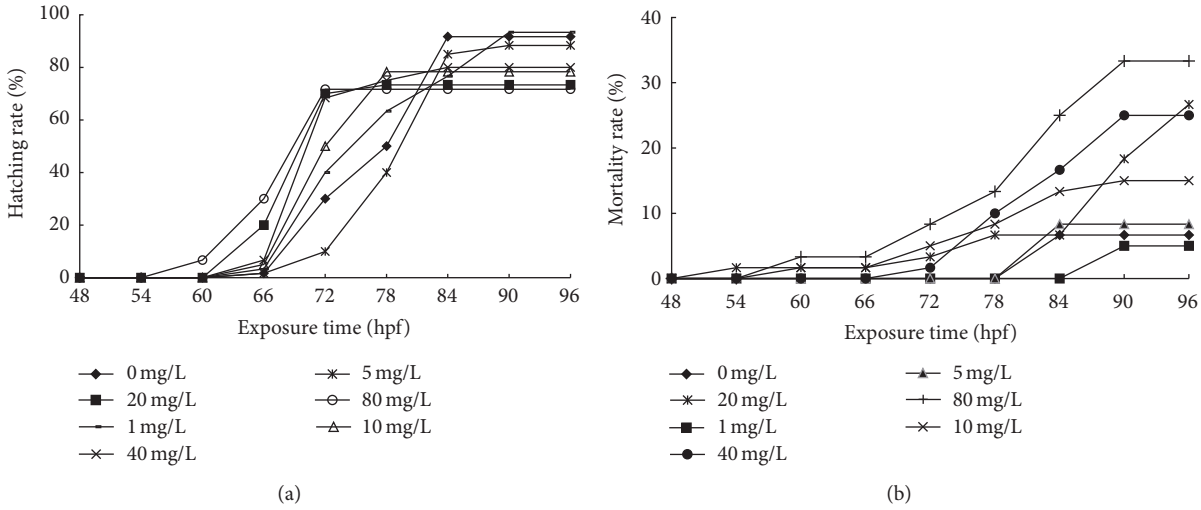

Figure 2: The hatching rate and mortality rate of rare minnow embryos exposed to different CDs concentration. The hatching rate (a) and mortality rate (b) for rare minnow embryos exposed to different CDs concentration. Triplicates were set for the tests, with 20 embryos/larvae each time.

performed by using PrimeScript ®RT reagent Kit with gDNA Eraser (Takara, Kyoto, Japan) following the manufacturer's instruction. The qPCR results were calculated using $2^{-\Delta\Delta CT}$ method [14].

2.8. Statistical Analysis. Statistical analysis was conducted with the one-way ANOVA or *t*-test depending on heterogeneity of variance (SPSS 17.0). Following the one-way ANOVA analysis, LSD multiple range test was employed for the evaluation between control and treated groups; otherwise *t-test* was performed between control and treated groups because of heterogeneity of variance. The differences were considered significant at $p < 0.05$ and extremely significant at $p < 0.01$.

3. Results

3.1. Morphological and Behavioral Analysis of Embryo Development of Rare Minnow. The toxicity effect of CDs on rare minnow embryos/larvae at different developmental stage was investigated in a concentration-dependent manner. As shown in Figure 1(a), in the stage of 12 hpf, no obvious developmental defects were observed in lower concentration groups (1, 5, 10, and 20 mg/L) compared with the control group. In higher concentration groups (40 mg/L and 80 mg/L), embryos yolk turbidity/agglutination was observed. Moreover, longer exposure time increased the malformation rate indicated by the shorter body length, tail/spinal curvature and pericardial edema, and yolk sac edema of the rare minnow embryos/larvae (Figure 1(b)).

The effects of CDs on hatching rate and mortality rate in embryos of rare minnow were tested. As shown in Figure 2, compared with the control group, the highest CDs concentration resulted in accelerated hatching. The hatched larvae were firstly observed at the stage of 54~60 hpf in the highest concentration group while they were detected at the stage of 60~66 hpf in control group. The hatching rate decreased significantly in response to the CDs treatment (Figure 2(a)). When the exposure time was extended to 96 hpf, most of unhatched embryos died.

Table 2: Effects of CDs on behavior and morphological parameter measurement of rare minnow embryos/larvae.

Indicator	0 mg/L	1 mg/L	5 mg/L	10 mg/L	20 mg/L	40 mg/L	80 mg/L
Spontaneous movements of 36 hpf (bends/30 seconds)	11.17 ± 2.32	9.50 ± 1.52	10.17 ± 1.47	8.17 ± 2.79**	6.83 ± 1.94**	7.83 ± 1.17**	9.17 ± 1.17
Heart rate of 60 hpf (bends/30 seconds)	67.00 ± 2.45	64.50 ± 2.88	60.67 ± 4.17*	64.00 ± 4.24	75.50 ± 3.27**	70.67 ± 5.74	71.00 ± 3.58
Malformation rate (%)	5.00 ± 1.00	6.67 ± 1.73	8.33 ± 1.73	13.30 ± 1.73**	26.67 ± 4.58**	25.00 ± 3.00**	43.33 ± 4.58**
SV-BA ($\times 10^2$ μm)	1.90 ± 0.19	2.07 ± 0.27	2.15 ± 0.28	2.70 ± 0.45**	3.13 ± 0.26**	3.05 ± 0.47**	3.32 ± 0.26**
Area of pericardial edema ($\times 10^4$ μm^2)	2.48 ± 0.53	2.60 ± 0.65	2.97 ± 0.32	4.05 ± 0.67**	5.43 ± 0.64**	5.50 ± 0.97**	5.55 ± 0.75**
Area of sac-yolk edema ($\times 10^5$ μm^2)	2.44 ± 0.10	2.56 ± 0.10	2.42 ± 0.22	2.83 ± 0.16**	3.17 ± 0.23**	3.49 ± 0.27**	3.41 ± 0.27**
Body length (mm)	3.11 ± 0.21	3.13 ± 0.18	3.16 ± 0.11	3.03 ± 0.08	2.96 ± 0.14	2.82 ± 0.20**	2.80 ± 0.18**

Values are presented as mean ± SD. Spontaneous movements, heart rate, SV-BA, area of pericardial edema, and area of sac-yolk edema ($n = 6$); body length ($n = 7$) and malformation rate ($n = 60$). Values that are significantly different from the control are indicated by asterisks (one-way ANOVA or *t-test*,* $p < 0.05$, ** $p < 0.01$).

Consistently, the increased mortality rate was observed in a concentration-dependent manner following the exposure to CDs at the stage of 96 hpf. It is interesting to note that no significant change among all concentration group treatments was detected before 72 hpf in contrast to the marked elevation of the mortality rate after 72 hpf (Figure 2(b)). It suggested that 72 hpf stage might be important for the fate determination of the rare minnow embryo development in response to the environmental stress introduced by the CDs.

The spontaneous embryonic movement at 36 hpf stage decreased in a concentration-dependent manner after the exposure to CDs. In the 10, 20, and 40 mg/L groups, the spontaneous embryonic movements decreased significantly against control group ($p < 0.01$). At the 60 hpf stage, the embryos heart rate in control group was 67.00 ± 2.45 beats per 30 seconds (mean ± SD) (Table 2). Embryos heart rates increased significantly in 20 mg/L group ($p < 0.01$). In the 40 and 80 mg/L group, heart rates just increased slightly. The malformation rates were increased in a concentration-dependent manner after the CDs exposure at the stage of 96 hpf. In 10~80 mg/L concentration group, the malformation rate was significantly increased compared with that in the control group ($p < 0.01$).

We also investigated the effects of CDs on hearts development of rare minnow embryos. In the 1 and 5 mg/L concentration group, compared with control, no significantly changed SV-BA distance was detected ($p < 0.05$) while, in the 10~80 mg/L concentration groups, the SV-BA distance was significantly increased ($p < 0.01$). The significant enlarged area of pericardial edema and sac-yolk edema appeared, respectively, in proportion to the increasing CDs concentration. In groups with concentration higher than 10 mg/L, the areas of pericardial edema and of sac-yolk edema were significantly decreased in comparison to control larvae ($p < 0.01$).

In addition, high concentration CDs treatment resulted in body length alteration of the larvae. At the 96 hpf stage, the larvae in control group have significantly shorter body length than that in higher concentration (40 and 80 mg/L) groups (Table 2) ($p < 0.01$).

3.2. Effects of CDs on Ca^{2+}-ATPase and Na^+/K^+-ATPase Activity of Rare Minnow Embryos/Larvae. As shown in Figure 3, the activities of Ca^{2+}-ATPase and Na^+/K^+-ATPase decreased in a concentration-dependent manner following exposure to CDs. In the highest concentration (80 mg/L) group, the Ca^{2+}-ATPase activities were decreased to 43%, 28%, 33%, and 25% of control at the stage of 12 hpf, 48 hpf, 72 hpf, and 96 hpf, respectively. Similarly, Na^+/K^+-ATPase activity decreased in a concentration-dependent manner following exposure to CDs. In the highest concentration (80 mg/L) group, the Na^+/K^+-ATPase activities were decreased to 40%, 47%, 65%, 63%, and 67% of control at the 12 hpf, 24 hpf, 48 hpf, 72 hpf, and 96 hpf stage, respectively.

3.3. Development Related Genes Expression. We discuss the effects of CDs on the expression pattern of the development related genes. As shown in Figure 4, *Wnt8a*, *Vezf1*, and *Mstn* mRNA levels at different concentrations (1, 5, 10, 20, 40, and 80 mg/L) were examined with *β-actin* gene as endogenous control. The values of the mRNA levels were assessed as the fold of control. At the 12 hpf stage, *Mstn* and *Wnt8a* showed the increased expression while the *Vezf1* expression is downregulated in all concentration group.

At 24 bpf stage, *Mstn* expression was upregulated. Further, with increasing of CDs concentration, these fold changes of *Mstn* expression showed the tendency as it rose up first and then went down. Further, with increasing concentration of CDs, *Mstn* expression showed the tendency as it rose up first and then went down. *Wnt8a* expression is upregulated. In 40 and 80 mg/L group, *Wnt8a* expression is significantly elevated compared to control ($p < 0.05$). In contrast, *Vezf1* expression is downregulated as the increased CDs concentration. In

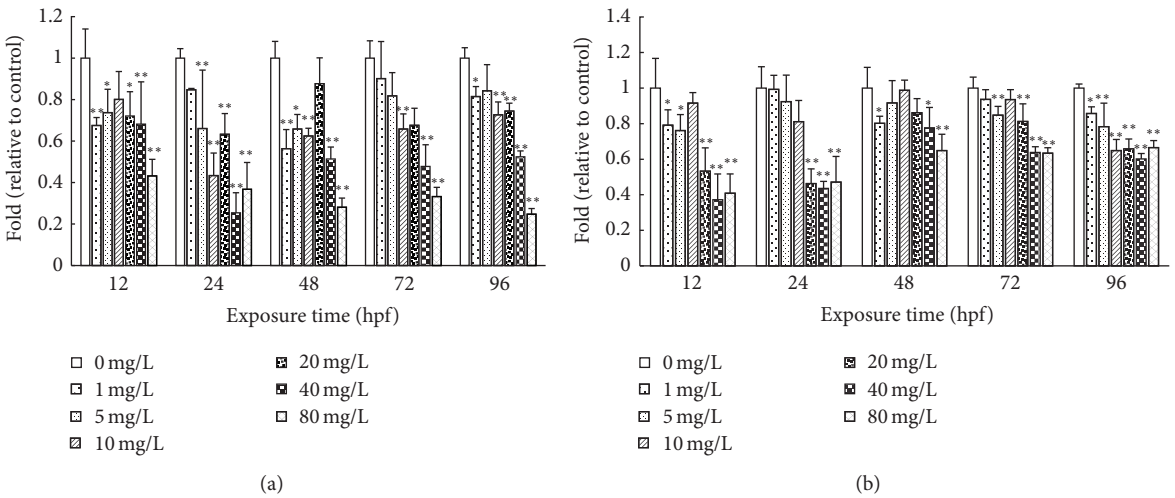

Figure 3: Effects of CDs on Ca^{2+}-ATPase and Na^+/K^+-ATPase activity of rare minnow embryos/larvae. The Ca^{2+}-ATPase (a) and Na^+/K^+-ATPase (b) activities for rare minnow embryos exposed to different concentration of CDs. Values are presented as mean ± SD ($n = 20$). Values that are significantly different from the control are indicated by asterisks (one-way ANOVA or *t-test*, $^*p < 0.05$, $^{**}p < 0.01$).

40 and 80 mg/L groups, *Vezf1* expression is significantly decreased compared to control.

At later stage (48–96 hpf), *Wnt8a* expression is upregulated as the increased CDs concentration. In response to the treatment of 80 mg/L CDs, the *Mstn* expression level increased significantly in company with the marked decrease of *Vezf1* expression at 48 hpf, 72 hpf, and 96 hpf stage (Figure 4).

3.4. Effects of CDs on SOD, CAT, and GPX Activities and MDA Contents of Rare Minnow Embryos/Larvae. We also investigated the effects of CDs on SOD, CAT, and GPX activities and MDA contents of rare minnow embryos/larvae (Figure 5). The SOD activity increased with the extending exposure duration compared with control group except at the 72 hpf stage. In the higher concentration (20, 40, and 80 mg/L) groups, significantly elevated SOD activity was detected compared with control ($p < 0.05$) (Figure 5(a)). The CAT activity alteration showed the similar pattern with that of SOD. With the extended exposure duration, significant higher CAT activity was detected accordingly (Figure 5(b)). GPX activity tended to rise up in relation to the increased CDs exposure duration. At each stage, higher CDs concentration treatment is induced sharply increase of the GPX activity ($p < 0.05$) (Figure 5(c)). CDs exposure increased the MDA content significantly compared to control at each developmental stage. As the exposure time got longer, the MDA content showed the tendency of increase which was more prominent in higher concentration groups (20, 40, and 80 mg/L) ($p < 0.01$) (Figure 5(d)).

3.5. DNA Damage Analysis. Through comet assay, we examined if the CDs exposure would induce the DNA damage in embryonic cells. The results showed that CDs exposure induces the DNA damage in cells (Figure 6). At 72 hpf stage, control cells showed uniform and regular round sized nucleus without tail (Figure 6(a)). In 1 mg/L concentration group, the cells showed oval nuclear staining without observed tail (Figure 6(b)). Elevated tail staining signal appeared in response to the increase of the CDs concentration (Figures 6(c)–6(g)).

Further, we tested if the tail length staining in cells is proportion to the CDs concentration with which the cells were treated. As shown in Figure 7, CDs treatment promotes the tail formation in cells. In 20, 40, and 80 mg/L group, the tail length staining is significantly stronger than control ($p < 0.01$). Except in the low concentration groups (1, 5, 10 mg/L), longer CDs exposure time promotes the length and DNA content of the comet tail. At later stage (48 hpf, 72 hpf, and 96 hpf), the length and DNA content of the comet tail increased in a concentration-dependent manner.

4. Discussion

4.1. Early Developmental Toxicity of CDs to Rare Minnow Embryos. A series of studies has shown the nanomaterials could induce the fish embryos' developmental defect among which the pericardial edema, yolk sac edema, and curvature of the spine appeared most frequently, suggesting the potential risky impacts of CDs on the natural water ecosystem.

Chen et al. have shown the abnormal condensation of embryonic eggs, pericardial edema, and curvature of the spine of zebrafish embryos/larvae following exposure to CdSe/ZnS QDs [15]. Kim and collogues showed that citrate-functionalized TiO_2 nanoparticles caused pericardial edema, yolk sac edema, craniofacial malformation, and opaque yolk in zebrafish embryos [16]. Lv showed that nano-ZnO induced zebrafish embryonic pericardial edema, yolk sac edema, and tail malformation [17].

Consistently, our results showed the CDs exposure also induced the pericardial edema, yolk sac edema, and tail malformation in the embryos/larvae of rare minnow. These data confirm the conclusion that the nanoparticle exposure would induce the developmental defects of fish embryos/larvae. On

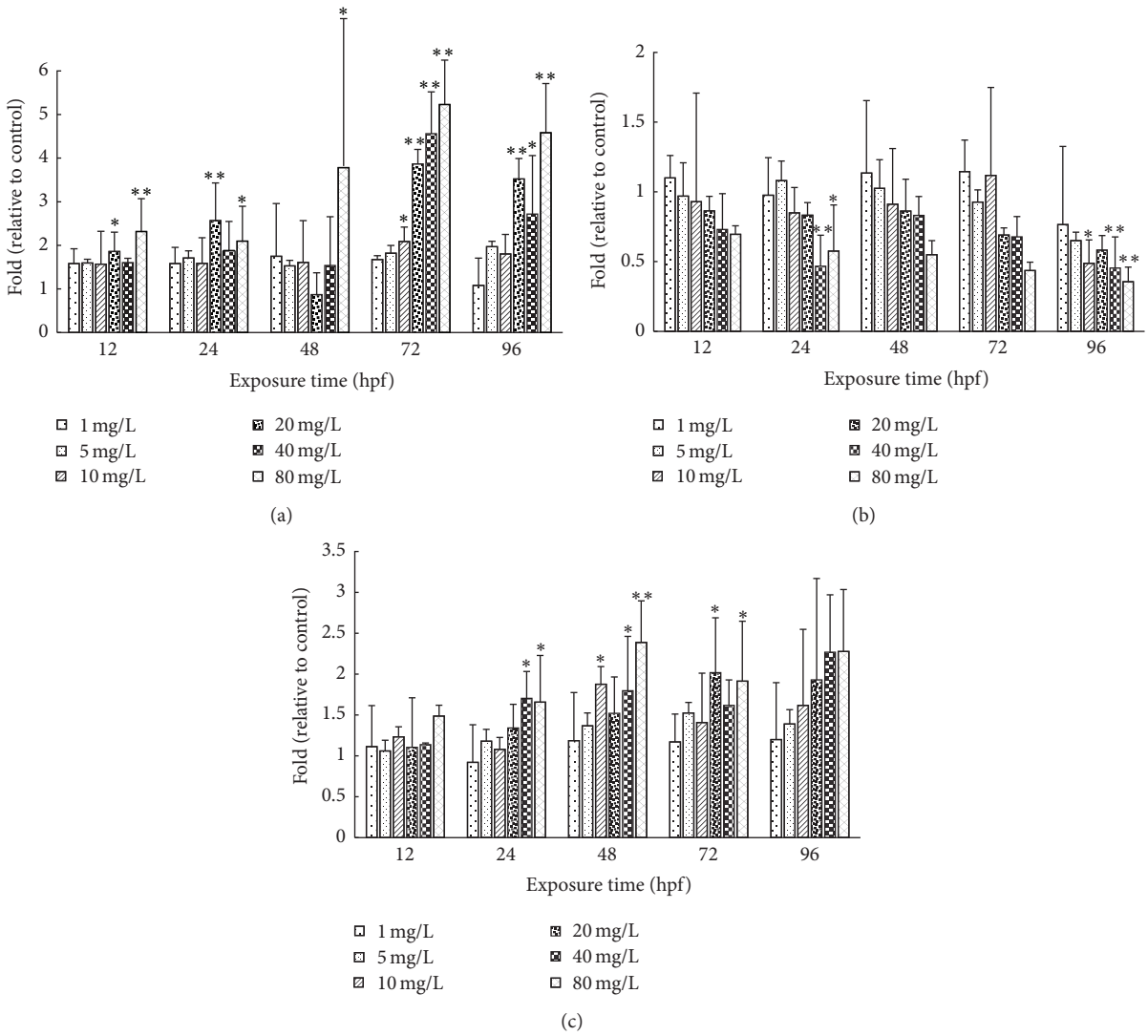

Figure 4: The *Mstn*, *Vezf1*, and *Wnt8a* mRNA levels for rare minnow embryos exposed to different concentration of CDs. The *Mstn* (a), *Vezf1* (b), and *Wnt8a* (c) mRNA levels for rare minnow embryos exposed to different concentration of CDs. Values are presented as mean ± SD ($n = 15$). Values that are significantly different from the control are indicated by asterisks (one-way ANOVA or *t-test*, $^{*}p < 0.05$, $^{**}p < 0.01$).

the other, our data also suggest the pericardial edema, yolk sac edema, and tail malformation are the main consequences of nanoparticles exposure in different fish spices other than the zebrafish, implying the common potential environmental risk of the CDs and the possible dysregulated molecular mechanism of the conserved development pathway in fish embryos/larvae.

4.2. Molecular Mechanism Underlined the Developmental Defect Induced by the CDs Exposure. Providing energy for the active movements of Na^+ and K^+ across the cell membrane and the epithelia and Na^+/K^+-ATPase plays a central role in whole body osmoregulation, ionic transportation, muscle function, and several other membrane transportation dependent physiological processes. Previous study has reported that the activity of Na^+/K^+-ATPase is important for the growth and survival for the *Penaeus vannamei* in the postlarval stage [18]. Hill et al. showed the significant decreased malformation rate induced by TCDD through regulating the osmotic pressure balance of the zebrafish embryos [19], suggesting the correlation between the chemical induced hydropic malformation and osmoregulation. In our study, CDs treatment decreased the Na^+/K^+-ATPase activity in concentration-dependent manner (Figure 4(b)). It might block the pumping out of the Na^+ and subsequently break the balance of Na^+ accumulation, which eventually result in the edema and destruction of cells [20].

The hatching process of fish eggs was largely determined by the collaboration between hatching enzymes and membrane lipid peroxidation, which weakened the egg membrane along with embryos squirm [21]. In the majority of fishes, hatching enzyme is synthesized by the hatching gland distributed on the outer surface of embryo and yolk sac [22]. In our study, by means of interferometer spectrometer, we

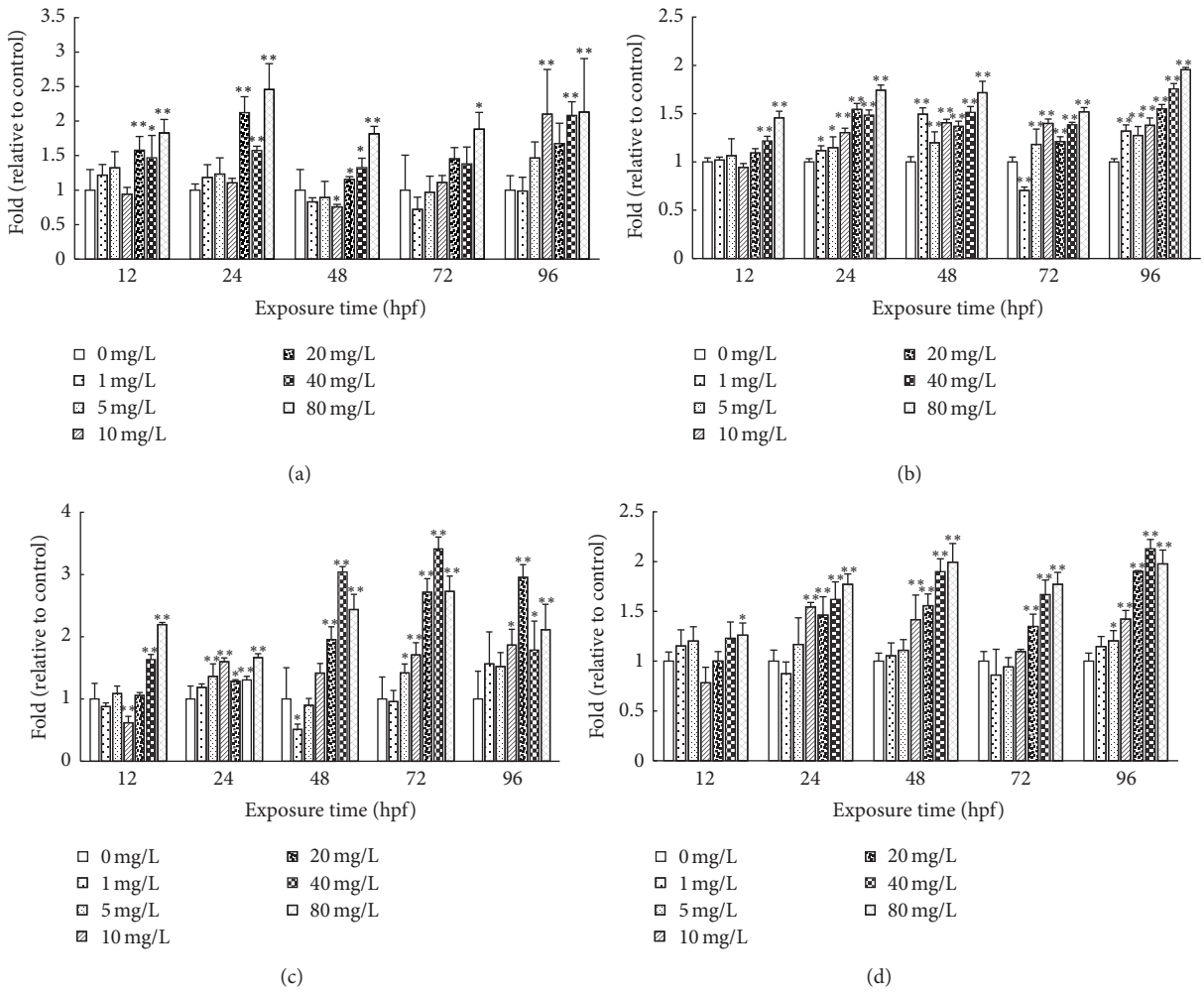

Figure 5: The SOD, CAT, and GPX activities and MDA contents for rare minnow embryos exposed to different concentration of CDs. The SOD (a), CAT (b), and GPX (c) activities and MDA contents (d) for rare minnow embryos exposed to different concentration of CDs. Values are presented as mean ± SD ($n = 20$). Values that are significantly different from the control are indicated by asterisks (one-way ANOVA or *t-test*, $^{*}P < 0.05$, $^{**}P < 0.01$).

did observe that, in rare minnow, the hatching gland cells were located on the surface of yolk sac (data not shown). Thus, the defective development of the yolk sac could trigger the inactivation of hatching gland. CDs could enter into the cytoplasm by endocytosis mechanism [23]. In addition, CDs could be complexed with proteins, polysaccharide, or other biological molecules in cells, which subsequently affect the hatching enzyme activity. It could explain the lower hatching rate result from the CDs treatment (80 mg/L).

In our study, the vascular endothelial zinc finger (*Vezf1*) expression level decreases with the increased CDs concentration (Figure 5(b)). *Vezf1* participates in the molecular pathways that control early blood vessel development. *Vezf1* may play an important role in the endothelial lineage determination and embryonic vasculogenesis and angiogenesis at later stages [24]. Silencing *Vezf1* on chicken embryo in vivo suggested that *Vezf1* is important for the development of blood vessel and heart [25]. Decreased expression levels of *Vezf1* influenced the function of cardiovascular system during early development. Eventually, the heart physiological compensation promotes the increased heart rate and SV-BA distance of the embryos in 10~80 mg/L concentration group (Table 2).

In our study, the Ca^{2+}-ATPase activities decreased with the increased CDs concentration and exposure duration (Figure 3(a)). The Ca^{2+}-ATPase plays a crucial role in maintaining the intracellular concentration of Ca^{2+} [26]. Inhibition of the activity of Ca^{2+}-ATPase leads to the intracellular accumulation of Ca^{2+} which induces the skeletal developmental defect. Myostatin (*Mstn*) and *Wnt8a* expressions were observed to be upregulated significantly in response to the CDs treatments in a concentration-dependent manner (Figures 4(a) and 4(c)). *Mstn* belongs to the transforming growth factor-b (TGF-b) family and has been identified as an important negative regulator of muscle development [27].

MOD mediated muscle development is tightly regulated by the TGF-β pathway. As the important transcriptional regulator of MOD, Mstn could be recruited by the SMAD

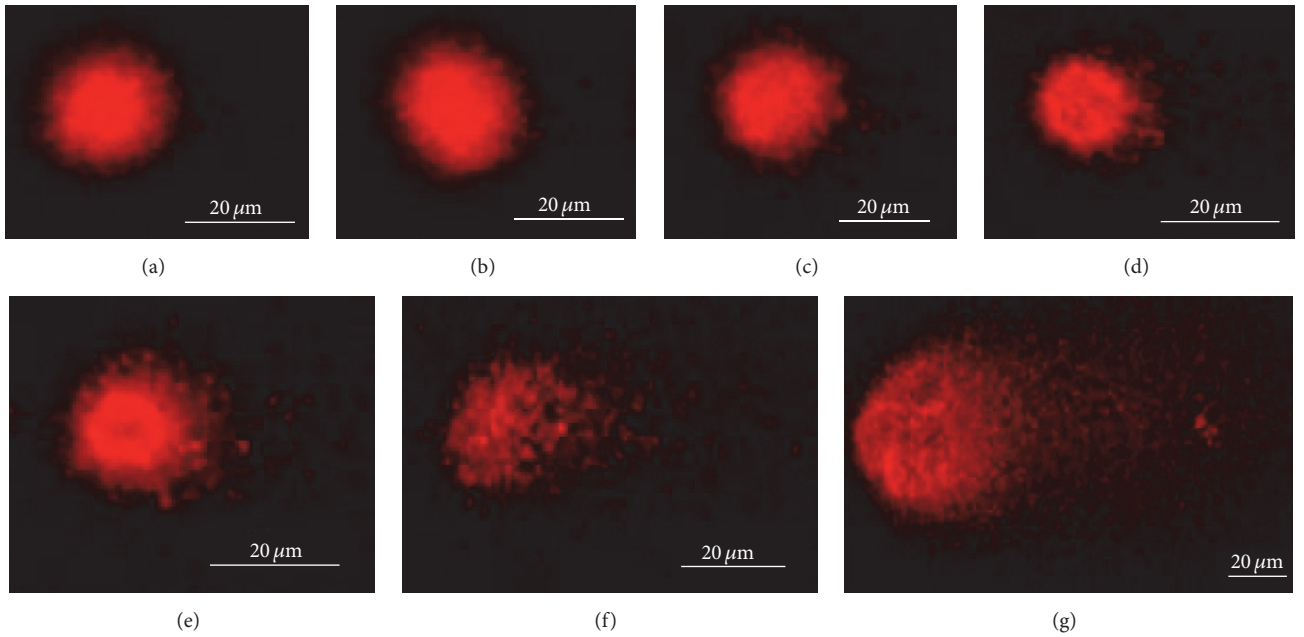

Figure 6: DNA damage. Effects of different concentration CDs (control (a), 1 mg/L (b), 5 mg/L (c), 10 mg/L (d), 20 mg/L (e), 40 mg/L (f), and 80 mg/L (g)) on DNA damage of rare minnow embryos/larvae cells by comet assay.

proteins to the regulatory sequences of MOD which account for the retarded muscle growth [28]. Wnt8a is a key factor in Wnt/β-catenin signaling pathway for the body axis extending [29]. Wnt8a initially locates at the bottom area of the animal pole of fertilized eggs which activate the classical Wnt/β-catenin signaling through translocating to the destined microtube region, contributing to the curvature of the spine or tail within the development progression [30]. Downregulated *Wnt8a* results in lacking of the tail shaft structure in zebrafish embryos/larvae [31]. The significant increased expression of *Wnt8a* indicates the inhibited body axis extension. Taken together, on one hand, both of the *Wnt8a* expression upregulation and the inhibited Ca^{2+}-ATPase activity promote the skeletal development and, on the other hand, increased *Mstn* expression blocks the muscle development which could explain the observed tail and spinal curvatures in this study.

It is noteworthy that the detailed mechanism underlined the CDs induced alteration of the target gene expression is poorly understood. Previous studies have shown that the CDs could be complexed with both double strand DNA (dsDNA) [32] and cellular functional proteins [9]. These results provide the probability that the CDs could affect the transcription of target gene through either cis- or transregulation. Accordingly, in our study, we reasoned that there are two possible mechanisms either working separately or together to alter the development related gene expression induced by CDs exposure: (1) the CDs might bind to the cis-elements which block the binding sites of transcriptional factors. (2) The CDs might be complexed with and dysregulated the transcriptional factors directly. However, the further study is needed to clarify this issue in the future.

4.3. Oxidative Stress and DNA Damage. Oxidative DNA damage and the inflammatory response by far are the two major involved mechanisms concerning the biological toxicity of the nanomaterials [33, 34]. In normal physiological condition, the endogenous antioxidant enzymes combat the reactive oxygen species (ROS) and prevent the oxidative damage to the organism. In fact, fish can combat the oxidative stress with the enzyme system consisting of SOD, CAT, and GPX. SOD convert superoxide anions (O_2^-) into H_2O_2 and then the enzymes of CAT and GPX catalyze the reaction to digest H_2O_2 into H_2O and O_2^- [35]. Upon exogenous stress, abnormal ROS accumulation would break this balance and generate cellular oxidative damage.

Environmental pollutants go into the body and produce active oxygen free radicals through a series of metabolic conversions. If they are not cleared promptly, the balance will be destroyed and cause organisms oxidative damage [36]. LPO can be defined as the oxidative damage of cell membrane lipids and has been used extensively as a biomarker of oxidative stress in vivo [37]. As one of the main products of cell membrane LPO, MDA level has been regarded as the indicator of the LPO level [38].

In the present study, the activities of SOD were increased following CDs treatments (Figure 5(a)), suggesting the occurrence of the oxidative stress. SOD act first to scavenge the O_2^-; then antioxidant system becomes active to defense and synchronizes the activity of SOD with that of CAT. These results are in agreement with the previous study [39] in which the correlations between SOD and CAT were found in the mussel *Mytilus galloprovincialis* upon the stress introduced by copper nanoparticles exposure. Moreover, due to the accumulating H_2O_2 generated from O_2^- by SOD, the CAT

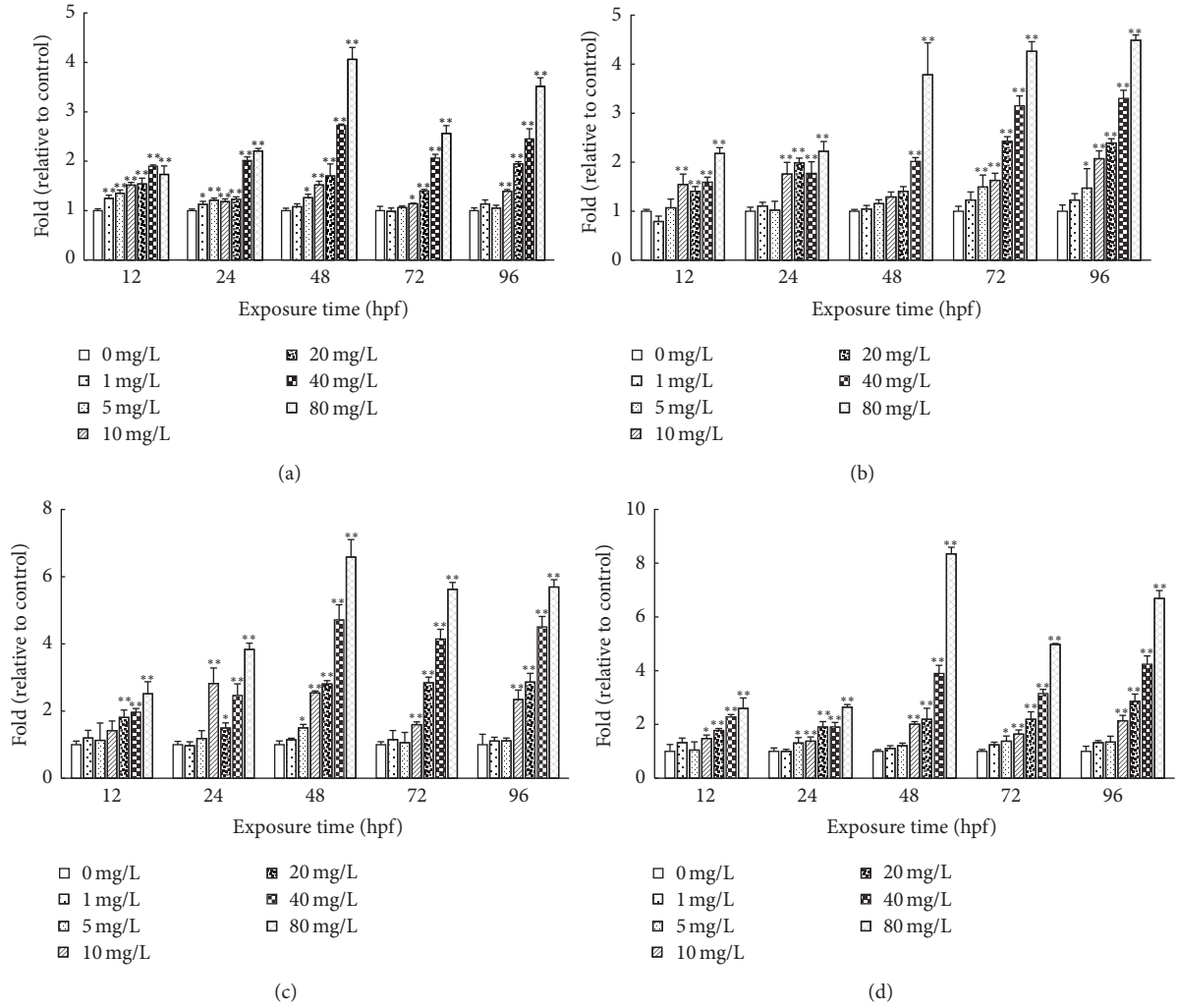

Figure 7: The comet tail length, tail DNA percent, tail moment, and olive tail moment for rare minnow embryos exposed to different concentration of CDs. The comet tail length (a), tail DNA percent (b), tail moment (c), and Olive tail moment (d) for rare minnow embryos exposed to different concentration of CDs. Values are presented as mean ± SD ($n = 20$). Values that are significantly different from the control are indicated by asterisks (one-way ANOVA or *t-test*, $^{*}p < 0.05$, $^{**}p < 0.01$).

turn active quickly to keep pace with SOD (Figure 5(b)). Also, the GPX activity is induced by the higher intensity of stress result from higher CDs concentration (Figure 5(c)).

In sum, in rare minnow, the antioxidant enzyme system consists of SOD, CAT, and GPX combined together that act against oxidative stress and keep the MDA content in a certain range in lower CDs concentration group. However, long time of CDs exposure in 20, 40, and 80 mg/L concentration groups breaks the organism antioxidant capacity and results in the increase of the MDA content (Figure 5(d)), indicating that CDs exposure induced the oxidative stress to the embryo. Consequently, the defective development of rare minnow embryo appeared.

With the increased CDs concentration and extended exposure time, serious DNA damage of rare minnow embryos/larvae cells was detected (Figures 6 and 7). It could be the reason for higher malformation and mortality rate. Further increase of the CDs concentration results in more serious DNA damage induced by the ROS attacking nucleotides. The damaged DNA cannot be repaired in time; thus the malformation rate and mortality rate increased significantly [40].

5. Conclusion

(1) In summary, the higher concentrations of CDs have significant development toxicity on rare minnow embryos which could be characterized as decreased spontaneous movements and body length, increased heart rate, and pericardial edema, yolk sac edema and tail/spinal curvature, various morphological malformations, and decreased hatching rate.

(2) The underlying mechanism of this developmental toxicity appears to be related to the generation of oxidative stress, repressed DNA repair efficacy, and altered development related gene expression.

Competing Interests

The authors declare that there is no conflict of interests regarding the publication of this paper.

Acknowledgments

The authors thank Dr. Haoxing Zhang and Dr. Xu Pang for the language editing of the manuscript. This work was supported by the Fundamental Research Funds for the Central Universities of China (XDJK2014C061 and XDJK2016E098).

References

[1] X. Wang, K. Qu, B. Xu, J. Ren, and X. Qu, "Multicolor luminescent carbon nanoparticles: synthesis, supramolecular assembly with porphyrin, intrinsic peroxidase-like catalytic activity and applications," *Nano Research*, vol. 4, no. 9, pp. 908–920, 2011.

[2] L. Cao, M. J. Meziani, S. Sahu, and Y.-P. Sun, "Photoluminescence properties of graphene versus other carbon nanomaterials," *Accounts of Chemical Research*, vol. 46, no. 1, pp. 171–180, 2013.

[3] L. Ma, *Study on the Synthesis of Carbon Nanodots and Its Application*, Henan Normal University, Xinxiang, China, 2014.

[4] Y. Song, W. Shi, W. Chen, X. Li, and H. Ma, "Fluorescent carbon nanodots conjugated with folic acid for distinguishing folate-receptor-positive cancer cells from normal cells," *Journal of Materials Chemistry*, vol. 22, no. 25, pp. 12568–12573, 2012.

[5] C. Liu, P. Zhang, X. Zhai et al., "Nano-carrier for gene delivery and bioimaging based on carbon dots with PEI-passivation enhanced fluorescence," *Biomaterials*, vol. 33, no. 13, pp. 3604–3613, 2012.

[6] F. Gottschalk, T. Sonderer, R. W. Scholz, and B. Nowack, "Modeled environmental concentrations of engineered nanomaterials (TiO_2, ZnO, Ag, CNT, fullerenes) for different regions," *Environmental Science and Technology*, vol. 43, no. 24, pp. 9216–9222, 2009.

[7] E. Oberdörster, S. Zhu, T. M. Blickley, P. McClellan-Green, and M. L. Haasch, "Ecotoxicology of carbon-based engineered nanoparticles: effects of fullerene (C_{60}) on aquatic organisms," *Carbon*, vol. 44, no. 6, pp. 1112–1120, 2006.

[8] X. Zhang, *The Safety Applied Study of Carbon Dots in the Biological and Medical Field*, Minnan Normal University, 2013.

[9] Z. Gao, G. Shen, X. Zhao et al., "Carbon dots: a safe nanoscale substance for the immunologic system of mice," *Nanoscale Research Letters*, vol. 8, no. 1, article 276, 2013.

[10] Y. Zhou, S. Cheng, H. Wei, and M. Sun, "A new toxicity test organism-Gobiocypris rarus," *Journal of Zoological Systematics and Evolutionary Research*, vol. 16, pp. 59–63, 1995.

[11] Z. Qun-Fang, J. Gui-Bin, and L. Ji-Yan, "Effects of sublethal levels of tributyltin chloride in a new toxicity test organism: the Chinese rare minnow (*Gobiocypris rarus*)," *Archives of Environmental Contamination and Toxicology*, vol. 42, no. 3, pp. 332–337, 2002.

[12] C. Schulte and R. Nagel, "Testing acute toxicity in the embryo of zebrafish, *Brachydanio rerio*, as an alternative to the acute fish test: preliminary results," *Alternatives to Laboratory Animals Atla*, vol. 22, no. 1, pp. 12–19, 1994.

[13] K. Kończaa, A. Lankoffb, A. Banasik et al., "A cross-platform public domain PC image-analysis program for the comet assay," *Mutation Research/fundamental and Molecular Mechanisms of Mutagenesis*, vol. 534, no. 1-2, pp. 15–20, 2003.

[14] K. J. Livak and T. D. Schmittgen, "Analysis of relative gene expression data using real-time quantitative PCR and the $2^{-\Delta\Delta C_T}$ method," *Methods*, vol. 25, no. 4, pp. 402–408, 2001.

[15] M.-F. Chen, C.-Z. Huang, D.-Y. Pu et al., "Toxic effects of CdSe/ZnS QDs to zebrafish embryos," *Environmental Science*, vol. 36, no. 2, pp. 719–726, 2015.

[16] M.-S. Kim, K. M. Louis, J. A. Pedersen, R. J. Hamers, R. E. Peterson, and W. Heideman, "Using citrate-functionalized TiO_2 nanoparticles to study the effect of particle size on zebrafish embryo toxicity," *Analyst*, vol. 139, no. 5, pp. 964–972, 2014.

[17] L. Lv, *The Developmental Toxicity Study of nano-ZnO on Zebrafish Embryos*, Harbin Institute of Technology, Harbin, China, 2013.

[18] P. Coutteau, M. R. Camara, and P. Sorgeloos, "The effect of different levels and sources of dietary phosphatidylcholine on the growth, survival, stress resistance, and fatty acid composition of postlarval *Penaeus vannamei*," *Aquaculture*, vol. 147, no. 3-4, pp. 261–273, 1996.

[19] A. J. Hill, S. M. Bello, A. L. Prasch, R. E. Peterson, and W. Heideman, "Water permeability and TCDD-induced edema in Zebrafish early-life stages," *Toxicological Sciences*, vol. 78, no. 1, pp. 78–87, 2004.

[20] Y. Wang, W. Dong, Z. Zhao et al., "Image quantitative assay of Na^+/K^+ ATPase and cytochrome oxidase activity changes in lung tissue of rabbit with pulmonary edema after seawater drowning," *Chinese Journal of Nautical Medicine*, vol. 5, no. 2, pp. 90–92, 1998.

[21] T. C. King-Heiden, P. N. Wiecinski, A. N. Mangham et al., "Quantum dot nanotoxicity assessment using the zebrafish embryo," *Environmental Science and Technology*, vol. 43, no. 5, pp. 1605–1611, 2009.

[22] H. E. Hagenmaier, "The hatching process in fish embryos-IV. The enzymological properties of a highly purified enzyme (chorionase) from the hatching fluid of the rainbow trout, Salmo gairdneri rich," *Comparative Biochemistry and Physiology—Part B*, vol. 49, no. 2, pp. 313–324, 1974.

[23] J. Zong, Y. Zhu, X. Yang, J. Shen, and C. Li, "Synthesis of photoluminescent carbogenic dots using mesoporous silica spheres as nanoreactors," *Chemical Communications*, vol. 47, no. 2, pp. 764–766, 2011.

[24] J.-W. Xiong, A. Leahy, H.-H. Lee, and H. Stuhlmann, "*Vezf1*: a Zn finger transcription factor restricted to endothelial cells and their precursors," *Developmental Biology*, vol. 206, no. 2, pp. 123–141, 1999.

[25] J. Ge, *Study on Funetion of Chiek Vascular Endothelial Zinc Finger-1 in Endothelial Cells Differentiation and Vessel Formation*, Xiamen Normal University, 2009.

[26] R. Moreau, G. Daoud, A. Masse, L. Simoneau, and J. Lafond, "Expression and role of calcium-ATPase pump and sodium-calcium exchanger in differentiated trophoblasts from human term placenta," *Molecular Reproduction and Development*, vol. 65, no. 3, pp. 283–288, 2003.

[27] J. M. Oldham, J. A. K. Martyn, M. Sharma, F. Jeanplong, R. Kambadur, and J. J. Bass, "Molecular expression of myostatin and MyoD is greater in double-muscled than normal-muscled cattle fetuses," *American Journal of Physiology—Regulatory Integrative and Comparative Physiology*, vol. 280, no. 5, pp. R1488–R1493, 2001.

[28] X. Zhu, S. Topouzis, L.-F. Liang, and R. L. Stotish, "Myostatin signaling through Smad2, Smad3 and Smad4 is regulated by the

inhibitory Smad7 by a negative feedback mechanism," *Cytokine*, vol. 26, no. 6, pp. 262–272, 2004.

[29] X. Zhao and G. Duester, "Effect of retinoic acid signaling on Wnt/β-catenin and FGF signaling during body axis extension," *Gene Expression Patterns*, vol. 9, no. 6, pp. 430–435, 2009.

[30] F.-I. Lu, C. Thisse, and B. Thisse, "Identification and mechanism of regulation of the zebrafish dorsal determinant," *Proceedings of the National Academy of Sciences of the United States of America*, vol. 108, no. 38, pp. 15876–15880, 2011.

[31] Y. Xiang, J. Gao, Z. Hu, and M. Zhou, "Category and function of Wnt gene," *Chemistry of Life*, vol. 27, no. 2, pp. 138–141, 2007.

[32] V. Milosavljevic, H. V. Nguyen, P. Michalek et al., "Synthesis of carbon quantum dots for DNA labeling and its electrochemical, fluorescent and electrophoretic characterization," *Chemical Papers*, vol. 69, no. 1, pp. 192–201, 2015.

[33] A. Nel, "Air pollution-related illness: effects of particles," *Science*, vol. 308, no. 5723, pp. 804–806, 2005.

[34] A. Nel, T. Xia, L. Mädler, and N. Li, "Toxic potential of materials at the nanolevel," *Science*, vol. 311, no. 5761, pp. 622–627, 2006.

[35] J. B. Pi, Q. Zhang, J. Fu et al., "ROS signaling, oxidative stress and Nrf2 in pancreatic beta-cell function," *Toxicology and Applied Pharmacology*, vol. 244, no. 1, pp. 77–83, 2010.

[36] S. K. Manna, S. Sarkar, J. Barr et al., "Single-walled carbon nanotube induces oxidative stress and activates nuclear transcription factor-κB in human keratinocytes," *Nano Letters*, vol. 5, no. 9, pp. 1676–1684, 2005.

[37] L. Jiang, L.-L. Che, and D.-S. Xiao, "Gender differences in lipid peroxidation stress and anti-oxidation reaction in rat cardiac muscles by long-term swimming exercise," *Journal of Clinical Rehabilitative Tissue Engineering Research*, vol. 11, no. 47, pp. 9475–9478, 2007.

[38] L. Hao and L. Chen, "Oxidative stress responses in different organs of carp (*Cyprinus carpio*) with exposure to ZnO nanoparticles," *Ecotoxicology and Environmental Safety*, vol. 80, pp. 103–110, 2012.

[39] T. Gomes, J. P. Pinheiro, I. Cancio, C. G. Pereira, C. Cardoso, and M. J. Bebianno, "Effects of copper nanoparticles exposure in the mussel Mytilus galloprovincialis," *Environmental Science and Technology*, vol. 45, no. 21, pp. 9356–9362, 2011.

[40] Q. Rahman, M. Lohani, E. Dopp et al., "Evidence that ultrafine titanium dioxide induces micronuclei and apoptosis in Syrian hamster embryo fibroblasts," *Environmental Health Perspectives*, vol. 110, no. 8, pp. 797–800, 2002.

Hindawi Publishing Corporation
BioMed Research International
Volume 2016, Article ID 4290793, 8 pages
http://dx.doi.org/10.1155/2016/4290793

Research Article

Spatiotemporal Distribution and Assemblages of Fishes below the Lowermost Dam in Protected Reach in the Yangtze River Main Stream: Implications for River Management

Junyi Li,[1,2] Hui Zhang,[2] Danqing Lin,[1,2] Jinming Wu,[2] Chengyou Wang,[2] Xuan Xie,[1,2] and Qiwei Wei[2]

[1]*College of Life Science, Southwest University, Chongqing, China*
[2]*Key Laboratory of Freshwater Biodiversity Conservation, Ministry of Agriculture of China, Yangtze River Fisheries Research Institute, Chinese Academy of Fishery Sciences, Wuhan, China*

Correspondence should be addressed to Qiwei Wei; weiqw@yfi.ac.cn

Received 7 July 2016; Accepted 20 September 2016

Academic Editor: Kaiyu He

Now more and more ecologists concern about the impacts of dam construction on fish. However, studies of fishes downstream Gezhouba Dam were rarely reported except Chinese sturgeon (*Acipenser sinensis* Gray). In this study, catch investigations and five hydroacoustic detections were completed from 2015 to 2016 to understand the distribution, size, and categories of fishes and their relationship with the environmental factors below Gezhouba Dam in protected reach in the Yangtze River main stream. Results showed significant differences in fish distribution and TS (target strength) between wet and flood seasons. Mean TS in five hydroacoustic detections were −59.98 dB, −54.70 dB, −56.16 dB, −57.90 dB, and −59.17 dB, respectively, and dominant fish species are *Coreius guichenoti* (Bleeker), *Siniperca chuatsi* (Basilewsky), and *Pelteobagrus vachelli* (Richardson). In the longitudinal direction, fish preferred to stay in some specific sections like reaches 2, 4, 7, 8, 11, and 16. Since hydrology factors change greatly in different seasons, environmental characteristics vary along the reaches, and human activities play an important role in the fish behavior, it is concluded that great cross-season changes in hydrology lead to the differences in TS and fish assemblages and that geography characteristics, especially channel geography, together with human activities influence fish longitudinal distribution. This finding provides basic knowledge of spatiotemporal distribution and assemblages of fishes in the extended reaches downstream Gezhouba Dam. In addition, it offers implications for river management. It could also serve as reference of future research on fish habitat.

1. Introduction

Yangtze River is the largest river in China and the third largest in the world. It originates in mount Tunggula and flows into the East China Sea, with the total length of about 6300 kilometers. The complex geological environment and climate conditions bring Yangtze River a high biodiversity [1]. There are more than 360 species of freshwater fishes in the Yangtze River. This river exhibits a seasonal flow. And water temperature is high in the summer and low in the winter. Other ecological environments also vary from season to season. Gezhouba Dam (lowermost dam in the Yangtze River), part of the Three Georges water conservancy project, was the first dam in the Yangtze main stream and located in Yichang city, Hubei province, China, about 40 kilometers away downstream Three Georges Dam.

With the development of the acoustic methods, hydroacoustic technology has been used in fisheries research successfully for decades. It was often used to estimate fish abundance and distribution and observe fish behaviors like swimming speed or direction not only in the marine but also in the river. This technology provides a convenient and direct means to observe fish in situ without disturbance or damage of various aquatic systems [2], and it has been successfully

used to monitor the fish in river both vertically [3, 4] and horizontally [5]. Horizontal sonar is usually used in shallow waters to study the fish size, migration, and abundance in the upper layer waters [6–8], and the "dead-zone" of layer waters was detected [9], while vertical sonar has been well applied to understanding of fish distribution and density in various waters including seawater and freshwater [2, 4]. Vertical sonar is also widely used in Chinese rivers [10–12]. Hydroacoustic technique has many advantages over traditional methods in studying fish size, abundance, and swimming speed, and it reduces manpower and reflects the fish behavior in natural state and is also less environment-dependent.

There existed more than 90 fish species in downstream section of the Gezhouba Dam in 1980s at the beginning of its construction. Among these species, there are some endangered and protected species at China national animal protection level, such as Chinese sturgeon (*Acipenser sinensis* Gray, CR, in the IUCN Red list) and Dabry's sturgeon. However, investigations on the catches in last decades showed that the reduction trend in fish species and fishery resources has become apparent in this downstream section [13, 14]. Since the construction of Three Gorges Dam, spatiotemporal distribution of dominant species was influenced by the changes in hydrological conditions [15]. Therefore, protection of fishery resources is of great significance, and the knowledge of the fish distribution and behavior is essential for river management.

Many studies of fish size and density in the downstream area of the Gezhouba Dam were carried out. However, almost all of them focused only on the area near the dam and the limited species like Chinese sturgeon (*Acipenser sinensis* Gray) [12, 15, 16], and the fish distribution in extended section remains unknown.

In this present study, acoustic detections coupled with fish sampling and the other datum collected were performed and this study is aimed at (1) understanding the fish distribution in the extended river section in downstream reach of Gezhouba Dam and its differences in different seasons, (2) finding out relations between the fish behaviors and environmental factors, (3) providing valuable information for fishery management and fish potential habitat.

2. Materials and Methods

2.1. Study Area. The study area covers the protected river reaches from downstream Gezhouba Dam (rkm 1678 km) to Songzi River (rkm 1598), with the span of about 80 km (Yangtze River estuary was defined as river kilometer (rkm) 0). The geomorphology of this area changes apparently from mountainous to flat and its hydrological characteristics are regulated by Gezhouba Dam and Three Georges Dam. The average annual flow discharge and water level at Yichang Hydrological Monitoring Station (YHMS) from 1950 to 2000, respectively, were 13900 m^3/s and 43.8 m [17]. In the study area, there are two tributaries, one is Qingjiang River which flows into the Yangtze River, and the other named Songzi River flows out. The reaches are microbend straight from Gezhouba Dam (rkm 1768) to Yidu city (rkm 1633) and tortuous in the last 35 km (Figure 1). The geographical advantages (river flows through the whole Yichang city and the study area is located at the junction of the upper and middle Yangtze River) and economic development in this area result in frequent human activities like shipping, wading engineering, and sewage disposal, which brings about tremendous pressure to the protection of aquatic environment in this area.

2.2. Hydroacoustic Detections. Five acoustic detections were performed in different seasons from 2015 to 2016, using a fiberglass-reinforced plastic boat with the length 6.3 m and engine power 85 hp, respectively. The echo sounder was equipped with a 199 kHz BioSonics DT-X with a 6.7° split-beam transducer and set to a source level of 221.0 dB re 1 μPa at 1 m and a receiver sensitivity of −51.3 dB re 1 μPa. While detecting, the pulse duration was 0.4 ms and pulse rate was 5 pings/s.

The transducer was anchored on the right side of the boat and at a depth 0.5 m into the water vertically so as to sample the entire water column from 1.5 m below the water surface to 0.5 m above the bottom. The vertical motion detection was performed at a speed of about 8–10 km/h with zigzag transects using a GPS receiver (JRC, Tokyo, Japan). It took 4 days to complete one detection due to the limited longitudinal detection distance of approximately 25 km one day. All the detections were performed in the daytime from 9:00 am to 17:00 pm (waterway transports make the detection in the night dangerous).

2.3. Fish Sampling. Fishing with various gillnets (6, 8 cm) was carried out to obtain catches and fish species. Investigations on catches were conducted in July, November, December 2015, and January 2016. Two different habitat types were selected to investigate catches and these two habitats were classified into running water area with fast flows and pool water area with smooth water surface. In the running water area, drift nets were used to fish, while in the pool water area, set gill nets were used. Body length (in millimeter) and weight (in grams) of each fish were measured. The fish sampling area covered the 20 km downstream reach from Gezhouba Dam.

2.4. River Environment. In river environment description, the waterway kilometrage was divided according to channel chart supplied by the Yangtze River navigation agencies. Frequency of the human activities was divided into two categories, frequent or less. Frequent category was classified into two main types: wading engineering (type I) and anchorage zone (type II), and less frequent category refers to nonwading engineering and nonanchorage zone as previously mentioned (Table 1).

The data of water level and flow discharge were obtained from China Three Gorges Corporation. The detection date was divided into two periods, wet seasons (area I) and flood seasons (area II) (Figure 2).

2.5. Acoustic and Fish Density Analysis. Acoustic data were processed by Echoview software v. 4.9 (Myriax Pty Ltd, Hobart, TAS, Australia) with times-varied gain (TVG) of

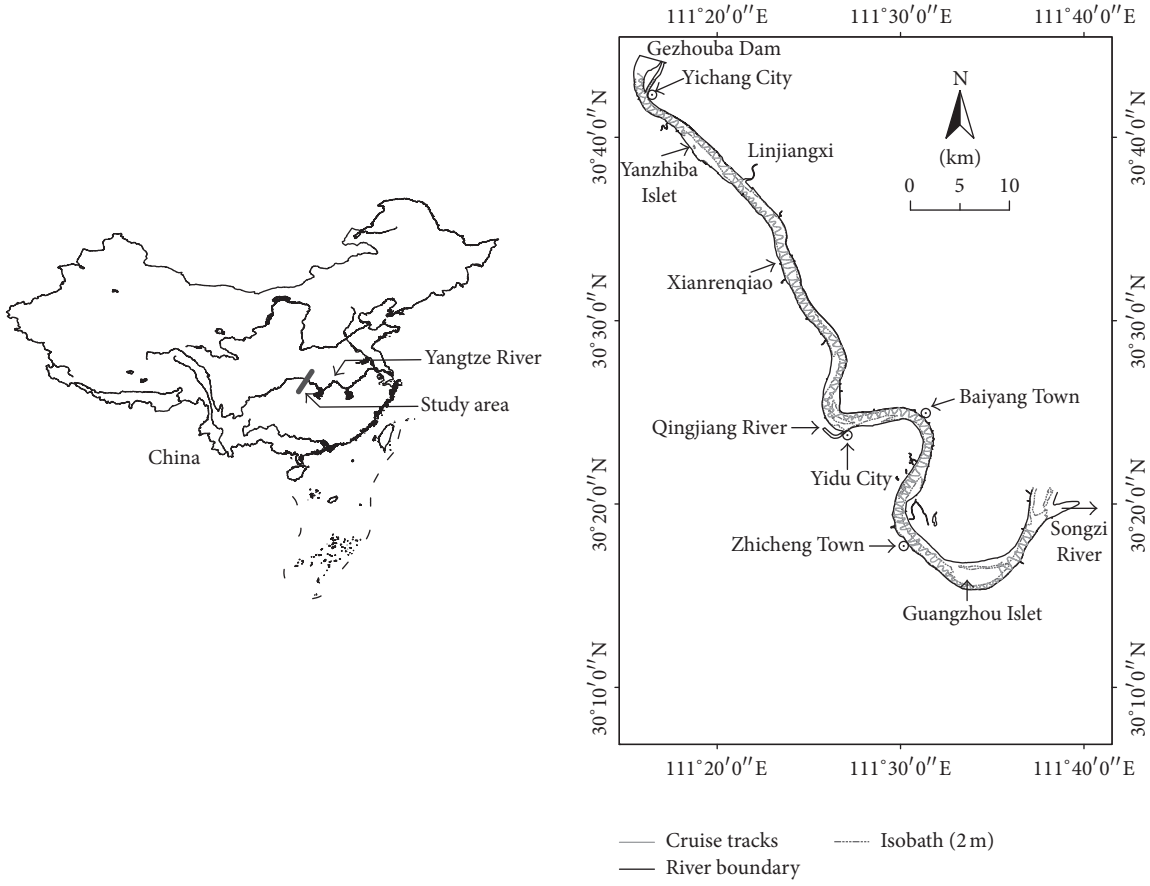

Figure 1: Study area, about 85 km in downstream reach of Gezhouba Dam, Yangtze River.

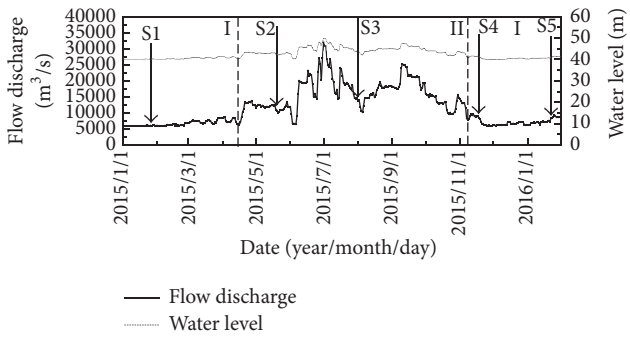

Figure 2: Flow discharge and water level in study area, 85 km downstream Gezhouba Dam, Yangtze River, 2015-2016.

20 log R. However, not all the acoustic data were chosen. Data from water surface to 1 m below surface was filtered through a straight line due to the movement of vessels and the existence of "dead-zone." In the same way, data of 0.5 m above the river bottom were also removed. Only the data of 1 m under the water surface and 0.5 m above river bottom were retained to be analyzed. Some noise echoes were manually identified and deleted. In the single-echo detection (SED) echogram, the maximum one-way gain compensation was set to 10 dB with TS threshold being −65 dB so as to exclude the echoes of fish below threshold value. When 4 single echoes were detected from one target with a maximum gap of 2 pings, one acceptable fish track detection (FTD) was obtained. Then information of every individual fish, such as TS, depth in water, location, and so on, was exported. The total length of every individual fish was usually calculated by a typical version equation: TS = 19.1 × log (TL) − 0.9 × log (Frequency) − 62.0 (Love, 1971) [18].

Fish density algorithm was calculated as follows:

$$\overline{\sigma}_{bs} = 10^{TS/10} \left(\mathrm{m}^2\right)$$
$$\rho_{vS} = \frac{S_v}{\overline{\sigma}_{bs}} \left(\mathrm{m}^{-3}\right). \quad (1)$$

$\overline{\sigma}_{bs}$ is the mean backscattering cross-section of all species (m^2), ρ_{vS} is the volumetric fish density in the region (fish/m^3), and S_v is the linear mean S_V value for the region (m^2/m^3).

3. Results

3.1. Assemblages of Fishes. Totally, 5687 fishes collected belong to 4 orders, 11 families, 38 genera, and 53 species. Of these 53 species, 13 species whose percentage (% N), respectively, exceeded 1% of the total number of catches

Table 1: Parameters of the divided reaches.

Reach ID	Left rank	Right rank	Human activity	Channel geography
1	Revetment	Revetment	Less	Curing
2	Revetment	Mountain	Less	Curing
3	Revetment	Revetment	Less	Straight
4	Revetment	Mountain and riffle	Frequent (II)	Straight
5	Revetment	Revetment	Less	Straight
6	Revetment	Revetment	Less	Straight
7	Revetment and riffle	Revetment and riffle	Frequent (II)	Straight
8	Mountain	Revetment and riffle	Less	Curing
9	Revetment and riffle	Revetment and riffle	Frequent (I)	Straight
10	Revetment	Revetment and riffle	Less	Straight
11	Mountain	Revetment and riffle	Less	Curing
12	Revetment	Revetment and riffle	Less	Straight
13	Revetment	Revetment	Less	Straight
14	Revetment	Revetment	Frequent (I)	Straight
15	Revetment and riffle	Revetment	Less	Curing
16	Revetment and riffle	Mountain	Less	Curing and straight

(5687) together account for 92.84% of the total number and 87.43% of the total weight of all catches. The breeding seasons of these 13 species are all in flood seasons about from March to August. 5 species are peculiar to the upper reaches of the Yangtze River whose stays are related to the lock and opening and flow discharge of Three Gorges Dam and Gezhouba Dam (Table 2).

3.2. Fish Vertical and TS Distribution. TS and TD (target depth) were obtained by Echoview analysis. Mean TS of the five detections were −59.98 dB, −54.70 dB, −56.16 dB, −57.90 dB, and −59.17 dB, respectively, and the mean target depth was 12.06 m, 11.47 m, 12.78 m, 13.72 m, and 12.44 m, respectively. Five acoustic detections indicated that differences of main TS distribution in various months were more significant than that of TD. The results of TS detection, respectively, in January 2015 November 2015, and January 2016 mainly ranged from −63 dB to −58 dB, while TS detection in May and July 2015 mainly ranged from −58 dB to −52 dB. In other words, target length converted from D1, D4, and D5 was bigger than that from D2 and D3 after using Love's TS-TL equation. Signals of TS > −30 dB were founded in each of five detections and they were maybe sent back by Chinese sturgeon (*Acipenser sinensis* Gray) [12]. The results of five TD detections concentrated in the depth layer from 5 to 15 m and

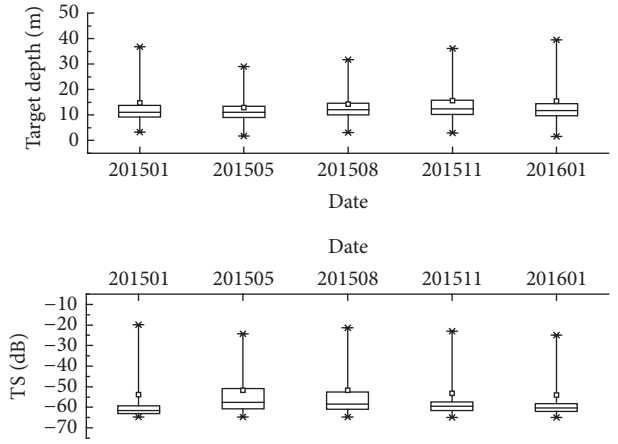

Figure 3: Fish vertical and TS distribution of the five hydroacoustic detections.

no obvious differences were found between these detections (Figure 3).

3.3. Fish Longitudinal Distribution. Fish longitudinal distribution was displayed by the fish density (ind/1000 m^3). Eighty kilometers of distance from the Gezhouba Dam to Songzi River was divided into 5 km interval reaches according to the river geomorphology and there were 16 reaches in total. Shades of the color represented the area density. Black area represented high density and white represented low density.

The fish gathering places were different in the five acoustic detections. Fish longitudinal distribution differed greatly between the flood and wet season. B (the hydroacoustic detection in May 2015) found that fishes mainly were distributed in the first eight reaches, while C (the hydroacoustic detection in August 2015) found more even distribution of fishes. Few fishes were distributed in reach 9 and reach 14 with anchorage zone there, and fish preferred to stay in some specific reaches like reaches 2, 4, 7, 8 11, and 16 (Figure 4).

4. Discussion

Most of the studies by using hydroacoustic technology focused on fish biomass, size, and distribution in large estuaries, lakes, and rivers [3, 19, 20]. Few studies reported the research findings in the longer downstream river section of a dam. This study indicated that the combination of hydroacoustic technology and traditional fish sampling turned out to be an effective way to understand the fish spatiotemporal distribution and assemblages downstream Gezhouba Dam in different seasons. The results showed significant differences in fish longitudinal distribution and size in different seasons. Fish preferred to stay in the specific reaches where river channel was curving, where there were geographical riffles and less human activities. There may be three reasons for the results. First, great changes in hydrology in different seasons may result in the different fish longitudinal distribution, assemblages, and size. Second, the geography characteristics of river channel in this study area vary along the reaches,

Table 2: Catches catalogue downstream Gezhouba Dam, Yangtze River.

Species	Number (N)	% N	Weight (W)	% W	Mean TL
Coreius guichenoti (Bleeker)	1665	29.28	363385.10	36.88	275
Siniperca chuatsi (Basilewsky)	1492	26.24	199257.10	20.22	156
Pelteobagrus vachelli (Richardson)	642	11.29	51837.86	5.26	154
Rhinogobio cylindricus Günther*	330	5.80	25424.00	2.58	201
Parabramis pekinensis (Basilewsky)	237	4.17	80081.90	8.13	283
Siniperca scherzeri Steindachner	188	3.31	36476.70	3.70	214
Rhinogobio typus Bleeker	145	2.55	20825.20	2.11	244
Xenocypris davidi Bleeker	130	2.29	11253.90	1.14	196
Mystus macropterus (Bleeker)	113	1.99	19892.90	2.02	278
Xenocypris davidi Bleeker	108	1.90	12287.60	1.25	146
Leiocassis crassilabris Günther	95	1.67	6657.00	0.68	138
Carassius auratus (Linnaeus)	77	1.35	21265.30	2.16	167
Leptobotia elongata (Bleeker)*	58	1.02	12850.30	1.30	258
Cyprinus carpio Linnaeus	52	0.91	40802.30	4.14	169
Pseudolaubuca sinensis Bleeker	49	0.86	2858.80	0.29	173
Saurogobio dabryi Bleeker	42	0.74	2664.00	0.27	183
Pelteobagrus fulvidraco (Richardson)	35	0.62	2601.00	0.26	162
Silurus asotus Linnaeus	27	0.47	15022.70	1.52	281
Squalidus argentatus (Sauvage et Dabry)	24	0.42	678.60	0.07	122
Hemibarbus maculatus Bleeker	18	0.32	2689.80	0.27	187
Pseudobrama simoni (Bleeker)	16	0.28	658.90	0.07	145
Pelteobagrus nitidus (Sauvage et Dabry)	14	0.25	309.50	0.03	128
Leiocassis longirostris Günther	13	0.23	4842.30	0.49	307
Hypophthalmichthys molitrix (Cuvier et Valenciennes)	11	0.19	2320.80	0.24	212
Coreius guichenoti (Sauvage et Dabry)*	10	0.18	5494.60	0.56	360
Squaliobarbus curriculus (Richardson)	9	0.16	2442.50	0.25	280
Silurus meridionalis Chen	9	0.16	12231.90	1.24	545
Megalobrama amblycephala Yih	8	0.14	5533.70	0.56	371
Pseudobagrus pratti Günther	7	0.12	327.20	0.03	184
Hemiculter bleekeri Warpachowsky	6	0.11	103.40	0.01	128
Pseudobagrus truncates (Regan)	6	0.11	102.00	0.01	117
Hemiculter leucisclus (Basilewsky)	5	0.09	204.90	0.02	123
Ctenopharyngodon idellus (Cuvier et Valenciennes)	5	0.09	13477.81	1.37	606
Tinca tinca (Linnaeus)	5	0.09	1690.90	0.17	284
Culter alburnus Basilewsky	5	0.09	2185.60	0.22	167
Odontobutis obscura (Temminck & Schlegel)	3	0.05	34.40	<0.01	10
Hyporhamphus intermedius (Cantor)	3	0.05	317.90	0.03	201
Jinshaia sinensis (Sauvage et Dabry)*	3	0.05	147.50	0.01	101
Parabotia fasciata Dabry	2	0.04	82.40	0.01	188
Lepturichthys fimbriata (Günther)	2	0.04	11.80	<0.01	116
Culter molitorella (Cuvier et Valenciennes)	2	0.04	170.70	0.02	219
Culter mongolicus mongolicus (Basilewsky)	2	0.04	1090.50	0.11	375
Culter oxycephaloides Kreyenberg et Pappenheim	2	0.04	1016.10	0.10	431
Myxocy prinus asiaticus (Bleeker)	2	0.04	235.40	0.02	183
Pelteobagrus eupogon (Boulenger)	2	0.04	110.00	0.01	19
Saurogobio gymnocheilus Lo Yao & Chen	1	0.02	67.60	0.01	224
Opsariichthys bidens Günther	1	0.02	32.00	<0.01	15
Misgurnus anguillicaudatus (Cantor)	1	0.02	37.00	<0.01	162
Channa argus (Cantor)	1	0.02	781.50	0.08	432
Gobiobotia filifer (Garman)	1	0.02	7.50	<0.01	107
Aristichthys nobilis (Richardson)	1	0.02	59.40	0.01	180
Rhinogobio ventralis Sauvage et Dabry*	1	0.02	179.60	0.02	251
Spinibarbus sinensis (Bleeker)	1	0.02	224.10	0.02	267
Total	5687	100	985343.47	100	

Number (N), percentage number (% N), weight (in grams, W), percent weight (% W), and mean total length (mm, mean TL). $*$ means that this species is peculiar to the upper reaches of the Yangtze River.

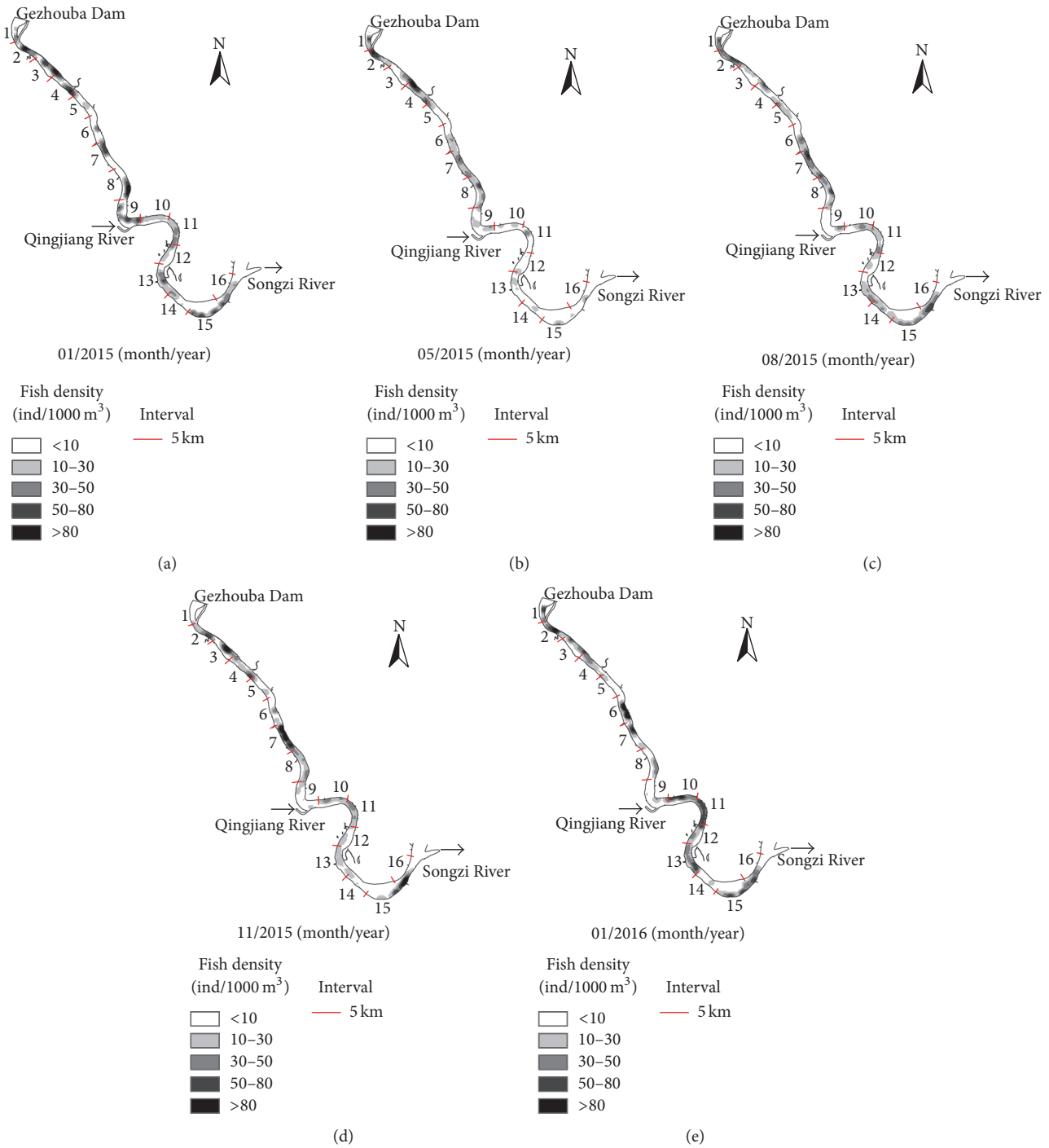

Figure 4: Fish longitudinal distribution of the five hydroacoustic detections. (a) Hydroacoustic detection in January 2015; (b) hydroacoustic detection in May 2015; (c) hydroacoustic detection in August 2015; (d) hydroacoustic detection in September 2015; (e) hydroacoustic detection in January 2016.

which may influence fish gathering. Third, human activity is also a limiting factor.

Fish distribution and abundance in rivers displayed longitudinal zonation from upstream to downstream [20, 21]. Water level changes from May to October in the Yangtze River, and many fishes migrate when water level changes seasonally in the Yangtze River. In flood seasons, hydrologic factors like water temperature, depth, flow velocity, flow discharge, and nutrients change rapidly. High flow discharge could bring high flow velocity and more nutrients, which play an important role in fish behaviors including migration, feeding, and reproduction. In addition, flood seasons are fish breeding periods for most of the species in this study area. Riverine fish assemblages change rapidly or gradually with

rapid or gradual changes in the physicochemical habitat [22]. Therefore, great differences in mean TS and fish longitudinal distribution between flood and wet seasons were found in this study.

Fish habitat is an essential component of ecosystem [23], while studies of fish habitats downstream Gezhouba Dam were merely limited to the habitats of large endangered individual Chinese sturgeon (*Acipenser sinensis* Gray) [24–27]. This study covers different reaches with different geography characteristics that are habitats of various fish species. Reaches 4 and 7 of this study area are straight geomorphologically with riffles where fish preferred to inhabit. Ranges of velocity and depth around the island are wider than those in other straight river sections without islands [28]. Reaches with riffles represent more complex environment beneficial for fish to avoid interference and predators. There also exists anchorage zone in reaches 4 and 7, and human waste such as deserted food and sanitary waste are discharged directly into the river here, which provides much more food and nutrients for these two reaches and make them an ideal habitat place for fish to feed and avoid disadvantage behaviors. Reaches 2, 8, 11, and 16 are curing section with mountains and riffles and with less human activities. Therefore, the environment of these reaches is much more natural and less disturbed externally. This may explain why fish preferred to stay in these reaches.

There are still some limitations in this study. Because of the fishing ban seasons (from March to May every year before 2015 and February to May from 2016), fish sampling and hydroacoustic detections could not be conducted simultaneously. The calculation results of the corresponding fish length of five acoustic detections were 1.64 cm, 3.09 cm, 2.59 cm, 2.10 cm, and 1.80 cm, respectively, by using the typical version equation: $TS = 19.1 \times \log(TL) - 0.9 \times \log(\text{Frequency}) - 62.0$ [18]. However, these calculation results significantly differ from actual measurement results of fish length of the catches. Since few researches on conversion equations of TS values and fish length about fish species in Yangtze River were reported, there have been no appropriate equations to match these two results so far. According to the average annual flow discharge and water level at YHMS in the last 50 years (from 1950 to 2000) and the situation of hydroacoustic detection in recent years [12, 17], the periods of wet seasons and flood seasons are almost the same every year. They could be divided into flood seasons and wet seasons (Figure 2). Therefore, five hydroacoustic detections were conducted in these two seasons: three in the wet seasons and two in the flood seasons. What is more, high flow discharge (when flow discharge $> 20000\,m^3/s$) in the flood seasons brings high velocity and much more bubbles which make the hydroacoustic detection unsafe and inaccurate. Therefore five hydroacoustic detections were conducted in the two periods (Figure 2, wet seasons and flood seasons).

Previous studies focused on the distribution and spawning grounds of Chinese sturgeon [16, 24, 29] or fish assemblages and behaviors in the downstream zone adjacent to Gezhouba Dam. This research extended the study area to 80 km away from Gezhouba Dam to offer the knowledge of fish longitudinal distribution and size in different seasons. Our study results demonstrated that fish distribution was influenced by both environment factors and human activities. Fish habitat loss has become a big threat to aquatic biodiversity [1]. Although quantitative factors like velocity, dissolved oxygen, and fish assemblages are not measured, the reaches of Yangtze River reported by this study where fish preferred to inhabit could be considered as potential fish habitats, which would be helpful for future research on fish habitat. Furthermore, how Gezhouba Dam affects the fish is still unknown, but the effects of Gezhouba Dam on fish survival were exemplified by the Acipenseriformes [30, 31]. Researches on the effects of Gezhouba Dam and conservations for fish biodiversity are also essential in the future work.

Based on this study findings, the suggestions for river management are as follows.

(1) Fishing ban seasons may be adjusted to containing the whole flooding seasons especially July and August since the breeding seasons of dominant fish species such as *Coreius guichenoti* (Bleeker), *Siniperca chuatsi* (Basilewsky), and *Pelteobagrus vachelli* (Richardson) in this study area are in the flooding seasons.

(2) Strengthen the supervision over poaching and overfishing in the specific reaches mentioned in this study where fishes prefer to inhabit.

(3) Select wading engineering location scientifically to avoid the loss of fish habitat.

Competing Interests

The authors declare that they have no competing interests.

Acknowledgments

Thanks are due to the members of the Endangered Fish Conservation Group of the Yangtze River Fisheries Research Institute, Chinese Academy of Fishery Sciences. This study was funded by the research (The Postenvironmental Impact Assessment of the Gezhouba Dam on the Yangtze River), which was supported by the China Three Gorges Corporation (no. 0799564), and it was also supported by the National Natural Science Foundation of China (no. 31602160).

References

[1] C. Fu, J. Wu, J. Chen, Q. Wu, and G. Lei, "Freshwater fish biodiversity in the Yangtze River basin of China: patterns, threats and conservation," *Biodiversity & Conservation*, vol. 12, no. 8, pp. 1649–1685, 2003.

[2] J. Simmonds and D. Maclennan, *Fisheries Acoustics: Theory and Practice*, John Wiley & Sons, New York, NY, USA, 2nd edition, 2007.

[3] J. Guillard, M. Simier, J.-J. Albaret, J. Raffray, I. Sow, and L. Tito de Morais, "Fish biomass estimates along estuaries: a comparison of vertical acoustic sampling at fixed stations and purse seine catches," *Estuarine, Coastal & Shelf Science*, vol. 107, pp. 105–111, 2012.

[4] V. Samedy, M. Wach, J. Lobry et al., "Hydroacoustics as a relevant tool to monitor fish dynamics in large estuaries," *Fisheries Research*, vol. 172, pp. 225–233, 2015.

[5] A. Duncan and J. Kubecka, "Patchiness of longitudinal fish distributions in a river as revealed by a continuous hydroacoustic survey," *ICES Journal of Marine Science*, vol. 53, no. 2, pp. 161–165, 1996.

[6] J. J. Burczynski and R. L. Johnson, "Application of dual-beam acoustic survey techniques to limnetic populations of juvenile sockeye salmon (*Oncorhynchus nerka*)," *Canadian Journal of Fisheries & Aquatic Sciences*, vol. 43, no. 9, pp. 1776–1788, 1986.

[7] B. H. Ransom, S. V. Johnston, and T. W. Steig, "Review on monitoring adult salmonid (*Oncorhynchus* and *Salmo* spp.) escapement using fixed-location split-beam hydroacoustics," *Fisheries Research*, vol. 35, no. 1-2, pp. 33–42, 1998.

[8] J. Kubecka and M. Wittingerova, "Horizontal beaming as a crucial component of acoustic fish stock assessment in freshwater reservoirs," *Fisheries Research*, vol. 35, no. 1-2, pp. 99–106, 1998.

[9] F. R. Knudsen and H. Sægrov, "Benefits from horizontal beaming during acoustic survey: application to three Norwegian lakes," *Fisheries Research*, vol. 56, no. 2, pp. 205–211, 2002.

[10] X. Tan, M. Kang, J. Tao, X. Li, and D. Huang, "Hydroacoustic survey of fish density, spatial distribution, and behavior upstream and downstream of the Changzhou Dam on the Pearl River, China," *Fisheries Science*, vol. 77, no. 6, pp. 891–901, 2011.

[11] J. Tao, Y. Gao, Y. Qiao et al., "Hydroacoustic observation of fish spatial patterns and behavior in the ship lock and adjacent areas of Gezhouba Dam, Yangtze River," *Acta Ecologica Sinica*, vol. 30, no. 4, pp. 233–239, 2010.

[12] H. Zhang, C. Y. Wang, D. G. Yang, H. Du, Q. W. Wei, and M. Kang, "Spatial distribution and habitat choice of adult Chinese sturgeon (*Acipenser sinensis* Gray, 1835) downstream of Gezhouba Dam, Yangtze River, China," *Journal of Applied Ichthyology*, vol. 30, no. 6, pp. 1483–1491, 2014.

[13] G. L. Yu, Y. G. Xu, X. C. Tan, Z. L. Deng, and J. B. Chang, "Status of fisheries in the section below the Gezhouba Dam of the Yangtze River," *Acta Hydrobiologica Sinica*, vol. 23, pp. 662–669, 1999 (Chinese).

[14] Q. Ma, P. C. Lin, H. Z. Liu, W. X. Cao, and X. Gao, "Effects of the gillnets on fish resources in the Yichang reaches of the Yangtze River," *Sichuan Journal of Zoology*, vol. 33, pp. 762–767, 2014 (Chinese).

[15] J. P. Tao, Y. T. Gong, X. C. Tan, Z. Yang, and J. B. Chang, "Spatiotemporal patterns of the fish assemblages downstream of the Gezhouba Dam on the Yangtze River," *Science China Life Sciences*, vol. 55, no. 7, pp. 626–636, 2012.

[16] Y. Qiao, X. Tang, S. Brosse, and J. Chang, "Chinese Sturgeon (*Acipenser sinensis*) in the Yangtze River: a hydroacoustic assessment of fish location and abundance on the last spawning ground," *Journal of Applied Ichthyology*, vol. 22, no. 1, pp. 140–144, 2006.

[17] W. C. Yu and J. Y. Lu, *Evolution of the Yangtze River and its Regulation*, China Water Power Press, Beijing, China, 2005 (Chinese).

[18] R. H. Love, "Dorsal-aspect target strength of an individual fish," *Journal of the Acoustical Society of America*, vol. 49, no. 3, pp. 816–823, 1971.

[19] U. Krumme and A. Hanning, "A floating device for stationary hydroacoustic sampling in shallow waters," *Fisheries Research*, vol. 73, no. 3, pp. 377–381, 2005.

[20] R. M. Hughes and J. R. Gammon, "Longitudinal changes in fish assemblages and water quality in the Willamette River, Oregon," *Transactions of the American Fisheries Society*, vol. 116, no. 2, pp. 196–209, 1987.

[21] E. Habit, M. C. Belk, R. Cary Tuckfield, and O. Parra, "Response of the fish community to human-induced changes in the Biobío River in Chile," *Freshwater Biology*, vol. 51, no. 1, pp. 1–11, 2006.

[22] W. J. Matthews, "Fish faunal 'breaks' and stream order in the eastern and central United States," *Environmental Biology of Fishes*, vol. 17, no. 2, pp. 81–92, 1986.

[23] J. A. Stefferud, K. B. Gido, and D. L. Propst, "Spatially variable response of native fish assemblages to discharge, predators and habitat characteristics in an arid-land river," *Freshwater Biology*, vol. 56, no. 7, pp. 1403–1416, 2011.

[24] B. Kynard, Q. W. Wei, and F. E. Ke, "Use of ultrasonic telemetry to locate the spawning area of Chinese sturgeons," *Chinese Science Bulletin*, vol. 40, pp. 669–671, 1995.

[25] H. Du, Q. W. Wei, H. Zhang, Z. Liu, C. Wang, and Y. Li, "Bottom substrate attributes relative to bedform morphology of spawning site of Chinese sturgeon *Acipenser sinensis* below the Gezhouba dam," *Journal of Applied Ichthyology*, vol. 27, no. 2, pp. 257–262, 2011.

[26] X. Ban, Y. Du, H. Z. Liu, and F. Ling, "Applying instream flow incremental method for the spawning habitat protection of Chinese sturgeon (*Acipenser sinensis*)," *River Research & Applications*, vol. 27, no. 1, pp. 87–98, 2011.

[27] C. Wang, B. Kynard, Q. Wei, H. Du, and H. Zhang, "Spatial distribution and habitat suitability indices for non-spawning and spawning adult Chinese sturgeons below Gezhouba Dam, Yangtze River: effects of river alterations," *Journal of Applied Ichthyology*, vol. 29, no. 1, pp. 31–40, 2013.

[28] X. Ban, H. Du, and Q. W. Wei, "Fish preference for hydraulic habitat in typical middle reaches of Yangtze River, China," *Journal of Applied Ichthyology*, vol. 29, no. 6, pp. 1408–1415, 2013.

[29] H. Zhang, Q. W. Wei, B. E. Kyanrd, H. Du, D. G. Yang, and X. H. Chen, "Spatial structure and bottom characteristics of the only remaining spawning area of Chinese sturgeon in the Yangtze River," *Journal of Applied Ichthyology*, vol. 27, no. 2, pp. 251–256, 2011.

[30] Q. W. Wei, F. F. Ke, J. M. Zhang et al., "Biology, fisheries, and conservation of sturgeons and paddlefish in China," *Environmental Biology of Fishes*, vol. 48, no. 1–4, pp. 241–255, 1997.

[31] J. M. Wu, C. Y. Wang, H. Zhang et al., "Drastic decline in spawning activity of Chinese sturgeon Acipenser sinensis Gray 1835 in the remaining spawning ground of the Yangtze River since the construction of hydrodams," *Journal of Applied Ichthyology*, vol. 31, no. 5, pp. 839–842, 2015.

Hindawi Publishing Corporation
BioMed Research International
Volume 2016, Article ID 2758168, 9 pages
http://dx.doi.org/10.1155/2016/2758168

Research Article

Isolation, Identification, and Optimization of Culture Conditions of a Bioflocculant-Producing Bacterium *Bacillus megaterium* SP1 and Its Application in Aquaculture Wastewater Treatment

Liang Luo, Zhigang Zhao, Xiaoli Huang, Xue Du, Chang'an Wang, Jinnan Li, Liansheng Wang, and Qiyou Xu

Heilongjiang River Fisheries Research Institute, Chinese Academy of Fishery Sciences, Harbin 150070, China

Correspondence should be addressed to Qiyou Xu; xuqiyou@hrfri.ac.cn

Received 24 June 2016; Accepted 29 September 2016

Academic Editor: Kaiyu He

A bioflocculant-producing bacterium, *Bacillus megaterium* SP1, was isolated from biofloc in pond water and identified by using both 16S rDNA sequencing analysis and a Biolog GEN III MicroStation System. The optimal carbon and nitrogen sources for *Bacillus megaterium* SP1 were 20 g L^{-1} of glucose and 0.5 g L^{-1} of beef extract at 30°C and pH 7. The bioflocculant produced by strain SP1 under optimal culture conditions was applied into aquaculture wastewater treatment. The removal rates of chemical oxygen demand (COD), total ammonia nitrogen (TAN), and suspended solids (SS) in aquaculture wastewater reached 64, 63.61, and 83.8%, respectively. The volume of biofloc (FV) increased from 4.93 to 25.97 mL L^{-1}. The addition of *Bacillus megaterium* SP1 in aquaculture wastewater could effectively improve aquaculture water quality, promote the formation of biofloc, and then form an efficient and healthy aquaculture model based on biofloc technology.

1. Introduction

Bioflocculant is an active substance produced by growing microorganisms and is composed of macromolecular polymers, such as glycoprotein, polysaccharide, protein, cellulose, and nucleic acid [1–3]. Bioflocculant offers many advantages for suspended solids (SS) removal, such as high security and efficiency, low cost, being nontoxic, and producing no secondary pollution for the environment [4–10]. The use of bioflocculant for SS removal has been widely used in industrial, domestic, and building material and livestock wastewater treatment as a new water treatment agent [11–14]. Although there were some general reports of bioflocculant in wastewater treatment, relevant research and application of bioflocculant in aquaculture wastewater treatment have rarely been reported.

In recent years, the aquaculture industry had developed rapidly with a worldwide presence, especially in China. However, low feeding utilization rates caused approximately 75% of the aquaculture feed to remain as nitrogen and phosphorous in the wastewater [15]. Aquaculture wastewater was discharged arbitrarily into rivers, lakes, and ocean, resulting in eutrophication and even red tide disasters. Many efforts have sought to reduce and regulate the generation and emission of aquaculture wastewater, such as upscaling aquaculture wastewater treatment by microalgal bacterial flocs [16], application of probiotics in carp aquacultures [17], removal of organic matter from polluted coastal waters by floating bed phytoremediation [18], and the application of artificial wetlands in multistage aquaculture wastewater purification [19]. Biofloc technology as one of the most advanced aquaculture technology models has been widely applied in shrimp, tilapia, and carp pond cultures. Using biofloc technology produced more aquaculture products without significantly increasing the usage of the basic natural resources of water and land, minimized damage to the environment, and provided an equitable cost/benefit ratio to support economic and social sustainability [20–24].

Compared with industrial and domestic wastewater, aquaculture wastewater is mainly composed of carbon, nitrogen, phosphorous, and other nutrients. Aquaculture wastewater also has its own characteristics, such as fewer poisonous metal materials and lower concentrations of nitrogen, phosphorous, SS, and chemical oxygen demand (COD). Therefore, bioflocculant-producing bacteria could feasibly be added to ponds and then used to effectively treat aquaculture wastewater. The aim of the present study was basically developed by two sections. The first section was to isolate and identify a bioflocculant-producing bacterium from fish pond and to optimize its culture conditions. In the second section, the bioflocculant produced by *Bacillus megaterium* SP1 was applied in the aquaculture wastewater treatment to reduce the COD and inorganic nitrogen, promote the formation of biofloc, improve the utilization rate of nitrogen, and ultimately form a highly efficient and healthy aquaculture model suitable for China's pond aquaculture.

2. Materials and Methods

2.1. Biofloc Samples and Isolation of Bioflocculant-Producing Bacterium. Biofloc samples were collected by Imhoff cones from the carp biofloc technology pond at Hulan experimental station of Heilongjiang River Fisheries Research Institute in Heilongjiang Province, China (45.97°N, 126.63°E). The samples were stored at 4°C in sterile containers. First, each biofloc sample was homogenized and serially diluted in sterile water. Second, each dilution was spread on enrichment medium and incubated at 30°C for 72 h. Strains with different colony morphology were taken and repeatedly cultivated for purification, and the single pure colony was saved for later use. Third, each pure colony was spread on fermentation medium and cultured at 30°C in a rotary shaker at 160 r min^{-1} for 72 h. The culture broth was used to determine for flocculating efficiency. The strain with the highest flocculating efficiency and good several subcultures was selected as the bioflocculant-producing bacterium for further study. Kaolin suspensions at a concentration of 5 g L^{-1} were then used to evaluate the flocculating capability of a series of the culture. Among them, the enrichment medium included beef extract (3 g L^{-1}), peptone (10 g L^{-1}), and NaCl (5 g L^{-1}) and was amended with 1.8% agar. The fermentation medium included glucose (20 g L^{-1}), KH_2PO_4 (2 g L^{-1}), K_2HPO_4 (5 g L^{-1}), $MgSO_4{\cdot}7H_2O$ (0.5 g L^{-1}), $(NH_4)_2SO_4$ (0.2 g L^{-1}), NaCl (0.1 g L^{-1}), urea (0.5 g L^{-1}), and yeast extract (0.5 g L^{-1}).

2.2. PCR Amplification and Phylogenetic Analysis. The bacterial genomic DNA of strain SP1 was extracted using the E.Z.N.A.® Bacterial DNA Kit (Omega Bio-Tek, Inc., USA). PCR amplification of the 16S rDNA was performed with universal primers (27F, 5′AGAGTTTGATCCTGGCTCAG3′, and 1492R, 5′GGTTACCTTGTTACGACTT3′). The amplification system was composed of a total volume of 50 μL containing 3 μL of total DNA, 1 μL of 27F, 1 μL of 1492R, 1 μL of dNTP, 5 μL of 10x buffer, 0.6 μL of Taq DNA polymerase, and 38.4 μL of ddH_2O [25]. The reaction conditions were as follows: 94°C for 4 min followed by 30 cycles of denaturation at 94°C for 1.5 min, annealing at 55°C for 1 min, and primer extension at 72°C for 1.5 min and a final extension at 72°C for 10 min [26]. PCR products were purified using PCR production purification kit, and the purified PCR products were sent to Suzhou GENEWIZ Biotechnologies Co. Ltd. (China) for sequencing. The sequence results were submitted (accession number: KU529280) to the GenBank database. Software MEGA 6.0 was used to construct a phylogenetic tree by the neighbor-joining method [27].

2.3. Identification with Biolog GEN III MicroStation System. The Biolog GEN III MicroStation System is an automated microbial identification system based on aerobic metabolic activities without the labor-intensive requirements of conventional strips or panels. The strain SP1 was characterized using Biolog GEN III microplate (Biolog Inc., Hayward, CA, USA). GEN III plate contains 95 different carbon substrates, which is based on interpreting patterns of sole-carbon substrate utilization indicated by color development in a 96-well microtiter plate. By analyzing the similarity of the metabolic fingerprints between SP1 and standard strains in the kinetic database by Biolog Retrospect 2.0 Data Management Software, the strain was identified. Among them, when SIM is > 0.5 and DIST is < 5.00, this is a more satisfactory result [28].

2.4. Analysis of Flocculating Efficiency. The flocculating efficiency of the bioflocculant produced by the bacterial culture was measured by kaolin suspension. In general, 2 mL of the bioflocculant (the culture broth of strain SP1), 5 mL of $CaCl_2$ (1%, w/v), and 93 mL of kaolin suspension were mixed in a 200-mL beaker. The mixture was stirred at 180 r min^{-1} for 1.5 min and at 80 r min^{-1} for 3 min with a vortex mixer (QL-861, Shanghai Jingmi Instrument Co., Ltd., China) and then kept still for 10 min. The supernatant portion was absorbed to determine its optical density (OD) at 550 nm by a 752 spectrophotometer [4]. The steps for the blank control were similar to the above steps except that the culture broth of strain SP1 was replaced with distilled water. All assays were conducted in three duplicates. The flocculating efficiency was defined and calculated as follows:

$$\text{Flocculating efficiency}\,(\%) = \frac{(A_0 - A)}{A_0} \times 100, \quad (1)$$

where A_0 and A were OD_{550} of the blank control and of the supernatant, respectively.

2.5. Optimization of Culture Conditions. Experiments were designed in which carbon and nitrogen sources of fermentation medium were replaced by various carbon and nitrogen sources in fresh fermentation medium. The one-way medium was used to determine the flocculating efficiency for kaolin suspension and to select the optimum carbon and nitrogen source for strain SP1.

According to the one-way experiment results, specific carbon and nitrogen sources in the original fermentation medium were replaced by the optimum carbon and nitrogen sources for optimal performance. The four factors of carbon

Table 1: Screening of bioflocculant-producing bacterium and its flocculating ratio for kaolin suspension.

Number	Flocculating ratio (%)	Number	Flocculating ratio (%)	Number	Flocculating ratio (%)	Number	Flocculating ratio (%)
1	58.2 ± 1.3^{e}	12	65.1 ± 3.2^{d}	25	68.5 ± 1.9^{cd}	*37*	91.9 ± 2.2^{a}
2	62.1 ± 1.2^{e}	14	54.5 ± 2.1^{e}	26	75.9 ± 1.6^{c}	38	73.9 ± 1.5^{c}
3	66.9 ± 2.2^{d}	15	41.9 ± 1.8^{g}	27	64.2 ± 2.3^{d}	39	78.1 ± 4.2^{bc}
4	65.1 ± 0.9^{d}	16	51.6 ± 1.1^{f}	28	52.5 ± 1.2^{f}	40	68.5 ± 3.1^{d}
5	89.2 ± 0.8^{a}	17	66.7 ± 0.8^{d}	29	58.1 ± 0.9^{e}	41	76.1 ± 2.1^{bc}
6	65.1 ± 1.7^{d}	18	78.4 ± 2.1^{b}	30	62.9 ± 2.1^{d}	42	52.1 ± 3.6^{f}
7	75.4 ± 1.5^{bc}	19	76.1 ± 3.2^{bc}	31	57.2 ± 1.7^{e}	43	60.3 ± 1.5^{e}
8	68.1 ± 1.9^{d}	20	70.3 ± 1.5^{c}	32	56.6 ± 1.2^{e}	44	73.5 ± 0.8^{c}
9	62.1 ± 2.1^{e}	21	65.2 ± 3.5^{d}	33	75.2 ± 4.3^{bc}	45	66.5 ± 1.3^{d}
10	70.3 ± 0.7^{c}	*22*	80.9 ± 2.1^{b}	*34*	88.7 ± 3.5^{a}	*46*	88.2 ± 2.7^{a}
11	42.1 ± 0.6^{g}	23	49.9 ± 1.4^{f}	35	75.2 ± 2.4^{bc}	47	77.9 ± 1.6^{b}
12	72.5 ± 1.5^{bc}	24	50.2 ± 2.3^{f}	36	43.9 ± 1.6^{g}	*48*	86.1 ± 2.1^{a}

Note. Each value represents a mean ± SE ($n = 3$). Values in the line with different superscript letters are significantly different ($P < 0.05$).

source, nitrogen source, initial pH, and temperature were the major factors influencing flocculation and were selected to design $L_{16}(4^5)$ orthogonal experiment. The optimum culture conditions were obtained by the analysis of the orthogonal experiment results.

2.6. Preliminary Application in Wastewater Treatment of Aquaculture. The aquaria (90 × 55 × 45 cm) selected for the experimental tanks had 100 L of three types of water (aquaculture wastewater, Hulan river water, and urban domestic wastewater) with continuous aeration. Culture broth of strain SP1 containing 1×10^7 CFU mL^{-1} was added to the aquaria water samples by an adding ratio of 1×10^4 CFU mL^{-1} to evaluate its effect on wastewater, especially by comparing how the data changed before and after inoculation. The experiment was divided into three groups, each group containing three duplicates. The indexes of chemical oxygen demand (COD), total ammonia nitrogen (TAN), suspended solids (SS), and volume of biofloc (FV) were determined.

2.7. Analytical Methods. The COD and SS were determined using the methods given by the National Standard of China, TAN was determined by the YSI Professional Plus (YSI Incorporated, Yellow Springs, USA), FV was determined by sampling 1000 mL pond water into a series of Imhoff cones [29], and the volume of the floc plug accumulating on the bottom of the cone was determined 15 min following sampling [20].

2.8. Statistical Analysis. Data analysis was performed by one-way ANOVA using SPSS 17.0 software for Windows. Duncan's multiple range tests were used to identify differences among experimental groups, and the level of statistical significance was accepted as $P < 0.05$.

3. Results and Discussion

3.1. Isolation of Bioflocculant-Producing Bacterium. Approximately 48 isolates were selected from the biofloc samples (Table 1). However, only six strains with flocculating efficiency exceeding 80% were able to actively flocculate kaolin suspension, as measured after five or more subcultures. Among them, the bacterium named SP1 with the highest flocculating efficiency was selected as the bioflocculant-producing bacterium for further study.

3.2. Identification and Characterization of Bioflocculant-Producing Bacterium. Strain SP1 was a circular, smooth, white, rod-shaped, Gram-positive bacterium with fermented liquid that was brown and turbid. Molecular analysis based on 16S rDNA confirmed the strain SP1 to be a *Bacillus* sp.; therefore, it was named *Bacillus* sp. SP1. The nucleotide sequence obtained in the present study had been submitted to GenBank and assigned accession number KU529280. In the phylogenetic tree, strain SP1 and the other closest *Bacillus* strains were grouped together (Figure 1). Strain SP1 was further identified using the Biolog GEN III MicroStation System, which was Biolog's latest generation product for the testing and microbial identification of aerobic Gram-negative and Gram-positive bacteria because they were in the same test panel; Gram stain and other pretests were no longer needed [30]. The results showed that strain SP1 was *Bacillus megaterium* (probability 59.6%, SIM 0.596, and DIST 5.883) based on the carbon source metabolic characteristics (Table 2). Therefore, this strain was named *Bacillus megaterium* SP1.

Bioflocculants were produced by many microorganisms widely distributed in soils and waters [31]. More than 70 bioflocculant-producing microorganisms have been reported, such as *Bacillus subtilis* [5], *Bacillus firmus* [32], *Bacillus licheniformis* [33], *Bacillus mucilaginosus* [2], *Proteus mirabilis* [34], and *Klebsiella* sp. [35]. However, bioflocculant produced by *Bacillus megaterium* and its application in wastewater treatment have rarely been reported. It was found that the extracellular polymeric substances (EPS) from *Bacillus megaterium* TF10 exhibit a high flocculation activity [36]. One report of a *Bacillus megaterium* strain producing a biodegradable flocculant was observed for turbidity and arsenic removal during growth [37]. Another bioflocculant produced by *Bacillus megaterium* YWO-5 was used for

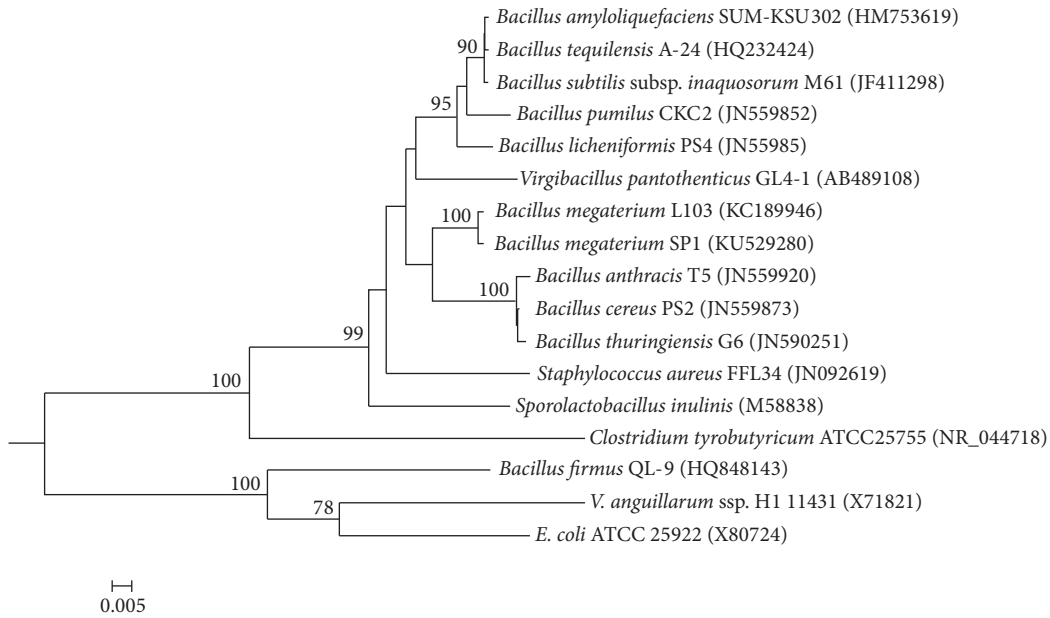

Figure 1: Neighbor-joining tree between *Bacillus megaterium* SP1 and its phylogenetically closest microorganisms based on the 16S rDNA. The scale bar indicates 0.005 substitutions per nucleotide position.

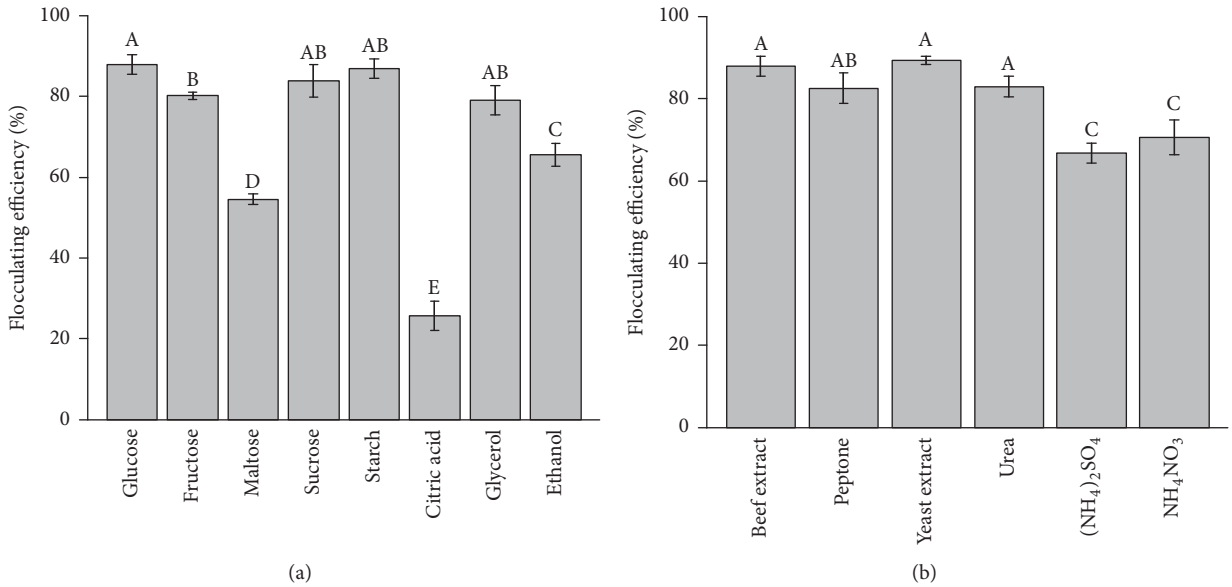

Figure 2: Effects of various carbon sources (a) and nitrogen sources (b) on flocculating efficiency. The bars are the respective standard deviations ($n = 3$), and values in the line with different superscript letters are significantly different ($P < 0.05$).

wastewater treatment [38]. In this work, the highly efficient bioflocculant-producing bacterium *Bacillus megaterium* SP1 was especially isolated from biofloc samples of aquaculture ponds for the purpose of accelerating biofloc formation and improving the water quality in aquaculture ponds.

3.3. Optimization of Culture Conditions

3.3.1. The Selection of the Optimum Carbon Source. Carbon source is a carbonaceous material used in microbial cells to supply energy for microbial growth, reproduction, and movement. To investigate the effect of various carbon sources on flocculating rate (in a kaolin suspension) under optimal culture conditions, the carbon source glucose (carbon content 0.4%) was used as fermentation medium in the control group and was replaced by various carbon sources (sucrose, fructose, maltose, soluble starch, citric acid, glycerol, and ethanol at the same concentration; other components remain unchanged) (Figure 2(a)). It was evident that glucose, fructose, sucrose, and soluble starch were suitable for bioflocculant production with the flocculating efficiency exceeding 80% after 72 h cultivation. The strain SP1 adapted well to a

Table 2: Carbon source metabolic characteristics of SP1 in GN III microplate.

Carbon source reactions	SP1
Polymers	
Dextrin	/
Glycogen	–
Tween 40	///
Sugars and sugar derivatives	
N-Acetyl-D-galactosamine	–
N-Acetyl-D-glucosamine	/
N-Acetyl-β-D-mannosamine	–
D-Arabitol	–
D-Cellobiose	–
D-Fructose	/
D-Fucose	/
D-Galactose	/
Gentiobiose	–
α-D-Glucose	/
3-Methyl-glucose	–
Myoinositol	–
α-D-Lactose	–
D-Salicin	–
D-Maltose	/
D-Mannitol	/
D-Mannose	–
D-Melibiose	–
β-Methyl-glucoside	/
Stachyose	–
D-Raffinose	/
L-Rhamnose	–
D-Sorbitol	–
Sucrose	+
D-Trehalose	/
D-Turanose	/
Methyl esters	
Methyl pyruvate	///
D-Lactic acid methyl ester	–
Carboxylic acids	
Acetic acid	–
Acetoacetic acid	/
Citric acid	–
Formic acid	/
L-Galactonic acid lactone	/
D-Galacturonic acid	/
D-Gluconic acid	/
D-Malic acid	–
L-Malic acid	+
D-Glucuronic acid	/
α-Hydroxy-butyric acid	–
β-Hydroxy-D,L butyric acid	/
ρ-Hydroxy-phenylacetic acid	–
D-Saccharic acid	–
Mucic acid	/
Carboxylic acids	
α-Keto butyric acid	–
α-Keto glutaric acid	–
L-Lactic acid	/
Propionic acid	–
Quinic acid	+
Bromosuccinic acid	/
Amides	
Glucuronamide	//
Amino acids, peptides, related chemicals	
L-Alanine	+
L-Aspartic acid	+
L-Glutamic acid	/
L-Histidine	/
Glycyl-L-proline	–
L-Pyroglutamic acid	/
D-Serine	–
L-Serine	–
D-Aspartic acid	–
L-Arginine	/
γ-Amino butyric acid	/
Nucleosides	
Inosine	–
Alcohols	
Glycerol	//
D-Glucose-6-phosphate	–
D-Fructose-6-phosphate	//
Else	
pH 5	+
pH 6	+
1% NaCl	+
4% NaCl	/
8% NaCl	/
1% sodium lactate	+
Fusidic acid	–
Troleandomycin	–
Rifamycin SV	–
Minocycline	–
Lincomycin	–
Guanidine HCl	–
Niaproof 4	–
Vancomycin	–
Tetrazolium violet	/
Tetrazolium blue	–
Nalidixic acid	–
Lithium chloride	/
Potassium tellurite	+
Aztreonam	/
Sodium butyrate	/
Sodium bromate	–

Note. +: positive response; −: negative response; /: borderline; //: mismatched positive; and ///: mismatched negative.

variety of carbon sources; the specific flocculating rates of glucose and soluble starch were 87.9% and 86.8%, respectively. Therefore, glucose was chosen as the optimum carbon source of strain SP1 because it had the highest flocculating activity and it has the lowest cost.

3.3.2. The Selection of the Optimum Nitrogen Source. Nitrogen sources provide the raw material for microbial amino acid synthesis. The effect of various nitrogen sources on the flocculating efficiency (in a kaolin suspension) after 72 h cultivation was observed. Beef extract, peptone, urea, $(NH_4)_2SO_4$, and

Table 3: The orthogonal experiment $L_{16}(4^5)$ of optimization of culture conditions.

	A ($g\,L^{-1}$)	B ($g\,L^{-1}$)	C (°C)	D	E	Flocculating ratio
1	1 (10.0)	1 (0.2)	1 (20)	1 (7.0)	1	0.785
2	1	2 (0.5)	2 (25)	2 (6.5)	2	0.813
3	1	3 (0.8)	3 (30)	3 (6.0)	3	0.839
4	1	4 (1.0)	4 (35)	4 (5.5)	4	0.765
5	2 (15.0)	1	2	3	4	0.786
6	2	2	1	4	3	0.822
7	2	3	4	1	2	0.806
8	2	4	3	2	1	0.836
9	3 (20.0)	1	3	4	2	0.840
10	3	2	4	3	1	0.866
11	3	3	1	2	4	0.858
12	3	4	2	1	3	0.856
13	4 (25.0)	1	4	2	3	0.788
14	4	2	3	1	4	0.906
15	4	3	2	4	1	0.827
16	4	4	1	3	2	0.808
I	0.800	0.800	0.818	0.838	0.828	
II	0.812	0.851	0.820	0.824	0.817	
III	0.855	0.833	0.855	0.825	0.826	
IV	0.832	0.816	0.806	0.813	0.829	
R	0.055	0.052	0.049	0.025	0.002	

Note. A: glucose; B: beef extract; C: culture temperature; D: medium initial pH; and E: blank control.

NH_4NO_3 replaced yeast extract (nitrogen content 0.03%) at the same concentration which was shown in Figure 2(b). The flocculating efficiency of six different nitrogen sources ranged from 66.88% to 89.37% and illustrated that certain nitrogen sources had a greater influence on the flocculating activity for the strain SP1. Specifically, beef extract and yeast extract produced bioflocculant with the flocculating efficiency exceeding 85% after 72 h cultivation. As a result, the beef extract was chosen as the best nitrogen source of strain SP1 for further study because of its high flocculating efficiency, complicated composition, and abundant nutrition.

3.4. Optimization of Culture Medium and Culture Conditions by Using Orthogonal Experiments. Orthogonal test factors and levels for flocculation of strains SP1, including glucose, beef extract, culture temperature, and culture medium initial pH values (with A, B, C, and D), were shown in Table 2. Orthogonal experiments were conducted to determine the optimal culture conditions. Orthogonal experimental results were shown in Table 3. The results of the range analysis suggested that the flocculating efficiency was influenced by the following factors in the descending order: glucose > beef extract > culture temperature > culture medium initial pH.

Microbial growth is influenced by culture medium composition and various survival factors. Lower concentration of carbon and nitrogen sources keeps strains such as SP1 from getting enough nutrients, thus affecting its growth and flocculating efficiency of the bioflocculant. In contrast, higher concentrations of carbon and nitrogen sources can make higher concentrations of inhibitory substances that negatively affect microbial growth as well as the flocculating rate of bioflocculant [31, 39, 40]. Microbial activity and metabolism are related to temperature; the suitable temperature is beneficial to microbial growth and metabolic rate. It was generally believed that the optimum temperature for bioflocculant formation was between 25 and 35°C, with low temperatures slowing bacterial growth and high temperatures changing the structure of the protein or peptide chain included in the bioflocculant (leading to degeneration) [41]. Initial pH also can affect the growth of bioflocculant-producing bacteria; in general, the optimal pH value of bioflocculant-producing bacteria is from neutral to weak alkaline. For different microorganism, the optimum pH value is not the same [42].

In this study, the optimal factor combination for flocculating efficiency from the result above was $A_3B_2C_3D_1$: 20 g of glucose, 0.5 g of beef extract, culture temperature of 30°C, and a medium initial pH of 7. Under these optimum culture conditions, the flocculating efficiency of bioflocculant produced by strain SP1 for kaolin suspension was 94.32%.

3.5. Preliminary Application in Wastewater Treatment of Aquaculture. Based on the orthogonal experiment results, two types of wastewater and Hulan river water were treated under optimal conditions ($A_3B_2C_3D_1$), and the results were shown in Figure 3. The aquaculture wastewater quality after the treatment improved significantly. COD decreased from 35.6 to 12.8 $mg\,L^{-1}$ ($P < 0.05$), TAN decreased from 6.43 to 2.34 $mg\,L^{-1}$ ($P < 0.05$), SS decreased from 27.1 to 4.43 $mg\,L^{-1}$ ($P < 0.05$), and FV increased from 4.93 to 25.97 $mL\,L^{-1}$ ($P < 0.05$). Under optimal culture conditions, the strain SP1 produced bioflocculant for aquaculture wastewater with a better purification effect: the removal rate of COD was from 44.19% to 64.04%, the removal rate of TAN was from 33.83% to 63.61%, and the removal rates of the SS were all over 70%. Interestingly, the FV ratio increased from 255.25% to 426.35%, which demonstrated that adding the culture broth of strain SP1 to wastewater could effectively accelerate the formation of biofloc. Adding SP1 could not only solve the problem of accumulation of harmful substances in aquaculture water but also promote the volume of biofloc which could be eaten by fish, improve the efficiency of protein generation in fish, reduce the feed demand for fish, and increase the income gained from aquaculture [20, 43].

High levels of inorganic nitrogen such as ammonia nitrogen and nitrite nitrogen are harmful to fish and are regarded as a limiting factor to production in intensive aquaculture [44]. Compared with residential and industrial sewage, the aquaculture wastewater had its own characteristics with low pollutant concentration and large water flow. Nitrogen, phosphorus concentration, suspended solid content, and the COD of aquaculture wastewater are lower than those of other types of wastewater. Bioflocculant-producing bacteria can use these substances, which are harmful to the growth of fish, and produce bioflocculant with high flocculating

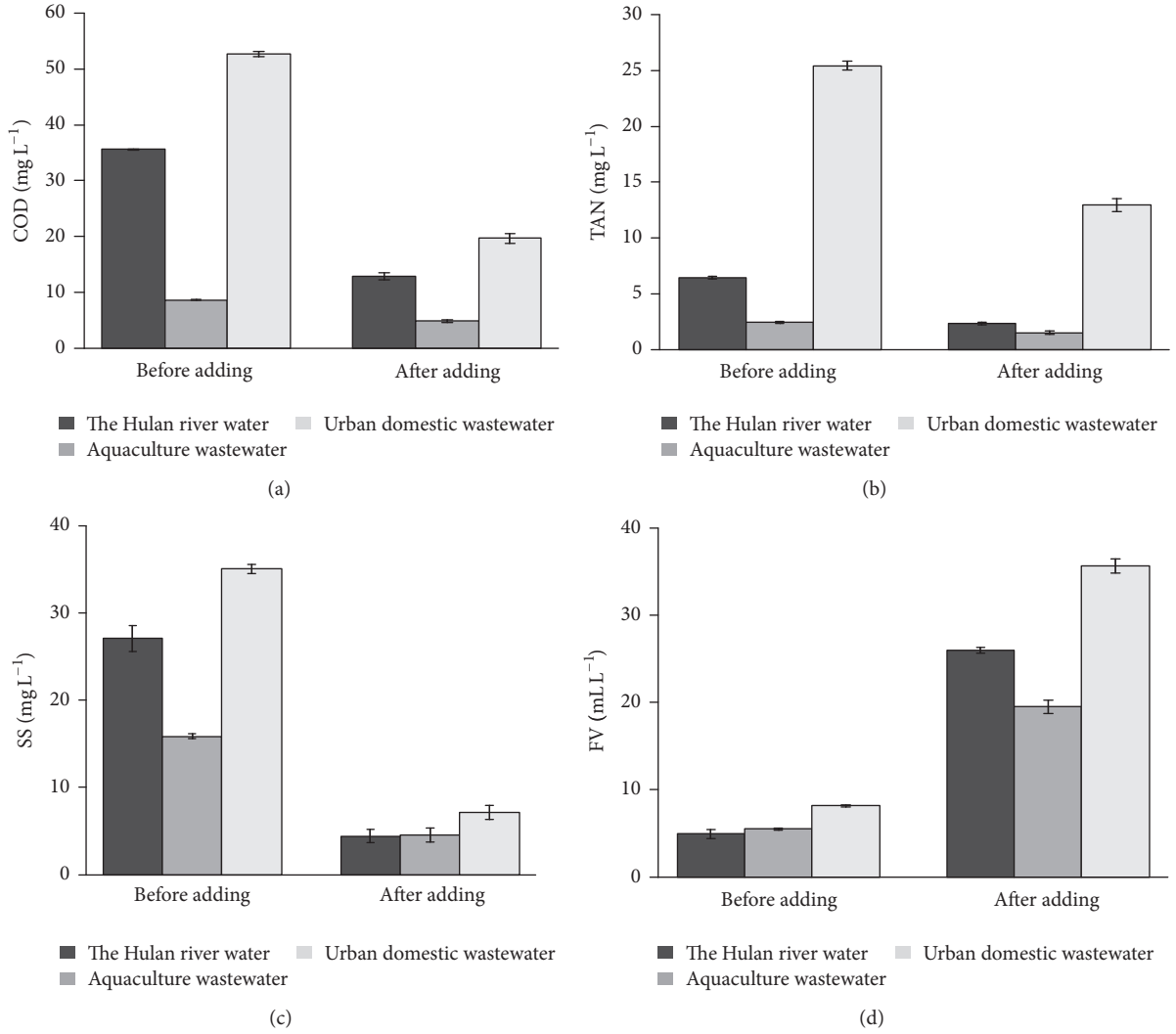

Figure 3: Effects of culture broth of strain SP1 on the chemical oxygen demand (COD), total ammonia nitrogen (TAN), suspended solids (SS), and volume of biofloc (FV) of aquaculture wastewater, the Hulan river water, and urban domestic wastewater. The bars are the respective standard deviations ($n = 3$).

activity. These bioflocculant-producing bacteria were successfully used to flocculate particulate and organic matter, improve water transparency and dissolved oxygen, reduce oxygen consumption, and thus improve environment and water quality of aquaculture.

It was of great significance to generate a mutual fusion between the bioflocculant technology of industrial wastewater treatment and biofloc technology of aquaculture to enhance the quality and efficiency of aquaculture and to promote characteristics of Chinese aquaculture that are being friendly to the environment, being healthy, and being sustainable for development.

4. Conclusions

In this study, a bioflocculant-producing bacterium *Bacillus megaterium* SP1 was isolated from biofloc in pond water. The optimal carbon and nitrogen sources for *Bacillus megaterium* SP1 were 20 g L^{-1} of glucose and 0.5 g L^{-1} of beef extract at 30°C and pH 7. Under these optimum culture conditions, the flocculating efficiency of bioflocculant produced by strain SP1 for kaolin suspension was 94.32%. It was demonstrated that adding strain SP1 to aquaculture wastewater could effectively reduce the COD, TAN, and SS and accelerate biofloc formation.

Abbreviations

COD: Chemical oxygen demand
TAN: Total ammonia nitrogen
SS: Suspended solids
FV: Volume of biofloc.

Competing Interests

There are no competing interests related to this paper.

Acknowledgments

This study was supported by the Central-Level Nonprofit Scientific Research Institutes Special Funds (HSY201407) and the China Agriculture Research System (CARS-46).

References

[1] J. Labille, F. Thomas, M. Milas, and C. Vanhaverbeke, "Flocculation of colloidal clay by bacterial polysaccharides: effect of macromolecule charge and structure," *Journal of Colloid and Interface Science*, vol. 284, no. 1, pp. 149–156, 2005.

[2] B. Lian, Y. Chen, J. Zhao, H. H. Teng, L. Zhu, and S. Yuan, "Microbial flocculation by *Bacillus mucilaginosus*: applications and mechanisms," *Bioresource Technology*, vol. 99, no. 11, pp. 4825–4831, 2008.

[3] J. Liu, J. Ma, Y. Liu, Y. Yang, D. Yue, and H. Wang, "Optimized production of a novel bioflocculant M-C11 by *Klebsiella sp*. and its application in sludge dewatering," *Journal of Environmental Sciences*, vol. 26, no. 10, pp. 2076–2083, 2014.

[4] R. Kurane, K. Hatamochi, T. Kakuno, M. Kiyohara, M. Hirano, and Y. Taniguchi, "Production of a bioflocculant by *Rhodococcus erythropolis* S-1 grown on alcohols," *Bioscience Biotechnology and Biochemistry*, vol. 58, no. 2, pp. 428–429, 1994.

[5] H. Yokoi, M. Shiraki, J. Hirose, S. Hayashi, and Y. Takasaki, "Flocculation properties of Xanthan produced by *Xanthomonas campestris*," *Biotechnology Techniques*, vol. 10, no. 10, pp. 789–792, 1996.

[6] C. G. Kumar, H.-S. Joo, J.-W. Choi, Y.-M. Koo, and C.-S. Chang, "Purification and characterization of an extracellular polysaccharide from haloalkalophilic Bacillus sp. I-450," *Enzyme and Microbial Technology*, vol. 34, no. 7, pp. 673–681, 2004.

[7] S. Deng, G. Yu, and Y. P. Ting, "Production of a bioflocculant by *Aspergillus parasiticus* and its application in dye removal," *Colloids and Surfaces B: Biointerfaces*, vol. 44, no. 4, pp. 179–186, 2005.

[8] R. Muñoz and B. Guieysse, "Algal-bacterial processes for the treatment of hazardous contaminants: a review," *Water Research*, vol. 40, no. 15, pp. 2799–2815, 2006.

[9] J. H. Yim, S. J. Kim, S. H. Ahn, and H. K. Lee, "Characterization of a novel bioflocculant, p-KG03, from a marine dinoflagellate, *Gyrodinium impudicum* KG03," *Bioresource Technology*, vol. 98, no. 2, pp. 361–367, 2007.

[10] Y. Zheng, Z.-L. Ye, X.-L. Fang, Y.-H. Li, and W.-M. Cai, "Production and characteristics of a bioflocculant produced by *Bacillus* sp. F19," *Bioresource Technology*, vol. 99, no. 16, pp. 7686–7691, 2008.

[11] S. B. Deng, R. B. Bai, X. M. Hu, and Q. Luo, "Characteristics of a bioflocculant produced by *Bacillus mucilaginosus* and its use in starch wastewater treatment," *Applied Microbiology and Biotechnology*, vol. 60, no. 5, pp. 588–593, 2003.

[12] S. Yan, N. Wang, Z. Chen et al., "Genes encoding the production of extracellular polysaccharide bioflocculant are clustered on a 30-kb DNA segment in *Bacillus licheniformis*," *Functional and Integrative Genomics*, vol. 13, no. 4, pp. 425–434, 2013.

[13] L. Y. Peng, C. P. Yang, G. M. Zeng et al., "Characterization and application of bioflocculant prepared by *Rhodococcus erythropolis* using sludge and livestock wastewater as cheap culture media," *Applied Microbiology and Biotechnology*, vol. 98, no. 15, pp. 6847–6858, 2014.

[14] S. S. Giri, M. Harshiny, S. S. Sen, V. Sukumaran, and S. C. Park, "Production and characterization of a thermostable bioflocculant from *Bacillus subtilis* F9, isolated from wastewater sludge," *Ecotoxicology and Environmental Safety*, vol. 121, pp. 45–50, 2015.

[15] R. Crab, Y. Avnimelech, T. Defoirdt, P. Bossier, and W. Verstraete, "Nitrogen removal techniques in aquaculture for a sustainable production," *Aquaculture*, vol. 270, no. 1–4, pp. 1–14, 2007.

[16] S. Van Den Hende, V. Beelen, G. Bore, N. Boon, and H. Vervaeren, "Up-scaling aquaculture wastewater treatment by microalgal bacterial flocs: from lab reactors to an outdoor raceway pond," *Bioresource Technology*, vol. 159, pp. 342–354, 2014.

[17] M. A. O. Dawood and S. Koshio, "Recent advances in the role of probiotics and prebiotics in carp aquaculture: a review," *Aquaculture*, vol. 454, pp. 243–251, 2016.

[18] L. Huang, J. Zhuo, W. Guo, R. G. M. Spencer, Z. Zhang, and J. Xu, "Tracing organic matter removal in polluted coastal waters via floating bed phytoremediation," *Marine Pollution Bulletin*, vol. 71, no. 1-2, pp. 74–82, 2013.

[19] S. Zhang, G. Li, X. Li, and L. Tao, "Multiple linear modeling of outflow nitrogen dynamics in vertical-flow constructed wetlands under two different operating states," *Ecological Engineering*, vol. 81, pp. 53–61, 2015.

[20] Y. Avnimelech, "Feeding with microbial flocs by tilapia in minimal discharge bio-flocs technology ponds," *Aquaculture*, vol. 264, no. 1–4, pp. 140–147, 2007.

[21] R. Crab, M. Kochva, W. Verstraete, and Y. Avnimelech, "Bio-flocs technology application in over-wintering of tilapia," *Aquacultural Engineering*, vol. 40, no. 3, pp. 105–112, 2009.

[22] E. Stokstad, "Down on the shrimp farm," *Science*, vol. 328, no. 5985, pp. 1504–1505, 2010.

[23] R. Crab, T. Defoirdt, P. Bossier, and W. Verstraete, "Biofloc technology in aquaculture: beneficial effects and future challenges," *Aquaculture*, vol. 356, pp. 351–356, 2012.

[24] Z. Zhao, Q. Xu, L. Luo, C. Wang, J. Li, and L. Wang, "Effect of feed C/N ratio promoted bioflocs on water quality and production performance of bottom and filter feeder carp in minimum-water exchanged pond polyculture system," *Aquaculture*, vol. 434, pp. 442–448, 2014.

[25] W. G. Weisburg, S. M. Barns, D. A. Pelletier, and D. J. Lane, "16S ribosomal DNA amplification for phylogenetic study," *Journal of Bacteriology*, vol. 173, no. 2, pp. 697–703, 1991.

[26] X. Zhang, J. Gao, F. Zhao, Y. Zhao, and Z. Li, "Characterization of a salt-tolerant bacterium *Bacillus* sp. from a membrane bioreactor for saline wastewater treatment," *Journal of Environmental Sciences*, vol. 26, no. 6, pp. 1369–1374, 2014.

[27] N. Saitou and M. Nei, "The neighbor-joining method: a new method for reconstructing phylogenetic trees," *Molecular Biology and Evolution*, vol. 4, no. 4, pp. 406–425, 1987.

[28] X.-J. Hu, Z.-J. Li, Y.-C. Cao, J. Zhang, Y.-X. Gong, and Y.-F. Yang, "Isolation and identification of a phosphate-solubilizing *bacterium Pantoea stewartii subsp. stewartii* g6, and effects of temperature, salinity, and pH on its growth under indoor culture conditions," *Aquaculture International*, vol. 18, no. 6, pp. 1079–1091, 2010.

[29] A. D. Eaton, L. S. Cleserci, and A. E. Greenberg, Eds., *Standard Methods for the Examination of Water and Waste Water*, American Public Health Association, Washington, DC, USA, 10th edition, 1995.

[30] P. Wragg, L. Randall, and A. M. Whatmore, "Comparison of Biolog GEN III MicroStation semi-automated bacterial identification system with matrix-assisted laser desorption ionization-time of flight mass spectrometry and 16S ribosomal RNA gene sequencing for the identification of bacteria of veterinary interest," *Journal of Microbiological Methods*, vol. 105, pp. 16–21, 2014.

[31] T. Zhang, Z. Lin, and H.-L. Zhu, "Microbial flocculant and its application in environmental protection," *Journal of Environmental Sciences*, vol. 11, no. 1, pp. 1–12, 1999.

[32] H. Salehizadeh and S. A. Shojaosadati, "Isolation and characterisation of a bioflocculant produced by *Bacillus firmus*," *Biotechnology Letters*, vol. 24, no. 1, pp. 35–40, 2002.

[33] I. L. Shih, Y. T. Van, L. C. Yeh, H. G. Lin, and Y. N. Chang, "Production of a biopolymer flocculant from *Bacillus licheniformis* and its flocculation properties," *Bioresource Technology*, vol. 78, no. 3, pp. 267–272, 2001.

[34] Z. Q. Zhang, S. Q. Xia, J. F. Zhao, and J. Zhang, "Characterization and flocculation mechanism of high efficiency microbial flocculant TJ-F1 from *Proteus mirabilis*," *Colloids and Surfaces B: Biointerfaces*, vol. 75, no. 1, pp. 247–251, 2010.

[35] A. K. Mandal, K. K. Yadav, I. K. Sen et al., "Partial characterization and flocculating behavior of an exopolysaccharide produced in nutrient-poor medium by a facultative oligotroph *Klebsiella sp*. PB12," *Journal of Bioscience and Bioengineering*, vol. 115, no. 1, pp. 76–81, 2013.

[36] S.-J. Yuan, M. Sun, G.-P. Sheng et al., "Identification of key constituents and structure of the extracellular polymeric substances excreted by *Bacillus megaterium* TF10 for their flocculation capacity," *Environmental Science and Technology*, vol. 45, no. 3, pp. 1152–1157, 2011.

[37] K. K. Devi and K. A. Natarajan, "Isolation and characterization of a bioflocculant from *Bacillus megaterium* for turbidity and arsenic removal," *Minerals and Metallurgical Processing*, vol. 32, no. 4, pp. 222–229, 2015.

[38] H.-C. Seo, S.-J. Yeo, H.-Y. Cho, and H.-C. Yang, "Some cultural characteristics of *Bacillus megaterium* YWO-5 producing bioflocculant for wastewater treatment," *The Korean Journal of Applied Microbiology and Biotechnology*, vol. 27, no. 1, pp. 80–85, 1999.

[39] Y. H. Wang, B. Dong, Y. B. Mao, and Y. S. Yan, "Bioflocculant-producing *Pseudomonas alcaligenes*: optimal culture and application," *The Chinese Journal of Environmental Science and Technology*, vol. 33, no. 3, pp. 68–71, 2010.

[40] R. Tao, Z. H. Yang, G. M. Zeng, E. J. Deng, and C. Li, "Screening and identification of bioflocculant-producing microorganism and optimal study on culture conditions," *The Chinese Journal of China Biotechnology*, vol. 25, no. 8, pp. 76–81, 2005.

[41] J. Bao-jun and Y. Jiang-mei, "The research status and development trend of microbial flocculant," *Physics Procedia*, vol. 24, pp. 425–428, 2012.

[42] W. Zhen, W. Kongxing, and X. Yumin, "Screening of flocculant-producing microorganisms and some characteristics of flocculants," *Biotechnology Techniques*, vol. 8, no. 11, pp. 831–836, 1994.

[43] M. A. Burford, P. J. Thompson, R. P. McIntosh, R. H. Bauman, and D. C. Pearson, "The contribution of flocculated material to shrimp (*Litopenaeus vannamei*) nutrition in a high-intensity, zero-exchange system," *Aquaculture*, vol. 232, no. 1–4, pp. 525–537, 2004.

[44] J. M. Ebeling, M. B. Timmons, and J. J. Bisogni, "Engineering analysis of the stoichiometry of photoautotrophic, autotrophic, and heterotrophic removal of ammonia-nitrogen in aquaculture systems," *Aquaculture*, vol. 257, no. 1–4, pp. 346–358, 2006.

Hindawi Publishing Corporation
BioMed Research International
Volume 2016, Article ID 5985987, 13 pages
http://dx.doi.org/10.1155/2016/5985987

Research Article

Microcystin Biosynthesis and *mcyA* Expression in Geographically Distinct *Microcystis* Strains under Different Nitrogen, Phosphorus, and Boron Regimes

Ankita Srivastava,[1] So-Ra Ko,[1] Chi-Yong Ahn,[1] Hee-Mock Oh,[1] Alok Kumar Ravi,[2] and Ravi Kumar Asthana[3]

[1]*Cell Factory Research Center, Korea Research Institute of Bioscience & Biotechnology, Daejeon, Republic of Korea*
[2]*Ocular Biochemistry, Dr. R. P. Centre for Ophthalmic Sciences, All India Institute of Medical Sciences, New Delhi 110029, India*
[3]*Centre of Advanced Study in Botany, Banaras Hindu University, Varanasi 221 005, India*

Correspondence should be addressed to Hee-Mock Oh; heemock@kribb.re.kr and Ravi Kumar Asthana; asthana.ravi@gmail.com

Received 1 June 2016; Accepted 1 September 2016

Academic Editor: Kaiyu He

Roles of nutrients and other environmental variables in development of cyanobacterial bloom and its toxicity are complex and not well understood. We have monitored the photoautotrophic growth, total microcystin concentration, and microcystins synthetase gene (*mcyA*) expression in lab-grown strains of *Microcystis* NIES 843 (reference strain), KW (Wangsong Reservoir, South Korea), and Durgakund (Varanasi, India) under different nutrient regimes (nitrogen, phosphorus, and boron). Higher level of nitrogen and boron resulted in increased growth (avg. 5 and 6.5 Chl *a* mg/L, resp.), total microcystin concentrations (avg. 1.185 and 7.153 mg/L, resp.), and *mcyA* transcript but its expression was not directly correlated with total microcystin concentrations in the target strains. Interestingly, Durgakund strain had much lower microcystin content and lacked microcystin-YR variant over NIES 843 and KW. It is inferred that microcystin concentration and its variants are strain specific. We have also examined the heterotrophic bacteria associated with cyanobacterial bloom in Durgakund Pond and Wangsong Reservoir which were found to be enriched in Alpha-, Beta-, and Gammaproteobacteria and that could influence the bloom dynamics.

1. Introduction

Bloom-forming freshwater cyanobacterial genera such as *Microcystis*, *Oscillatoria*, *Anabaena*, and *Nostoc* produce toxins and other bioactive compounds that can poison and kill humans and livestock [1, 2]. *Microcystis* sp. is the most frequently encountered one in freshwater bodies and is associated with production of hepatotoxic microcystin (MC) [3]. MCs are coded by the microcystins synthetase (*mcy*) gene cluster having 10 genes [4]. The gene cluster is transcribed in two polycistronic transcripts (*mcyABC* and *mcyDEFGHIJ*). The larger, *mcyD-J*, encodes a modular polyketide synthase (PKS) (*mcyD*), two hybrid enzymes comprising nonribosomal peptide synthetase (NRPS) and PKS modules (*mcyE* and *mcyG*), and enzymes putatively involved in the tailoring (*mcyJ*, *F*, and *I*) and transport (*mcyH*) of the toxins. The smaller operon, *mcyA-C*, encodes three NRPS enzymes. More than 89 MC variants have been described from natural blooms and laboratory cultures of cyanobacteria [2]. The physiological role of MCs in the producing organism is little understood. However, their roles were proposed in extracellular signaling and autoinduction [5, 6], photosynthesis [7], protein modulation [8], scavenging of oxygen radicals [9], and maintenance of colonies [10].

Parameters like light intensity, pH, temperature, nutrients, and trace metals could play a critical role in MCs production [11, 12]. Various field studies have demonstrated that nutrient enrichment of aquatic bodies by nitrogen (N) and/or phosphorus (P) could promote toxic blooms of *Microcystis* [13, 14]. In large aquatic systems highly complex interactions among the physical, chemical, and biological variables regulate the proliferation of *Microcystis* blooms and

toxin production, which could lead to contradicting results [13]. Laboratory studies have also shown the effects of nutrients on the growth and MC production of *Microcystis* [15, 16]. Only a few studies have focused on response of *Microcystis* to differing nutrient concentrations and trace metals on *mcy* transcription and MCs production [17, 18]. Recently, bacterial population associated with *Microcystis* bloom also received attention for its role in development of bloom [19]. A potential role of boron (B) in signaling and bacterial interspecies communication [20] aroused interest in studying its role in growth of *Microcystis* sp. and MC production in lab cultures, in addition to N and P.

A part of gene *mcyA* codes for the section of the condensation domain that contains the conserved motif C5 and is essentially required for MC biosynthesis in *Microcystis* sp. [4]. Therefore, we have monitored the *mcyA* gene expression and MC production and growth of three different strains of *Microcystis*, namely, *M. aeruginosa* NIES 843 (reference strain), *M. aeruginosa* KW (Wangsong Reservoir, South Korea), and *Microcystis* sp. (local pond, Durgakund, India), under selected nutrient regimes. As we had accessibility to natural algal bloom material from Durgakund Pond and Wangsong Reservoir, a seasonal variation in community dynamics of bacteria associated with cyanobacteria was also investigated.

2. Materials and Methods

2.1. Photoautotrophic Growth of Target Strains of Microcystis sp. and MC Analysis. Culture of *M. aeruginosa* NIES 843 strain and *M. aeruginosa* KW strain was maintained in BG-11 medium [21]. *M. aeruginosa* Durgakund strain was isolated from bloom samples collected from Durgakund Pond, Varanasi, India (25°17′20″N, 82°59′58″E), in which cyanobacterial blooms were noticed throughout the year. Our previous study characterized the real state of cyanobacterial bloom composition and the levels of MC variants in the target pond [12]. This pond lies 8.77 m above the sea level and has an area of 8010 m^2 with a mean depth 26.6 m. The pond is not connected to any river with exception of incoming water from adjacent temples and is often used for various religious activities. Samples were purified by repetitive subculturing in solid (soft agarose) and liquid culture media alternately [22]. The strains were grown in 165 mL sterilized BG-11 in 250 mL flasks. The cultures in all of the experiments were incubated at 25 ± 0.5°C with cool white fluorescent lights (80 μmol photons m^{-2} s^{-1}, 18 h light/6 h dark).

Growth and MC production curves of all three strains were determined under different nutrient (N, P, and B) regimes. Nutrients levels were selected based on the concentrations in BG-11 medium (comparatively nutrient rich media) and further decreased according to N/P ratio in cells [23]. *Microcystis* strains were individually grown in 250 mL culture flasks for 15 days in sterile BG-11 medium under low nitrate (0.015 mM), low phosphate (0.001 mM), and low boron (0.23 μM) separately. The growth of the cultures was followed up every alternate day. Samples were filtered (GF/C, Whatman, UK) and suspended in 80% acetone for overnight in dark (4°C). The supernatant was used to measure chlorophyll *a* (Chl *a*) (665 nm) according to Myers and Kratz [24]. A known volume of samples was collected four times (days 1, 3, 5, and 11) during the study period, filtered (GF/C, Whatman, UK), and stored until use for total (intracellular and extracellular) MC analysis. MC data are expressed as total MC concentration and as a ratio to Chl *a* to indicate the change in MC content. Extraction and estimation of three MC variants (MC-LR, -RR, and -YR) were carried out as previously described [12]. After starvation, 15 mL culture was washed and transferred separately to 250 mL flasks containing 150 mL sterilized BG-11 with higher N concentrations (1.5 mM and 17.6 mM) while P and B concentrations were kept constant as those of standard BG-11 medium. The experiment design was the same for all the three strains for higher P (0.1 mM and 0.23 mM) and B (23 μM and 46 μM) levels.

2.2. RNA Extraction, cDNA Synthesis, and Real-Time RT-PCR. *Microcystis* cultures (15 mL) were harvested on 11th day (exponential phase) by centrifugation at 6,000 ×g for 10 min, and the cell pellets were resuspended in 1 mL TRI Reagent® (Sigma-Aldrich, USA). Zirconia beads (0.5 g, 0.2 mm; Biospec, Bartlesville, OK, USA) were added to the cell suspension and cells were disrupted by vortex for 60 s. Total RNA was isolated according to the manufacturer's instructions for the reagent and resuspended in 30 μL of DEPC-H_2O. RNA integrity was verified by agarose electrophoresis with ethidium bromide staining. The quantity and quality of RNA were assessed with a NanoDrop ND-1000 Spectrophotometer (NanoDrop Technologies, Inc.). For construction of cDNA, total RNA was digested using DNase I (New England BioLabs, MA, USA) to remove genomic DNA according to the manufacturer's instructions. The RNA was reverse transcribed into cDNA in 20 μL reactions using iScript™ cDNA synthesis kit (Bio-Rad, Hercules, CA) according to the manufacturer's instructions. Negative controls containing no reverse transcriptase were run simultaneously.

Real-time RT-PCR was carried out using CFX 96 C 1000™ Thermal cycler (Bio-Rad, Hercules, CA). The reaction mixture consisted of 10 μL of SsoFast EvaGreen Supermix, 1 μL of each primer set for *mcyA* and 16S rRNA (Table 1), 1 μL 1 : 5 dilution of cDNA, and 7 μL of sterile Milli-Q-H_2O. Negative controls (without template DNA) were run simultaneously. The quantitative PCR program consisted of 94°C (5 min) and 40 cycles of 94°C (30 s), 60°C (30 s), and 72°C (30 s) with a final extension of 72°C (5 min). The annealing temperature for 16S rRNA gene was increased to 62°C. The fold change in the expression of the target gene relative to the control cells (grown in low nutrient concentrations) was calculated using CFX Manager Software (Version 2.1) and normalized with the expression of 16S rRNA (reference gene) [30].

2.3. Field Samples. Water samples were collected in 2 L acid washed glass bottles (Durgakund Pond) and 20 L polyethylene bottles (Wangsong Reservoir) from surface above a depth of 20 cm after some mixing and stored immediately at 4°C until the laboratory analysis was done. The samples were collected monthly from May 2010 to April 2011 and July 2010 to November 2010 during the cyanobacterial bloom only from Durgakund Pond and Wangsong Reservoir, respectively. The samples were filtered (0.2 μm cellulose nitrate

Table 1: Primers used in this study.

Primers	Sequence	Description	Reference
mcyA-Cd 1F (forward)	5′-AAAATTAAAAGCCGTATCAAA-3′	*mcyA* (condensation domain)	[25]
mcyA-Cd 1R (reverse)	5′-AAAAGTGTTTTATTAGCGGCTCAT-3′		
GM5F-GC-clamp[a,b]	5′-GC-clamp-CCTACGGGAGGCAGCAG-3′	16S rRNA gene DGGE fragment amplification	[26]
786R (reverse)	5′-CTACCAGGGTATCTAATC-3′	16S rRNA amplification for real-time RT-PCR	[27]
27F (forward)	5′-AGAGTTTGATCMTGGCTCAG-3′	Complete sequence of 16S rRNA for nested-PCR	[28]
1525R (reverse)	5′-AAGGAGGTGATCCAGCC-3′	Complete sequence of 16S rRNA for nested-PCR	[28]
907R (reverse)	5′-CCGTCAATTCCTTTGAGTTT-3′	16S rRNA gene DGGE fragment amplification	[29]

[a]GC-clamp: 5′-CGCCCGCCGCGCGCGGCGGGCGGGGCGGGGGCACGGGGGG-3′.
[b]GM5F (without GC-clamp) was used as forward primer for real-time RT-PCR.

filter, Sartorius, Germany) to harvest most of the bacteria on the same day of collection and stored (−20°C) until use for molecular analyses.

2.4. DNA Extraction, PCR, and DGGE. DNA was extracted from the filter by grinding in liquid nitrogen and suspending in TE buffer (pH 8.0, 10 mM Tris-HCl and 1 mM EDTA) followed by phenol/chloroform method [31]. A nested-PCR was carried out for the amplification of nearly complete sequence of 16S rRNA with primers 27F and 1525R (Table 1). PCR was performed in a 50 μL final volume of reaction mixture with 5 μL of 10× buffer, 5 μL of 2.5 mM dNTP mixture, 1.5 μL of the respective primer sets (10 pmol), 1 μL of template DNA, and 5 U of Ex-Taq DNA polymerase (Takara, Japan). The PCR protocol consisted of initial denaturation at 94°C (5 min) and 30 cycles of 94°C (30 s), 56°C (30 s), and 72°C (45 s) with a final extension of 72°C (10 min). This was followed by a touchdown PCR [32] with primers 341F (with 40 bp long-GC-clamp) and 907R (Table 1). The PCR protocol consisted of initial denaturation at 94°C (5 min) and 30 cycles of 94°C (45 s) and 72°C (45 s) with annealing temperature set to 65°C and decreased by 0.5°C at every cycle for 20 cycles, and then 15 additional cycles were performed with the annealing temperature at 55°C and a final extension of 72°C (10 min).

The amplified products were separated in a denaturing gradient gel of a 12% polyacrylamide gel [acrylamide-bisacrylamide (37.5 : 1, w/v)] containing a linear 30–60% denaturant gradient (100% denaturant corresponded to 7 M urea and 40% (v/v) formamide). DGGE was run for 18 h at 110 V on the DCode system (Bio-Rad, Hercules, CA, USA). The gel was stained with ethidium bromide and visualized by UV transillumination. Thereafter, the bands were excised from the DGGE gel and incubated in Milli-Q-water (30 μL) for 24 h at 4°C. The eluent was then again amplified using the same PCR condition and primers but without GC-clamp.

2.5. Cloning and Sequencing. The amplified PCR products were purified using the QIAquick® Gel Extraction Kit (Qiagen, Hilden, Germany) and ligated into the pGEM-T Easy Vector (Promega, Madison, WI) according to the manufacturer's protocols. They were transformed into HIT™ competent *Escherichia coli* DH5-α (RBC Bioscience, New Taipei, Taiwan) and plated on Luria-Bertani agar plates in the presence of ampicillin. The white colonies were selected and incubated in Luria-Bertani broth containing ampicillin (50 μg/mL). DNA was purified using the QIAprep® Spin Mini-Prep Kit (Qiagen, Hilden, Germany). The purified products were sequenced by Solgent Inc. (Daejeon, South Korea), using an ABI 3730XL automatic DNA sequence (Carlsbad, CA, USA).

2.6. Statistical Analysis. All experiments were carried out in triplicate with standard deviation (SD) represented as bars wherever necessary using Microcal™ Origin® Version 6.0. Effects of N, P, and B supplementation to the growth medium on total MCs production, Chl *a*, and MC content were statistically analyzed using multivariate analysis of variance (ANOVA). Data were explored using SPSS 16.0 software and log-transformed to give these an approximate normal distribution.

3. Results

3.1. Photoautotrophic Growth of the Target Strains in Different Nutrient Regimes (N, P, and B). Photoautotrophic growth of target strains was monitored in low levels of nutrients (N, 0.015 mM; P, 0.001 mM; B, 0.23 μM). These strains were transferred separately in medium having selected higher nutrient concentrations and growth behavior was monitored up to 15th d by measuring Chl *a* at periodic intervals (Figure 1). Chl *a* was significantly influenced by different concentrations of N ($F_{1,12} = 120$, $p < 0.001$), P ($F_{1,12} = 5.4$, $p < 0.05$), and B ($F_{1,12} = 26.4$, $p < 0.001$) in all three strains. Increased level of the N in the medium resulted in the higher Chl *a* yield (avg. 5 mg/L, 11th d) in the target strains. The yield was approximately 1.1 times higher in the cultures of all strains with 17.6 mM N. It was interesting that 100 times more concentration of N (1.5 mM) did not affect the Chl *a* yield (avg. 4.1 mg/L) in the target strains as compared to the growth in the lowest N concentration. The growth of Durgakund strain was lower as compared to NIES 843 and KW strains.

Likewise, the strains grown in varying levels of P behaved differently. The Chl *a* yield of the strains in low level of P (0.001 mM) was 1.67 times lower on an average basis as compared to the cultures with low level of N. Increase in the P concentration (100 times) in the growth medium increased the growth of the target strains by 1.21 times (avg. 3.4 mg/L)

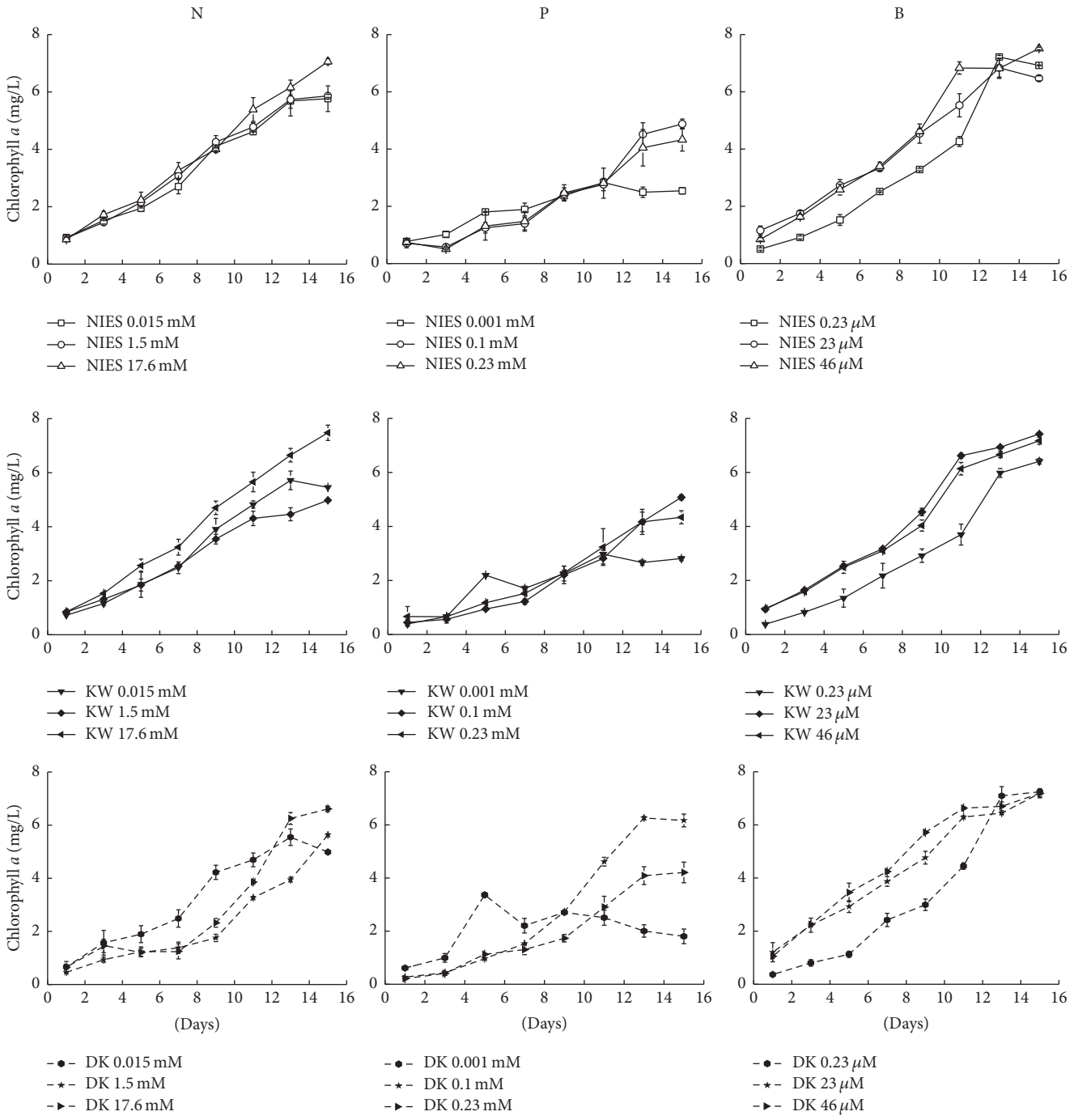

Figure 1: Growth curves of *M. aeruginosa* NIES 843, KW, and Durgakund (DK) strains under different concentrations of N, P, and B.

(Figure 1). The growth of Durgakund strain was better as compared to NIES 843 and KW strains. Decrease in the Chl *a* yield (1.1 times) of the target strains at 0.23 mM P indicated that there was no increase in the growth beyond a critical threshold level of P (0.1 mM). This was in contrast to the level of N in the cultures favoring the growth of the target strains. Interestingly, photoautotrophic growth of the strains was favored with increase in B levels (Figure 1). Average Chl *a* yield of the strains was 4.1, 6.2, and 6.5 mg/L in low (0.23 μM) and higher concentrations (23 and 46 μM), respectively.

3.2. Effect of Nutrient Concentrations on MC Variants. Samples were collected simultaneously from the same set of cultures on 1, 3, 5, and 11 d for MC analysis. Intracellular and extracellular MCs were referred to as total MC for each variant. All three MC variants (MC-LR, -RR, and -YR) were detected in both NIES 843 and KW strains at different N concentrations with predominance of MC-RR (Figure 2). MC-YR was not detected in cultures of Durgakund strain at any of the N addition experiments. Total MC was significantly influenced by N ($F_{1,12} = 653$, $p < 0.001$), P ($F_{1,12} = 1179$,

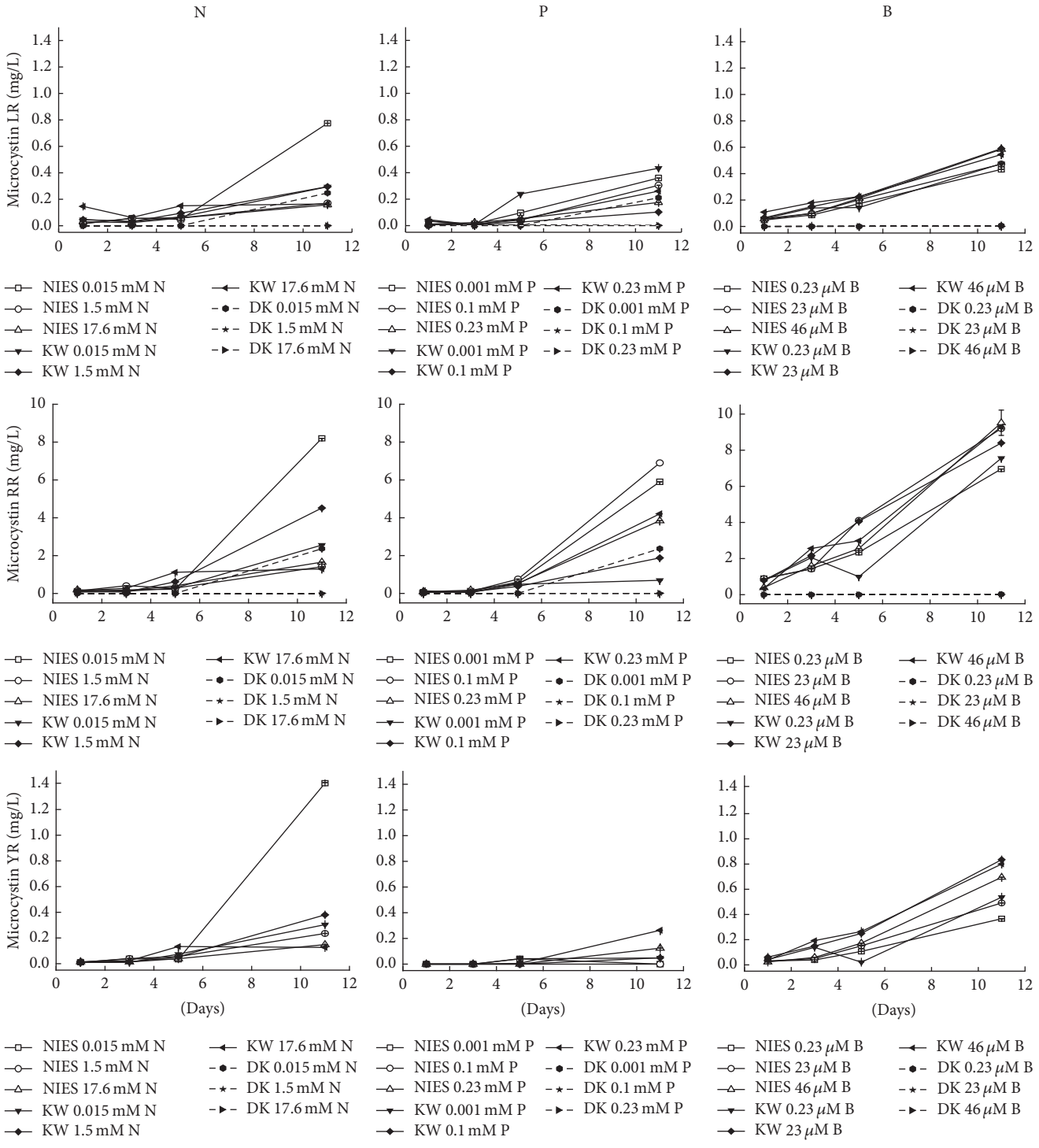

Figure 2: Variations in MC-LR, -RR, and -YR of *M. aeruginosa* NIES 843, KW, and Durgakund (DK) strains under different concentrations of N, P, and B.

$p < 0.001$), and B ($F_{1,12} = 1131$, $p < 0.001$) in the target strains. MC content was also significantly influenced by N ($F_{1,12} = 381$, $p < 0.001$), P ($F_{1,12} = 194$, $p < 0.001$), and B ($F_{1,12} = 718$, $p < 0.001$). The highest levels of MC-LR (0.77 mg/L), -RR (8.2 mg/L), and -YR (1.4 mg/L) were recorded at 0.015 mM N in NIES 843. However, at higher concentrations of N (1.5 and 17.6 mM), the same levels of MC variants were recorded in both NIES 843 and KW strains (Figure 2). In comparison, Durgakund strain had the lowest concentration of MC-LR and -RR.

Likewise MC-YR was not detected in Durgakund strain growing in any of the P concentrations while higher level of

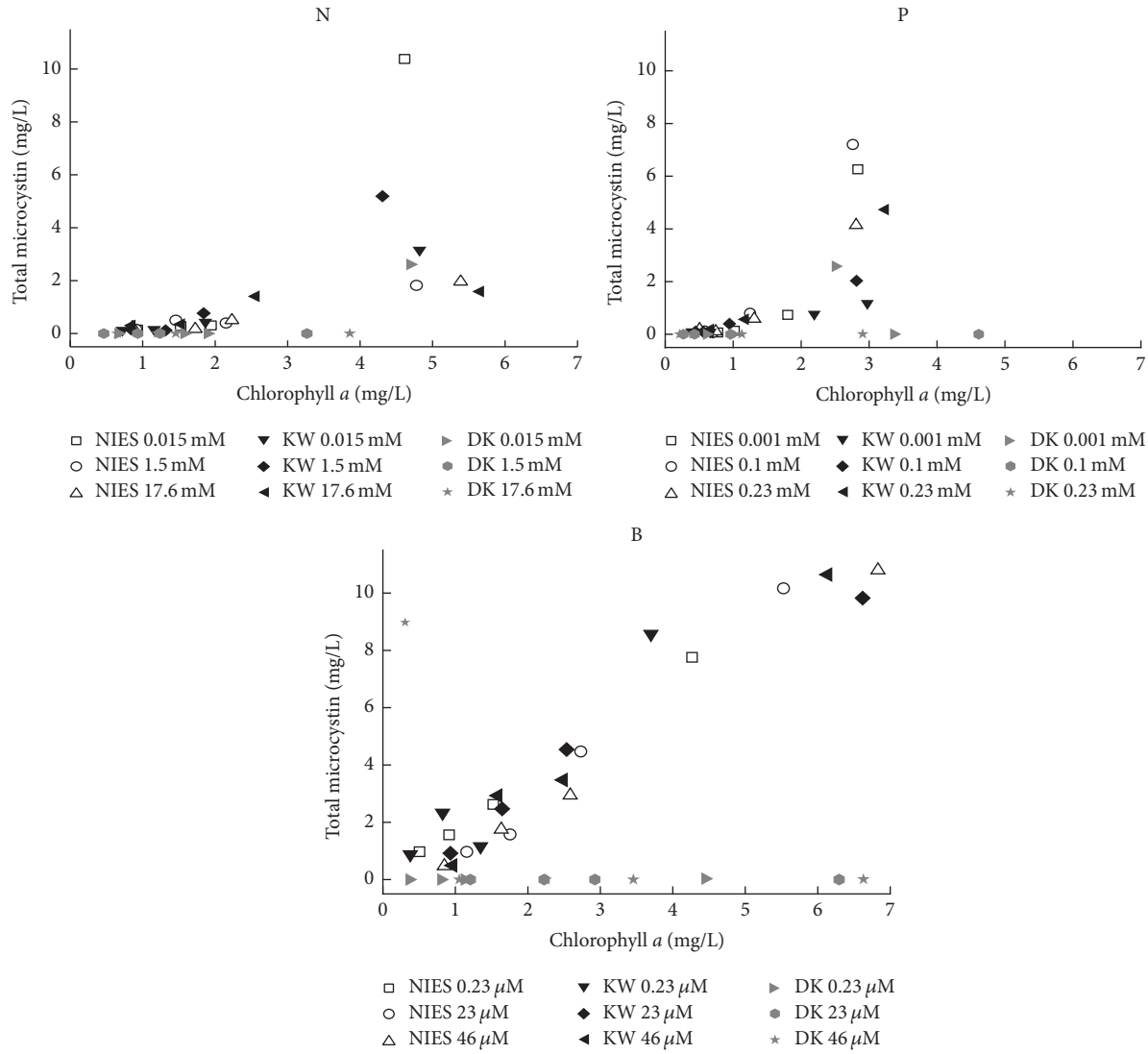

Figure 3: Total MC concentration as a function of chlorophyll *a* concentration in *M. aeruginosa* NIES 843, KW, and Durgakund (DK) strains under different concentrations of N, P, and B.

MC-YR was recorded in KW strain at 0.23 mM P. Highest level of MC-LR and -RR was recorded in NIES 843 strain followed by KW strain and Durgakund strain (Figure 2). Higher level of P (0.23 mM) favored the production of MC-LR, -RR, and -YR in NIES 843. MC-YR was again not detected in Durgakund strain at any of the B incubated cultures. Higher B concentrations favored all MC variants in both NIES 843 and KW strains (Figure 2).

The total MC concentration in the cultures of the target strains linearly increased with the Chl *a* concentration (Figure 3). Very high total MC concentration was observed under different concentrations of B in NIES 843 and KW strains while total MC concentration was much lower in DK strain under various N, P, and B concentrations (Figure 3). Highly significant correlation was observed between MC concentration and total MC content under variable concentrations of N, P, and B in the target strains (Figure 4).

3.3. Effect of Nutrient Concentrations on mcyA Expression. Real-time RT-PCR was used to measure the expression of *mcyA* at different nutrient concentrations (N, P, and B) in the target strains (Figure 5). *mcyA* transcript increased at 1.5 and 17.6 mM N relative to the control (0.015 mM N). Maximum increase (12.4-fold) in *mcyA* transcript was recorded in Durgakund strain and only 2.3-fold increase in NIES 843. *mcyA* transcript in KW strain decreased (0.19-fold) relative to the control at 17.6 mM N. However, *mcyA* transcript increased in the target strains at 1.5 μM N indicating a threshold level of N for optimum expression of *mcyA*. Similarly, increase in P levels (0.1 and 0.23 mM) increased the *mcyA* transcript in NIES 843 and Durgakund strains while only 0.23 mM P slightly increased the expression of *mcyA*. The maximum increase of *mcyA* transcript (10-fold) was recorded in NIES 843 at 0.1 mM P. In B-containing cultures, concentration-dependent increase in *mcyA* transcript was recorded in the

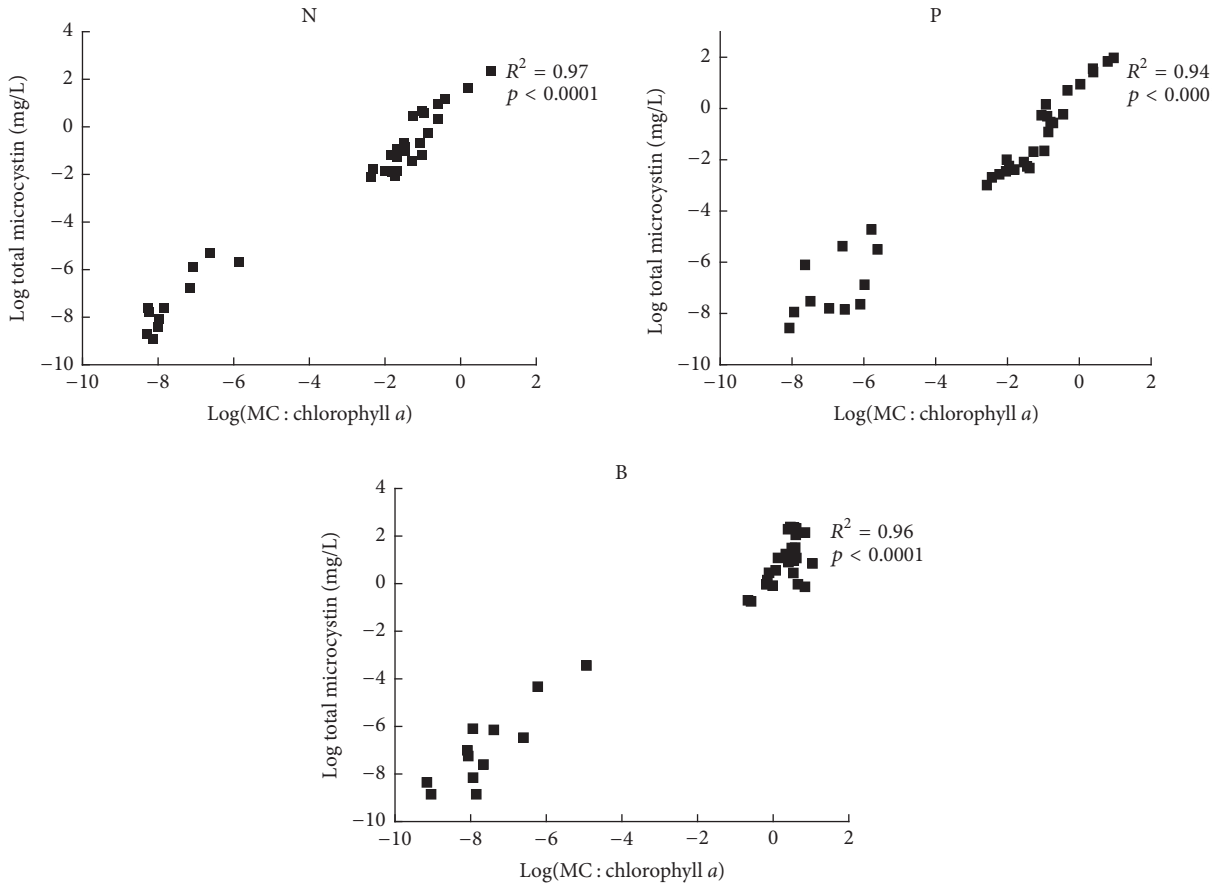

Figure 4: Relationship between MC content and total MC concentration in *M. aeruginosa* NIES 843, KW, and Durgakund (DK) strains under different concentrations of N, P, and B.

Table 2: Coefficient of determination (R^2) among chlorophyll *a*, microcystin concentrations and content, and *mcyA* expression in *Microcystis* strains (NIES 843, KW, and Durgakund)[a].

	Chlorophyll *a* (mg/L)	Total MC (mg/L)	MC content (mg/Chl *a*)	*mcyA* (fold change)
Chlorophyll *a*	1			
Total MC	0.110	1		
MC content	0.002	0.769***	1	
mcyA	0.000	0.083	0.087	1

MC: microcystin; Chl *a*: chlorophyll *a*.
[a]Calculations based on data at 11th d, *** p < 0.0001.

target strains. The maximum increase (19-fold) in *mcyA* transcript was recorded in NIES 843 at 46 μM B followed by Durgakund (2.8-fold) and KW strain (1.4-fold).

The correlation among growth, MC concentrations, MC content, and *mcyA* expression for the target strains is represented in Table 2. MC content per biomass increased with the total MC concentrations as significant correlation was observed among these (p < 0.0001, R^2 = 0.769). Chl *a* concentration and MC production were closely related in different concentrations of P in NIES 843 (p < 0.0001, R^2 = 0.835) and KW strains (p = 0.001, R^2 = 0.669) and of B in NIES 843 (p < 0.0001, R^2 = 0.960) and KW strains (p < 0.0001, R^2 = 0.918). Such relationship was rather weak in different concentrations of N in NIES 843 (p = 0.033, R^2 = 0.378) and KW strains (p = 0.004, R^2 = 0.584). In different nutrient regimes the expression of *mcyA* was not correlated with MC concentration (p = 0.222, R^2 = 0.342) and content (p = 0.333, R^2 = 0.232) in NIES 843. Similar trend was evident in Durgakund strain with MC concentration (p = 0.958, R^2 = 0.001) and content (p = 0.945, R^2 = 0.001). Contrary to this, *mcyA* expression pattern is directly reflected on MC concentration (p = 0.011, R^2 = 0.834) and content (p = 0.044, R^2 = 0.679) in KW strain.

3.4. Bacterial Community. DGGE profile of water samples, collected during cyanobacterial bloom, from Durgakund

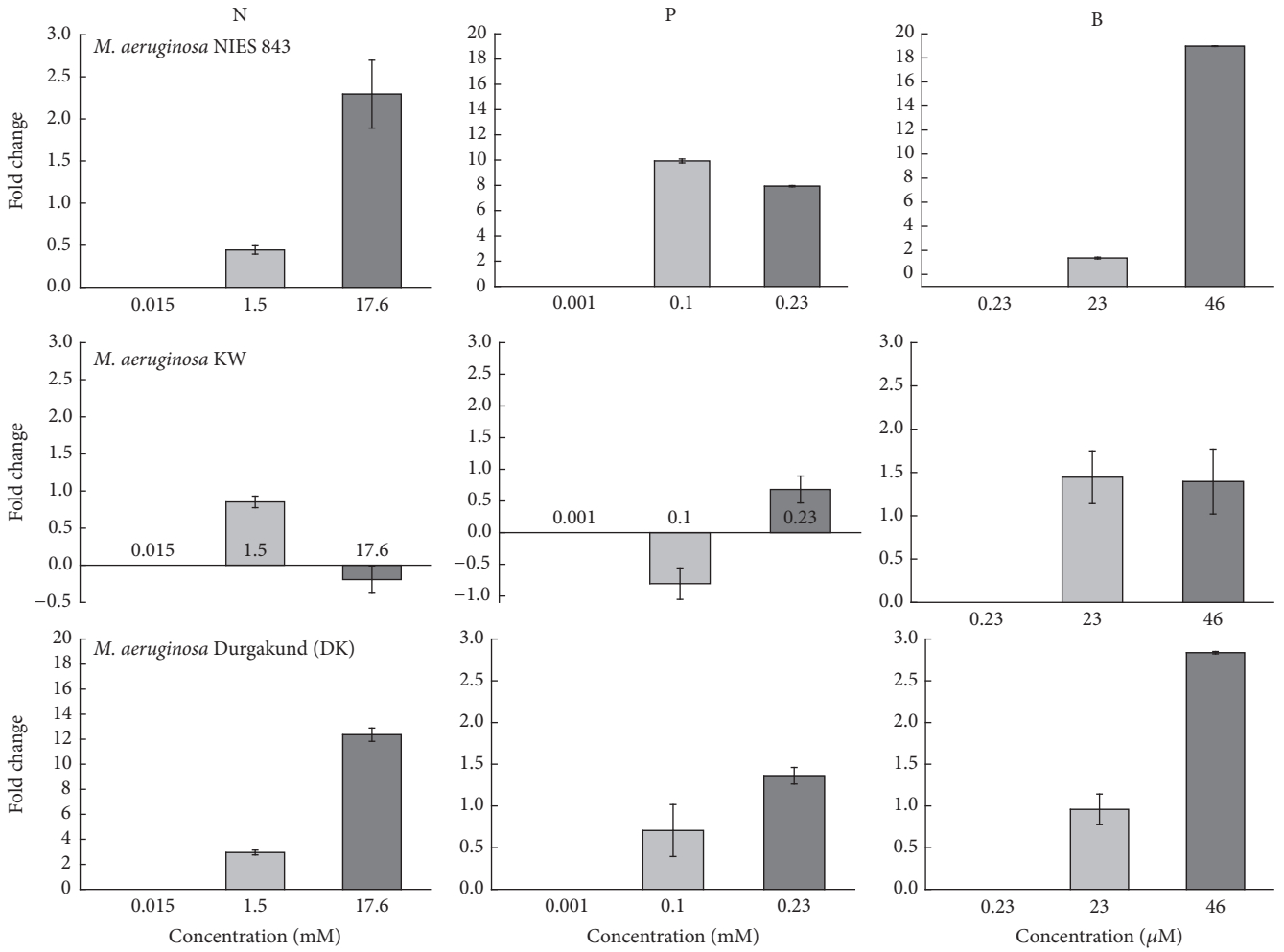

Figure 5: Effect of different concentrations of N, P, and B on *mcyA* expression of *M. aeruginosa* NIES 843, *M. aeruginosa* KW, and *Microcystis* Durgakund (DK) strain. The data were calculated relative to the expression in control cells (grown in low nutrient concentration) and normalized with the expression of the reference gene (16S rRNA).

Pond and Wangsong Reservoir for bacterial and cyanobacterial 16S rRNA gene is shown in Figure 6. All labeled bands were sequenced and most of the analyzed sequences showed 99% similarity to their closest relatives in the database (Table 3). Six sequences (bands 5, 10, 16, 17, 18, and 19) were related to Alphaproteobacteria and retrieved from all the samples except for August and September in Durgakund while bands 17 and 18 appeared in July and August in Wangsong Reservoir samples. Sequence related to Betaproteobacteria (band 4) appeared in August and September. One bacterial sequence (band 9) was related to Xanthomonadales order within Gammaproteobacteria and found in the Durgakund samples of all months. Among the cyanobacterial community, bands 8, 12, and 13 (intense) showed similarity to *M. aeruginosa* and were present in all the samples of Durgakund and Wangsong Reservoir. Interestingly, sequence (band 6) related to *M. wesenbergii* was more intense in August and September samples of Durgakund Pond. Sequence (band 2) related to *Merismopedia glauca* belonging to order Chroococcales was also seen in all the samples of Durgakund. In general, the banding pattern of DGGE in August and September samples differed from the samples of other months in Durgakund (Figure 6).

4. Discussion

Net production of MC was shown to be influenced by growth rate, that is, cell division process, reflecting a nearly linear correlation between them [33]. In the present study, the MC content per biomass increased with the total MC concentration but growth could not be correlated with total MC concentration in the target strains (Table 2). This was in tune with observations recorded earlier in the hepatotoxic *Microcystis* strains [15]. In this study, low N (0.015 mM) approximated eutrophic conditions in water bodies; therefore increased N concentration (maximum 17.6 mM) favored growth in the target strains. Higher level of N (1.5 mM and 17.6 mM) resulted in increased MC concentrations in the strains which is consistent with previous lab studies [34, 35]. Fluctuations in MC level of cyanobacteria with respect to N concentrations

Table 3: Phylogenetic affinity of *16S rRNA* gene sequences retrieved from monthly cyanobacterial bloom samples.

Band number	Name	Accession number	Similarity (%)	Taxonomic group
		Durgakund Pond		
1	Uncultured bacterium	JQ906016	99	Uncultured bacterium
2	*Merismopedia glauca*	AJ781044	99	Chroococcales, Cyanobacteria
3	Uncultured bacterium[a]	KF418783	—	Uncultured bacterium
4	Uncultured beta-proteobacterium	JN371632	95	Betaproteobacteria
5	*Porphyrobacter* sp.	AB299749	99	Sphingomonadales, Alphaproteobacteria
6	*Microcystis wesenbergii*	AB666079	99	Chroococcales, Cyanobacteria
7	Uncultured bacterium	HQ653656	97	Uncultured bacterium
8	*Microcystis aeruginosa*	AF139304	99	Chroococcales, Cyanobacteria
9	*Aquimonas* sp.[a]	KF418784	—	Xanthomonadales, Gammaproteobacteria
10	*Roseomonas* sp.	HM124370	98	Rhodospirillales, Alphaproteobacteria
		Wangsong Reservoir		
11	*Acinetobacter* sp.	KM108563	79	Pseudomonadales, Gammaproteobacteria
12	*Microcystis aeruginosa*	KF372572	98	Chroococcales, Cyanobacteria
13	*Microcystis aeruginosa*	KJ746519	100	Chroococcales, Cyanobacteria
14	*Malikia spinosa*	NR114228	99	Burkholderiales, Betaproteobacteria
15	*Aeromonas* sp.	KM363229	99	Aeromonadales, Gammaproteobacteria
16	*Rhodobacter* sp.	AB251408	93	Rhodobacterales, Alphaproteobacteria
17	Uncultured alpha-proteobacterium	HM153675	98	Alphaproteobacteria
18	*Roseomonas lacus*	JQ349047	99	Rhodospirillales, Alphaproteobacteria
19	Uncultured alpha-proteobacterium	HM153673	100	Alphaproteobacteria

[a]All the bands except 3 and 9 were based on published papers; therefore bands 3 and 9 were submitted to Genbank (BankIt1645319 Seq1 KF418783 for DGGE band #3; BankIt1646633 Seq1 KF418784 for DGGE band #9).

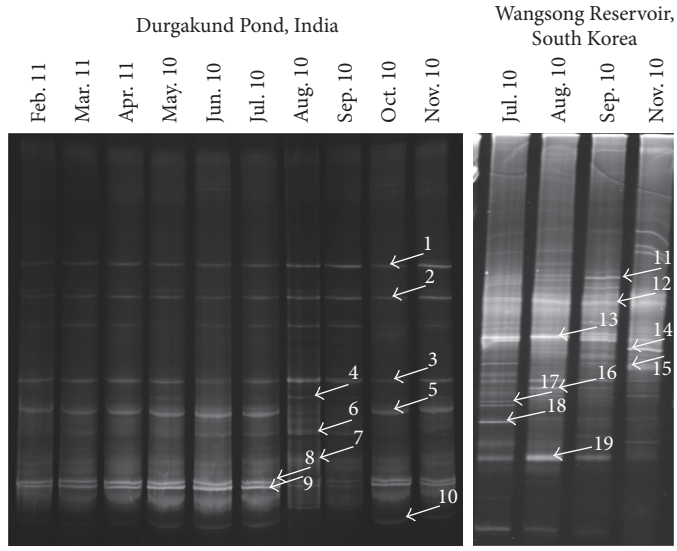

Figure 6: DGGE profile of 16S rDNA fragments of bacteria and cyanobacteria in bloom samples collected monthly from Durgakund Pond and Wangsong Reservoir. All labeled bands were excised from the gel, reamplified, and sequenced.

in medium have already been reported [16, 33, 36]. Recent study also demonstrated that N-limited conditions reduced the MC quota in *Microcystis aeruginosa* relative to nutrient-saturated conditions [37]. Increased MC content in higher levels of N seemed to be rational in this context; however composition and presence of MC variants also changed with strains. Composition and dominance of MC-RR variant in the present context could be explained on the basis that MC is an N-rich compound (over 14% of MC-LR on molecular weight basis) [38] and increased intracellular content of the N-rich amino acid arginine promotes production of the [Asp^3] MC-RR variant in *M. aeruginosa* [35, 39].

The target strains showed better growth at 0.1 mM P, indicating it is a threshold limit. *M. aeruginosa* NIES 843 and KW

followed the same trend in growth, while Durgakund strain seemed more sensitive to the changes in P concentrations. Fluctuations in MC levels of the target strains under varying P concentrations again indicate strain specific response to P. Interestingly, significant decrease in the total MC level was observed in Durgakund strain under higher P concentrations (0.1 and 0.23 mM). There are some reports where P limitation slightly reduced or did not influence the toxicity of *M. aeruginosa* [36, 37], while increase in MC production by *Microcystis* was also reported with decreasing concentrations of P in culture conditions [40, 41]. In contrast to these results, a positive correlation between MC content and increasing phosphate was observed in natural ecosystems suggesting that raised level of P increased the relative contribution of toxigenic cyanobacteria to total phytoplankton biomass [42, 43]. Several reports have also emphasized the importance of N : P ratios in MC production due to variations in response of *Microcystis* strains to N and P [14, 15, 44, 45]. For example, Lee et al. [44] reported higher MC and Chl *a* content at total N : P atomic ratios of 16 : 1 and 50 : 1. Furthermore, it was suggested that cellular MC content is a function of cellular nitrogen status and found to be strongly correlated with cellular protein content at N : P ratios between 18 and 51 in *M. aeruginosa* [34].

It is hard to devise a clear role of N and/or P in development of bloom and its toxicity; therefore we also investigated the effect of B, which has a potential role in signaling and interspecies communication. The role of B has also been shown in organization of cell walls, membrane function, metabolic activities, and stabilization of heterocyst in cyanobacteria [46]. Recently, a B-containing signal molecule (autoinducer AI-2), encoded by AI-2 synthase (*luxS*), has been reported by Chen et al. [20]. AI-2 is produced by a large number of bacterial species and proposed to serve as a universal signal for interspecies communication [47]. The production of signaling molecules called N-acyl homoserine-lactones (AHLs) was also reported for the first time in *Gloeothece* sp. [48] and *M. aeruginosa* [49]. They demonstrated that the concentration of the AHLs was cell density dependent and might play an important role in bloom formation. Since one of the potential roles of MCs in the producing organism was proposed in extracellular signaling, autoinduction, and maintenance of colonies [5, 6, 10], we studied the effect of B on MC production in *Microcystis* strains in the current study. It was interesting that B favored growth of all the target strains along with MC concentrations (Figure 3). The total concentrations of MC variants in Durgakund strain were lowest as compared to NIES 843 and KW strains under different concentrations of N, P, and B. This could be explained on the basis that the presence of toxic strains of cyanobacteria does not always indicate toxicity, as MC-producing cell quota may vary up to 3-4 orders of magnitude [50]. Since we have done lab-based study, cyanobacteria also undergo changes in loss of toxin production [51] and colonial morphology in *Microcystis*, if maintained in the culture for prolonged period [52].

Transcription of *mcy* genes in *M. aeruginosa* occurs *via* a central bidirectional promoter between *mcyA* and *mcyD*. A total of three NtcA (global nitrogen regulator) binding sites were identified in the *mcyA*/*D* promoter region, suggesting the role of nitrogen in controlling MC biosynthesis [53]. In this study, the overall patterns in *mcyA* expression were somewhat consistent with MC levels measured under different N concentrations in all the three strains but not directly correlated with the total MC concentrations ($p = 0.273$, $R^2 = 0.287$). This finding is consistent with observation where low N resulted in decrease in transcript levels of MC synthesizing genes [54]. However, Sevilla et al. [17] reported that the MC concentration in the cultures correlated with *mcyD* expression but the transcript level remained constant and was independent of nitrate availability. Recently, Horst et al. [37] suggested that MC quota was not driven by decrease in copy number of the *mcyB* gene but mediated by phenotypic responses of individual cells to N availability. As MC is made up of different modules, each having specific enzymatic function [4], N might be helpful in assembly of these modules explaining the increased MC concentration without any direct correlation with upregulation of transcription. An alternative explanation could be that there might be an initial accumulation of MC quota in the cells and since prokaryotic mRNA is highly unstable, these might have already been transcribed and translated leading to variable results at the time of expression analysis. However, further research on time dependent real-time analysis is needed.

In this study, *mcyA* transcript increased under higher P levels in the target strains. In another study, insignificant changes were observed in the relative quantification of *mcyD* in *M. aeruginosa* PCC 7806 under excess phosphate, while P-deficiency (N/P = 40 : 1) led to an increase in *mcyD* transcript and MC-LR per cell [55]. Increases in MC quotas and *mcyE* expression were also reported in Lake Rotorua with the increase in *Microcystis* cell concentrations [56]. They demonstrated that MC production was not always continuous and significant changes in *mcyE* expression occurred over smaller time frames.

Increase in *mcyA* expression in the target strains was consistent but not correlated with MCs levels under selected concentrations of B. Correlation analysis revealed that *mcyA* expression in only KW strain was directly linked with MC content ($p = 0.044$, $R^2 = 0.679$) and concentrations ($p = 0.011$, $R^2 = 0.834$) under different levels of N, P, and B. Increase in photoautotrophic growth and MC concentrations in the target strains suggested an indirect role of B but its role in nonheterocystous cyanobacteria is still not well documented. Furthermore, it was suggested that accumulation of *mcyB* in the lysing *Microcystis* cells stimulated the production of MCs in the remaining intact *Microcystis* cells [6]. Therefore, a more detailed study on direct role of B in signaling or MC production is needed particularly in nonnitrogen fixing species like *Microcystis*. Various field and laboratory studies failed to assign a single major factor responsible for promoting cyanobacterial bloom and its toxicity. This indicated a complex regulation of bloom development and its toxicity by biological and environmental variables. Induction of the growth of toxic *Microcystis* bloom is not yet known in spite of the fact that cyanobacterial blooms are regulated by various environmental factors. This study focused on response of *Microcystis* to differing nutrient concentrations

on *mcy* transcription and MCs production which could help to decipher the possible regulation of the bloom growth and its toxicity and in timely management of the water bodies.

The interaction between bacteria and cyanobacteria is one of the biotic factors that influence the bloom dynamics [57]. Therefore, we also investigated the community compositional plasticity of heterotrophic bacteria associated with cyanobacterial blooms in Durgakund Pond and Wangsong Reservoir (Figure 6, Table 3). Bacterial groups, such as Alphaproteobacteria, Betaproteobacteria, and Gammaproteobacteria, were frequently found to be the dominant groups during the bloom of *Microcystis*. Earlier we have reported the dominance of *Microcystis* sp. in Durgakund Pond with the highest proportion of potentially toxigenic *Microcystis* sp. (14%) and MCs concentration in September [12]. Our observation was in tune with the findings that *Microcystis* bloom changed the microhabitat and quantity and quality of exudates and also microbes have the potential to control bloom development of potentially toxic cyanobacteria [9, 57]. However, in future a more comprehensive comparative study of bacteria associated with cyanobacteria and MC production in the field and lab cultures may provide insight in the complex regulatory mechanisms of MC production.

5. Conclusions

In summary, a comparison of photoautotrophic growth, MC content and concentration, and *mcyA* gene expression of three lab-grown *Microcystis* strains (NIES 843, KW, and Durgakund) in different nutrient regimes revealed that MC content per biomass and total MC concentration were highly correlated. MC production increased with increase in growth and this could have important implications for the management of freshwater bodies during *Microcystis* bloom upsurge. Lack of MC-YR in Durgakund strain indicated that MC concentration and variants were strain specific. Expression of *mcyA* showed nutrient concentration-dependent tendency but was not correlated with total MC concentration and therefore necessitates a time dependent real-time analysis for understanding the role of nutrients and other ecological variables in MC production. Natural associations of heterotrophic bacteria and cyanobacterial bloom were somewhat similar in freshwater bodies; however bacterial community showed variation during the different phases of the cyanobacterial bloom.

Competing Interests

The authors declare that they have no competing interests.

Acknowledgments

Financial support from DST (Department of Science and Technology), New Delhi, to Ankita Srivastava (IF 10355, Date: 26 November, 2010) is gratefully acknowledged. A grant from the host institution through the KRIBB Research Initiative Program is acknowledged. Financial support by the Basic Core Technology Development Program for the Oceans and the Polar Regions of the National Research Foundation (NRF) funded by the Ministry of Science, ICT and Future Planning (2016MIA5A1027453) is gratefully acknowledged. Ravi Kumar Asthana is thankful to UGC (University Grants Commission), New Delhi, Project Code no. P-01/623, and UGC, UPE support from the university, for financial support.

References

[1] W. W. Carmichael, "Health effects of toxin-producing cyanobacteria: 'The CyanoHABs'," *Human and Ecological Risk Assessment*, vol. 7, no. 5, pp. 1393–1407, 2001.

[2] M. Welker and H. Von Döhren, "Cyanobacterial peptides—nature's own combinatorial biosynthesis," *FEMS Microbiology Reviews*, vol. 30, no. 4, pp. 530–563, 2006.

[3] H. K. Hudnell, Q. Dortch, and H. Zenick, "An overview of the interagency, international symposium on cyanobacterial harmful algal blooms (ISOC-HAB): advancing the scientific understanding of freshwater harmful algal blooms," in *Cyanobacterial Harmful Algal Blooms: State of the Science and Research Needs*, H. K. Hudnell, Ed., pp. 1–16, Springer, Berlin, Germany, 2008.

[4] D. Tillett, E. Dittmann, M. Erhard, H. Von Döhren, T. Börner, and B. A. Neilan, "Structural organization of microcystin biosynthesis in *Microcystis aeruginosa* PCC7806: an integrated peptide-polyketide synthetase system," *Chemistry and Biology*, vol. 7, no. 10, pp. 753–764, 2000.

[5] E. Dittmann, M. Erhard, M. Kaebernick et al., "Altered expression of two light-dependent genes in a microcystin-lacking mutant of *Microcystis aeruginosa* PCC 7806," *Microbiology*, vol. 147, no. 11, pp. 3113–3119, 2001.

[6] D. Schatz, Y. Keren, A. Vardi et al., "Towards clarification of the biological role of microcystins, a family of cyanobacterial toxins," *Environmental Microbiology*, vol. 9, no. 4, pp. 965–970, 2007.

[7] S. Jähnichen, B. M. Long, and T. Petzoldt, "Microcystin production by *Microcystis aeruginosa*: direct regulation by multiple environmental factors," *Harmful Algae*, vol. 12, pp. 95–104, 2011.

[8] R. Alexova, P. A. Haynes, B. C. Ferrari, and B. A. Neilan, "Comparative protein expression in different strains of the bloom-forming cyanobacterium *Microcystis aeruginosa*," *Molecular and Cellular Proteomics*, vol. 10, no. 9, Article ID M110.003749, 2011.

[9] C. Dziallas and H.-P. Grossart, "Increasing oxygen radicals and water temperature select for toxic *Microcystis* sp," *PLoS ONE*, vol. 6, no. 9, Article ID e25569, 2011.

[10] N. Gan, Y. Xiao, L. Zhu et al., "The role of microcystins in maintaining colonies of bloom-forming *Microcystis* spp.," *Environmental Microbiology*, vol. 14, no. 3, pp. 730–742, 2012.

[11] M. Lukač and R. Aegerter, "Influence of trace metals on growth and toxin production of *Microcystis aeruginosa*," *Toxicon*, vol. 31, no. 3, pp. 293–305, 1993.

[12] A. Srivastava, G.-G. Choi, C.-Y. Ahn, H.-M. Oh, A. K. Ravi, and R. K. Asthana, "Dynamics of microcystin production and quantification of potentially toxigenic *Microcystis* sp. using real-time PCR," *Water Research*, vol. 46, no. 3, pp. 817–827, 2012.

[13] J. M. Rinta-Kanto, E. A. Konopko, J. M. DeBruyn, R. A. Bourbonniere, G. L. Boyer, and S. W. Wilhelm, "Lake Erie *Microcystis*: relationship between microcystin production, dynamics of genotypes and environmental parameters in a large lake," *Harmful Algae*, vol. 8, no. 5, pp. 665–673, 2009.

[14] H. W. Paerl, W. S. Gardner, M. J. McCarthy, B. L. Peierls, and S. W. Wilhelm, "Algal blooms: noteworthy nitrogen," *Science*, vol. 346, no. 6206, p. 175, 2014.

[15] C. Vézie, J. Rapala, J. Vaitomaa, J. Seitsonen, and K. Sivonen, "Effect of nitrogen and phosphorus on growth of toxic and nontoxic *Microcystis* strains and on intracellular microcystin concentrations," *Microbial Ecology*, vol. 43, no. 4, pp. 443–454, 2002.

[16] R. Dai, H. Liu, J. Qu, X. Zhao, J. Ru, and Y. Hou, "Relationship of energy charge and toxin content of *Microcystis aeruginosa* in nitrogen-limited or phosphorous-limited cultures," *Toxicon*, vol. 51, no. 4, pp. 649–658, 2008.

[17] E. Sevilla, B. Martin-Luna, L. Vela, M. Teresa Bes, M. Luisa Peleato, and M. F. Fillat, "Microcystin-LR synthesis as response to nitrogen: transcriptional analysis of the *mcyD* gene in *Microcystis aeruginosa* PCC7806," *Ecotoxicology*, vol. 19, no. 7, pp. 1167–1173, 2010.

[18] R. Alexova, M. Fujii, D. Birch et al., "Iron uptake and toxin synthesis in the bloom-forming *Microcystis aeruginosa* under iron limitation," *Environmental Microbiology*, vol. 13, no. 4, pp. 1064–1077, 2011.

[19] A. E. Kirkwood, C. Nalewajko, and R. R. Fulthorpe, "The effects of cyanobacterial exudates on bacterial growth and biodegradation of organic contaminants," *Microbial Ecology*, vol. 51, no. 1, pp. 4–12, 2006.

[20] X. Chen, S. Schauder, N. Potier et al., "Structural identification of a bacterial quorum-sensing signal containing boron," *Nature*, vol. 415, no. 6871, pp. 545–549, 2002.

[21] R. Rippka, J. Deruelles, J. B. Waterbury, M. Herdman, and R. Y. Stanier, "Generic assignments, strain histories and properties of pure cultures of cyanobacteria," *Microbiology*, vol. 111, no. 1, pp. 1–61, 1979.

[22] M. Shirai, A. Ohotake, T. Sano et al., "Toxicity and toxins of natural blooms and isolated strains of *Microcystis* spp. (Cyanobacteria) and improved procedure for purification of cultures," *Applied and Environmental Microbiology*, vol. 57, no. 4, pp. 1241–1245, 1991.

[23] A. C. Redfield, "On the proportions of organic derivations in seawater and their relation to the composition of plankton," in *James Johnstone Memorial Volume*, R. J. Daniel, Ed., pp. 177–192, University Press of Liverpool, 1934.

[24] J. Myers and W. A. Kratz, "Relation between pigment content and photosynthetic characteristics in a blue-green algae," *The Journal of General Physiology*, vol. 39, no. 1, pp. 11–22, 1955.

[25] M. Hisbergues, G. Christiansen, L. Rouhiainen, K. Sivonen, and T. Börner, "PCR-based identification of microcystin-producing genotypes of different cyanobacterial genera," *Archives of Microbiology*, vol. 180, no. 6, pp. 402–410, 2003.

[26] G. Muyzer, E. C. De Waal, and A. G. Uitterlinden, "Profiling of complex microbial populations by denaturing gradient gel electrophoresis analysis of polymerase chain reaction-amplified genes coding for 16S rRNA," *Applied and Environmental Microbiology*, vol. 59, no. 3, pp. 695–700, 1993.

[27] B. J. Paster, F. E. Dewhirst, I. Olsen, and G. J. Fraser, "Phylogeny of *Bacteroides*, *Prevotella*, and *Porphyromonas* spp. and related bacteria," *Journal of Bacteriology*, vol. 176, no. 3, pp. 725–732, 1994.

[28] D. J. Lane, "*16S/23S rRNA* sequencing," in *Nucleic Acid Techniques in Bacterial Systematics*, E. Stackebrandt and M. Goodfellow, Eds., pp. 115–175, John Wiley & Sons, Chichester, UK, 1991.

[29] A. Teske, C. Wawer, G. Muyzer, and N. B. Ramsing, "Distribution of sulfate-reducing bacteria in a stratified fjord (Mariager Fjord, Denmark) as evaluated by most-probable-number counts and denaturing gradient gel electrophoresis of PCR-amplified ribosomal DNA fragments," *Applied and Environmental Microbiology*, vol. 62, no. 4, pp. 1405–1415, 1996.

[30] M. W. Pfaffl, "A new mathematical model for relative quantification in real-time RT-PCR," *Nucleic Acids Research*, vol. 29, no. 9, article e45, 2001.

[31] J. Sambrook and D. W. Russell, *Molecular Cloning, a Laboratory Manual*, Cold Spring Harbor Laboratory Press, Cold Spring Harbor, NY, USA, 3rd edition, 2001.

[32] R. H. Don, P. T. Cox, B. J. Wainwright, K. Baker, and J. S. Mattick, "'Touchdown' PCR to circumvent spurious priming during gene amplification," *Nucleic Acids Research*, vol. 19, no. 14, p. 4008, 1991.

[33] B. M. Long, G. J. Jones, and P. T. Orr, "Cellular microcystin content in N-limited *Microcystis aeruginosa* can be predicted from growth rate," *Applied and Environmental Microbiology*, vol. 67, no. 1, pp. 278–283, 2001.

[34] T. G. Downing, C. S. Sember, M. M. Gehringer, and W. Leukes, "Medium N:P ratios and specific growth rate comodulate microcystin and protein content in *Microcystis aeruginosa* PCC7806 and *M. aeruginosa* UV027," *Microbial Ecology*, vol. 49, no. 3, pp. 468–473, 2005.

[35] D. B. Van de Waal, J. M. H. Verspagen, M. Lürling, E. Van Donk, P. M. Visser, and J. Huisman, "The ecological stoichiometry of toxins produced by harmful cyanobacteria: an experimental test of the carbon-nutrient balance hypothesis," *Ecology Letters*, vol. 12, no. 12, pp. 1326–1335, 2009.

[36] G. A. Codd and A. M. Poon, "Cyanobacterial toxins," in *Biochemistry of the Algae and Cyanobacteria: Proceedings of the Phytochemistry Society of Europe*, L. L. Rogers and J. R. Gallon, Eds., vol. 28, pp. 283–296, Oxford University Press, Oxford, UK, 1988.

[37] G. P. Horst, O. Sarnelle, J. D. White, S. K. Hamilton, R. B. Kaul, and J. D. Bressie, "Nitrogen availability increases the toxin quota of a harmful cyanobacterium, *Microcystis aeruginosa*," *Water Research*, vol. 54, pp. 188–198, 2014.

[38] D. P. Botes, P. L. Wessels, H. Kruger et al., "Structural studies on cyanoginosins-LR, -YR, -YA and -YM, peptide toxins from *Microcystis aeruginosa*," *Journal of the Chemical Society, Perkin Transactions*, vol. 1, pp. 2747–2748, 1985.

[39] D. B. Van de Waal, G. Ferreruela, L. Tonk et al., "Pulsed nitrogen supply induces dynamic changes in the amino acid compositionand microcystin production of the harmful cyanobacterium *Planktothrix agardhii*," *FEMS Microbiology Ecology*, vol. 74, no. 2, pp. 430–438, 2010.

[40] H.-M. Oh, S. J. Lee, M.-H. Jang, and B.-D. Yoon, "Microcystin production by *Microcystis aeruginosa* in a phosphorus-limited chemostat," *Applied and Environmental Microbiology*, vol. 66, no. 1, pp. 176–179, 2000.

[41] K. Kameyama, N. Sugiura, H. Isoda, Y. Inamori, and T. Maekawa, "Effect of nitrate and phosphate concentration on production of microcystins by *Microcystis viridis* NIES 102," *Aquatic Ecosystem Health and Management*, vol. 5, no. 4, pp. 443–449, 2002.

[42] A. Giani, D. F. Bird, Y. T. Prairie, and J. F. Lawrence, "Empirical study of cyanobacterial toxicity along a trophic gradient of lakes," *Canadian Journal of Fisheries and Aquatic Sciences*, vol. 62, no. 9, pp. 2100–2109, 2005.

[43] K. Izydorczyk, T. Jurczak, A. Wojtal-Frankiewicz, A. Skowron, J. Mankiewicz-Boczek, and M. Tarczyńska, "Influence of abiotic and biotic factors on microcystin content in *Microcystis aeruginosa* cells in a eutrophic temperate reservoir," *Journal of Plankton Research*, vol. 30, no. 4, pp. 393–400, 2008.

[44] S. J. Lee, M.-H. Jang, H.-S. Kim, B.-D. Yoon, and H.-M. Oh, "Variation of microcystin content of *Microcystis aeruginosa* relative to medium N:P ratio and growth stage," *Journal of Applied Microbiology*, vol. 89, no. 2, pp. 323–329, 2000.

[45] W. M. Lewis, W. A. Wurtsbaugh, and H. W. Paerl, "Rationale for control of anthropogenic nitrogen and phosphorus to reduce eutrophication of inland waters," *Environmental Science and Technology*, vol. 45, no. 24, pp. 10300–10305, 2011.

[46] P. H. Brown, N. Bellaloui, M. A. Wimmer et al., "Boron in plant biology," *Plant Biology*, vol. 4, no. 2, pp. 205–223, 2002.

[47] M. G. Surette, M. B. Miller, and B. L. Bassler, "Quorum sensing in *Escherichia coli*, *Salmonella typhimurium*, and *Vibrio harveyi*: a new family of genes responsible for autoinducer production," *Proceedings of the National Academy of Sciences of the United States of America*, vol. 96, no. 4, pp. 1639–1644, 1999.

[48] D. I. Sharif, J. Gallon, C. J. Smith, and E. D. Dudley, "Quorum sensing in *Cyanobacteria*: *N*-octanoyl-homoserine lactone release and response, by the epilithic colonial cyanobacterium *Gloeothece* PCC6909," *ISME Journal*, vol. 2, no. 12, pp. 1171–1182, 2008.

[49] C. Zhai, P. Zhang, F. Shen, C. Zhou, and C. Liu, "Does *Microcystis aeruginosa* have quorum sensing?" *FEMS Microbiology Letters*, vol. 336, no. 1, pp. 38–44, 2012.

[50] S. I. Blackburn, C. J. S. Bolch, G. J. Jones, A. P. Negri, and P. T. Orr, "Cyanobacterial blooms: why are they toxic?" in *Managing Algal Blooms: Outcomes from the CSIRO Blue Green Algal Research Program*, J. R. D. Davis, Ed., pp. 67–77, CSIRO Land and Water, Canberra, Australia, 1997.

[51] D. Schatz, Y. Keren, O. Hadas, S. Carmeli, A. Sukenik, and A. Kaplan, "Ecological implications of the emergence of non-toxic subcultures from toxic *Microcystis* strains," *Environmental Microbiology*, vol. 7, no. 6, pp. 798–805, 2005.

[52] M. Zhang, F. Kong, X. Tan, Z. Yang, H. Cao, and P. Xing, "Biochemical, morphological, and genetic variations in *Microcystis aeruginosa* due to colony disaggregation," *World Journal of Microbiology and Biotechnology*, vol. 23, no. 5, pp. 663–670, 2007.

[53] H. P. Ginn, L. A. Pearson, and B. A. Neilan, "NtcA from *Microcystis aeruginosa* PCC 7806 is autoregulatory and binds to the microcystin promoter," *Applied and Environmental Microbiology*, vol. 76, no. 13, pp. 4362–4368, 2010.

[54] M. J. Harke and C. J. Gobler, "Global transcriptional responses of the toxic cyanobacterium, *Microcystis aeruginosa*, to nitrogen stress, phosphorus stress, and growth on organic matter," *PLoS ONE*, vol. 8, no. 7, Article ID e69834, 2013.

[55] T. M. Kuniyoshi, E. Sevilla, M. T. Bes, M. F. Fillat, and M. L. Peleato, "Phosphate deficiency (N/P 40:1) induces *mcyD* transcription and microcystin synthesis in *Microcystis aeruginosa* PCC7806," *Plant Physiology and Biochemistry*, vol. 65, pp. 120–124, 2013.

[56] S. A. Wood, A. Rueckert, D. P. Hamilton, S. C. Cary, and D. R. Dietrich, "Switching toxin production on and off: intermittent microcystin synthesis in a *Microcystis* bloom," *Environmental Microbiology Reports*, vol. 3, no. 1, pp. 118–124, 2011.

[57] C. Dziallas and H.-P. Grossart, "Temperature and biotic factors influence bacterial communities associated with the cyanobacterium *Microcystis* sp," *Environmental Microbiology*, vol. 13, no. 6, pp. 1632–1641, 2011.

Hindawi Publishing Corporation
BioMed Research International
Volume 2016, Article ID 9837598, 7 pages
http://dx.doi.org/10.1155/2016/9837598

Research Article

Sequestration and Distribution Characteristics of Cd(II) by *Microcystis aeruginosa* and Its Role in Colony Formation

Xiangdong Bi,[1,2] Ran Yan,[2] Fenxiang Li,[1] Wei Dai,[2] Kewei Jiao,[1] Qixing Zhou,[1] and Qi Liu[2]

[1]*Key Laboratory of Pollution Processes and Environmental Criteria, College of Environmental Science and Engineering, Nankai University, Ministry of Education, Tianjin 300071, China*
[2]*Key Laboratory of Aquatic-Ecology and Aquaculture of Tianjin, Department of Fisheries Sciences, Tianjin Agricultural University, Tianjin 300384, China*

Correspondence should be addressed to Qixing Zhou; zhouqx@nankai.edu.cn

Received 28 May 2016; Accepted 5 July 2016

Academic Editor: Zhi-Hua Li

To investigate the sequestration and distribution characteristics of Cd(II) by *Microcystis aeruginosa* and its role in *Microcystis* colony formation, *M. aeruginosa* was exposed to six different Cd(II) concentrations for 10 days. Cd(II) exposure caused hormesis in the growth of *M. aeruginosa*. Low concentrations of Cd(II) significantly induced formation of small *Microcystis* colonies ($P < 0.05$) and increased the intracellular polysaccharide (IPS) and bound extracellular polysaccharide (bEPS) contents of *M. aeruginosa* significantly ($P < 0.05$). There was a linear relationship between the amount of Cd(II) sequestrated by algal cells and the amount added to cultures in the rapid adsorption process that occurred during the first 5 min of exposure. After 10 d, *M. aeruginosa* sequestrated nearly 80% of 0.2 mg L^{-1} added Cd(II), while >93% of Cd(II) was sequestrated in the groups with lower added concentrations of Cd(II). More than 80% of the sequestrated Cd(II) was bioadsorbed by bEPS. The Pearson correlation coefficients of exterior and interior factors related to colony formation of *M. aeruginosa* revealed that Cd(II) could stimulate the production of IPS and bEPS via increasing Cd(II) bioaccumulation and bioadsorption. Increased levels of cross-linking between Cd(II) and bEPS stimulated algal cell aggregation, which eventually promoted the formation of *Microcystis* colonies.

1. Introduction

Microcystis blooms frequently occur in eutrophic freshwaters and their outbreaks always lead to water deoxygenation, microcystin pollution, and fish kill. During *Microcystis* blooms, algal cells aggregate largely on the surface of water and can be visible. Colony formation plays a vital role in the occurrence of *Microcystis* blooms [1]. It protects *Microcystis* cells from zooplankton grazing [2], viral or bacterial attack, and other potential negative environmental factors [3] and also provides a competitive advantage over other phytoplankton species [4]. However, how unicellular *Microcystis* cells aggregate into colonies exactly is not yet known. Previous studies have found that both biotic and abiotic factors, such as zooplankton grazing, nutritive salt, and microcystins, could stimulate *Microcystis* colony formation [2, 4]. Both zooplankton grazing and microcystins were reported to increase the amount of extracellular polysaccharides (EPS) and eventually stimulate aggregation of *Microcystis* cells [2].

Cyanobacterial blooms frequently occur in eutrophic waters with serious metal pollution [5, 6]. Cadmium (Cd), as a nonessential metal for biology, has become an important pollutant in natural freshwaters due to increasing use in industry, agriculture, and anthropogenic activities [7]. The negative effects of Cd on the environment have been recognized and it readily accumulates in living organisms. It was documented that cyanobacteria (*Synechocystis* sp. BASO670 and *Synechocystis* sp. BASO672) had high tolerance to Cd(II)-induced toxic effects, and Cd(II) could significantly stimulate EPS production in these two *Synechocystis* isolates [8]. In our previous study, we found there were significant differences in cadmium accumulation in four sizes of *Microcystis* colony [9] and cadmium accumulation decreased with increasing *Microcystis* colony sizes. We speculated that cadmium ions

might play an important role in the early stage of *Microcystis* colony formation in natural waters [9].

To better predict, prevent, and control *Microcystis* blooms in natural waters, it is important to understand all the factors involved in triggering colony formation of *Microcystis* species. In this study, both sequestration and distribution characteristics of Cd(II) by toxic *M. aeruginosa* and physiological responses related to colony formation were investigated in laboratory conditions.

2. Materials and Methods

2.1. Cyanobacterial Culture. *M. aeruginosa* FACHB-905, a very common microcystin-producing *Microcystis* strain, which was provided by the Institute of Hydrobiology of China, can form large visible colonies with non-microcystin-producing *Microcystis* strains in natural waters. *M. aeruginosa* FACHB-905 were cultured in conical flasks containing sterilized BG11 medium (without EDTA) under a 12 light:12 dark cycle with a light density of 60 μmol m^{-2} s^{-1} at 25°C. To reduce any effects related to minor differences in photon irradiance and to maintain homogeneity, the flasks were shaken slightly four times every day and rearranged randomly. Cultures were grown until the exponential growth phase.

2.2. Experimental Design. $CdCl_2$ (Merck, Germany) was dissolved in distilled water to prepare a stock solution (20000 mg L^{-1}). Based on the median effective concentration EC_{50}-96 h = 0.383 mg L^{-1}, determined by the method of Vanewijk and Hoekstra [10] of Cd(II) on *M. aeruginosa* obtained in preliminary experiments, Cd(II) was added to algal culture at an initial density of 5.473×10^6 ind mL^{-1} to final concentrations of 0 (control), 0.0125, 0.025, 0.05, 0.1, 0.2, and 0.4 mg L^{-1}, with three replicate flasks per concentration. Samples were removed from the cultures at 0, 5, 10, 20, 60, and 120 min and then daily until the 10th day of the experiment, to determine the algal cell density, colony numbers, bioadsorption and bioaccumulation characteristics of Cd(II), and bound extracellular polysaccharide (bEPS) and intracellular polysaccharide (IPS) contents of *M. aeruginosa*.

2.3. Effects of Cd(II) on Growth and Colony Formation of M. aeruginosa. Algal cell density and *M. aeruginosa* colonies were measured using a hemocytometer under a light microscope (×40). To reduce erroneous results, samples were taken 1 cm below the water surface with movement by a wide-mouth pipette, and the flasks were shaken up slightly 30 min before taking samples. The inhibition rate (IR), the decrease of intact algae in suspension, was calculated using the following formula: IR (%) = $(N_0 - N_S)/N_0 \times 100$, where N_0 is algal cell density in the control (ind L^{-1}) and N_S is algal cell density in the Cd(II)-added treatment (ind L^{-1}) [11]. *M. aeruginosa* were classified as unicellular, two-cell aggregation or colony (aggregation of ≥3 cells).

2.4. Determination of Bioadsorption and Bioaccumulation of Cd(II) by M. aeruginosa. Algal culture (500 mL) was centrifuged at 10,000 ×g for 10 min at 4°C, and the supernatant was dried to constant weight at 180°C to determine the content of Cd(II) in the medium (μg L^{-1}). The algal cell deposit was resuspended in 1.0×10^{-3} mol L^{-1} EDTA solution and then stirred with glass beads for 30 min to detach bEPS associated with the algal cells. After centrifugation at 10,000 ×g for 30 min at 4°C, the algal cell deposit was used to determine Cd(II) content accumulated inside algal cells (pg $cell^{-1}$). The resulting supernatant was dried to constant weight at 180°C to determine Cd(II) content bioadsorbed on the algal cell walls. The resulting solid was precisely weighed (0.5 g) and transferred into a polytetrafluoroethylene, where 7 mL of HNO_3 and 1 mL of H_2O_2 were added. The digester was sealed tightly and placed in a microwave digestion system (ETHOS One, Milestone, Italy). The procedure for microwave digestion is summarized as follows: the digester was heated from 25°C to 180°C over 10 min and then held for 25 min to digest the samples. After complete digestion, the digestion solution was evaporated to 2.5 mL, transferred to a 50 mL volumetric flask, and diluted with deionized water. A reagent blank was prepared using the same chemicals and digestion procedure as a comparison. Content of Cd(II) in collected samples was measured using Inductively Coupled Plasma-Atomic Emission Spectrometry (ICP-AES) using an ICP-9000 (N + M) (Thermo Jarrell Ash, USA), for which the detection limit of Cd is 0.01 mg kg^{-1}.

2.5. Effects of Cd(II) on bEPS and IPS Production by M. aeruginosa. Algal culture (50 mL) was centrifuged at 5,000 ×g for 10 min at 4°C, and the cell pellet was washed with 1.0×10^{-3} mol L^{-1} EDTA solution using a glass rod. The resulting suspension was stirred with glass beads to detach bEPS associated with the algal cells. After centrifugation at 10,000 ×g for 30 min at 4°C, the algal cell pellet and supernatant were collected to determine IPS and bEPS contents (pg $cell^{-1}$), respectively. To precipitate proteins from the supernatant, trichloroacetic acid (TCA) was added to a final concentration of 10% and the precipitated proteins were removed by centrifugation at 10,000 ×g for 20 min at 4°C. The clear supernatant was precipitated overnight at 4°C with six volumes of 95% ethanol. TCA precipitation and ethanol precipitation were repeated once. After centrifugation (12,000 ×g for 30 min at 4°C), the deposit obtained was dissolved in distilled water, dialyzed (3,600 mol wt cutoff tubing) against distilled water at 4°C for 24 h with 2 times, and then concentrated to 2 mL by rotary evaporation. The content of bEPS (pg $cell^{-1}$) was estimated using the phenol-sulfuric acid method [12]. Algal cells were disrupted by freezing and thawing repeatedly to obtain IPS and then treated as for bEPS measurement.

2.6. Statistical Analysis. Results are expressed as means ± SD and were subjected to Fisher's least significant difference test (SPSS version 17.0) to determine significant differences ($P < 0.05$) among groups [13]. The Pearson correlation coefficient was examined by paired t-test (SPSS version 17.0) [14].

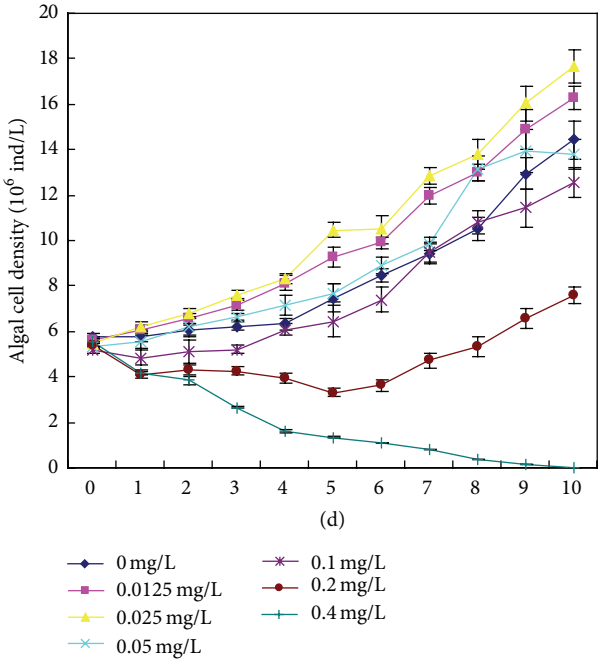

Figure 1: Effects of various concentrations of Cd(II) on algal cell density of *M. aeruginosa*.

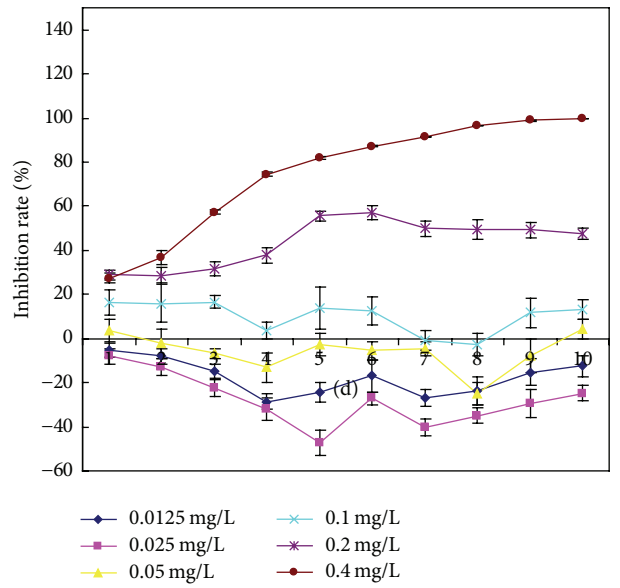

Figure 2: Effects of various concentrations of Cd(II) on the inhibition rate of *M. aeruginosa*.

3. Results and Discussion

3.1. Effects of Cd(II) on Growth of M. aeruginosa. The growth of *M. aeruginosa* FACHB-905 was affected in a Cd(II) concentration-dependent manner. With increasing exposure time, *M. aeruginosa* cell densities increased in low concentration Cd(II)-added groups (0.0125 and 0.025 mg L^{-1}) and decreased in high-concentration Cd(II)-added groups (0.05, 0.1, 0.2, and 0.4 mg L^{-1}) as compared with the control groups (Figure 1). These results indicated that Cd(II) had a dual effect (promotion and inhibition) on the growth of *M. aeruginosa*. Such an effect is described as hormesis, a dose-response relationship characterized by low-dose stimulation and high-dose inhibition [15]. Gong et al. found that inorganic arsenic could also cause hormesis in *M. aeruginosa* FACHB 905 [16]. In our experiment, high Cd(II) of concentrations inhibited the growth, possibly because the Cd(II) concentration exceeded the tolerance limit of *M. aeruginosa* cells, causing cell structure damage and disintegration. Among the tested concentrations, 0.4 mg L^{-1} Cd(II) exhibited the strongest inhibitory effects, with a 4-day IR of 74.752% and a 10-day IR of 99.992% (Figure 2). It is documented that *M. aeruginosa* PCC 7806 was susceptible to trace metal toxicity [17], while a *M. aeruginosa* strain isolated in the Czech Republic had high tolerance to 5.0–10.0 mg L^{-1} Cd(II) [18]. Therefore, it is possible that different strains of *M. aeruginosa* have different sensitivities to Cd(II)-induced toxicity.

3.2. Effects of Cd(II) on Colony Formation by M. aeruginosa. Compared with colonial forms that predominate in natural conditions, *Microcystis* exists mainly as noncolonial (single and a few paired) cells in culture [19]. Colony formation

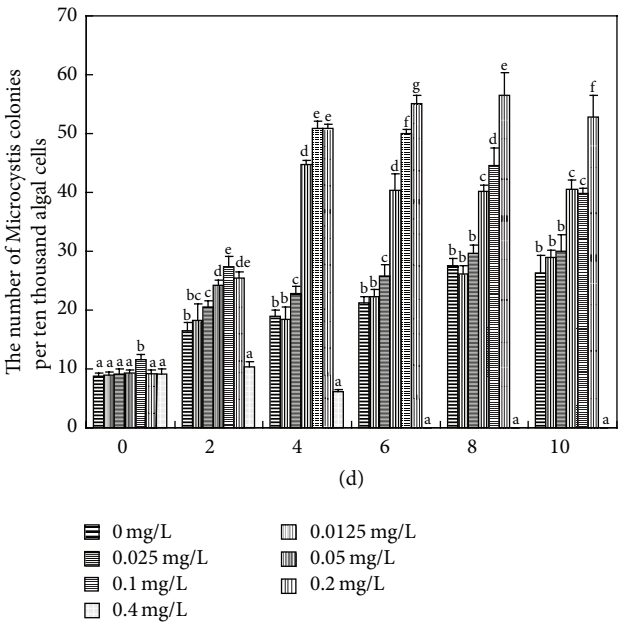

Figure 3: Effects of Cd(II) on colony formation by *M. aeruginosa*. Values sharing the same letters are not significantly different, whereas those marked with different letters are significantly different ($P < 0.05$).

of *M. aeruginosa* is a phenotypic response of single cells to environmental stress [3]. Colonial *Microcystis* had higher endurance to heavy metal-induced stress than noncolonial *Microcystis* [20]. Our results show that three concentrations of Cd(II) (0.05, 0.1, and 0.2 mg L^{-1}) significantly induced *Microcystis* colony formation ($P < 0.05$), and 0.2 mg L^{-1} Cd(II) had the highest inductive effect (Figure 3). The proportion of *Microcystis* colonies was significantly decreased in

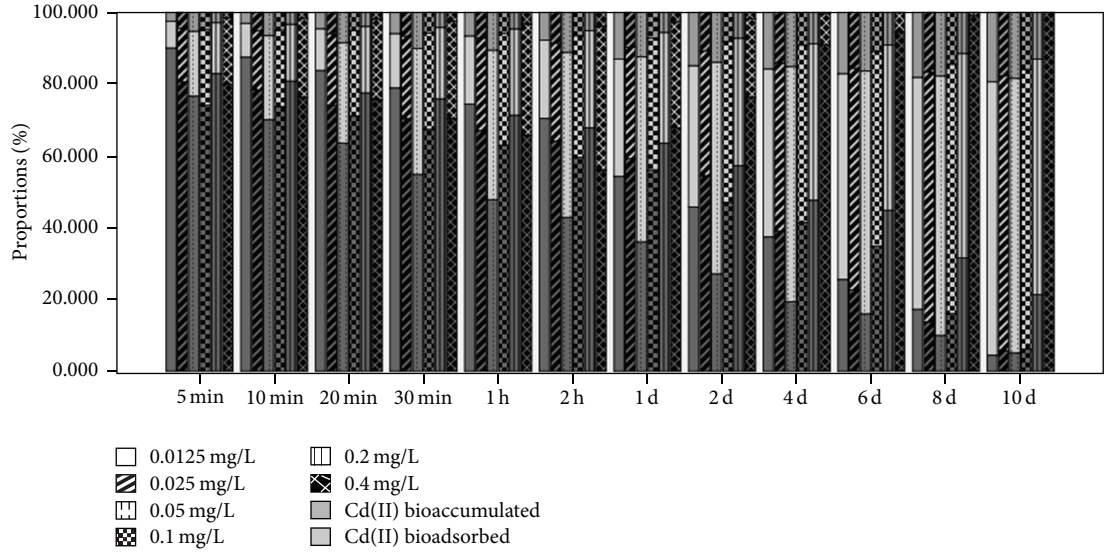

Figure 4: Changes in the proportions of Cd(II) bioadsorbed by bEPS and bioaccumulated inside algal cells and of Cd(II) in the culture medium for *M. aeruginosa* exposed to various concentrations of Cd(II).

the 0.4 mg L^{-1} Cd(II)-added group after 4 d, and no *Microcystis* colonies could be observed under the microscope after 6 d, which might result from the strong inhibitory effects of 0.4 mg L^{-1} Cd(II) on the growth of *M. aeruginosa* (Figures 1, 2, and 3). No colonies with five or more cells were observed during the whole experimental period. Unlike Fe, Al, Mn, Pb, and Cr, Cd was the only heavy metal element accumulated much higher in small *Microcystis* colony than in middle, large, and super-large colonies in natural waters [9]. These observations indicate that Cd(II) may play an important role in the early stage of *Microcystis* colony formation in natural waters [9].

3.3. Sequestration and Distribution Characteristics of Cd(II) by Microcystis Cells. When *Microcystis* cells were exposed to Cd(II), a rapid adsorption process occurred in the first 5 min. There was a linear relationship between Cd(II) sequestrated by algal cells (including Cd(II) bioadsorbed on bEPS and bioaccumulated inside cells) and the added Cd(II) concentrations during this time period ($y = 8.5326x - 8.664$; $R^2 = 0.9864$). More chances for metal ions to combine with cation-chelating binding sites in bEPS were provided with the increasing Cd(II) concentrations [21, 22]. Once Cd(II) was bioadsorbed onto the external cell wall, an internal bioaccumulation process would begin immediately [23]. Use of different strains of *M. aeruginosa* might lead to a longer adsorption process (10 min) [24]. In our experiment, there was also a slow adsorption process following the initial 5 min rapid adsorption, suggesting that Cd(II) was removed via interactions with functional groups on the cell surface [8, 17].

On longer Cd(II) exposure the proportion of Cd(II) sequestrated in *Microcystis* cells increased, reaching >93% at the end of the 10th day in the groups exposed to ≤0.1 mg L^{-1} Cd(II) (Figure 4). *M. aeruginosa* sequestrated >80% of the 0.2 mg L^{-1} added Cd(II). We suggest that when 0.2 mg L^{-1} Cd(II) was added, Cd(II) sequestration by *M. aeruginosa* cells reached its saturation level. Considering the sequestration Cd(II) in *M. aeruginosa*, >80% was bioadsorbed by bEPS and <20% was bioaccumulated inside algal cell (Figures 5 and 6), which is consistent with the results of Parker et al. [25] and Ozturk et al. [8].

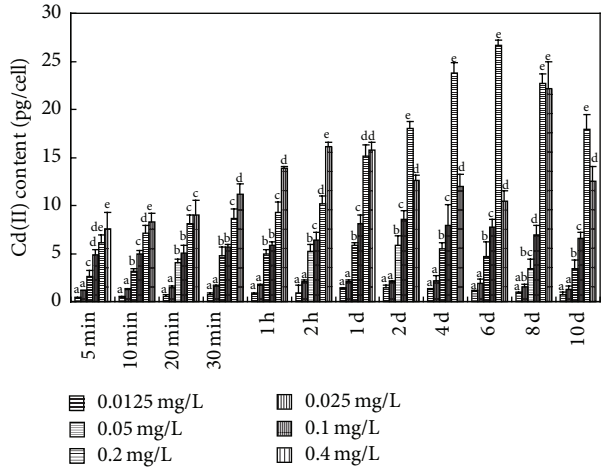

Figure 5: Cd(II) content bioaccumulated inside algal cells. Values sharing the same letters are not significantly different, whereas those marked with different letters are significantly different ($P < 0.05$).

3.4. Effects of Cd(II) on bEPS and IPS Production by M. aeruginosa. Under normal physiological conditions, polysaccharide produced in cells can be partially secreted to form EPS. The cyanobacterial EPS can be divided into two main groups: polysaccharides bound to the cell surface (bEPS) and soluble polysaccharides released into the surrounding environment (soluble extracellular polysaccharide, sEPS) [26]. Bound

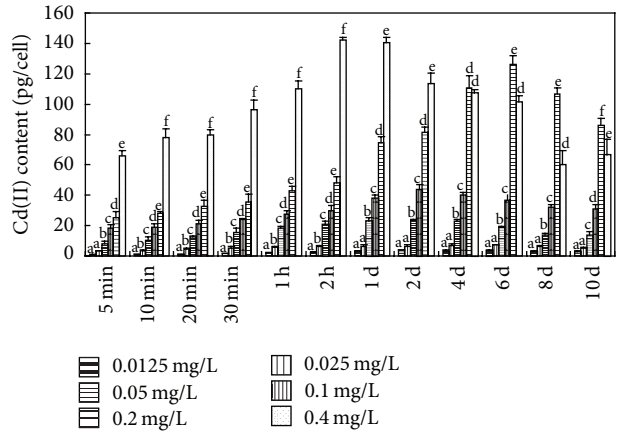

Figure 6: Cd(II) bioadsorbed by bEPS. Values sharing the same letters are not significantly different, whereas those marked with different letters are significantly different ($P < 0.05$).

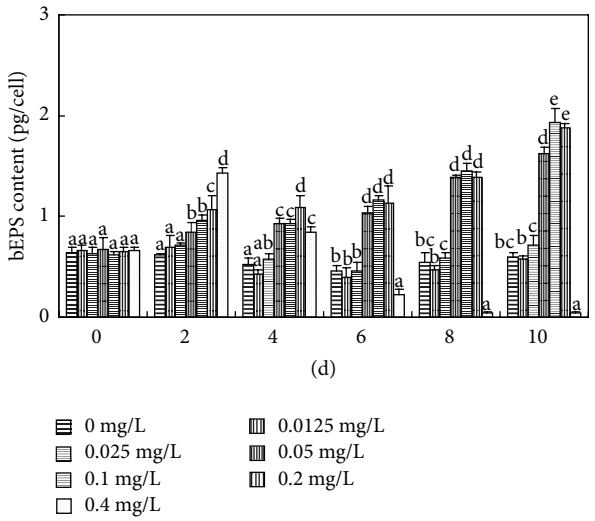

Figure 7: Effects of various concentrations of Cd(II) on the bEPS content of *M. aeruginosa* (pg/cell). Values sharing the same letters are not significantly different, whereas those marked with different letters are significantly different ($P < 0.05$).

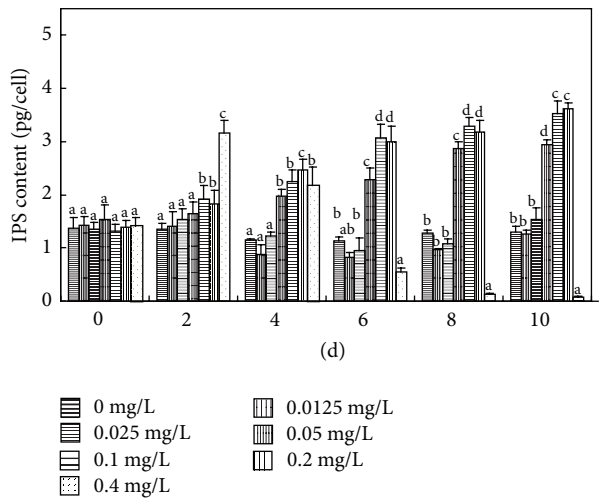

Figure 8: Effects of various concentrations of Cd(II) on the IPS content of *M. aeruginosa* (pg/cell). Values sharing the same letters are not significantly different, whereas those marked with different letters are significantly different ($P < 0.05$).

extracellular polysaccharide, referred to as sheath, capsule, or slime, plays an important role in the attachment of *M. aeruginosa* cells into colonies and in protecting cells from unfavorable environmental conditions [26]. Compared to the control, no significant changes in IPS content were observed in *M. aeruginosa* exposed to 0.0125 and 0.025 mg L^{-1} Cd(II) throughout the experiment, and a similar result was obtained for bEPS for the first 6 days (Figures 7 and 8), because *M. aeruginosa* in long-term laboratory culture responded only slowly to slight environmental disturbance [27]. Higher concentrations of Cd(II) (0.05, 0.1, and 0.2 mg L^{-1}) significantly and simultaneously increased IPS and bEPS levels throughout the experimental period ($P < 0.05$) (Figures 7 and 8). IPS and bEPS contents changed in the same way as each other after Cd(II) exposure and had a high Pearson correlation coefficient throughout the experiment (Table 1), suggesting *Microcystis* cells could respond positively to Cd(II) stress by secreting organic substances (mainly polysaccharides) via active transport [28] (Figures 7 and 8). It is also worth noting that Cd(II) could significantly stimulate bEPS production of *M. aeruginosa* at relatively low concentrations, while the stimulatory activities of Pb(II) were observed at much higher concentrations [29]. Therefore, we speculate that Cd(II) at low concentration could promote the early formation of *Microcystis* colonies by stimulating bEPS production in natural waters.

3.5. Role of Cd(II) in Colony Formation of M. aeruginosa. The Pearson correlation coefficients of exterior and interior factors related to colony formation by *M. aeruginosa* are shown in Table 1. With increasing concentrations of Cd(II) added to the culture medium, Cd(II) bioadsorption onto bEPS and Cd(II) bioaccumulation inside algal cells significantly increased. Increased Cd(II) bioaccumulation inside algal cells stimulated more IPS production. We suggest that, through active transport [28], more IPS was secreted outside the cells, leading to an increased chance of cross-linking between Cd(II) and bEPS [30]. Algal cell aggregation was stimulated by this increased cross-linking, which eventually promoted the formation of *Microcystis* colonies.

4. Conclusions

M. aeruginosa was very sensitive to Cd(II) compared to other heavy metal ions and adsorbed >93% of the Cd(II) in the culture medium when exposed to ≤0.1 mg L^{-1} Cd(II). Among the sequestrated Cd(II) in *M. aeruginosa*, >80% was bioadsorbed by bEPS, and <20% was bioaccumulated inside algal cells. Under the stress of Cd(II), *M. aeruginosa* increased the production of IPS and bEPS, which could significantly

Table 1: Pearson correlation coefficients of exterior and interior factors related to the colony formation of *M. aeruginosa*.

Time	Relationship of initial Cd(II) concentrations with amounts of Cd(II) bioabsorbed on bEPS per unit algal cell	Relationship of initial Cd(II) concentrations with amounts of Cd(II) bioaccumulated inside per unit algal cell	Relationship of amounts of Cd(II) bioabsorbed per unit algal cell with amounts of bEPS per unit algal cell	Relationship of amounts of Cd(II) bioaccumulated inside per unit algal cell with amounts of IPS per unit algal cell	Relationship of bEPS per unit algal cell with IPS per unit algal cell	Relationship of initial Cd(II) concentrations with *Microcystis* colony formation
2 d	0.994**	0.977**	0.897**	0.513*	0.891**	0.724**
4 d	0.988**	0.980**	0.829**	0.821**	0.985**	0.823**
6 d	0.976**	0.975**	0.667**	0.732**	0.981**	0.914**
8 d	0.978**	0.978**	0.628**	0.682**	0.990**	0.955**
10 d	0.987**	0.986**	0.737**	0.795**	0.997**	0.933**

**Correlation is significant at the 0.01 level (two-tailed). *Correlation is significant at the 0.05 level (two-tailed).

promote the formation of small colonies. Notably, this phenomenon occurred at low Cd(II) concentrations, close to those found in natural waters. Moreover, we have found that Pb(II) in the tolerance range of *M. aeruginosa* could stimulate bEPS production, which promoted colony formation [29]. Therefore, heavy metals with different stimulatory effects on different stages of the formation of *Microcystis* colonies might be one factor that contributes to the occurrence of *M. aeruginosa* blooms in natural conditions.

Abbreviations

IPS: Intracellular polysaccharide
bEPS: Bound extracellular polysaccharide
sEPS: Soluble extracellular polysaccharide
EPS: Extracellular polysaccharide
IR: Inhibition rate
ICP-AES: Inductively Coupled Plasma-Atomic Emission Spectrometry.

Competing Interests

The authors declare that they have no competing interests.

Acknowledgments

This work was supported by grants from China National Critical Project for Science and Technology on Water Pollution Prevention and Control (2012ZX07501002-001), the National Natural Science Foundation of China (Grant no. 31300393), China Postdoctoral Science Foundation (Grant nos. 2015T80212 and 2014M551013), Project of Tianjin Science and Technology (Grant nos. 16JCYBJC29900 and 15ZCZDNC00230), and Project of Tianjin Municipal Science and Technology Support Program (Grant no. 12ZCDZNC05300).

References

[1] L. F. Zhao, L. Lu, M. Li, Z. R. Xu, and W. Zhu, "Effects of Ca and Mg levels on colony formation and EPS content of cultured *M. aeruginosa*," *Procedia Environmental Sciences B*, vol. 10, pp. 1452–1458, 2011.

[2] Z. Yang, F. X. Kong, X. L. Shi, M. Zhang, P. Xing, and H. S. Cao, "Changes in the morphology and polysaccharide content of *Microcystis aeruginosa* (Cyanobacteria) during flagellate grazing," *Journal of Phycology*, vol. 44, no. 3, pp. 716–720, 2008.

[3] W. Wang, Y. Liu, and Z. Yang, "Combined effects of nitrogen content in media and *Ochromonas* sp. grazing on colony formation of cultured *Microcystis aeruginosa*," *Journal of Limnology*, vol. 69, no. 2, pp. 193–198, 2010.

[4] N. Q. Gan, Y. Xiao, L. Zhu et al., "The role of microcystins in maintaining colonies of bloom-forming *Microcystis* spp," *Environmental Microbiology*, vol. 14, no. 3, pp. 730–742, 2012.

[5] H. Z. Yuan, J. Shen, and E. F. Liu, "Assessment and characterization of heavy metals and nutrients in sediments from Taihu lake," *Journal of Environmental Sciences-China*, vol. 32, no. 3, pp. 649–657, 2011.

[6] F. Liu, D.-G. Deng, L. Yang, Y.-Q. Shao, P.-F. Zhu, and L. Ji, "Risk evaluation of heavy metals in the surface sediments of lake chaohu in China," *Fresenius Environmental Bulletin*, vol. 22, no. 7, pp. 1807–1813, 2013.

[7] M. Tsezos, "Biosorption of metals. The experience accumulated and the outlook for technology development," *Hydrometallurgy*, vol. 59, no. 2-3, pp. 241–243, 2001.

[8] S. Ozturk, B. Aslim, and Z. Suludere, "Cadmium (II) sequestration characteristics by two isolates of *Synechocystis* sp. in terms of exopolysaccharide (EPS) production and monomer composition," *Bioresource Technology*, vol. 101, no. 24, pp. 9742–9748, 2010.

[9] X. Bi, W. Dai, S. Zhang, K. Xing, and X. Zhang, "Accumulation and distribution characteristics of heavy metals in different size *Microcystis* colonies from natural waters," *Fresenius Environmental Bulletin*, vol. 24, no. 3, pp. 773–779, 2015.

[10] P. H. Vanewijk and J. A. Hoekstra, "Calculation of the EC50 and its confidence interval when subtoxic stimulus is present," *Ecotoxicology and Environmental Safety*, vol. 25, no. 1, pp. 25–32, 1993.

[11] S. L. Zhang, B. Zhang, K. Z. Xing, X. Zhang, X. Tian, and W. Dai, "Inhibitory effects of golden thread (*Coptis chinensis*) and berberine on *Microcystis aeruginosa*," *Water Science and Technology*, vol. 61, no. 3, pp. 763–769, 2010.

[12] M. Dubois, K. A. Gilles, J. K. Hamilton, P. A. Rebers, and F. Smith, "Colorimetric method for determination of sugars and

related substances," *Analytical Chemistry*, vol. 28, no. 3, pp. 350–356, 1956.

[13] U. Meier, "A note on the power of Fisher's least significant difference procedure," *Pharmaceutical Statistics*, vol. 5, no. 4, pp. 253–263, 2006.

[14] A. Jeremy and P. Ingela, "2010 Quantifying colocalization by correlation: the Pearson correlation coefficient is superior to the Mander's overlap coefficient," *Cytometry*, vol. 77A, no. 8, pp. 733–742, 2010.

[15] E. J. Calabrese, "Hormesis: why it is important to toxicology and toxicologists," *Environmental Toxicology and Chemistry*, vol. 27, no. 7, pp. 1451–1474, 2008.

[16] Y. Gong, H. Y. Ao, B. B. Liu et al., "Effects of inorganic arsenic on growth and microcystin production of a *Microcystis* strain isolated from an algal bloom in Dianchi Lake, China," *Chinese Science Bulletin*, vol. 56, no. 22, pp. 2337–2342, 2011.

[17] B. Huang, S. Xu, A. Miao, L. Xiao, and L. Yang, "Cadmium toxicity to *Microcystis aeruginosa* PCC 7806 and its microcystin-lacking mutant," *PLoS ONE*, vol. 10, no. 1, Article ID e0116659, 2015.

[18] P. Rzymski, B. Poniedziałek, P. Niedzielski, P. Tabaczewski, and K. Wiktorowicz, "Cadmium and lead toxicity and bioaccumulation in *Microcystis aeruginosa*," *Frontiers of Environmental Science & Engineering*, vol. 8, no. 3, pp. 427–432, 2014.

[19] Z.-X. Wu and L.-R. Song, "Physiological comparison between colonial and unicellular forms of *Microcystis aeruginosa* Kütz. (Cyanobacteria)," *Phycologia*, vol. 47, no. 1, pp. 98–104, 2008.

[20] Z.-X. Wu, N.-Q. Gan, Q. Huang, and L.-R. Song, "Response of *Microcystis* to copper stress—do phenotypes of *Microcystis* make a difference in stress tolerance?" *Environmental Pollution*, vol. 147, no. 2, pp. 324–330, 2007.

[21] F. Pagnanelli, M. Petrangeli Papini, L. Toro, M. Trifoni, and U. F. Vegliò, "Biosorption of metal ions on *Arthrobacter* sp.: biomass characterization and biosorption modeling," *Environmental Science and Technology*, vol. 34, no. 13, pp. 2773–2778, 2000.

[22] S. J. Chen, W. J. Zheng, and F. Yang, "Study advances on heavy metals bio-adsorbed by cyanobacteria," *Marine Environmental Science*, vol. 25, no. 4, pp. 103–106, 2006.

[23] N. Rangsayatorn, E. S. Upatham, M. Kruatrachue, P. Pokethitiyook, and G. R. Lanza, "Phytoremediation potential of *Spirulina* (*Arthrospira*) platensis: biosorption and toxicity studies of cadmium," *Environmental Pollution*, vol. 119, no. 1, pp. 45–53, 2002.

[24] J. Zeng, D. Y. Zhao, Y. B. Ji, and Q. L. Wu, "Comparison of heavy metal accumulation by a bloom-forming cyanobacterium, *Microcystis aeruginosa*," *Chinese Science Bulletin*, vol. 57, no. 28-29, pp. 3790–3797, 2012.

[25] D. L. Parker, L. C. Rai, N. Mallick, P. K. Rai, and H. D. Kumar, "Effects of cellular metabolism and viability on metal ion accumulation by cultured biomass from a bloom of the cyanobacterium *Microcystis aeruginosa*," *Applied and Environmental Microbiology*, vol. 64, no. 4, pp. 1545–1547, 1998.

[26] R. D. Philippis and M. Vincenzini, "Outermost polysaccharidic investments of cyanobacteria: nature, significance and possible applications," *Recent Research Developments in Microbiology*, vol. 7, pp. 13–22, 2003.

[27] C. S. Reynolds, G. Jaworski, H. Cmiech, and G. Leedale, "On the annual cycle of the blue-green alga *Microcystis aeruginosa* Kütz. emend. Elenkin," *Philosophical Transactions of the Royal Society B: Biological*, vol. 293, no. 1068, pp. 419–477, 1981.

[28] S. M. Myklestad, "Release of extracellular products by phytoplankton with special emphasis on polysaccharides," *Science of the Total Environment*, vol. 165, no. 1–3, pp. 155–164, 1995.

[29] X.-D. Bi, S.-L. Zhang, W. Dai, K.-Z. Xing, and F. Yang, "Effects of lead(II) on the extracellular polysaccharide (EPS) production and colony formation of cultured *Microcystis aeruginosa*," *Water Science and Technology*, vol. 67, no. 4, pp. 803–809, 2013.

[30] T. C. Lau, P. O. Ang, and P. K. Wong, "Development of seaweed biomass as a biosorbent for metal ions," *Water Science and Technology*, vol. 47, no. 10, pp. 49–54, 2003.

Hindawi Publishing Corporation
BioMed Research International
Volume 2016, Article ID 6861702, 7 pages
http://dx.doi.org/10.1155/2016/6861702

Research Article

Interaction Effects between Organochlorine Pesticides and Isoflavones *In Vitro* and *In Vivo*

Yunbo Zhang, Jipeng Guo, Xiao Zhang, Jingjing Guo, Ming Zhang, Yang Yang, and Xiaolin Na

Department of Environmental Hygiene, Public Health College, Harbin Medical University, Harbin, Heilongjiang 150081, China

Correspondence should be addressed to Xiaolin Na; naxiaolin1495@sohu.com

Received 30 March 2016; Revised 25 May 2016; Accepted 16 June 2016

Academic Editor: Kaiyu He

Organochlorine pesticides (OCPs) have caused increasing global concern due to their high toxicity, persistence, bioaccumulation, and significant adverse effects on human health. This study was to explore the interaction effects between OCPs and isoflavones. Six kinds of OCPs and 2 kinds of isoflavones-genistein and daidzein were included to study their effect on MCF-7 cells *in vitro*. Eighty-one female Sprague-Dawley rats were randomized to 9 groups according to factorial design to study the interaction effect between isoflavones and γ-HCH. Compared to organochlorine pesticides alone group, proliferation rate of MCF-7 cells was lower in 100 μmol/L genistein + organochlorine pesticides and 100 μmol/L daidzein + organochlorine pesticides group ($p < 0.05$). *In vivo* study showed that there are interaction effects on kidney weight and liver weight when treated with isoflavones and γ-HCH. The changes in uterine morphology and positive expression of ERα showed inhibition effects between isoflavones and γ-HCH. In conclusion, the data suggests that there are interactions between isoflavones and OCPs *in vitro* and *in vivo*.

1. Introduction

The research on endocrine-disrupting chemicals (EDCs) has attracted more and more interest of scientists. Organochlorine pesticides (OCPs), which are one of the EDCs, can be lipophilic, stable, difficult to be degraded, volatile, and accumulative. They are easy to be accumulated in environment, and humans can absorb them via food chain enrichment through the digestive tract, respiratory tract, and skin [1, 2]. The OCPs are usually divided into three main groups including DDT and its derivatives (DDTs and DDEs), HCHs, and chlorinated cyclodiene such as chlordane. DDEs are the main bioaccumulative metabolite of the organochlorine insecticide DDT. Exposure of men or animals to OCPs can cause some side effects including reproductive toxicity and even cancer [3, 4].

Soybean isoflavones are a kind of plant estrogen, extracted in soybean, mainly including genistein and daidzein. Genistein is the most frequently studied isoflavone due to its biological activities of improving cardiovascular, bone, and postmenopausal health. Daidzein, a major component of soy with structural similarities to estrogen, can exert effects of anti-inflammatory, lowering lipid levels and increasing mitochondrial biogenesis. Many studies have indicated that the isoflavones or single components (genistein or daidzein) have many important biological activities; for example, they can improve the women's menopause syndrome and prevent osteoporosis. Messina et al. found that higher isoflavones intake was associated with 25% reduction in recurrence in 9,514 breast cancer survivors over 7.4-year follow-up period [5]. Moreover, although the antiproliferation effect in different breast tumor cell types treated with different concentration of genistein and daidzein varied, their effects were related to ERα and c-erbB-2 expression [6].

Breast cancer is the most common and leading type of cancer in women, and the survival rates are very poor in developing countries. Human breast cancer cell line MCF-7 was used as the hormone-responsive breast cancer cell line in many studies. Estrogen can make the pathological progress of mammary gland cells accelerate, which is a major cause of estrogen dependent breast cancer. A large number of studies showed that OCPs could combine with estrogen receptor to cause some side effects including reproductive toxicity [7, 8]. According to Shekhar, p,p′-DDT could evoke responses and

further enhance the responses together with estradiol or o,p′-DDT in estrogen receptor-positive breast cancer cells [9]. However, studies showed that both genistein and DDT can be combined with estrogen receptor. High concentrations of genistein can inhibit the proliferation of cells while DDTs promote the proliferation of cells, although the effects of isoflavones on breast cancer remain controversial and human clinical investigations are needed [10]. We can still predict that more phytoestrogen dietary intake may drop the weakness of exogenous estrogen.

OCPs affect human health mainly by continuous exposures at low dose [11]. And human can be exposed to isoflavones by daily food. It has practical significance to carry out research on interactions between OCPs and isoflavones.

2. Material and Methods

2.1. In Vitro Experiment

2.1.1. Chemicals. β-HCH, γ-HCH, o,p′-DDT, p,p′-DDT, p,p′-DDE, and chlordane were purchased from Dr. Ehrenstorfer GmbH Ltd. Co. (Germany). Genistin (Gen, purity ≥ 99%), daidzein (Dai, purity ≥ 99%), estradiol (E_2), and methyl thiazolyl tetrazolium (MTT) were purchased from Sigma Chemical Co. (St. Louis, MO).

2.1.2. Cell Culture and Treatment. MCF-7 cells were cultured in a 37°C, 5% CO_2 saturated humidity incubator with DMEM (containing 100 IU/mL penicillin/streptomycin and 10% FBS). The cells had digestive transfer culture after being grown to 80% cell density. Discard DMEM and rinse it two times by PBS (pH 7.4) solution. 0.05% trypsin (1 mL) was added to cover cell layer for 2-3 minutes. After discarding dispersed liquid, 5 mL DMEM was added in culture bottle. Cells were made into single cell suspension and placed into culture flask at 37°C.

2.1.3. MTT Experiment. MCF-7 cells were cultured in phenol red-free DMEM (Sigma-Aldrich) with 100 IU/mL penicillin/streptomycin and 10% charcoal stripped estrogen-free FBS (Invitrogen). Cells were treated with the following solutions: (i) DMEM medium alone (the control group); (ii) 100 μmol/L genistein group; (iii) 100 μmol/L daidzein group; (iv) 1 μmol/L o,p′-DDT, 1 μmol/L p,p′-DDT, 1 μmol/L γ-HCH, 1 μmol/L chlordane, 10 μmol/L p,p′-DDE, and 20 μmol/L β-HCH; (v) 100 μmol/L genistein + 1 μmol/L o,p′-DDT, 100 μmol/L genistein + 1 μmol/L p,p′-DDT, 100 μmol/L genistein + 1 μmol/L γ-HCH, 100 μmol/L genistein + 1 μmol/L chlordane, 100 μmol/L genistein + 10 μmol/L p,p′-DDE, and 100 μmol/L genistein + 20 μmol/L β-HCH; (vi) 100 μmol/L daidzein + 1 μmol/L o,p′-DDT, 100 μmol/L daidzein + 1 μmol/L p,p′-DDT, 100 μmol/L daidzein + 1 μmol/L γ-HCH, 100 μmol/L daidzein + 1 μmol/L chlordane, 100 μmol/L daidzein + 10 μmol/L p,p′-DDE, and 100 μmol/L daidzein + 20 μmol/L β-HCH. Cell growth and inhibition rate was measured by 3-(4,5-dimethylthiazol-2-yl)-2,5-diphenyltetrazolium bromide (MTT) assay.

Table 1: Groups by 3 ∗ 3 factorial design with different dose of isoflavones and γ-HCH (n = 9/group).

γ-HCH (mg/kg bw)	Isoflavones (mg/kg diet)		
	900	600	0
8	1	4	7
4	2	5	8
0	3	6	9

Note: factorial design with 2 factors of 3 levels. Three levels of γ-HCH: 8 mg/kg bw, 4 mg/kg bw, and 0 mg/kg bw. Three levels of isoflavones: 900 mg/kg diet, 600 mg/kg diet, and 0 mg/kg diet.

Cells were seeded in 96-well plates (cell density of 3×10^4/mL) for 24 h and exposed to various concentrations of genistein, daidzein, or OCPs for 48 h. Then the cells were incubated with 20 μL 5 mg/mL MTT in the dark for 4 h at 37°C. Absorbance values (optical density, OD) were obtained using a microplate reader (model 680: Bio-Rad Laboratories, Inc., Hercules, CA, USA) at a wavelength of 490 nm. Wells containing cells in DMEM were served as the normal control. To convert OD values to proliferation rate, the following equation was used: proliferation rate (PR) = OD of test concentration/OD of control ∗ 100%. Each concentration was measured in 3–5 repeated wells, and every assay was tested ≥3 times.

2.2. In Vivo Experiment

2.2.1. Chemical. Isoflavones were purchased from Rongsheng Ltd. Co. (Xi'an, China) with purity ≥98%. γ-HCH was purchased from Qinchengletter Ltd. Co. (Beijing, China) with purity of 99.4%.

2.2.2. Animals. Prior to study initiation, the experimental protocol was reviewed and approved by the Committee on Animal Research and Ethics of Harbin Medical University (Harbin, China). Eighty-one female Sprague-Dawley (SD) rats, weighing 60–80 g, were purchased from Weitonglihua Experimental Animal Ltd. Co. (Beijing, China, Batch number SCXK (jing) 2012-0001). The animals were caged in a room maintained at 23 ± 2°C. After adaption for 1 week, rats were randomly divided into 9 groups in single cage. Each group was divided by 3 ∗ 3 factorial design with different dose of isoflavones and γ-HCH (Table 1). Isoflavones were added into diet. γ-HCH was dissolved with corn oil and administrated by intragastric administration.

SD rats were fed in the standard animal laboratory for 4 weeks. At the end of the experiment, rats were sacrificed after being fasted for 12 h. Body organs such as brain, liver, kidney, spleen, and the parametrial and perirenal fat pads of rats were dissected and weighed. Blood was collected from the sacrificed animals and serum was separated from the blood (3,000 rpm, 15 min) for the determination of estradiol and testosterone using radioimmunoassay and serum glucose using automatic biochemical analyzer (Hitachi 7100, Japan). The reagent kits were bought from Northern Institution of

Biotechnology (Beijing, China). Histopathological examination was performed on 5 μm paraffin sections with standard hematoxylin-eosin (HE) staining. The examination was performed blindly. Immunohistochemistry was performed to investigate the expression of ERα in uterus with ERα antibody from Zhongshan Technology Ltd. Co. (Beijing, China). The representative pictures were digitized by inverted microscope (Nikon Ti-S, Japan). The immunohistochemistry staining was quantified by using Image-Pro Plus software (Media Cybernetics, USA).

2.3. Statistics. The statistical analyses were performed with the SPSS program. Data was expressed as means ± SD. Data in this work were normally distributed determined with the Kolmogorov-Smirnov test. The data of cell culture study was analyzed with one-way ANOVA. Animal study was analyzed using a two-way ANOVA with isoflavones and OCPs treatments as factors, followed by a post hoc test with Fisher's least significant difference (LSD). p value < 0.05 was considered significant for all statistical analyses.

3. Results

3.1. In Vitro. The interaction of genistein and daidzein with OCPs in MCF-7 cells was shown in Figure 1. Compared to control group, OCPs could increase proliferation rate of MCF-7 cell line while genistein and daidzein could inhibit the growth of MCF-7 cell observably ($p < 0.05$). Compared with OCPs alone group (o,p′-DDT, p,p′-DDT, β-HCH, and γ-HCH), proliferation rate of MCF-7 cells was lower in both 100 μmol/L genistein + OCPs group and daidzein + OCPs group ($p < 0.05$). Furthermore, proliferation rate of MCF-7 cells in genistein treatment group was lower than daidzein treatment group in o,p′-DDT, p,p′-DDT, and β-HCH group, higher in γ-HCH group.

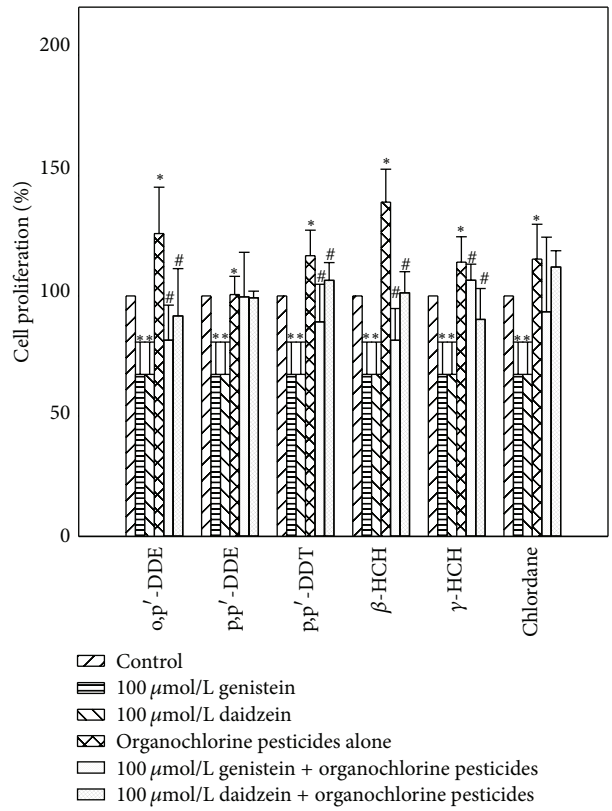

Figure 1: Interaction of genistein and daidzein with OCPs on proliferation rate of MCF-7 cells. * p value < 0.05 was considered significant compared with control group; # p value < 0.05 was considered significant compared with organochlorine pesticides alone group.

Table 2: Two-way ANOVA analysis of effect of isoflavones and γ-HCH treatment on rats (p value).

	Main effect		Interaction effect
	Isoflavones	γ-HCH	
Blood glucose	0.022*	0.423	0.419
Estradiol	0.159	0.003*	0.652
Testosterone	0.749	0.020*	0.110
Spleen weight	0.015*	0.012*	0.795
Kidney weight	0.529	0.566	0.047*
Liver weight	0.283	0.050	0.033*

* p value < 0.05 was considered significant.

3.2. In Vivo

3.2.1. Effect of Isoflavones and γ-HCH on Body Weight. Effect of isoflavones and γ-HCH on body weight was shown in Figure 2. Rats grew normally and the body weight increased step by step from beginning of experiment to the end. Two-way ANOVA indicated that no significant differences were found in rats' body weight treated with different dosage of isoflavones and γ-HCH ($p > 0.05$).

3.2.2. Interaction of Isoflavones and γ-HCH. The main effects of isoflavones and γ-HCH and their interaction were shown in Table 2. According to Table 2, the effect of isoflavones treatment on fasting blood glucose was significant ($p = 0.022$); that is, serum glucose levels in 600 mg/kg diet isoflavones treatment groups were increased markedly compared to 0 mg/kg diet isoflavones treatment groups (6.1 ± 0.2 mmol/L in 900 mg/kg diet treatment groups, 6.8 ± 0.2 mmol/L in 600 mg/kg diet treatment groups, and 6.2 ± 0.2 mmol/L in 0 mg/kg diet treatment groups). No main effect of γ-HCH and interaction effects were found in serum fasting blood glucose. In addition, the main effect of γ-HCH in serum estradiol and testosterone levels was prominent; that is, γ-HCH could reduce serum level of estradiol and testosterone notably (estradiol: 33.64 ± 2.39 pg/mL in 8 mg/kg bw, 36.45 ± 2.39 pg/mL in 4 mg/kg bw, and 45.37 ± 2.51 pg/mL in 0 mg/kg bw; testosterone: 1.45 ± 0.22 ng/mL in 8 mg/kg bw, 1.66 ± 0.22 ng/mL in 4 mg/kg bw, and 2.30 ± 0.22 ng/mL in 0 mg/kg bw). No main effect of isoflavones and interaction effects were found. Furthermore, both isoflavones and γ-HCH could alter spleen weight significantly. Isoflavones had a tendency of increase, while γ-HCH could reduce spleen weight (data not shown). Overall, there are no interactions

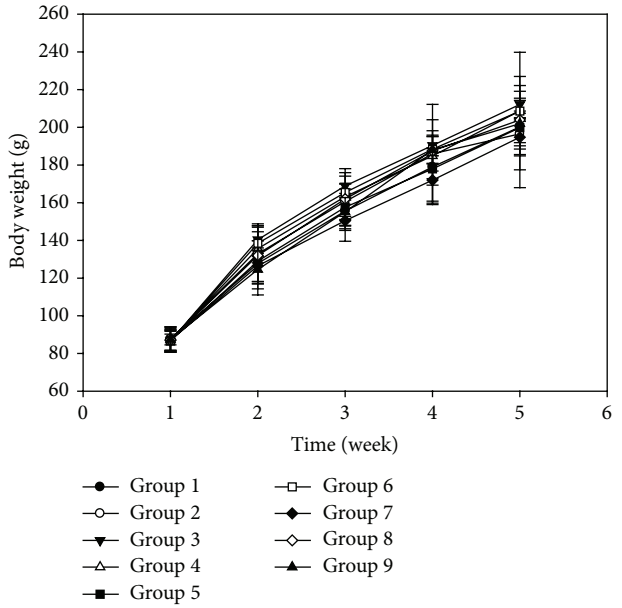

Figure 2: Effect of isoflavones and γ-HCH on body weight in female SD rats. Group 1: 900 mg/kg diet isoflavones and 8 mg/kg bw γ-HCH; group 2: 900 mg/kg diet isoflavones and 4 mg/kg bw γ-HCH; group 3: 900 mg/kg diet isoflavones and 0 mg/kg bw γ-HCH; group 4: 600 mg/kg diet isoflavones and 8 mg/kg bw γ-HCH; group 5: 600 mg/kg diet isoflavones and 4 mg/kg bw γ-HCH; group 6: 600 mg/kg diet isoflavones and 0 mg/kg bw γ-HCH; group 7: 0 mg/kg diet isoflavones and 8 mg/kg bw γ-HCH; group 8: 0 mg/kg diet isoflavones and 4 mg/kg bw γ-HCH; group 9: 0 mg/kg diet isoflavones and 0 mg/kg bw γ-HCH.

between isoflavones and γ-HCH except kidney ($p = 0.047$) and liver weight ($p = 0.033$). The changes of liver weight in isoflavones 900 mg/kg diet group were different from isoflavones 600 mg/kg diet along with the increase of γ-HCH dose. In isoflavones 600 mg/kg diet group, liver weight was increased significantly with the increase of γ-HCH dose (γ-HCH 8 mg/kg bw group: 7.36 ± 0.69 g; γ-HCH 4 mg/kg bw group: 6.97 ± 1.19 g; γ-HCH 0 mg/kg bw group: 6.55 ± 0.84 g). However, in isoflavones 900 mg/kg diet, liver weight was highest in γ-HCH 8 mg/kg bw group (7.70±0.52 g) and lowest in γ-HCH 4 mg/kg bw group (6.80 ± 0.32 g). In addition, the changes of kidney weight in γ-HCH 8 mg/kg bw were different from γ-HCH 4 mg/kg bw along with the increase of isoflavones dose. In γ-HCH 8 mg/kg bw group, kidney weight was highest in isoflavones 600 mg/kg diet group (900 mg/kg diet: 1.55 ± 0.14 g; 600 mg/kg diet: 1.74 ± 0.13 g; 0 mg/kg diet: 1.54±0.13 g). But in γ-HCH 4 mg/kg bw group, kidney weight was highest in isoflavones 0 mg/kg diet group (900 mg/kg diet: 1.63 ± 0.14 g; 600 mg/kg diet: 1.63 ± 0.27 g; 0 mg/kg diet: 1.69 ± 0.18 g).

3.2.3. Interaction of Isoflavones and γ-HCH on Uterine Morphology. To make the comparison simpler and easier, only uterine morphology in groups 1, 3, 7, and 9 was analyzed. The interaction of isoflavones and γ-HCH on uterine morphology was shown in Figure 3. Compared with control group, tissue morphology was changed significantly in isoflavones treatment group and γ-HCH treatment group. High columnar endometrial glandular epithelial cells were found in isoflavones treatment group, while low columnar endometrial glandular epithelial cells were shown in γ-HCH treatment group. Furthermore, although high columnar endometrial glandular epithelial cells were found in group 1 with mixed treatment of 900 mg/kg diet isoflavones and 8 mg/kg bw γ-HCH, the degree of hyperplasia was lower than isoflavones treatment group and higher than γ-HCH treatment group (Figure 3(a)). In addition, the changes of expression of ERα in uterus were similar to the changes of uterine morphology (Figure 3(b)). Compared with control group, the positive expression of ERα in isoflavones treatment group was significantly higher ($p < 0.001$) and lower in γ-HCH treatment group ($p = 0.025$). The positive expression rate of ERα in group 1 with 900 mg/kg diet isoflavones and 8 mg/kg bw γ-HCH was lower than isoflavones treatment group and higher than γ-HCH treatment group (Figure 3(c)).

4. Discussion

EDCs are chemicals that may interfere with the body's endocrine system and produce adverse developmental, reproductive, neurological, and immune effects in both humans and wildlife. EDCs are derived from a wealth of sources, including OCPs, xenoestrogens, long-chain alkylphenols, and phytoestrogen. MCF-7 cells derived from human breast cancer cells, which are positive to ER and sensitive to estrogen, have been widely used to evaluate environmental estrogen and explore the development mechanism of estrogen on breast cancer occurrence [12, 13]. Genistein is a phytoestrogen with a plant-derived phenolic compound that structurally mimics the hormone 17 β-estradiol. Previous studies revealed that genistein could significantly inhibit the proliferation of MCF-7 cells in a dose-dependent manner. High dose of genistein could inhibit proliferation rate of MCF-7 cells [6, 12, 14]. Besides, daidzein and genistein exhibited biphasic effects (stimulatory or inhibitory) on proliferation and ERα expression in MCF-7 cells. That is, 1 μmol/L daidzein significantly stimulates cell growth and 200 μmol/L daidzein could inhibit cell proliferation [6]. In this study, we found that both 100 μmol/L genistein and 100 μmol/L daidzein could inhibit proliferation of MCF-7 cells. The dichlorodiphenyltrichloroethane (DDT), a known endocrine disruptor, links to animal and human disorders [15]. Payne et al. found that o,p′-DDT, p,p′-DDE, β-HCH, and p,p′-DDT produce proliferative effects in MCF-7 cells. Furthermore, combined effects were demonstrated by regression analyses even when each mixture component was present at levels or below its individual no-observed-effect concentration [16]. However, the research on interaction between soy isoflavones (genistein and daidzein) and OCPs was little. According to Charles et al., both *in vitro* and *in vivo*, low concentrations of the six synthetic chemicals (SCs, including o,p-DDT) failed to increase estrogenic responses which were induced by plant-derived phytoestrogens (PEs) alone. *In vitro*, interactions

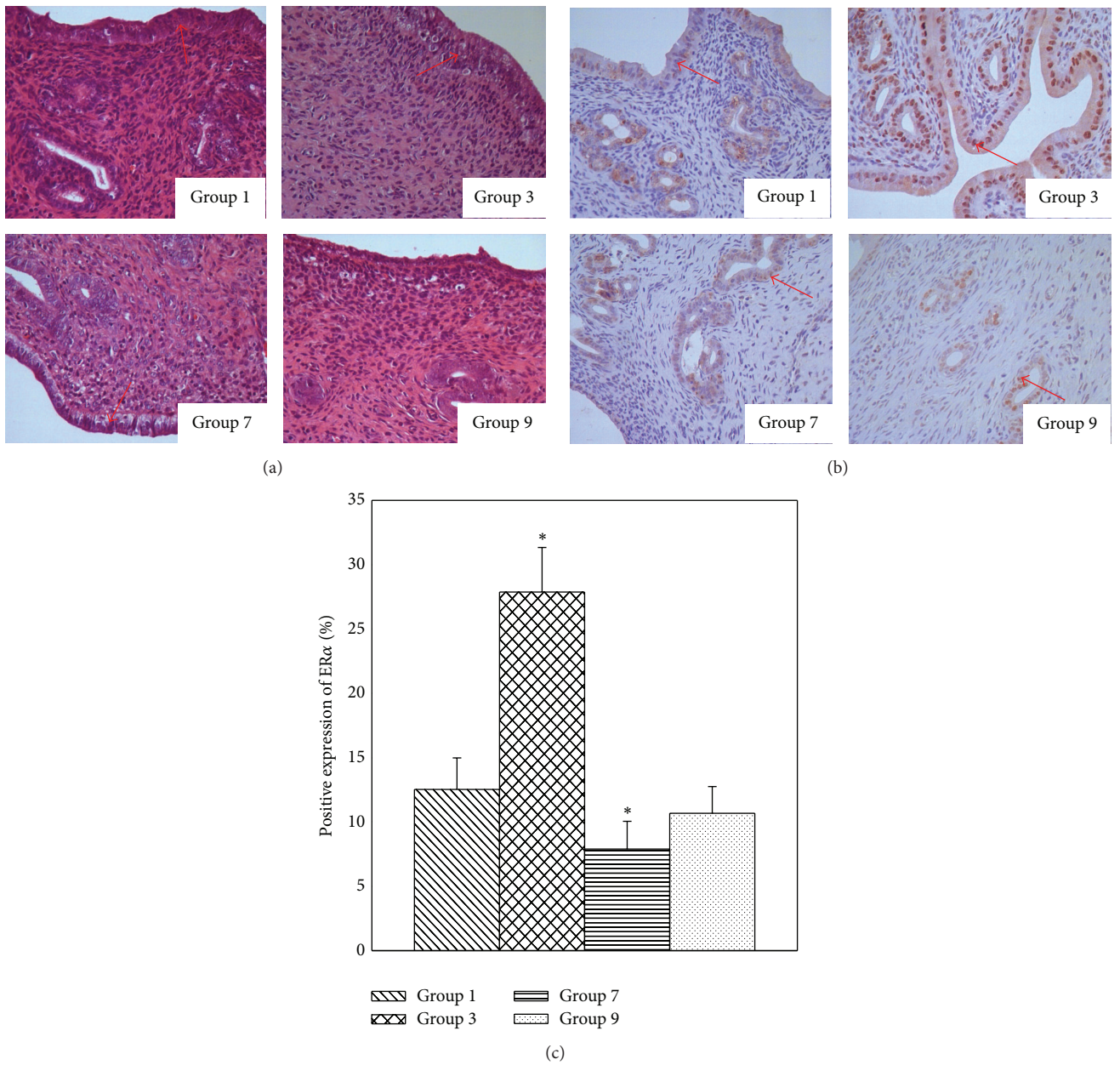

FIGURE 3: Interaction of isoflavones and γ-HCH on uterine morphology and expression of ERα. (a) showed interaction of isoflavones and γ-HCH on uterine morphology. Compared with control group (group 9), high columnar endometrial glandular epithelial cells were found in group 3, while low columnar endometrial glandular epithelial cells were shown in group 7. Furthermore, although high columnar endometrial glandular epithelial cells were found in group 1, the degree of hyperplasia was lower than isoflavones treatment group and higher than γ-HCH treatment group. (b) showed interaction of isoflavones and γ-HCH on expression of ERα. Compared to group 9, ERα expression was higher in group 3 ($p \leq 0.05$), while being lower in group 7 ($p \leq 0.05$). Moreover, ERα expression in group 1 was lower than group 3 and higher than group 7. (c) showed positive expression of ERα in immunohistochemistry. $^{*}p$ value < 0.05 was considered significant compared with control group (group 9). Group 1 was treated with 900 mg/kg diet isoflavones and 8 mg/kg bw γ-HCH; group 3 was treated with 900 mg/kg diet isoflavones alone; group 7 was treated with 8 mg/kg bw γ-HCH alone; group 9 was treated with 0 mg/kg diet isoflavones and 0 mg/kg bw γ-HCH.

between high dosages of SCs and PEs were greater than mixtures of SCs in the absence of PEs [17]. In our study, soy isoflavones (genistein and daidzein) could repair the damage of OCPs; that is, isoflavones could inhibit breast cell proliferation triggered by OCPs except p,p′-DDE and chlordane.

In vivo test was conducted according to the results of *in vitro* experiment. We used soy isoflavones as a mixture of

genistein and daidzein. Overall, isoflavones could influence blood glucose and spleen weight in female rats; γ-HCH could affect estradiol and testosterone levels in serum and spleen weight in high dose treatment. Furthermore, there is interaction effect on kidney weight and liver weight when treated with isoflavones and γ-HCH. No other effects were found in body weight, brain weight, fat weight, and so forth.

Previous study showed that soy isoflavones could significantly decrease body weight [18], while HCB, p,p′-DDE, and β-HCH showed quadratic associations with BMI [19]. In this study, no significant changes were found in isoflavones and OCPs treatment. Ye et al. found that both daidzein and genistein did not have a significant effect on glycemic control and insulin sensitivity over a 6-month supplementation period in Chinese women [20]. Another research showed that isoflavones mixture could lower blood glucose level in serum in high-fat diet fed C57BL/6J mice for 92 days [21]. But in this study, low dosage of isoflavones (600 mg/kg diet) could increase blood glucose level in female rats. The possible causes of differences between previous study and the current study are as follows: (1) SD rats were used in the present study instead of C57/BL6 mice, which have different absorption and ingestion for different species; (2) natural synthesis isoflavones were used as the intervention medicine, and they were different from the mixture of daidzin and glycitin used in their study. Otherwise, the interaction effect of isoflavones and γ-HCH on kidney weight and liver weight indicated that they could resist their side effects to produce healthy condition.

A wide number of pesticides, including OCPs, such as γ-HCH, may induce reproductive and developmental alterations by altering steroid hormone metabolism or binding to the estrogen/androgen receptors. Exposure to γ-HCH with dose of 25 mg/kg bw *in vivo* could increase absolute and relative uterus weight in F1 pups on postnatal day 22 and change vaginal patency and reduce diameters of primary oocytes at fully sexual maturity [22]. According to findings of Huang et al., both chlordane and γ-HCH treatment could increase estrogen, reduce testosterone, and alter morphology of the masculine appendage in shrimp [23]. In our study, estradiol and testosterone levels in serum were reduced in female rats treated with γ-HCH. Furthermore, the changes of uterine morphology and expression of ERα showed that there was interaction effect between isoflavones and γ-HCH.

5. Conclusions

In summary, high dosage of genistein and daidzein could inhibit proliferation of MCF-7 cells treated with OCPs. Besides, there are interaction effects between isoflavones and γ-HCH in uterine morphology and expression of ERα. The mechanisms of interactions between OCPs and isoflavones are not clear. Competitive inhibition effect may possibly be involved in the mechanism. Isoflavones show stronger affinity to ER, which may inhibit the combination of γ-HCH to ER.

Competing Interests

The authors declare that there is no conflict of interests regarding the publication of this paper.

Acknowledgments

This study was supported by the National Natural Science Foundation of China (81202190, 30972439, and 81273079) and the Innovation Fund of Harbin Medical University.

References

[1] A. F. A. Mahmoud, Y. Ikenaka, Y. B. Yohannes et al., "Distribution and health risk assessment of organochlorine pesticides (OCPs) residue in edible cattle tissues from northeastern part of Egypt: High accumulation level of OCPs in tongue," *Chemosphere*, vol. 144, pp. 1365–1371, 2016.

[2] F.-L. Tang, M. Zhang, J.-F. Xu et al., "Pollution characteristics and health risk assessment of organochlorine pesticides (OCPs) in the water of Lake Qiandao and its major input rivers," *Huan Jing Ke Xue*, vol. 35, no. 5, pp. 1735–1741, 2014.

[3] J.-Z. Yang, Z.-X. Wang, L.-H. Ma et al., "The organochlorine pesticides residues in the invasive ductal breast cancer patients," *Environmental Toxicology and Pharmacology*, vol. 40, no. 3, pp. 698–703, 2015.

[4] N. Pi, S. E. Chia, C. N. Ong, and B. C. Kelly, "Associations of serum organohalogen levels and prostate cancer risk: results from a case-control study in Singapore," *Chemosphere*, vol. 144, pp. 1505–1512, 2016.

[5] M. Messina, B. J. Caan, D. I. Abrams, M. Hardy, and G. Maskarinec, "It's time for clinicians to reconsider their proscription against the use of soyfoods by breast cancer patients," *Oncology*, vol. 27, no. 5, pp. 430–437, 2013.

[6] E. J. Choi and G.-H. Kim, "Antiproliferative activity of daidzein and genistein may be related to ERα/c-erbB-2 expression in human breast cancer cells," *Molecular Medicine Reports*, vol. 7, no. 3, pp. 781–784, 2013.

[7] D. Pestana, D. Teixeira, A. Faria, V. Domingues, R. Monteiro, and C. Calhau, "Effects of environmental organochlorine pesticides on human breast cancer: putative involvement on invasive cell ability," *Environmental Toxicology*, vol. 30, no. 2, pp. 168–176, 2015.

[8] V. Briz, J.-M. Molina-Molina, S. Sánchez-Redondo et al., "Differential estrogenic effects of the persistent organochlorine pesticides dieldrin, endosulfan, and lindane in primary neuronal cultures," *Toxicological Sciences*, vol. 120, no. 2, pp. 413–427, 2011.

[9] P. V. M. Shekhar, J. Werdell, and V. S. Basrur, "Environmental estrogen stimulation of growth and estrogen receptor function in preneoplastic and cancerous human breast cell lines," *Journal of the National Cancer Institute*, vol. 89, no. 23, pp. 1774–1782, 1997.

[10] Y. Kwon, "Effect of soy isoflavones on the growth of human breast tumors: findings from preclinical studies," *Food Science & Nutrition*, vol. 2, no. 6, pp. 613–622, 2014.

[11] R. Cholewa, D. Beutling, J. Budzyk, M. Pietrzak, and S. Walorczyk, "Persistent organochlorine pesticides in internal organs of coypu, Myocastor coypus," *Journal of Environmental Science and Health—Part B Pesticides, Food Contaminants, and Agricultural Wastes*, vol. 50, no. 8, pp. 590–594, 2015.

[12] P. Fan, S. Fan, H. Wang et al., "Genistein decreases the breast cancer stem-like cell population through Hedgehog pathway," *Stem Cell Research & Therapy*, vol. 4, no. 6, article 146, 2013.

[13] G. Dall, J. Vieusseux, A. Unsworth, R. Anderson, and K. Britt, "Low dose, low cost estradiol pellets can support MCF-7 tumour growth in nude mice without bladder symptoms," *Journal of Cancer*, vol. 6, no. 12, pp. 1331–1336, 2015.

[14] E. J. Choi, J. Y. Jung, and G.-H. Kim, "Genistein inhibits the proliferation and differentiation of MCF-7 and 3T3-L1 cells via the regulation of ERα expression and induction of apoptosis," *Experimental and Therapeutic Medicine*, vol. 8, no. 2, pp. 454–458, 2014.

[15] M. R. Bratton, D. E. Frigo, H. C. Segar et al., "The organochlorine o,p′-DDT plays a role in coactivator-mediated MAPK crosstalk in MCF-7 breast cancer cells," *Environmental Health Perspectives*, vol. 120, no. 9, pp. 1291–1296, 2012.

[16] J. Payne, M. Scholze, and A. Kortenkamp, "Mixtures of four organochlorines enhance human breast cancer cell proliferation," *Environmental Health Perspectives*, vol. 109, no. 4, pp. 391–397, 2001.

[17] G. D. Charles, C. Gennings, B. Tornesi et al., "Analysis of the interaction of phytoestrogens and synthetic chemicals: an in vitro/in vivo comparison," *Toxicology and Applied Pharmacology*, vol. 218, no. 3, pp. 280–288, 2007.

[18] Z. Zhu, L. Li, X. Jin, J. Fang, and D. Zhang, "Er-Xian Decoction, a traditional Chinese herbal formula, intervening early in hypothalamic-pituitary axis of male rats with delayed puberty," *Pharmacognosy Magazine*, vol. 10, no. 40, pp. 517–521, 2014.

[19] J. P. Arrebola, R. Ocaña-Riola, A. L. Arrebola-Moreno et al., "Associations of accumulated exposure to persistent organic pollutants with serum lipids and obesity in an adult cohort from Southern Spain," *Environmental Pollution*, vol. 195, pp. 9–15, 2014.

[20] Y.-B. Ye, A.-L. Chen, W. Lu et al., "Daidzein and genistein fail to improve glycemic control and insulin sensitivity in Chinese women with impaired glucose regulation: a double-blind, randomized, placebo-controlled trial," *Molecular Nutrition and Food Research*, vol. 59, no. 2, pp. 240–249, 2015.

[21] Y. Zang, K. Igarashi, and C. Yu, "Anti-obese and anti-diabetic effects of a mixture of daidzin and glycitin on C57BL/6J mice fed with a high-fat diet," *Bioscience, Biotechnology, and Biochemistry*, vol. 79, no. 1, pp. 117–123, 2015.

[22] E. Di Consiglio, G. De Angelis, M. E. Traina, E. Urbani, and E. Testai, "Effect of lindane on CYP-mediated steroid hormone metabolism in male mice following in utero exposure," *Journal of Applied Toxicology*, vol. 29, no. 8, pp. 648–655, 2009.

[23] D.-J. Huang, S.-Y. Wang, and H.-C. Chen, "Effects of the endocrine disrupter chemicals chlordane and lindane on the male green neon shrimp (Neocaridina denticulata)," *Chemosphere*, vol. 57, no. 11, pp. 1621–1627, 2004.

Hindawi Publishing Corporation
BioMed Research International
Volume 2016, Article ID 4532697, 13 pages
http://dx.doi.org/10.1155/2016/4532697

Research Article

Effects of Acute and Chronic Heavy Metal (Cu, Cd, and Zn) Exposure on Sea Cucumbers (*Apostichopus japonicus*)

Li Li, Xiangli Tian, Xiao Yu, and Shuanglin Dong

The Key Laboratory of Mariculture, Ministry of Education, Fisheries College, Ocean University of China, Qingdao 266003, China

Correspondence should be addressed to Xiangli Tian; xianglitian@ouc.edu.cn

Received 4 March 2016; Revised 2 May 2016; Accepted 12 May 2016

Academic Editor: Ping Li

Acute and chronic toxicity tests were conducted with sea cucumber (*Apostichopus japonicus*) exposed to heavy metals. Acute toxicity values (96 h LC50) were 2.697, 0.133, and 1.574 mg L^{-1} for Zn, Cu, and Cd, respectively, and were ranked in order of toxicity: Cu > Cd > Zn. Under chronic metal exposure the specific growth rates of sea cucumbers decreased with the increase of metal concentration for all the three metals. After acute metal exposure, the oxygen consumption rate (OCR) decreased. The OCRs in all groups were significantly different than control ($P < 0.05$) except in the group treated with 1.00 mg L^{-1} Zn ($P < 0.05$), where the increase of OCR was observed. The OCRs in groups chronically exposed to metals were significantly lower than that in the control group ($P < 0.05$). The activity of both pyruvate kinase (PK) and hexokinase (HK) in sea cucumbers followed: respiratory tree > muscle > intestine in natural sea water. After chronic Zn, Cu, and Cd exposure, the change pattern of HK and PK in respiratory tree, muscle, and intestine varied slightly. However, the activity of the enzyme showed a general trend of increase and then decrease and the higher the exposure concentration was, the earlier the highest point of enzyme activity was obtained.

1. Introduction

The sea cucumber *Apostichopus japonicus* is a dominant mariculture species in northern coastal areas in China with the production of 194,000 t in 2013 [1, 2]. However, with the rapid development of intensive farming and industry activities, more liquid effluents with high levels of heavy metals have been discharged into the environment, which posed a potential threat to sea cucumber culture [3]. In general, heavy metals could be divided into different categories according to their toxicity and function. Metals such as cadmium (Cd) and lead (Pb) are biologically nonessential and their toxicities rise with increasing concentrations. Metals such as copper (Cu), zinc (Zn), and iron (Fe) are essential elements playing important roles in biological systems. However, the essential elements can also be detrimental to living organism at high concentrations [4].

Heavy metal exposure was considered to be associated with fish deformities and has been a subject of concern for many decades [4]. Meanwhile, studies have shown that exposure to heavy metals in aquatic environment could change the metabolic activities and many other physiological characteristics in crustaceans [5]. As fundamental physiological activities of animal energy metabolism, respiration is directly associated with the amount of energy released from the oxidation of food substratum. Therefore, it is a good indicator to evaluate the toxicant effects caused by heavy metals [5, 6]. For example, oxygen consumption rate (OCR) was used to study the adverse effect of heavy metal exposure on Pacific white shrimp, Green-lipped mussel, and ridgetail white prawn [6–8]. Both pyruvate kinase (PK) and hexokinase (HK) are key enzymes of glycolysis. The alteration of activity of these enzymes could change the metabolic level of the animal. Several environmental factors such as salinity, temperature, and diet can influence the glucose metabolism in aquatic animals by altering the enzyme activities [2, 9].

Although the effect of heavy metal exposure on crustaceans and molluscan has been extensively studied, there is not much information available as to what happens in sea cucumber. In the present study, we evaluated the effect of one commonly found nonessential element (Cd) and two essential elements (Zn and Cu) on the survival, specific

growth rate (SGR), OCR, and activity of metabolic enzymes in sea cucumber. This study provides a reference of the safety concentration of heavy metals in sea cucumber culture and most importantly provides basic data about the toxicity mechanism of sea cucumber to heavy metal exposure.

2. Materials and Methods

2.1. Collection and Maintenance of Animals. Juvenile sea cucumbers (*Apostichopus japonicus*) around 15 g were purchased from a local farm in Jiaonan district and transported to the laboratory located on the campus of Ocean University of China (Qingdao, Shandong, China). The animals were acclimated for 10 days in nature seawater continuously aerated with air stones. One-half or one-third of the rearing water was exchanged by fresh equitemperature seawater every day to ensure high water quality. The sea cucumbers were fed ad libitum every day at 08:00 on formulated feed (crude protein ≥ 23.0%, 3.0–5.0% fat, ash ≤ 18%, fiber ≤ 8.0%, and moisture ≤ 11.0%). After acclimation, the healthy individuals with an average weight of 15.42 ± 2.07 g were selected for the toxicity study.

The metal salts $ZnSO_4{\cdot}7H_2O$, $CuSO_4{\cdot}5H_2O$, and $CdCl_2{\cdot}2.5H_2O$ were dissolved in deionized water to prepare stock metal solution and stored at 4°C. Seawater used in the experiment was precipitated and filtered by a composite sand filter. The temperature, salinity, and pH of the seawater used during the experiment were controlled at 17.2 ± 0.2°C, 29.0 ± 2.0‰, and 7.87 ± 0.29, respectively. The ammonia and nitrite concentrations were kept at less than 0.011 and 0.0026 mg L^{-1}, respectively.

2.2. Acute Toxicity Study. A preliminary experiment was conducted to determine the highest concentrations of Zn, Cu, and Cd, respectively, causing no mortality and the lowest concentrations of Zn, Cu, and Cd, respectively, causing 100% mortality of sea cucumber in 96 h. Concentrations of the treatments were set up based on the equal logarithm intervals method with nature seawater as control (Table 1). Using Zn as an example, the highest concentration of Zn causing no mortality was 1 mg L^{-1} and the low lowest concentration of Zn causing 100% mortality was 6 mg L^{-1}. The logarithms of 1 and 6 to base 10 were 0 and 0.78, respectively. The interval between 0 and 0.78 was divided into five equal parts with six numbers. Using the number 10 as the base and the six corresponding numbers as exponent, the concentrations of treatments were set up as Table 1. The study was conducted in glass aquariums (53 cm × 28 cm × 34 cm) with five sea cucumbers in each aquarium. Five replicates were conducted for each treatment. The sea cucumbers were not fed two days before the study to empty intestine. The culture water was 100% changed every 24 h. The activities of the experimental animals were continuously observed and the dead individuals were picked out. The number of death was recorded at 24 h, 48 h, 72 h, and 96 h.

The LC50 is the concentration of toxicant causing 50% mortality of the test animals. The probit analysis (PB) method, the linear regression of probit mortality on log dosage, was employed to obtain a regression equation to estimate the 24 h, 48 h, 72 h, and 96 h LC50 [10]. The maximum allowable toxicant concentration (MATC) is the concentration of toxicant that may be present without causing harm. It can be calculated by multiplying the 96 h LC50 by application factor (AF). An AF of 0.05 is suggested by Boyd for general use [11].

Table 1: The experimental design and nominal concentrations of Zn, Cu, and Cd in acute toxicity experiment test.

Cation	Concentration (mg L^{-1})						
	CA0	CA1	CA2	CA3	CA4	CA5	CA6
Zn	Control	1.00	1.43	2.05	2.94	4.21	6.00
Cu	Control	0.02	0.03	0.05	0.08	0.13	0.20
Cd	Control	0.50	0.66	0.87	1.15	1.51	2.00

Note: comparison was conducted among different concentration groups within each metal.

Table 2: The experimental design and nominal concentrations of Zn, Cu, and Cd in chronic toxicity test.

Cation	Concentration (mg L^{-1})				
	CC0	CC1	CC2	CC3	CC4
Zn	Control	0.040	0.070	0.150	0.770
Cu	Control	0.003	0.005	0.010	0.050
Cd	Control	0.022	0.044	0.088	0.440

Note: comparison was conducted among different concentration groups within each metal.

2.3. Chronic Toxicity Study

2.3.1. Experimental Design and Management. A 15 d chronic toxicity test was conducted in glass aquariums (53 cm × 28 cm × 34 cm). Concentrations of Zn, Cu, and Cd were set up as 1/200, 1/100, 1/50, and 1/10 of 24 h LC50 value of each element with nature sea water as control (Table 2). Ten replicates were conducted for each treatment. Sea cucumbers were randomly picked up in five of ten replicates and assigned to samples for HK and PK analysis. Muscle, intestine, and respiratory tree samples were collected on 0 h, 12 h, 24 h, 5 d, 10 d, and 15 d during the experiment. Three animals were randomly sampled from five aquariums. Muscle was removed from the posterior of the body. The whole intestine was removed by an incision at the esophagus and cloaca. It was then cut longitudinally and washed thoroughly in ice-cold distilled water. After rinsing, the three tissues were dried with filter paper, and each sample was frozen with liquid nitrogen in an Eppendorf tube (1.5 mL) and stored at −80°C until analysis.

Metal concentration in the test solution used in the acute and chronic toxicity study was measured using the inductively coupled plasma-optical emission spectrophotometer (ICP-OES; VISTA-MPX, VARIAN). The nominal and measured concentrations of metals were listed in Table 3.

2.3.2. Enzyme Activity Determination. A 0.1–0.3 g of each of the three tissues was homogenized and the ice-cold saline of quadrupled volume of the tissue was added to each sample to make a 20% homogenate. The homogenates were

Table 3: Nominal and measured concentrations (mean ± SD, $n = 3$) of Zn, Cu, and Cd in test solutions.

Zn			Cu			Cd		
Nominal concentration ($mg\,L^{-1}$)	Measured ($mg\,L^{-1}$)	%	Nominal concentration ($mg\,L^{-1}$)	Measured ($mg\,L^{-1}$)	%	Nominal concentration ($mg\,L^{-1}$)	Measured ($mg\,L^{-1}$)	%
0.00	0.020 ± 0.001	—	0.00	0.003 ± 0.001	—	0.00	0.001 ± 0.000	—
0.04	0.036 ± 0.004	90.0	0.003	0.004 ± 0.000	133.3	0.022	0.026 ± 0.004	118.2
0.07	0.038 ± 0.001	54.3	0.005	0.006 ± 0.000	120.0	0.044	0.053 ± 0.001	120.5
0.15	0.121 ± 0.003	80.7	0.01	0.011 ± 0.000	110.0	0.088	0.097 ± 0.001	110.2
0.77	0.682 ± 0.005	88.6	0.02	0.019 ± 0.004	95.0	0.44	0.419 ± 0.001	95.2
1.00	0.932 ± 0.002	93.2	0.03	0.029 ± 0.004	96.7	0.50	0.437 ± 0.001	87.4
1.43	1.321 ± 0.080	92.4	0.05	0.043 ± 0.003	86.0	0.66	0.575 ± 0.003	87.1
2.05	1.980 ± 0.003	96.6	0.05	—	—	0.87	0.784 ± 0.002	90.1
2.94	2.820 ± 0.056	95.9	0.08	0.069 ± 0.007	86.3	1.15	1.030 ± 0.005	89.6
4.21	4.110 ± 0.073	97.6	0.13	0.123 ± 0.001	94.6	1.51	1.480 ± 0.001	98.0
6.00	5.230 ± 0.126	87.2	0.20	0.184 ± 0.001	92.0	2.00	1.820 ± 0.005	91.0

immediately centrifuged for 10 min at 4°C and 2000 r/min. The protein concentrations of the samples were determined with Folin phenol reagent [12]. Collected supernatants were used for the determination of activities of PK and HK using a commercial kit (Nanjing Jiancheng Bioengineering Institute, China).

The activity of PK was determined by continuously monitoring the decrease in absorbance at 340 nm using NADH-linked methods [13]. PK activities were calculated using the molar extinction coefficient of NADH ($6.22\,mmol^{-1}\,cm^{-1}$). The HK activity was determined by reading the absorbance values using spectrophotometer at 340 nm [14]. All enzyme activities were expressed as $U\,mg^{-1}$ (unit per milligram protein), where U was defined as the enzyme causing the conversion of 1 μmol of substrate min^{-1} [15].

2.3.3. Specific Growth Rate. Sea cucumbers in five aquariums for each treatment were assigned to measure the growth rate of animals. The wet weight of the sea cucumbers before and after the experiment was recorded to calculate the specific growth rate (SGR) of the animal using the following equation. Before weighing, the animals were fasted for 24 h to evacuate their guts:

$$\text{Specific growth rate (SGR)} = \left[\frac{(\ln W_2 - \ln W_1)}{(t_2 - t_1)}\right] \times 100\%, \quad (1)$$

where W_1 and W_2 were the weights at times t_1 and t_2, respectively, with t_1 and t_2 being the first and final day of the experiment, respectively.

2.4. Oxygen Consumption Rate Determination. The oxygen consumption rates were measured for the sea cucumbers after 96 h acute toxicity and 15 d chronic toxicity test at all the treatments and control except the CA5 and CA6 groups (Table 1) according to the methods described by Dong et al. [16]. The two groups were not measured because of the high mortality of the animals after 96 h acute metal exposure. Briefly, an individual sea cucumber was put into a 3-L conical flask. Four replicates in each treatment and one blank control to correct for the respiration of bacteria in the water were set up. When it became quiescent after 12 h, change in oxygen content was determined before and after the test over 24 h using the Winkler method [17].

The oxygen consumption rate (R_0) of sea cucumber was calculated from the following equation [18]:

$$R_0\left(mg\,O_2 * g^{-1} * h^{-1}\right) = \frac{(C_0 - C_t)\,V}{WT}, \quad (2)$$

where C_t and C_0 are the change in oxygen content ($mg\,O_2\,L^{-1}$) before and after test in the test bottles and blank bottles, respectively; V is the volume of the bottle (L); W and T are the wet weight of sea cucumbers (g) and time of duration (h), respectively.

2.5. Statistical Analysis. Statistical analyses were performed using SPSS (version 17.0). The comparisons of weight, specific growth rate, and oxygen consumption rate among treatments were done by one-way ANOVA, followed by Duncan's multiple comparison tests if significant difference was reported by ANOVA. All the data were expressed as mean ± standard error.

3. Results

3.1. Acute Toxicity of Zn, Cu, and Cd on Survival and Behavior of Sea Cucumber and the LC50 Values. Effects of acute toxicity of the three metals (Zn, Cu, and Cd) on survival rate of sea cucumber are listed in Table 4. With the increase of concentration and time duration of metal exposure, the survival rate of sea cucumber decreased. The sea cucumber showed similar toxicity symptom under the stress of the three metals. In the low concentration groups, that is, the concentration with Zn of $2.05\,mg\,L^{-1}$, Cu of $0.08\,mg\,L^{-1}$,

Table 4: Effects of acute Zn, Cu, and Cd stress on the survival rate of *Apostichopus japonicus*.

Cations	Concentration (mg L^{-1})	24 h Survival rate (%)	48 h Survival rate (%)	72 h Survival rate (%)	96 h Survival rate (%)
Zn	1.00	100	100	100	100
	1.43	100	100	100	100
	2.05	100	94.44	83.33	77.78
	2.94	94.44	83.33	66.67	33.33
	4.21	83.33	66.67	38.89	16.67
	6.00	66.67	38.89	11.11	0
Cu	0.02	100	100	100	100
	0.03	100	100	100	100
	0.05	100	100	100	100
	0.08	94.44	88.89	77.78	77.78
	0.13	88.89	77.78	55.56	50.00
	0.20	77.78	61.11	38.89	27.78
Cd	0.50	100	100	100	100
	0.66	100	100	100	100
	0.87	100	100	100	100
	1.15	94.44	88.89	77.78	66.67
	1.51	88.89	77.78	66.67	50.00
	2.00	33.33	72.22	55.56	38.89
	Control	100	100	100	100

Table 5: The regression equation and medium lethal concentration (LC50) of *Apostichopus japonicus* exposed to various Zn, Cu, and Cd concentrations calculated by probit analysis.

Cation	Time/h	Regression equation	R^2	LC50 (mg L^{-1})	MATC* (mg L^{-1})
Zn	24 h	$y = 3.8072x + 1.6268$	0.9970	7.691	
	48 h	$y = 3.9949x + 2.1415$	0.9968	5.200	
	72 h	$y = 4.6655x + 2.4832$	0.9873	3.467	
	96 h	$y = 6.439x + 2.2450$	0.9723	2.679	0.135
Cu	24 h	$y = 2.1241x + 5.6999$	0.9924	0.468	
	48 h	$y = 2.3553x + 6.3485$	0.9884	0.267	
	72 h	$y = 2.6206x + 7.1363$	0.9943	0.153	
	96 h	$y = 3.3879x + 7.9710$	0.9985	0.133	0.007
Cd	24 h	$y = 2.7053x + 3.2471$	0.9866	4.446	
	48 h	$y = 2.6388x + 3.6658$	0.9280	3.206	
	72 h	$y = 2.5822x + 4.0910$	0.9978	2.250	
	96 h	$y = 2.9672x + 4.4159$	0.9837	1.574	0.079

*MATC (maximum allowable toxicant concentration).

and Cd of 1.15 mg L^{-1}, the activities of the sea cucumbers were similar to the animal in the control group in the first 24 h. The sea cucumber was absorbed on the wall or bottom of the aquarium. However, with the extension of exposure time, the absorption capacity of ambulacral foot weakened and some of the animals dropped on to the bottom of the aquarium accompanied by twisting and contraction of the body. Few individuals spontaneously rejected internal organs, that is, evisceration, followed by disappearance of spines on the body and after evisceration the individuals started to rot. The sea cucumbers were more sensitive to high concentration (Zn of 6.00 mg L^{-1}, Cu of 0.20 mg L^{-1}, and Cd of 2.00 mg L^{-1}) metal exposure. Immediately after exposure, some individuals dropped on the bottom of the aquarium, twisted, and contracted the body followed by evisceration and death.

As exhibited in Table 5, with the extension of exposure time, the LC50 for the three metals all decreased demonstrating that the toxicity of the three metals to sea cucumber increased as the exposure time increased. The 96 h LC50 values for Zn, Cu, and Cd were 2.679, 0.133, and 1.574 mg L^{-1}, respectively, while the maximum allowable toxicant concentrations (MATC) for the three metals (Zn, Cu, and Cd) were 0.135, 0.007, and 0.079 mg L^{-1}, respectively.

Table 6: The survival rate and specific growth rate of *Apostichopus japonicus* exposed to various concentrations of Zn, Cu, and Cd for 15 days. Different letters indicate significant differences ($P < 0.05$).

Cations	Concentration (mg L^{-1})	Survival rate (%)	Initial wet weight (g)	Final wet weight (g)	Specific growth rate (% d^{-1})
Zn	Control	100	16.36 ± 0.25^{ac}	21.32 ± 0.23^{a}	21.64 ± 1.75^{a}
	0.040	100	15.58 ± 0.15^{b}	19.30 ± 0.25^{b}	16.67 ± 1.29^{b}
	0.070	100	15.74 ± 0.45^{ab}	18.02 ± 0.61^{c}	10.66 ± 1.45^{c}
	0.150	100	16.12 ± 0.52^{acb}	16.98 ± 0.60^{d}	4.18 ± 0.38^{d}
	0.770	58.30	16.48 ± 0.33^{c}	13.07 ± 0.52^{e}	-19.15 ± 1.73^{e}
Cu	Control	100	16.36 ± 0.25^{a}	21.32 ± 0.23^{a}	21.64 ± 1.75^{a}
	0.003	100	15.95 ± 0.04^{bc}	19.05 ± 0.63^{b}	14.11 ± 2.76^{b}
	0.005	100	16.18 ± 0.11^{ab}	18.30 ± 0.32^{bc}	9.94 ± 2.33^{c}
	0.010	100	15.75 ± 0.37^{c}	17.72 ± 0.68^{c}	9.26 ± 1.62^{c}
	0.050	75.00	16.88 ± 0.09^{d}	14.31 ± 0.31^{d}	-13.94 ± 1.52^{d}
Cd	Control	100	16.36 ± 0.25^{ab}	21.32 ± 0.23^{a}	21.64 ± 1.75^{a}
	0.022	100	16.64 ± 0.26^{b}	20.82 ± 0.64^{a}	18.63 ± 1.55^{a}
	0.044	100	16.67 ± 0.27^{b}	19.27 ± 0.63^{b}	12.09 ± 2.16^{b}
	0.088	100	15.94 ± 0.2^{a}	17.97 ± 0.41^{c}	9.53 ± 2.65^{b}
	0.440	83.30	16.05 ± 0.1^{a}	13.23 ± 0.11^{d}	-15.51 ± 1.26^{c}

3.2. Effects of Chronic Toxicity of Metals on Survival and Growth of Sea Cucumber. The survival rate and SGR of sea cucumber after chronic metal exposure are listed in Table 6. With the increase of metal concentration, the SGR of sea cucumber decreased for all the three metals. The SGRs in groups treated with Zn and Cu were significantly lower than that in control ($P < 0.05$). When the Cd concentration was over 0.044 mg L^{-1}, the SGRs of sea cucumbers were significantly lower than those in control and the low concentration (0.022 mg L^{-1}) treatments. Apparent uneaten feeds were found on the 7th d with Zn at the concentration of 0.150 mg L^{-1}, the 10th d with Cu at the concentration of 0.010 mg L^{-1}, and 12th d with Cd at the concentration of 0.088 mg L^{-1}. After that, all the sea cucumbers stopped eating and began to contract their bodies into balls. Negative SGRs were recorded in treatments with the Zn, Cu, and Cd concentrations of 0.770, 0.050, and 0.440 mg L^{-1} and their survival rates were 58.3%, 75.0%, and 83.3%, respectively.

3.3. Effects of Metal Stress on OCR and Metabolic Enzymes of Sea Cucumber

3.3.1. Acute Zn, Cu, and Cd Stress on OCR of Sea Cucumber. Significant differences were found on OCR between sea cucumbers acutely exposed to different concentrations of Zn, Cu, Cd, and control ($P < 0.05$). The OCR increased significantly in the group treated with 1.00 mg L^{-1} Zn ($P < 0.05$), while in the other groups, similar trend was observed: with the increase of metal concentrations, the OCRs decreased and were significantly lower than that in control ($P < 0.05$) (Figure 1).

3.3.2. Chronic Zn, Cu, and Cd Stress on OCR of Sea Cucumber. The OCRs in groups chronically exposed to metals were significantly lower than that in the control group ($P < 0.05$) (Figure 2). Significant difference for the OCR occurred only between CC4 and CC1 groups under Zn exposure ($P < 0.05$), while no significant differences were observed among the CC2, CC3, and CC4 groups. The same law was found in the Cd treated groups. In the Cu treated groups, the OCR of the highest concentration treated group was significantly lower than that in the lowest concentration treated group but not different from CC2.

3.3.3. Effects of Chronic Zn, Cu, and Cd Exposure on HK and PK in Different Tissues of Sea Cucumber. In the nature seawater, the HK and PK activities in the respiratory tree were larger than those in the muscle followed by intestine (Figure 3). Under chronic low Cu exposure (0.003 mg L^{-1}), the HK activity in the intestine did not change much and there was a slight trend of increase in the CC2 group (0.005 mg L^{-1}) (Figure 3). However, the HK activity increased rapidly and reached the highest point on the 10th day of exposure and then decreased in the high concentration groups (CC3 and CC4). In the respiratory tree, which has a higher concentration of HK than the intestine under normal conditions, the change pattern of HK was different from the intestine. An increase of HK activity was observed in the low concentration group (CC1). In the other three groups, the HK activity increased at first and then decreased under chronic Cu exposure. The higher the exposure concentration was, the earlier the highest point of HK activity obtained. In the muscle, a slight increase of HK activity occurred in the two low concentration groups (CC1 and CC2), while in the two high concentration groups (CC3 and CC4), the HK activity increased rapidly and then decreased (Figure 3).

The PK in the respiratory tree responded similarly to the HK in this tissue (Figure 3). An increase of PK activity was observed in the low concentration group (CC1). In the other three groups, the PK activity increased at first and then decreased under chronic Cu exposure. The higher the exposure concentration was, the earlier the highest point of

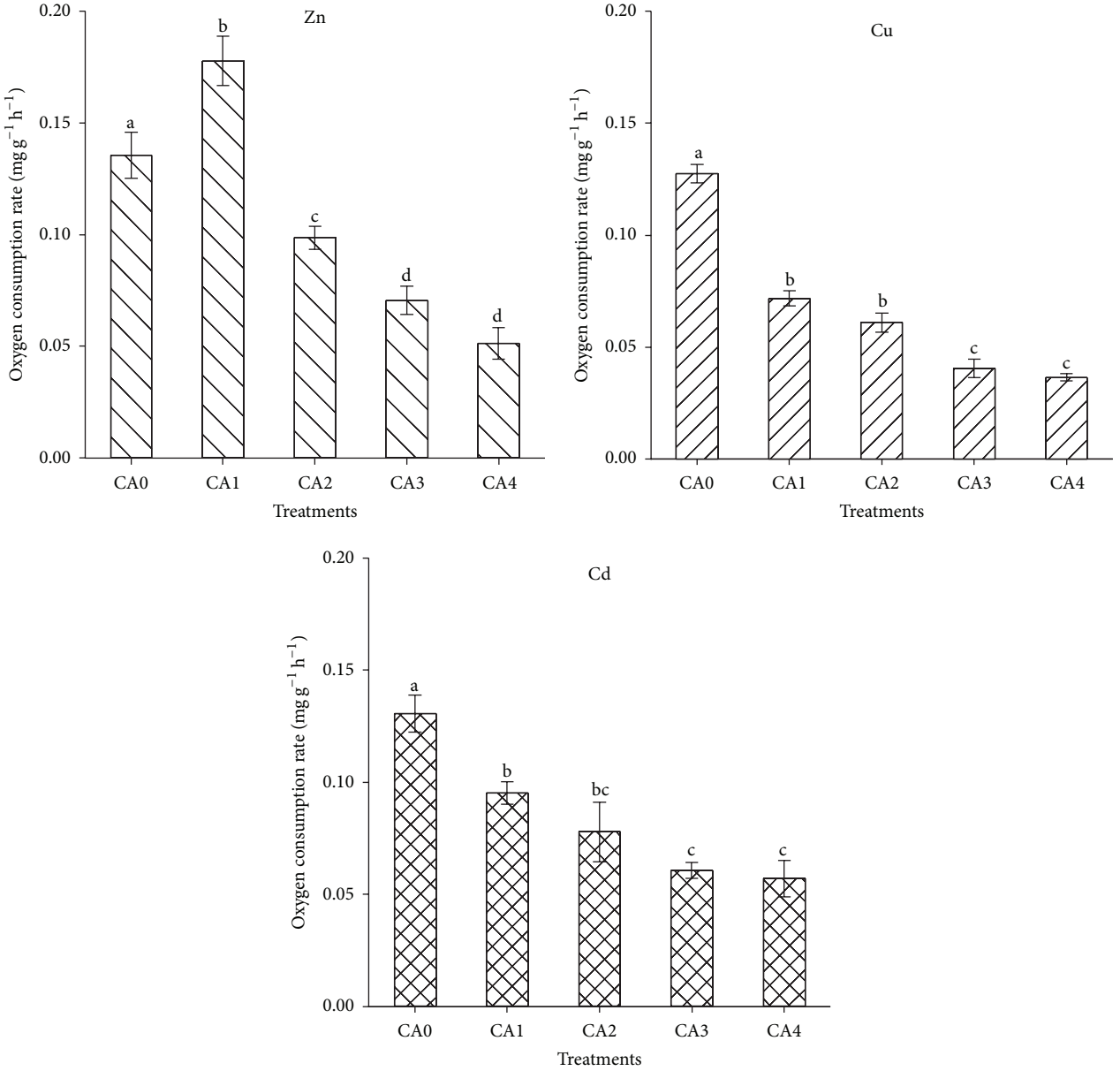

Figure 1: Levels of oxygen consumption rate of *Apostichopus japonicus* after 96 h acute exposure to various Zn, Cu, and Cd concentrations. The bars are the respective standard deviations ($n = 3$), and different letters above the bars indicate significant differences ($P < 0.05$).

PK activity reached. A trend of increase was observed in both the intestine and muscle in the CC3 and CC4 groups. In the muscle, the PK in the low concentration groups (CC1 and CC2) fluctuated around the value in the nature seawater (Figure 3).

Generally, the HK activity increased first and then decreased in all the three tissues under chronic Cd exposure in the CC2, CC3, and CC4 groups. The higher the exposure concentration was, the earlier the highest point of HK activity reached (Figure 4). For example, the highest concentrations of HK activity in the respiratory tree of the three groups, that is, CC4 (0.440 mg L^{-1}), CC3 (0.088 mg L^{-1}), and CC2 (0.044 mg L^{-1}), were obtained on days 0.5, 5, and 10 of exposure, respectively. In the low concentration group (CC1), the HK activity decreased in the respiratory tree, increased in the muscle, and fluctuated around the value in the nature seawater in the intestine. The change pattern of PK was similar to HK and the PK activity increased first and then decreased in the CC2, CC3, and CC4 groups. The higher the exposure concentration was, the earlier the highest point of PK activity reached. The PK fluctuated around the value of control in the low concentration group (CC1) in the intestine and respiratory tree (Figure 4).

Under chronic Zn exposure, in the CC2, CC3, and CC4 groups, the HK activity generally increased at first and then decreased in the respiratory tree and intestine (Figure 5). In the muscle, the HK activity increased in the four treatments and kept increasing in the CC1, CC2, and CC3 groups at

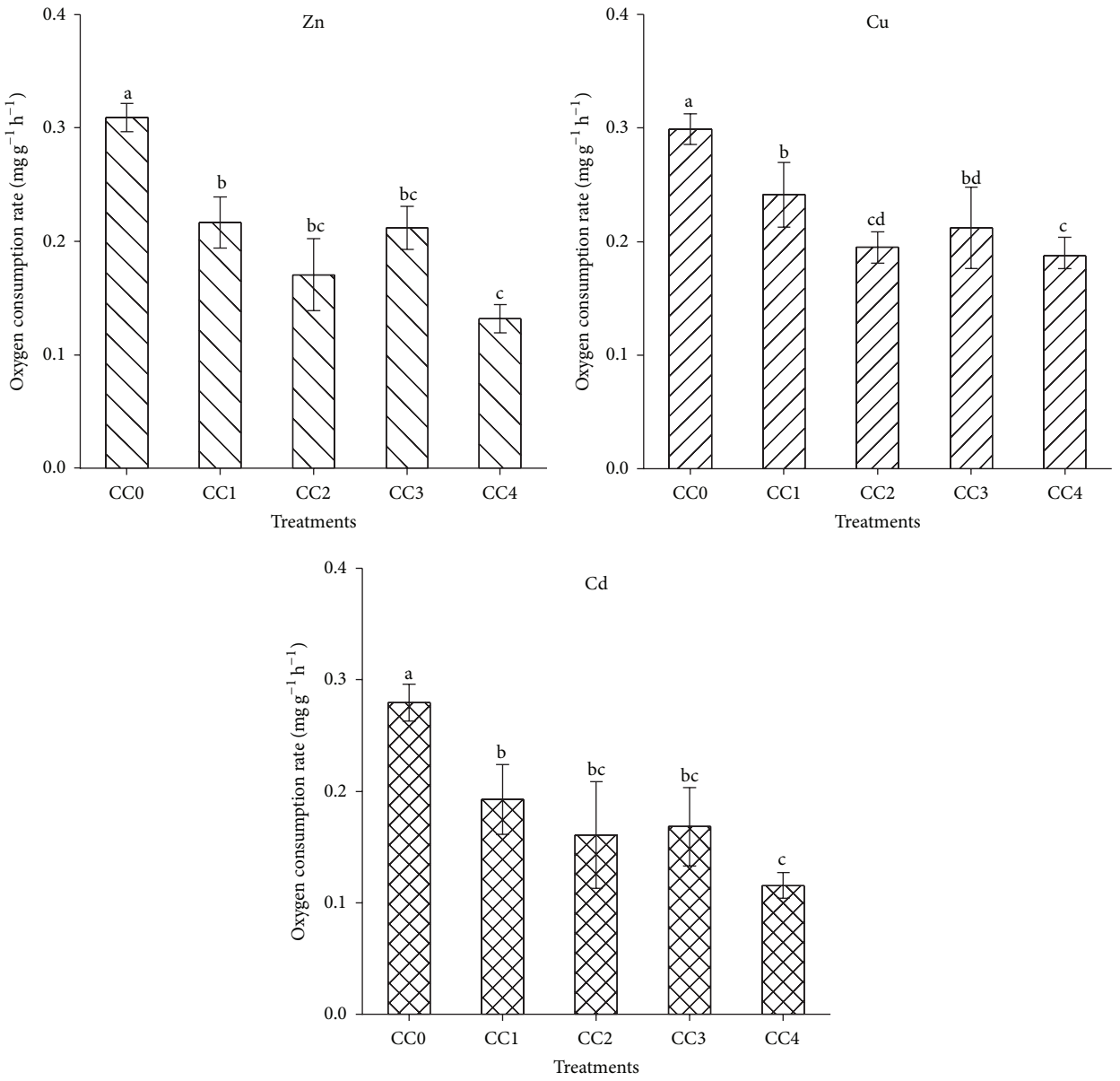

Figure 2: Levels of oxygen consumption rate of *Apostichopus japonicus* after 15 d chronic exposure to various Zn, Cu, and Cd concentrations. The bars are the respective standard deviations ($n = 3$), and different letters above the bars indicate significant differences ($P < 0.05$).

the last sampling of this study. The PK activity increased and then decreased only in the intestine and muscle of the high concentration group, that is, CC4 group with a Zn concentration of 0.770. In the other treatments and tissues, the PK activity all decreased or fluctuated around control (Figure 5).

4. Discussion

When the sea cucumbers were acutely exposed to metals, severe mortality was observed in this study. However, mortality only occurred in groups treated with the highest concentration of heavy metals in the chronic toxicity test. This might be because of the acclimation response of the sea cucumber under chronic metal exposure. It has been reported that fish can be physiologically acclimated to chronic Zn exposure by reducing the branchial influx rate of Zn and restoring plasma calcium concentrations [19]. Cadmium is the most commonly found nonessential heavy metal in aquatic environments and it tends to bioaccumulate in living organisms. The metal, which could disrupt calcium absorption, can lead to acute hypocalcaemia and growth reduction, problematic reproduction, and impairments in development and behavior in aquatic species [4, 20]. As a key constituent of metabolic enzymes, Cu is an essential micronutrient for living organisms [4]. However, it can be toxic to aquatic organisms when exceeding normal levels. The toxic effect includes reduced growth rate, behavioral changes, and deformities in fish larvae [4]. An essential element for living organisms, Zn, is crucial to over 300 enzymes and other

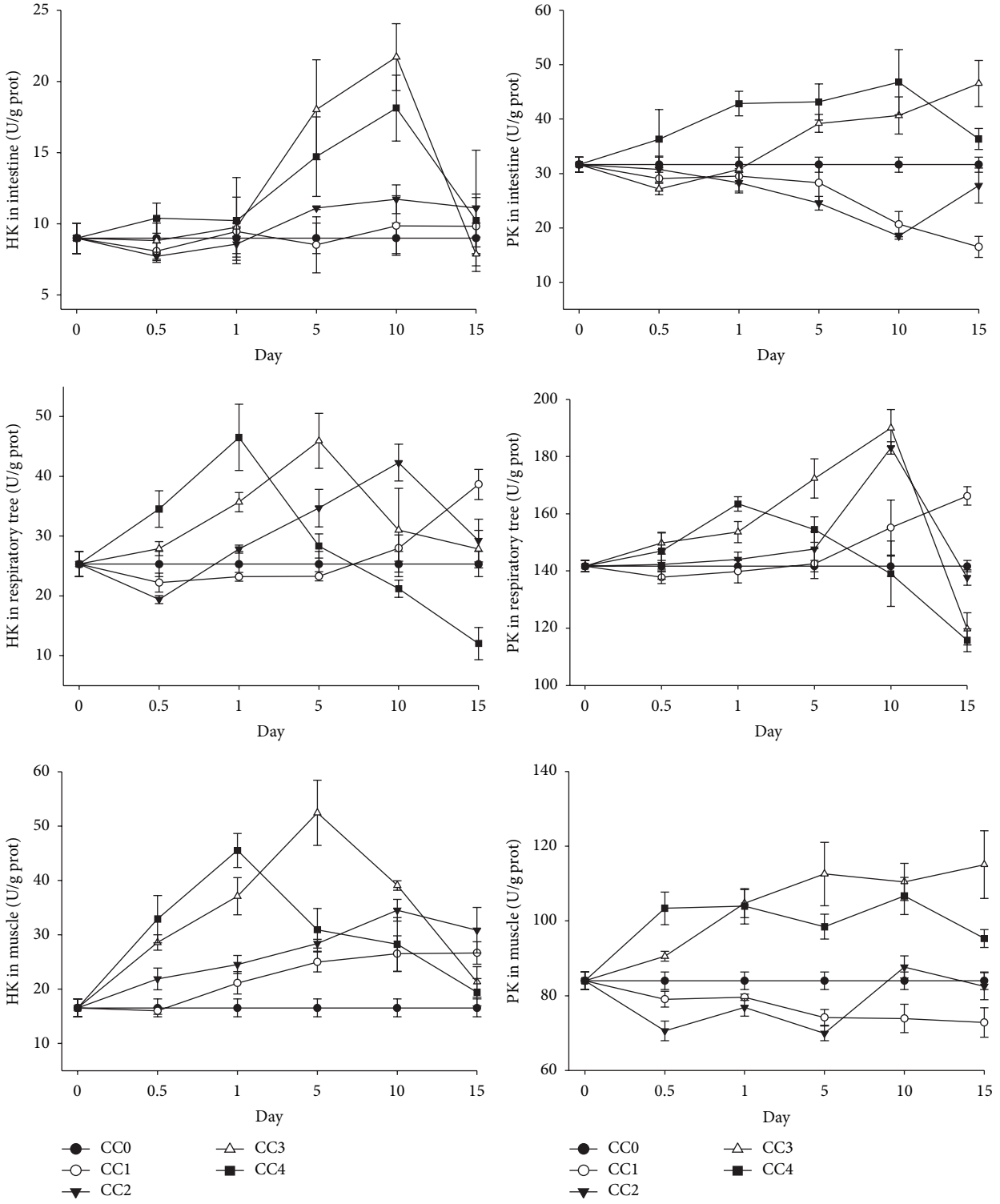

Figure 3: Levels of hexokinase (HK) and pyruvate kinase (PK) in intestine, respiratory tree, and muscle of *Apostichopus japonicus* during chronic Cu exposure. The bars are the respective standard deviations ($n = 3$).

proteins and also a vital component of all their tissues and fluids of organs [21, 22]. However, it may have detrimental effects on the development and survival of many aquatic organisms when reaching a threshold [4]. The mechanism of its toxicity is similar to Cd, that is, disrupting calcium homeostasis through the induction of hypocalcaemia and disturbing acid-base balance [19].

The toxicity of certain metals is species-dependent. The 96 h LC50 value for Cd in sea cucumber is 1574 $\mu g\,L^{-1}$ (Table 5), while that for the rainbow trout, zebrafish, and

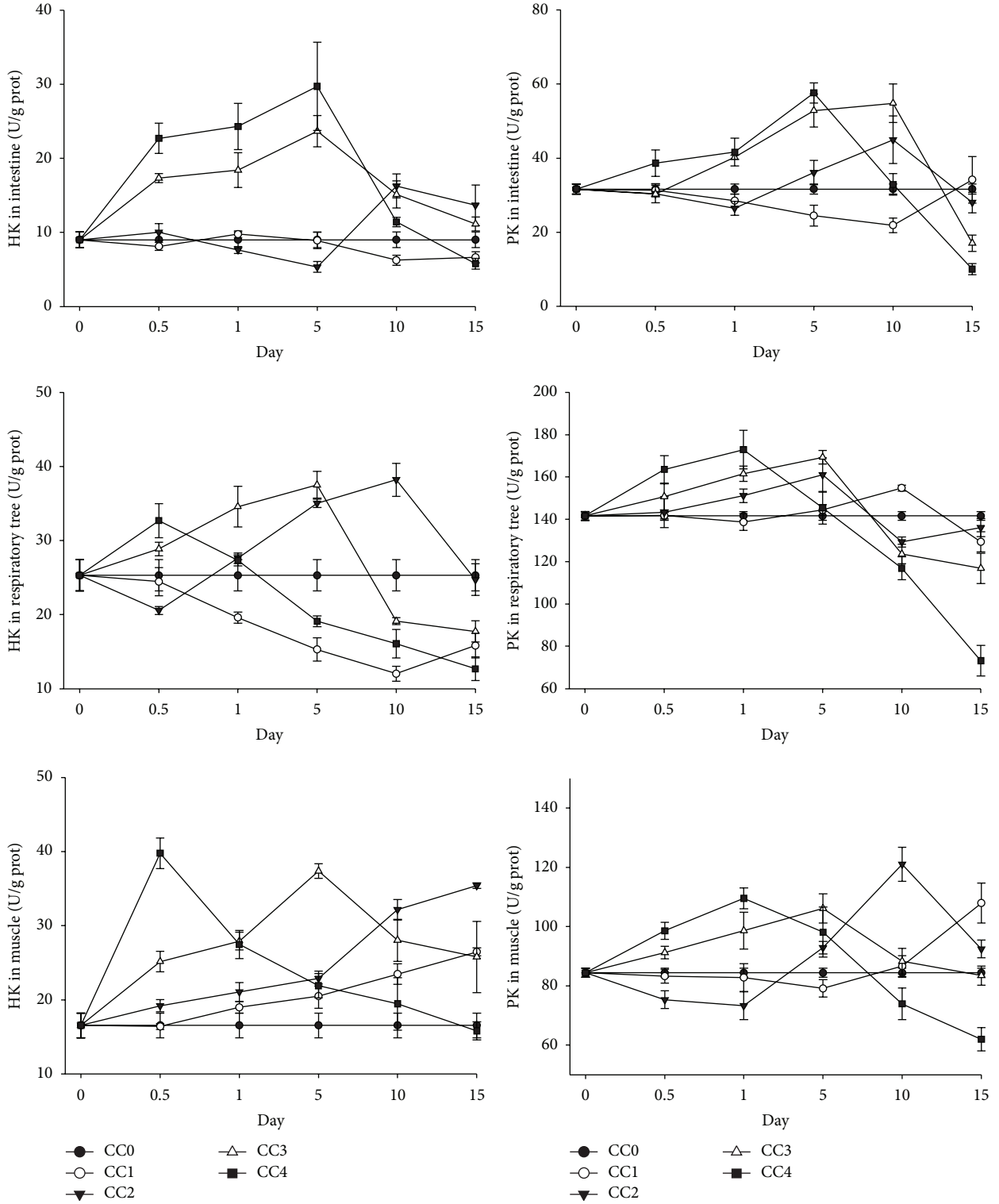

Figure 4: Levels of hexokinase (HK) and pyruvate kinase (PK) in intestine, respiratory tree, and muscle of *Apostichopus japonicus* during chronic Cd exposure. The bars are the respective standard deviations ($n = 3$).

perch is 19, 3822, and 8141 $\mu g\,L^{-1}$, respectively. This indicates that the sea cucumber is less sensitive to Cd toxicity than the rainbow trout, but more sensitive than the zebrafish and perch [23, 24]. The 96 h LC50 for Cu in sea cucumber is 133 $\mu g\,L^{-1}$, which is higher than rainbow trout, but lower than the zebrafish [24, 25]. The 96 h LC50 for Zn in sea cucumber is 2697 $\mu g\,L^{-1}$ and the sea cucumber is more tolerant to Zn toxicity than the rainbow trout, which has a

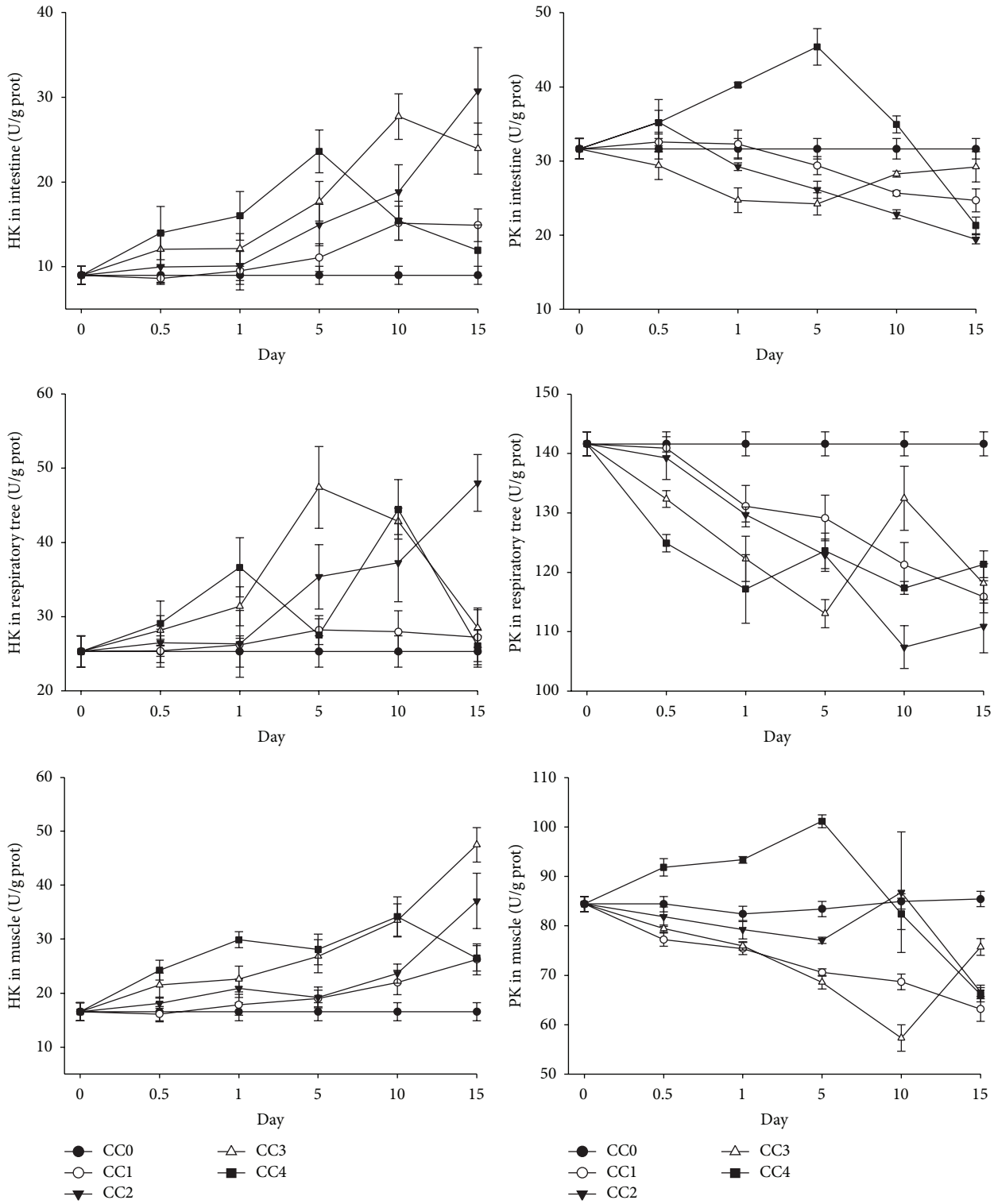

Figure 5: Levels of hexokinase (HK) and pyruvate kinase (PK) in intestine, respiratory tree, and muscle of *Apostichopus japonicus* during chronic Zn exposure. The bars are the respective standard deviations ($n = 3$).

96 h LC50 of 869 μg L^{-1} [26]. However, some other aquatic species, such as guppy, are extremely tolerant to Zn toxicity with a 96 h LC50 of 30826 μg L^{-1} [27]. The sea cucumber's sensitivity to metals was metal-dependent. In this study, the sea cucumber is more sensitive to Cu than Cd. Similar result was reported for common carp and zebrafish [24]. However, some other species such as ridgetail white prawn (*Exopalaemon carinicauda*) are more sensitive to Cd than Cu

[6], while other species, such as rainbow trout, are sensitive to both Cu and Cd [24]. The mechanisms leading to different sensitivities among species remain not clear and it may be related to differences in the regulation and affinity of metal uptake [24].

The change of oxygen consumption rate was reported in *Apostichopus japonicus* after evisceration or under fluctuant temperatures [16, 28]. Both Cd and Cu exposure could cause significant inhibition of OCR in *Exopalaemon carinicauda*. Similar results were also reported in *Farfantepenaeus paulensis* and *L. vannamei*, which was acutely exposed to Zn and Cd [5, 6, 8]. In this study, acute Cu and Cd stress resulted in the decrease of OCR in sea cucumber, which is consistent with previous reports. The decrease of OCR in *L. vannamei* was attributed to histopathological alterations in the gills after acute exposure to Cd and Zn [6, 29], while inhabitation of respiration by heavy metal in mussel has been attributed to mucus production because it reduces the efficiency of gaseous exchange [30]. However, the physiological mechanism for respiratory impairment in sea cucumber is not clear. Though OCRs were generally decreased when the aquatic animals were acutely exposed to heavy metals [5], it is interesting to find that the OCR in sea cucumber increased under acute low concentration Zn exposure (1.00 mg L^{-1}). The exact reason for the surprising elevation of OCR in sea cucumber remains unknown. However, elevated OCR was observed in Green-lipped mussels after chronic exposure to raised Cd for one week and was interpreted as "an augmented expenditure of energy reserves characteristic of a stress compensation process" [7]. The primary respiratory organ in the sea cucumber is the respiratory tree and the animal could also obtain oxygen via cutaneous respiration [28]. The increase of OCR in the sea cucumber indicated elevated activity of the two parts.

In the nature seawater, the HK in the three tissues in sea cucumber followed: respiratory tree > muscle > intestine. Therefore, the metabolic responses of the three organs to heavy metal exposure were different and the respiratory tree was the most active metabolic place. The HK in the respiratory tree showed a trend of increase and then decrease in all the treatments except groups treated with the lowest concentration for all metals in chronic exposure test. And the higher the exposure concentration was, the earlier the highest point of HK activity obtained. HK is a key enzyme of glycolysis by converting glucose to glucose-6-phosphate [31]. The elevation of HK might be related to the glycolytic pathway to derive energy from glucose. The HK activity decreased when the time of duration of metal exposure increased indicating that the sea cucumber could not maintain the energy support from the glycolysis. The HK activity was reported to be affected by several factors such as salinity, dietary carbohydrate, and molt cycle in shrimp [14], while in sea cucumber, the variation of HK under metal exposure was not reported. In the present study, certain level of chronic metal stress seemed to promote glycolysis at initial phase. However, as the duration of metal stress lasted, the glycolysis was inhibited. The higher the metal concentration was, the early the inhibition happened.

The PK in the three tissues in sea cucumber also followed: respiratory tree > muscle > intestine. As a major site of acute hormone action, pyruvate kinase (PK) is also one of the key enzymes in control of the glycolytic pathways [32]. It catalyzes the transfer of a phosphate group from phosphoenolpyruvate (PEP) to ADP, yielding one molecule of pyruvate and one molecule of ATP (PEP + ADP → pyruvate + ATP) [33]. The specific activity of PK is affected by several factors such as different diets, while prolonged starvation could reduce the activity of PK in vertebrates. The mechanism of inhibition of PK is a hormone and metabolite-mediated mechanism in the regulation of the enzyme-gene expression [32]. Under chronically higher concentration Cd and Cu exposure, the PK in the respiratory tree increased at first and then decreased, while in the lowest groups (CC0), the PK slightly increased or fluctuated around the value in control. However, no elevation of PK levels was observed in the respiratory tree of sea cucumber exposed to chronic Zn stress indicating that sea cucumber might be more tolerant to Zn than the Cu and Cd.

5. Conclusion

We conducted chronic and acute toxicity test to evaluate the effect of one commonly found nonessential element (Cd) and two essential elements (Zn and Cu) on survival, specific growth rate, oxygen consumption rate, and activity of metabolic enzymes in sea cucumber. From this study, it demonstrated that chronic metal exposure could inhibit the growth of the sea cucumber and the specific growth rate of sea cucumber decreased with the increase of metal concentration. The 96 h LC50 values were calculated as 2.697, 0.133, 1.574 mg L^{-1} for Zn, Cu, and Cd, respectively, and the three metals were ranked in order of toxicity: Cu > Cd > Zn. The maximum allowable toxicant concentrations causing no harm to sea cucumber for the three metals are 0.135, 0.007, and 0.079 mg L^{-1} for Zn, Cu, and Cd, respectively. Under acute or chronic heavy metal stress, the sea cucumber has many physiological adaption mechanisms including decrease or increase of oxygen consumption rate and adjusted activity of metabolic enzymes.

Abbreviations

OCR: Oxygen consumption rate
HK: Hexokinase
PK: Pyruvate kinase
SGR: Specific growth rate
MATC: Maximum allowable toxicant concentration
AF: Application factor.

Competing Interests

There are no competing interests related to this paper.

Acknowledgments

This study was supported by the National Great Project of Scientific and Technical Supporting Programs (Grant no. 2011BAD13B03), the Programs for Excellent Youth Foundation of Shandong Province (Grant no. JQ201009),

and National Natural Science Foundation of China (no. 31402317).

References

[1] C. Shi, S. Dong, F. Wang, Q. Gao, and X. Tian, "Effects of the sizes of mud or sand particles in feed on growth and energy budgets of young sea cucumber (*Apostichopus japonicus*)," *Aquaculture*, vol. 440, pp. 6–11, 2015.

[2] B. Xia, Q.-F. Gao, J. Wang, P. Li, L. Zhang, and Z. Zhang, "Effects of dietary carbohydrate level on growth, biochemical composition and glucose metabolism of juvenile sea cucumber *Apostichopus japonicus* (Selenka)," *Aquaculture*, vol. 448, pp. 63–70, 2015.

[3] J. Wang, T. Ren, Y. Han et al., "Effects of dietary vitamin C supplementation on lead-treated sea cucumbers, *Apostichopus japonicus*," *Ecotoxicology and Environmental Safety*, vol. 118, pp. 21–26, 2015.

[4] D. G. Sfakianakis, E. Renieri, M. Kentouri, and A. M. Tsatsakis, "Effect of heavy metals on fish larvae deformities: a review," *Environmental Research*, vol. 137, pp. 246–255, 2015.

[5] E. Barbieri and E. T. Paes, "The use of oxygen consumption and ammonium excretion to evaluate the toxicity of cadmium on *Farfantepenaeus paulensis* with respect to salinity," *Chemosphere*, vol. 84, no. 1, pp. 9–16, 2011.

[6] C. Zhang, F. Li, and J. Xiang, "Acute effects of cadmium and copper on survival, oxygen consumption, ammonia-N excretion, and metal accumulation in juvenile Exopalaemon carinicauda," *Ecotoxicology and Environmental Safety*, vol. 104, no. 1, pp. 209–214, 2014.

[7] S. G. Cheung and R. Y. H. Cheung, "Effects of heavy metals on oxygen consumption and ammonia excretion in green-lipped mussels (*Perna viridis*)," *Marine Pollution Bulletin*, vol. 31, no. 4–12, pp. 381–386, 1995.

[8] J. P. Wu and H.-C. Chen, "Effects of cadmium and zinc on oxygen consumption, ammonium excretion, and osmoregulation of white shrimp (*Litopenaeus vannamei*)," *Chemosphere*, vol. 57, no. 11, pp. 1591–1598, 2004.

[9] E. Gómez-Milán, G. Cardenete, and M. J. Sánchez-Muros, "Annual variations in the specific activity of fructose 1,6-bisphosphatase, alanine aminotransferase and pyruvate kinase in the *Sparus aurata* liver," *Comparative Biochemistry and Physiology Part B: Biochemistry and Molecular Biology*, vol. 147, no. 1, pp. 49–55, 2007.

[10] W.-M. Ray, Y.-H. Chien, and C.-H. Chen, "Comparison of probit analysis versus arcsine square root transformation on LC_{50} estimation," *Aquacultural Engineering*, vol. 15, no. 3, pp. 193–207, 1996.

[11] C. E. Boyd, *Water Quality: An Introduction*, Kluwer Academic, 2000.

[12] O. H. Lowry, N. J. Rosebrough, A. L. Farr, and R. J. Randall, "Protein measurement with the Folin phenol reagent," *The Journal of Biological Chemistry*, vol. 193, no. 1, pp. 265–275, 1951.

[13] S. R. Speed, J. Baldwin, R. J. Wong, and R. M. G. Wells, "Metabolic characteristics of muscles in the spiny lobster, *Jasus edwardsii*, and responses to emersion during simulated live transport," *Comparative Biochemistry and Physiology—B Biochemistry and Molecular Biology*, vol. 128, no. 3, pp. 435–444, 2001.

[14] G. Gaxiola, G. Cuzon, T. García et al., "Factorial effects of salinity, dietary carbohydrate and moult cycle on digestive carbohydrases and hexokinases in *Litopenaeus vannamei* (Boone, 1931)," *Comparative Biochemistry and Physiology—A Molecular and Integrative Physiology*, vol. 140, no. 1, pp. 29–39, 2005.

[15] Y. Lu, F. Wang, and S. Dong, "Energy response of swimming crab *Portunus trituberculatus* to thermal variation: implication for crab transport method," *Aquaculture*, vol. 441, pp. 64–71, 2015.

[16] Y. Dong, S. Dong, X. Tian, F. Wang, and M. Zhang, "Effects of diel temperature fluctuations on growth, oxygen consumption and proximate body composition in the sea cucumber *Apostichopus japonicus* Selenka," *Aquaculture*, vol. 255, no. 1–4, pp. 514–521, 2006.

[17] J. D. H. Strickland and T. R. Parsons, "A practical handbook of seawater analysis," *Bulletin of the Fisheries Research Board of Canada*, vol. 167, pp. 1–11, 1968.

[18] M. Omori and T. Ikeda, *Methods in Marine Zooplankton Ecology*, John Wiley & Sons, New York, NY, USA, 1984.

[19] S. Niyogi and C. M. Wood, "Interaction between dietary calcium supplementation and chronic waterborne zinc exposure in juvenile rainbow trout, *Oncorhynchus mykiss*," *Comparative Biochemistry and Physiology Part C: Toxicology & Pharmacology*, vol. 143, no. 1, pp. 94–102, 2006.

[20] F. Dang and W.-X. Wang, "Assessment of tissue-specific accumulation and effects of cadmium in a marine fish fed contaminated commercially produced diet," *Aquatic Toxicology*, vol. 95, no. 3, pp. 248–255, 2009.

[21] M. S. Tellis, M. M. Lauer, S. Nadella, A. Bianchini, and C. M. Wood, "Sublethal mechanisms of Pb and Zn toxicity to the purple sea urchin (*Strongylocentrotus purpuratus*) during early development," *Aquatic Toxicology*, vol. 146, pp. 220–229, 2014.

[22] T. Muralisankar, P. Saravana Bhavan, S. Radhakrishnan, C. Seenivasan, V. Srinivasan, and P. Santhanam, "Effects of dietary zinc on the growth, digestive enzyme activities, muscle biochemical compositions, and antioxidant status of the giant freshwater prawn *Macrobrachium rosenbergii*," *Aquaculture*, vol. 448, pp. 98–104, 2015.

[23] S. Niyogi, P. Couture, G. Pyle, D. G. McDonald, and C. M. Wood, "Acute cadmium biotic ligand model characteristics of laboratory-reared and wild yellow perch (*Perca flavescens*) relative to rainbow trout (*Oncorhynchus mykiss*)," *Canadian Journal of Fisheries and Aquatic Sciences*, vol. 61, no. 6, pp. 942–953, 2004.

[24] D. Alsop and C. M. Wood, "Metal uptake and acute toxicity in zebrafish: common mechanisms across multiple metals," *Aquatic Toxicology*, vol. 105, no. 3-4, pp. 385–393, 2011.

[25] L. N. Taylor, C. M. Wood, and D. G. McDonald, "An evaluation of sodium loss and gill metal binding properties in rainbow trout and yellow perch to explain species differences in copper tolerance," *Environmental Toxicology and Chemistry*, vol. 22, no. 9, pp. 2159–2166, 2003.

[26] D. H. Alsop, J. C. McGeer, D. G. McDonald, and C. M. Wood, "Costs of chronic waterborne zinc exposure and the consequences of zinc acclimation on the gill/zinc interactions of rainbow trout in hard and soft water," *Environmental Toxicology and Chemistry*, vol. 18, no. 5, pp. 1014–1025, 1999.

[27] A. Gül, M. Yilmaz, and Z. Işilak, "Acute toxicity of zinc sulphate ($ZnSO_4.H_2O$) to guppies (*Poecilia reticulata* P., 1859)," *Gazi University Journal of Science*, vol. 22, no. 2, pp. 59–65, 2009.

[28] Y. Zang, X. Tian, S. Dong, and Y. Dong, "Growth, metabolism and immune responses to evisceration and the regeneration of viscera in sea cucumber, *Apostichopus japonicus*," *Aquaculture*, vol. 358-359, pp. 50–60, 2012.

[29] J.-P. Wu, H.-C. Chen, and D.-J. Huang, "Histopathological alterations in gills of white shrimp, *Litopenaeus vannamei* (Boone) after acute exposure to cadmium and zinc," *Bulletin of Environmental Contamination and Toxicology*, vol. 82, no. 1, pp. 90–95, 2009.

[30] T. J. Naimo, G. J. Atchison, and L. E. Holland-Bartels, "Sublethal effects of cadmium on physiological responses in the pocketbook mussel, Lampsilis ventricosa," *Environmental Toxicology and Chemistry*, vol. 11, no. 7, pp. 1013–1021, 1992.

[31] C. K. Miyasaka, R. B. Azevedo, R. Curi, J. M. Filho, and F. M. Lajolo, "Administration of fish oil by gavage increases the activities of hexokinase, glucose-6-phosphate dehydrogenase, and citrate synthase in rat lymphoid organs," *General Pharmacology: The Vascular System*, vol. 27, no. 6, pp. 991–994, 1996.

[32] M. Salomon, P. Mayzaud, and F. Buchholz, "Studies on metabolic properties in the Northern Krill, *Meganyctiphanes norvegica* (Crustacea, Euphausiacea): influence of nutrition and season on pyruvate kinase," *Comparative Biochemistry and Physiology—A Molecular and Integrative Physiology*, vol. 127, no. 4, pp. 505–514, 2000.

[33] X. Yuan, Y. Zhou, X.-F. Liang et al., "Molecular cloning, expression and activity of pyruvate kinase in grass carp *Ctenopharyngodon idella*: effects of dietary carbohydrate level," *Aquaculture*, vol. 410-411, pp. 32–40, 2013.